



Universiteit
Leiden
The Netherlands

Towards treatment of liver fibrosis: Cells, targets and models

Helm, D. van der

Citation

Helm, D. van der. (2021, February 11). *Towards treatment of liver fibrosis: Cells, targets and models*. Retrieved from <https://hdl.handle.net/1887/139202>

Version: Publisher's Version

License: [Licence agreement concerning inclusion of doctoral thesis in the Institutional Repository of the University of Leiden](#)

Downloaded from: <https://hdl.handle.net/1887/139202>

Note: To cite this publication please use the final published version (if applicable).

Cover Page



Universiteit Leiden

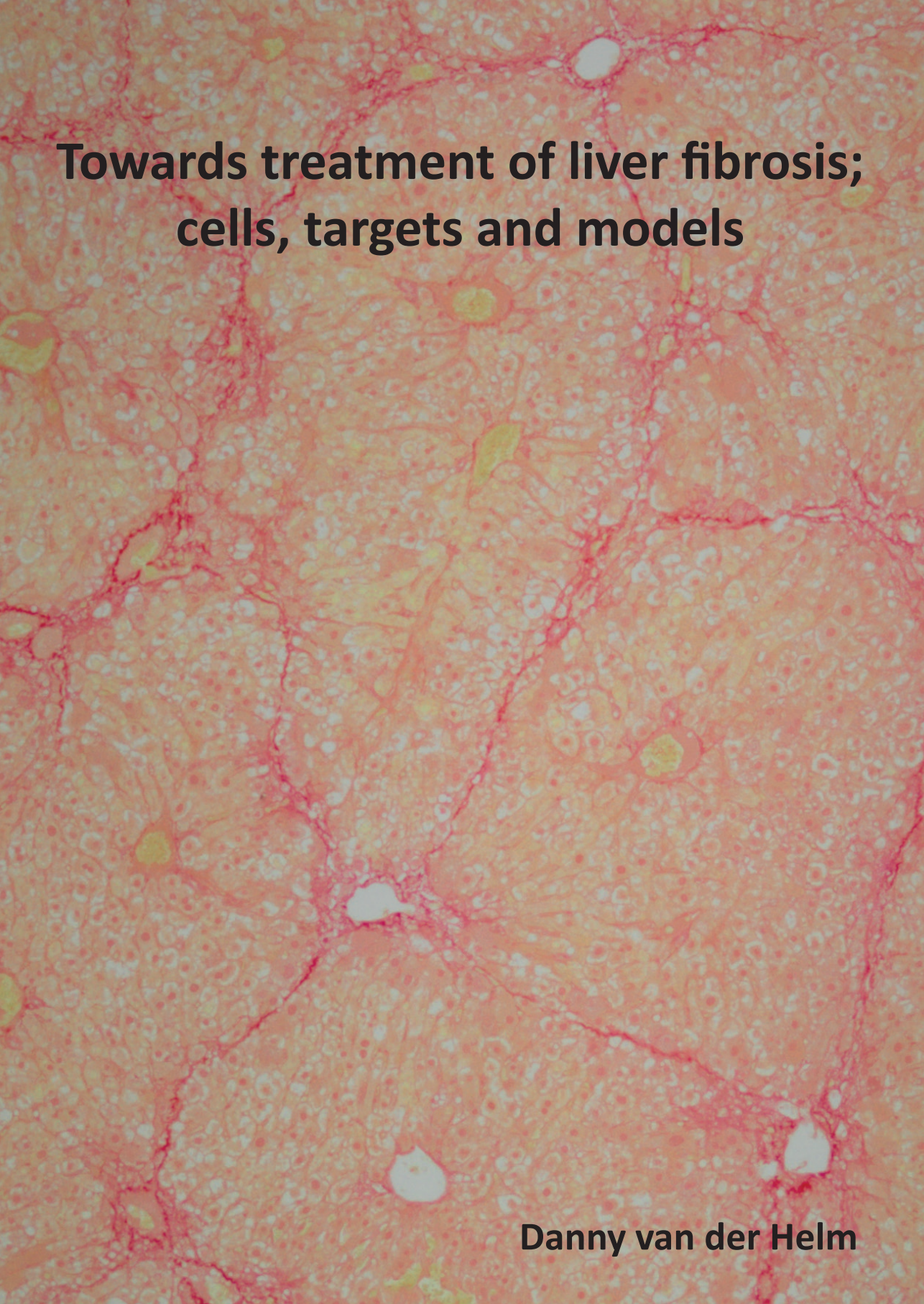


The handle <http://hdl.handle.net/1887/139202> holds various files of this Leiden University dissertation.

Author: Helm, D. van der

Title: Towards treatment of liver fibrosis: Cells, targets and models

Issue date: 2021-02-11



**Towards treatment of liver fibrosis;
cells, targets and models**

Danny van der Helm

**Towards treatment of liver fibrosis;
cells, targets and models**

Copyright © 2020 Danny van der Helm. All rights reserved. No part of this thesis may be reproduced, stored or transmitted in any way or by any means without the prior permission of the author, or when applicable, of the publishers of the scientific papers.

ISBN: 978-94-6423-074-1

Design, Lay-out and Printing: ProefschriftMaken

The printing of this thesis was financially supported by: Nederlandse Vereniging voor Gastroenterologie (NVGE) and Sectie Experimentele Gastroenterologie (SEG)

Towards treatment of liver fibrosis; cells, targets and models

Proefschrift

ter verkrijging van
de graad van Doctor aan de Universiteit Leiden,
op gezag van Rector Magnificus Prof. dr. ir. H. Bijl,
volgens besluit van het College voor Promoties
te verdedigen op donderdag 11 februari 2021
klokke 13:45 uur

Door

Danny van der Helm

geboren op 15 januari 1987 te Rotterdam

Promotoren: Prof. dr. ir. H.W. Verspaget
Prof. dr. B. van Hoek

Co-promotor: Dr. M.J. Coenraad

Promotiecommissie: Prof. dr. P.S. Hiemstra
Prof. dr. I.P.J. Alwayn
Prof. dr. B.E. Snaar-Jagalska
Prof. dr. M.E.J. Reinders (Erasmus MC)
Dr. M.J. Hoogduijn (Erasmus MC)

Table of Contents

Chapter 1	General Introduction	7
Chapter 2	Local but not systemic administration of mesenchymal stromal cells ameliorates fibrogenesis in regenerating livers	27
Chapter 3	VCAM-positive mesenchymal stromal cells are most instrumental in ameliorating experimental liver fibrogenesis	55
Chapter 4	Mesenchymal stromal cells prevent progression of liver fibrosis in a novel zebrafish embryo model	77
Chapter 5	Local and systemic elevated Cripto levels during liver fibrogenesis	101
Chapter 6	CRIPTO promotes an aggressive tumour phenotype and resistance to treatment in hepatocellular carcinoma	119
Chapter 7	General Discussion	153
Appendix	Nederlandse samenvatting	170
	Curriculum vitae	175
	Publications	176
	Dankwoord	179

CHAPTER 1



General Introduction

Liver cirrhosis, the second phase in the fibrosis-cirrhosis-hepatocellular carcinoma (HCC) cascade, is the fourth most common cause of death in Europe (170.000 deaths per year) and the 14th worldwide (>1 million deaths per year), with an expected increasing incidence in the nearby future^{1,2}. Cirrhosis is becoming a major health problem and therapeutics directly targeting the process of liver fibrogenesis, thereby preventing the progression of the disease in the fibrosis-cirrhosis-HCC cascade, are not yet available.

Aetiological factors that can cause cirrhosis include hepatitis viruses (B, C and D), chronic alcohol intake (alcoholic liver disease, ALD), auto-immune hepatitis (AIH), drug-induced liver injury (DILI), genetic disorders (like α 1-antitrypsin deficiency, Wilson disease and hereditary haemochromatosis), obesity and diabetes mellitus (non-alcoholic fatty liver disease, NAFLD), and cholestatic diseases (like primary biliary cholangitis, PBC, and primary sclerosing cholangitis, PSC)²⁻⁵. The prevalence of these aetiologies is region related^{2,6-8}. In the Western world, liver cirrhosis mostly evolves in a background of alcohol intake (ALD) and lifestyle-induced NAFLD^{7,9,10}. Due to the increasing prevalence of overweight and diabetes over the past decades, NAFLD has become an endemic cause of liver disease^{9,10}. In Asia and sub-Saharan Africa, cirrhosis is mostly induced by viral hepatitis B or C infection^{6,7}. In general, these aetiological factors lead to the onset of liver fibrogenesis and eventually to fibrosis and cirrhosis^{3,4,11}. Liver fibrogenesis starts by damaged and apoptotic hepatocytes which trigger the proliferation and activation of liver-resident stellate cells^{3,4,11}. These activated stellate cells differentiate into myofibroblasts and subsequently start to secrete excessive amounts of extracellular matrix (ECM) leading to fibrogenesis (Figure 1). The liver has an efficient regenerative capacity to overcome acute damage induced by injuring stimuli such as toxins, viral infection, auto-immunity, cholestasis, metabolic disorders, trauma or surgical interventions¹²⁻¹⁶. In response to these acute injuring stimuli, stellate cells become activated and the liver starts regenerative cascades that promote survival and proliferation of endogenous liver cells. At the end of these regenerative processes, the activated stellate cells are silenced and shift to their inactivated state¹⁴⁻¹⁶. When the liver is chronically challenged, despite some regeneration, the liver will be unable to recover in the period between the injuring insults. This continuous fibrogenesis leads to diminished liver function and eventually to fibrosis and finally cirrhosis^{4,11}.

In a healthy steady-state situation, stellate cells reside in the space of Disse near the portal triads¹⁷. The space of Disse is the area between the hepatocytes and the liver sinusoids, with the fenestrated endothelium in between. During liver fibrogenesis, the activated and proliferating stellate cells migrate and populate these spaces where they secrete ECM components and form the so-called septa that eventually bridge the entire space between portal triads (porto-portal septa), between centrilobular veins (centro-central septa), and between portal triads and centrilobular veins (porto-central septa). In the clinic, the produced ECM deposition is used to assess the severity of liver fibrosis¹⁸. Besides these myofibroblasts and their secreted ECM components, the septa are also filled with invading Kupffer- and T-cells¹⁸. After a long

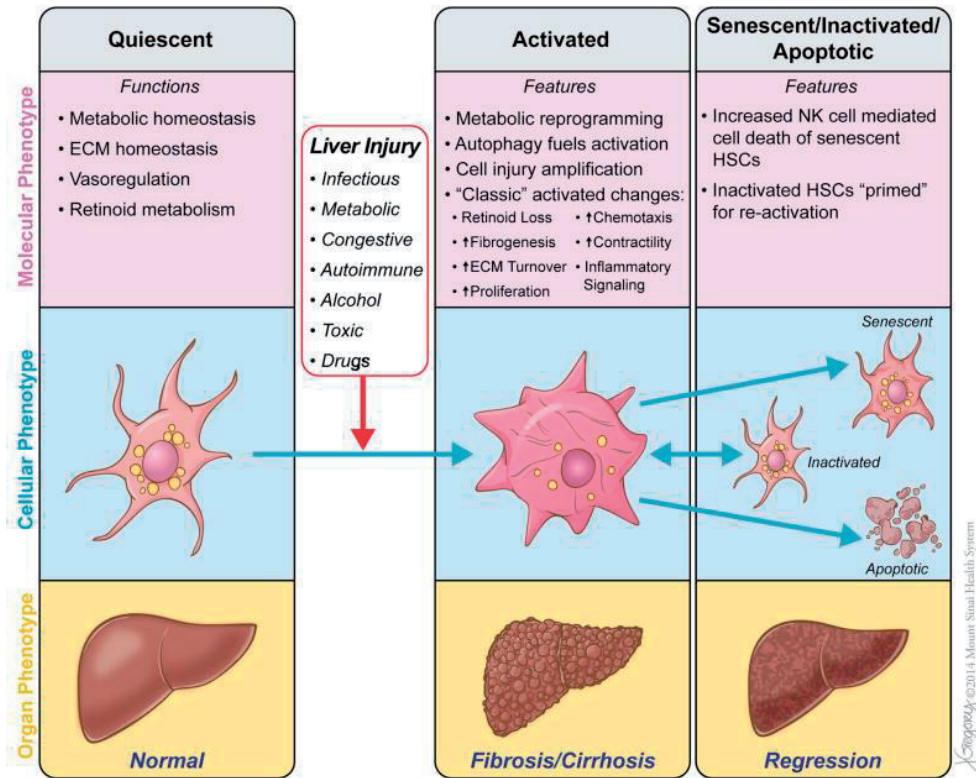


Figure 1: Stellate cells during the induction and regression of liver fibrogenesis. In the healthy situation, quiescent stellate cells are involved in metabolic homeostasis, vaso-regulation and retinoid metabolism. Due to liver injuring stimuli, the stellate cells become activated and differentiate into myofibroblasts. This shift is accompanied by metabolic reprogramming, retinoid loss, increased ECM secretion, increased proliferation, and increased inflammatory signalling of stellate cells. Removal of the injuring stimuli may lead to the regression of fibrogenesis, which is initiated by myofibroblasts that become apoptotic or shift to their inactivated or senescent state. Reproduced from [Pathobiology of liver fibrosis: a translational success story, Y.A. Lee, M.C. Wallace, S.L. Friedman, 64(5):830-41 2014] with permission from the illustrator and BMJ Publishing Group Ltd¹¹.

period of sustained fibrogenesis, the blood-flow through the liver becomes hampered which leads to fewer nutrients and oxygen supply and subsequently more cell death in the liver which eventually enhances the ongoing fibrogenesis. During the last phase, the liver will fail to perform its many functions, which indicates end-stage liver cirrhosis. During this final stage there is an increased risk of decompensated cirrhosis, characterized by variceal bleeding, ascites, hepatic encephalopathy, and multi-organ failure. Furthermore, cirrhosis also predisposes towards development of hepatocellular carcinoma (HCC)^{19,20}.

Treatment of liver fibrosis and cirrhosis is limited to removal of the injuring stimuli, such as anti-viral therapies or refraining from alcohol consumption^{21,22}. For example, sustained response to antiviral therapy in patients with HBV- or HCV-induced fibrosis can lead to the reversal of

the relative stage of fibrosis^{23,24}. Due to this successful treatment strategy, less patients with HCV-induced cirrhosis are now in need of orthotopic liver transplantation (OLT)²⁵. Nevertheless, OLT is currently the only curative treatment for end-stage cirrhosis with deteriorating function and decompensation^{9,21,24}. Although OLT is performed for decades already, it is still a major intervention with substantial risks^{26,27}. Furthermore, the possibility to perform OLT depends on the general condition of the patient and on donor availability^{28,29}. Recently, hepatocyte and liver organoid transplantations were tested as alternative treatment strategies for end-stage liver cirrhosis. These therapies were found to improve liver function and overall survival in mice with fulminant liver failure^{30,31}. However, in mouse models for liver fibrosis, these treatments were ineffective in resolving fibrosis, and also showed low engraftment in the damaged liver. Altogether these observations indicate the need for alternative treatment strategies which preferably directly target fibrogenesis³²⁻³⁴.

Mesenchymal stromal cells (MSCs)

The applicability of MSC therapy is well studied in a variety of diseases, and research in this context made huge progress in the basic and functional characterisation of this cell type³⁵⁻³⁷. Some of these studies showed that MSCs have functional characteristics that might be applicable to reverse liver fibrogenesis^{33,37-39}. MSCs can easily be isolated from different tissues such as adipose-, umbilical cord-, and bone marrow-tissue, and are identified by their ability to adhere to plastic, their ability to differentiate into osteoblasts, adipocytes and chondrocytes, and their expression of certain membrane markers^{37,38,40}. The literature, however, is less unambiguous regarding the precise subset of these membrane markers⁴¹. In general, mouse-derived MSCs are known to express CD29 (β 1-integrin), Stem Cell Antigen-1 (SCA-1) and CD44 but not the hematopoietic cell marker CD45 and endothelial cell marker CD31^{42,43}. Endoglin (CD105) and vascular cell adhesion molecule 1 (VCAM-1, CD106) membrane expression are inconsistently used as identification markers for MSCs^{41,44-47}.

MSCs exert multiple unique features that make them of interest for therapeutic use. One of these features is that resting MSCs are not expressing MHC class II proteins, unless activated, and are therefore not recognised and not rejected by the host immune system after transplantation⁴⁸. Furthermore, MSCs can easily be expanded *in vitro* while maintaining their phenotype and can easily be cryopreserved, which makes it possible to treat multiple patients with the same MSC product³⁸.

In relation to their potential therapeutic use, MSCs are known to be able to inhibit inflammatory responses, for example suppressing T-cell responses and promoting anti-inflammatory macrophage differentiation^{49,50}. Because of these immune-regulatory properties, MSCs have already been used after kidney or bone-marrow transplantation for the prevention of rejection^{36,51,52}. Furthermore, MSCs promote regeneration and repair of damaged tissue as, for example, observed in the MSC treatment of perianal fistulas in Crohns disease⁵³. Tissue

repair, tissue regeneration and immune-responses are also important processes during the regression of liver fibrogenesis, and therefore the use of MSCs might be of interest as potential treatment strategy for liver fibrosis⁴⁰.

Fibroblasts and MSCs have multiple phenotypic similarities which makes it somewhat difficult to distinguish these cell types. Literature suggests that MSCs, in contrast to fibroblasts, are positive for SCA-1 and that this marker therefore may be used to distinguish both cell types⁵⁴. It is also suggested that fibroblasts and MSCs share some functional characteristics in immunomodulation and tissue regeneration⁵⁴⁻⁵⁷. However, the comparison in their ability to reverse liver fibrogenesis has not been studied before.

MSC therapy as potential therapeutic strategy to resolve liver fibrosis

Sakaida et al. published in 2004 *in vivo* studies showing that MSC treatment could inhibit and prevent the induction of liver fibrosis⁵⁸. Since that time several *in vivo* and clinical studies assessed whether liver fibrosis and cirrhosis could be reversed by MSC therapy^{39,40,59-61}. Most of these studies revealed positive and promising results showing that MSCs are able to effectively reverse liver fibrogenesis and thereby ameliorate fibrosis or cirrhosis. Furthermore, no serious side-effects or unsafety signals were observed in all these studies. In literature, different working mechanisms have been suggested. One of the suggested theories includes the ability of MSCs to stimulate the survival and proliferation of endogenous liver cells upon tissue damage (Figure 2). For example, Fouraschen et al. showed that livers that underwent a partial hepatectomy regenerate faster with MSC therapy¹². It was suggested that MSCs express and secrete hepatocyte growth factor (HGF), vascular endothelial growth factor (VEGF), insulin-like growth factor-1 (IGF-1), and stromal derived growth factor-1 (SDF-1) and thereby stimulate survival and proliferation of hepatocytes, that might explain the pro-regenerative capacities of MSC therapy^{12,62-66}. In relation to the anti-inflammatory capacities of MSCs, it is thought that MSCs reverse fibrogenesis by suppression and/or redirecting of innate- and adaptive-immune responses (Figure 3). For example, MSCs are known to directly inhibit B- and T-cell proliferation, thereby inhibiting immune-responses. In relation to the innate immune system, MSCs are thought to secrete IGF-1 and interleukin-10 (IL-10) in response to the fibrogenic environment, which stimulates macrophage M2 polarization. M2 macrophages are anti-inflammatory and are able to silence some of the immune-reactions which occur during fibrogenesis^{63,67}. Furthermore, MSCs are also known to suppress dendritic and NK cell function (Figure 3).

Another suggested mechanism is a direct anti-fibrogenic effect of MSCs by the release of cytokines such as HGF which directly targets the stellate cells and myofibroblasts. HGF is known to directly inhibit the activation and proliferation of stellate cells, thereby directly targeting the initiation steps of fibrogenesis. Furthermore, HGF is also known to silence myofibroblasts (activated stellate cells), thereby directly silencing fibrogenesis (Figure 2)^{37,66,68-70}. MSCs are

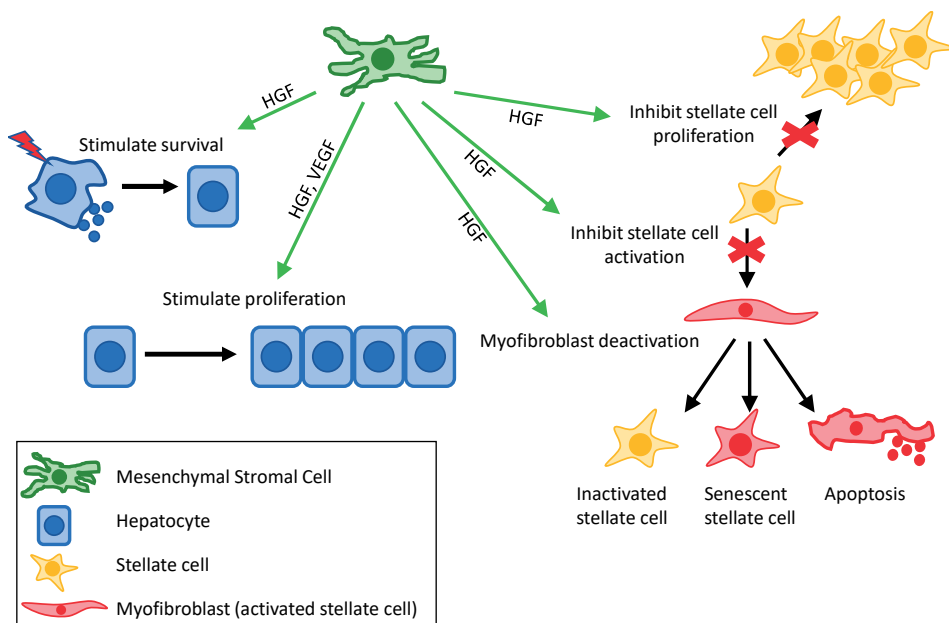


Figure 2: Potential therapeutic interactions of MSCs with endogenous liver cells for the treatment of liver fibrosis. Schematic overview of suggested working mechanisms of MSC therapy for the regression of liver fibrogenesis.

even thought to be able to differentiate into hepatocytes or hepatocyte-like cells^{33,38}. These differentiated cells exert similar functional properties as observed in normal hepatocytes, such as glycogen storage, low density lipoprotein (LDL) uptake, and the production of albumin and urea. However, while these hepatocyte-like cells, like hepatocyte organoids, may improve liver function, they show low engraftment in the liver and are also ineffective for induction of regression of ongoing fibrogenesis³²⁻³⁴. The precise working mechanisms of MSCs are still largely unknown, but probably encompass a combination of the above mentioned mechanisms that contribute to their efficacy in the observed reversal of fibrogenesis.

The importance of study design and MSC characterisation in MSC-related therapy

Despite the promising previously performed studies and the proposed mechanisms, the use of MSC therapy for liver fibrosis is still in its infancy. Most *in vivo* and clinical studies are using different study designs, which makes it difficult to compare these studies and to evaluate the overall efficacy of MSC therapy^{37,59,60,71}. For example, the disease stage (fibrosis vs cirrhosis) or aetiological factors can be different between studies and these might affect the study outcome. Furthermore, the effectiveness of MSC therapy could also be affected by technical variables in the study design such as the dosage and -administration routes (i.e., local- vs intravenous- vs portal-administration) of MSCs^{39,59-61,71}. Moreover, many studies are using MSCs isolated from different sources, while it is known that adipose-, umbilical cord-

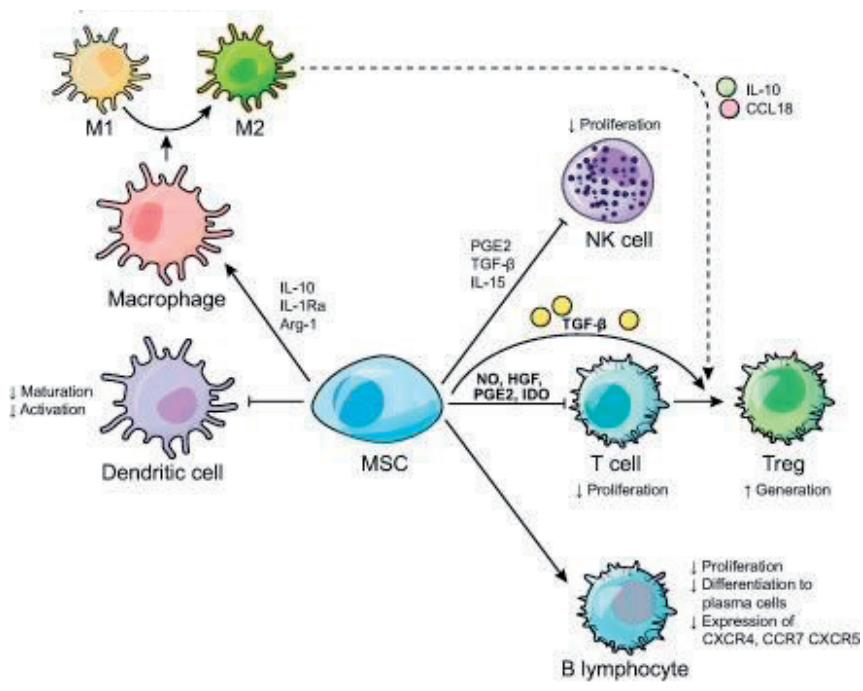


Figure 3: The putative interplay between MSCs and immune cells in the treatment of liver fibrosis. Schematic overview of suggested immunoregulatory mechanisms of MSC therapy that might lead to the regression of liver fibrogenesis. Reprinted from [Mesenchymal stromal cell therapy for liver Diseases, 68(6):1272-1285 2018, M. Alfaifi, Y.W. Eom, P.N. Newsome, S.K. Baik] with permission from Elsevier⁶¹.

and bone marrow-derived MSCs can behave differently, suggesting that the source of MSCs might also be important to induce the regression of fibrogenesis^{46,72}. Furthermore, recently published studies revealed the possible existence of different subpopulations of MSCs which might explain the different findings in the literature^{43,45,46,71}. With the currently used isolation protocols, a heterogeneous population of cells is isolated which are all positive for most of the known MSC characterisation markers^{46,73,74}. For example, VCAM (CD106) and Endoglin (CD105) membrane expression are not used as a standard for MSC characterisation while literature already suggested that subpopulations identified by the presence or absence of these proteins might exert different functional properties⁴⁴⁻⁴⁶. Anderson et al. showed that Endoglin-negative MSC populations seem to have better immunoregulatory properties compared to Endoglin-positive MSC populations⁴⁵. Other studies have shown that VCAM-positive MSC subpopulations are more pro-regenerative and immunosuppressive compared to VCAM-negative MSC subpopulations^{44,46}. These findings indicate that the use of different subpopulations of MSCs probably affect therapy efficacy. Therefore, these variables might explain the different and sometimes contradictive study outcomes, warranting further research to identify an optimal MSC therapy for liver fibrosis.

Animal models to study liver fibrogenesis

Various *in vitro* and *in vivo* models are being used to study the pathogenesis of liver fibrogenesis and to test alternative treatments to reverse this pathological process^{75,76}. Acute and chronic liver fibrogenesis can be induced *in vivo* by genetic modifications, mechanical alterations or administration of hepatotoxic compounds⁷⁵.

The latter is most frequently used since these models most resemble the human viral- or alcohol-induced liver diseases. Thioacetamide (TAA) and carbon tetrachloride (CCL4) are well-known and frequently used hepatotoxic compounds to induce acute- and chronic- liver injury in mice and rats^{75,76}. Hepatocytes metabolise both compounds into hepatotoxic metabolites that subsequently induce apoptosis of the hepatocytes and thereby initiate the induction of fibrogenesis^{75,76}. The duration of the administration-period of these compounds correlates to the severity and progression of the disease. This correlation makes it possible to study different disease stages within the same model system^{76,77}. CCL4- and TAA-induced animal models for liver fibrosis have shown to be predictable and reliable but are also expensive and sometimes acute toxicities with subsequent animal death are observed. Moreover, it takes a relative long period to induce chronic liver fibrosis (6 weeks) or cirrhosis (12 weeks). Within these periods, animals are in need of frequent check-ups and regular administration of the toxic compounds, making these models time-consuming and labour-intensive⁷⁵. These observations indicate that CCL4 and TAA rodent models are robust but less attractive for high throughput compound screening.

Zebrafish embryos, on the other hand, are small, less expensive, easy to maintain, have a short regeneration time and also showed huge physiological similarities with man⁷⁸⁻⁸⁰. In relation to that latter, livers of zebrafish are constructed with the same cells as in humans and show a further resemblances of 70%^{78,81}. Moreover, zebrafish embryos are suitable for high throughput screening as observed in non-hepatic related studies⁸⁰. However, the use of these embryos in respect to liver fibrogenesis is limited, and a detailed description of a zebrafish embryo model which resembles chronic human liver fibrogenesis had not been presented yet.

Some studies observed that acute liver injury in zebrafish embryos leads to increased collagen and Hand-2 expression, which is indicative for the activation of stellate cells, and for the onset of fibrosis⁸²⁻⁸⁵. Furthermore, similarities to the well-known human and mouse pathogenesis of liver fibrogenesis were observed when TAA or ethanol was administered to mature zebrafish⁸⁶⁻⁸⁸. The zebrafish embryo might thus be an attractive high throughput model system to study chronic liver fibrogenesis. The abilities of TAA and CCL4 to induce fibrogenesis in zebrafish embryos and the possible involved pathways have not yet been described. If these compounds induce fibrogenesis in zebrafish embryos with similar pathological mechanisms as observed in humans it would be a perfect high throughput screening model for the identification of alternative therapeutics to reduce fibrogenesis.

Cripto-1: a new player in the fibrosis-cirrhosis–HCC cascade

As mentioned earlier, therapies directly targeting fibrogenesis are needed. In order to discover new targets for intervention, it is important to increase our basic understanding and knowledge of the fibrosis-cirrhosis-HCC cascade and the underlying pathological mechanisms.

In 2018, Zhang et al. described elevated Cripto-1 (Teratocarcinoma-Derived Growth Factor 1; TGDF1) protein levels in blood of patients with HBV- and HCV-induced cirrhosis⁸⁹. Cripto-1 belongs to the epidermal growth factor-Cripto/frl/cryptic (EGF-CFC) family and is a GPI-anchored signaling protein that is important during embryogenesis and believed to be silenced after birth⁹⁰⁻⁹². Surprisingly, recent discoveries indicate that Cripto-1 is re-expressed postnatally in different neoplastic processes but a link to fibrogenesis was never observed⁹⁰. Oncogenesis, embryogenesis, fibrogenesis, tissue repair, and tissue regeneration are different processes but also share multiple similarities including cell proliferation, cell survival, and cell differentiation¹⁴⁻¹⁶. Cripto-1 is known to be an important protein for these cellular features during embryogenesis and oncogenesis^{92,93}. One might therefore speculate that Cripto-1 expression during fibrogenesis could be involved in the survival, proliferation and plasticity of liver cells as protective mechanism to overcome the injuring stimuli. When this would be true it could imply a functional role for Cripto-1 in the fibrosis–cirrhosis-HCC cascade. Altogether, these observations warrant further research to disentangle the contribution of Cripto-1 in liver fibrogenesis, which in the future may contribute to the identification of new leads for antifibrotic therapy.

Cripto-1 in Hepatocellular carcinoma

Hepatocellular carcinoma is the second leading cause of cancer-related death worldwide⁹⁴. HCC mostly arises in a background of cirrhosis in the last phase of the fibrosis-cirrhosis-HCC pathological disease course^{95,96}. HCCs are known to be invasive and to have a high metastatic potential leading to poor prognosis of patients. The treatments for early and intermediate tumor stages include resection, OLT and/or minimally invasive image-guided therapies such as local ablation by trans-arterial chemoembolization (TACE) or radiofrequency ablation (RFA)^{97,98}. For advanced tumor stages, systemic treatments such as Sorafenib and Regorafenib are being used^{98,99}. However, these palliative systemic therapies can have substantial side-effects, are effective in only a minority of the patients and lead to an average survival benefit of only 6 months^{98,100}. Despite these different treatment strategies the overall patient prognosis for HCC remains poor due to tumor recurrence and non-response to therapy⁹⁸.

Biomarkers for HCCs that correlate with tumor stage and which are able to predict the progression of the tumor could be of help in the early detection and treatment of HCC¹⁰¹. In the clinic, alpha-fetoprotein (AFP) is used as a biomarker but as sole marker is insufficient for diagnosis since it does not predict disease stage and serum levels are not elevated in 30% of the HCCs^{98,102}. However, in the cases where AFP is elevated those serum levels do

correlate to tumor size and tumor progression, and therefore in these cases it can be used to evaluate response to therapy and follow-up of the disease¹⁰³. The mechanisms behind the development, progression, invasion, and metastasis of HCCs are largely unknown. Elucidation of these processes might lead to the identification of new biomarkers and new (personalized)-therapies. For example, biomarkers which could distinguish Sorafenib responders from non-responders would lead to a better and more personalized treatment. As mentioned earlier, Cripto-1 is re-expressed during oncogenesis where it is involved in cancer progression and metastasis^{91,104-110}. Moreover, Wang et al. recently showed that Cripto-1 expression in HCC correlates to poor patient survival and faster tumor recurrence in HCC patients but the precise contribution of Cripto-1 is unclear^{92,111}. Suggested mechanisms include Cripto-1 involvement in pathways leading to faster proliferation and onset of epithelial to mesenchymal transition of tumour cells^{92,112-117}. The exact function of Cripto-1 in HCC and its possible usage as a biomarker, however, need to be further studied. As described, Cripto-1 is also observed in blood of patients with cirrhosis without the presence of HCC or any other neoplasms⁸⁹. One might speculate that hepatocytes expressing Cripto-1 during fibrogenesis may be the cells with the highest potential to become oncogenic and thereby may be identified as the “cancer stem cells”. In the future, unravelling the role of Cripto-1 in the fibrosis-cirrhosis-HCC pathological disease course might lead to the identification of new targets for HCC and antifibrotic therapies.

Outline and aims of the studies described in this thesis

Currently, MSCs have been tested in clinical trials, often with promising results but also sometimes with a lack of effectivity regarding the reversal of fibrosis, cirrhosis and end-stage liver disease^{39,61,118}. Results from the literature are difficult to compare since there are multiple differences in study design such as underlying disease aetiology, disease stage, administration route- and dosage- and source- of MSCs, which could affect the study outcomes^{60,61,71}. Therefore, in the study of **chapter 2**, the therapeutic potential of MSCs and fibroblasts were assessed and compared, in combination with partial hepatectomy as regenerating stimulus, in CCL4-induced fibrosis and cirrhosis in mice. Furthermore, the impact of route of administration and dosage of MSCs on the therapeutic efficacy of MSCs was evaluated. Specifically the local administration of the MSCs in regenerating fibrotic and cirrhotic livers was thought to be able to ameliorate fibrogenesis.

The use of different MSC subpopulations might also contribute to the contrasting findings in literature^{44-46,119}. In the study of **chapter 3**, the pro-regenerative and anti-fibrotic abilities of four different subpopulations of MSCs, selected on their Endoglin and/or vascular cell adhesion molecule (VCAM) expression, was compared. This approach was used to evaluate whether different subpopulations of MSCs could lead to different outcomes, which might explain the contradictory results observed in literature.

Rodent models for liver fibrosis have been widely used, but are not suitable for high throughput screening purposes⁷⁵. Therefore we aimed to translate the widely used CCL4 and TAA mouse models for liver fibrosis to zebrafish embryos as a new model suitable for fast screening (**chapter 4**). The applicability to study new therapeutic interventions was evaluated by the administration of MSCs and fibroblasts as potential novel cell therapies for liver fibrogenesis.

Therapies directly targeting fibrogenesis are needed. More knowledge of the pathological mechanisms underlying the fibrosis-cirrhosis-HCC cascade could lead to identification of new leads for the development of alternative treatment strategies. Interestingly, a recent study reported elevated Cripto-1 protein levels in plasma of patients with cirrhosis⁸⁹. This was the first study that suggested a connection between Cripto-1 expression and fibrogenesis. In order to compare Cripto-1 expression of normal and fibrogenic liver tissue of humans, mice, and zebrafish embryos a study was performed to evaluate whether Cripto-1 is expressed by liver cells (**chapter 5**). Furthermore, the Cripto-1 level in blood and its expression in liver tissue were assessed to evaluate whether it relates with the disease stage. If this would be the case, it could imply a contribution of Cripto-1 in the fibrosis–cirrhosis-HCC cascade which warrant further studies.

Cripto-1 is known for its role in cancer progression and metastasis⁹⁰. In HCC, Cripto-1 expression correlates with poor prognosis and overall survival, however, the functional role of Cripto-1 in HCC is largely unknown^{89,111}. Therefore, as described in **chapter 6** the role of Cripto-1 in HCCs *in vitro* and *in vivo* was studied. In addition it was assessed whether Cripto-1 expression might affect the use of conventional systemic therapies.

Finally, in the overall discussion of **chapter 7** the implications of the findings of the different studies is discussed and directions for future research are indicated.

References

1. Lozano, R., Naghavi, M., Foreman, K. *et al.* Global and regional mortality from 235 causes of death for 20 age groups in 1990 and 2010: a systematic analysis for the Global Burden of Disease Study 2010. *Lancet* 2012; **380**: 2095-2128.
2. Blachier, M., Leleu, H., Peck-Radosavljevic, M. *et al.* The burden of liver disease in Europe: a review of available epidemiological data. *J Hepatol* 2013; **58**: 593-608.
3. Bataller, R. & Brenner, D. A. Liver fibrosis. *J Clin Invest* 2005; **115**: 209-218.
4. Friedman, S. L. Mechanisms of hepatic fibrogenesis. *Gastroenterology* 2008; **134**: 1655-1669.
5. Mitchell, E. L. & Khan, Z. Liver Disease in Alpha-1 Antitrypsin Deficiency: Current Approaches and Future Directions. *Curr Pathobiol Rep* 2017; **5**: 243-252.
6. Jefferies, M., Rauff, B., Rashid, H. *et al.* Update on global epidemiology of viral hepatitis and preventive strategies. *World J Clin Cases* 2018; **6**: 589-599.
7. Asrani, S. K., Devarbhavi, H., Eaton, J. *et al.* Burden of liver diseases in the world. *J Hepatol* 2019; **70**: 151-171.
8. Setiawan, V. W., Stram, D. O., Porcel, J. *et al.* Prevalence of chronic liver disease and cirrhosis by underlying cause in understudied ethnic groups: The multiethnic cohort. *Hepatology* 2016; **64**: 1969-1977.
9. European Association for the Study of the Liver, European Association for the Study of Diabetes & European Association for the Study of Obesity. EASL-EASD-EASO Clinical Practice Guidelines for the management of non-alcoholic fatty liver disease. *Diabetologia* 2016; **59**: 1121-1140.
10. Vernon, G., Baranova, A. & Younossi, Z. M. Systematic review: the epidemiology and natural history of non-alcoholic fatty liver disease and non-alcoholic steatohepatitis in adults. *Aliment Pharmacol Ther* 2011; **34**: 274-285.
11. Lee, Y. A., Wallace, M. C. & Friedman, S. L. Pathobiology of liver fibrosis: a translational success story. *Gut* 2015; **64**: 830-841.
12. Fouraschen, S. M. G., Pan, Q. W., de Ruiter, P. E. *et al.* Secreted Factors of Human Liver-Derived Mesenchymal Stem Cells Promote Liver Regeneration Early After Partial Hepatectomy. *Stem Cells Dev* 2012; **21**: 2410-2419.
13. Tranchart, H., Catherine, L., Maitre, S. *et al.* Efficient Liver Regeneration following Temporary Portal Vein Embolization with Absorbable Gelatin Sponge Powder in Humans. *J Vasc Interv Radiol* 2015; **26**: 507-515.
14. Fausto, N. & Campbell, J. S. The role of hepatocytes and oval cells in liver regeneration and repopulation. *Mech Dev* 2003; **120**: 117-130.
15. Fausto, N., Campbell, J. S. & Riehle, K. J. Liver regeneration. *Hepatology* 2006; **43**: S45-53.
16. Gilgenkrantz, H. & Collin de l'Hortet, A. Understanding Liver Regeneration: From Mechanisms to Regenerative Medicine. *Am J Pathol* 2018; **188**: 1316-1327.
17. Higashi, T., Friedman, S. L. & Hoshida, Y. Hepatic stellate cells as key target in liver fibrosis. *Adv Drug Deliv Rev* 2017; **121**: 27-42.

18. Lo, R. C. & Kim, H. Histopathological evaluation of liver fibrosis and cirrhosis regression. *Clin Mol Hepatol* 2017; **23**: 302-307.
19. D'Amico, G., Morabito, A., D'Amico, M. *et al.* Clinical states of cirrhosis and competing risks. *J Hepatol* 2018; **68**: 563-576.
20. D'Amico, G., Morabito, A., D'Amico, M. *et al.* New concepts on the clinical course and stratification of compensated and decompensated cirrhosis. *Hepatol Int* 2018; **12**: 34-43.
21. Mathurin, P., Hadengue, A., Bataller, R. *et al.* EASL Clinical Practical Guidelines: Management of Alcoholic Liver Disease. *J Hepatol* 2012; **57**: 399-420.
22. Liver, E. A. S. EASL Recommendations on Treatment of Hepatitis C 2016. *J Hepatol* 2017; **66**: 153-194.
23. Lee, Y. A. & Friedman, S. L. Reversal, maintenance or progression: What happens to the liver after a virologic cure of hepatitis C? *Antivir Res* 2014; **107**: 23-30.
24. Marcellin, P., Gane, E., Buti, M. *et al.* Regression of cirrhosis during treatment with tenofovir disoproxil fumarate for chronic hepatitis B: a 5-year open-label follow-up study. *Lancet* 2013; **381**: 468-475.
25. Belli, L. S., Perricone, G., Adam, R. *et al.* Impact of DAAs on liver transplantation: Major effects on the evolution of indications and results. An ELITA study based on the ELTR registry. *J Hepatol* 2018; **69**: 810-817.
26. Angaswamy, N., Tiriveedhi, V., Sarma, N. J. *et al.* Interplay between immune responses to HLA and non-HLA self-antigens in allograft rejection. *Hum Immunol* 2013; **74**: 1478-1485.
27. Maynard, E. Liver Transplantation: Patient Selection, Perioperative Surgical Issues, and Expected Outcomes. *Surg Clin North Am* 2019; **99**: 65-72.
28. Lucidi, V., Gustot, T., Moreno, C. *et al.* Liver transplantation in the context of organ shortage: toward extension and restriction of indications considering recent clinical data and ethical framework. *Curr Opin Crit Care* 2015; **21**: 163-170.
29. Reddy, M. S., Rajalingam, R. & Rela, M. Liver transplantation in acute-on-chronic liver failure: lessons learnt from acute liver failure setting. *Hepatol Int* 2015; **9**: 508-513.
30. Boudechiche, L., Tranchart, H., Branchereau, S. *et al.* Improvement of Hepatocyte Transplantation Efficiency in the *mdr2*^{-/-} Mouse Model by Glyceryl Trinitrate. *Transplantation* 2015; **99**: 36-40.
31. Gramignoli, R., Vosough, M., Kannisto, K. *et al.* Clinical Hepatocyte Transplantation: Practical Limits and Possible Solutions. *Eur Surg Res* 2015; **54**: 162-177.
32. Dhawan, A., Puppi, J., Hughes, R. D. *et al.* Human hepatocyte transplantation: current experience and future challenges. *Nat Rev Gastroenterol Hepatol* 2010; **7**: 288-298.
33. Forbes, S. J., Gupta, S. & Dhawan, A. Cell therapy for liver disease: From liver transplantation to cell factory. *J Hepatol* 2015; **62**: S157-169.
34. Matsumoto, T., Takami, T. & Sakaida, I. Cell transplantation as a non-invasive strategy for treating liver fibrosis. *Expert Rev Gastroenterol Hepatol* 2016; **10**: 639-648.
35. Molendijk, I., Barnhoorn, M. C., de Jonge-Muller, E. S. *et al.* Intraluminal Injection of Mesenchymal Stromal Cells in Spheroids Attenuates Experimental Colitis. *J Crohns Colitis* 2016; **10**: 953-964.

36. Reinders, M. E., Bank, J. R., Dreyer, G. J. *et al.* Autologous bone marrow derived mesenchymal stromal cell therapy in combination with everolimus to preserve renal structure and function in renal transplant recipients. *J Transl Med* 2014; **12**: 331.
37. Alfaifi, M., Eom, Y. W., Newsome, P. N. *et al.* Mesenchymal stromal cell therapy for liver diseases. *J Hepatol* 2018; **68**: 1272-1285.
38. Eom, Y. W., Kim, G. & Baik, S. K. Mesenchymal stem cell therapy for cirrhosis: Present and future perspectives. *World J Gastroenterol* 2015; **21**: 10253-10261.
39. Berardis, S., Dwisthi Sattwika, P., Najimi, M. *et al.* Use of mesenchymal stem cells to treat liver fibrosis: current situation and future prospects. *World J Gastroenterol* 2015; **21**: 742-758.
40. Parekkadan, B. & Milwid, J. M. Mesenchymal Stem Cells as Therapeutics. *Annu Rev Biomed Eng* 2010; **12**: 87-117.
41. Sung, J. H., Yang, H. M., Park, J. B. *et al.* Isolation and characterization of mouse mesenchymal stem cells. *Transplant Proc* 2008; **40**: 2649-2654.
42. Li, H., Ghazanfari, R., Zacharaki, D. *et al.* Isolation and characterization of primary bone marrow mesenchymal stromal cells. *Ann N Y Acad Sci* 2016; **1370**: 109-118.
43. Morikawa, S., Mabuchi, Y., Kubota, Y. *et al.* Prospective identification, isolation, and systemic transplantation of multipotent mesenchymal stem cells in murine bone marrow. *J Exp Med* 2009; **206**: 2483-2496.
44. Yang, Z. X., Han, Z. B., Ji, Y. R. *et al.* CD106 identifies a subpopulation of mesenchymal stem cells with unique immunomodulatory properties. *PLoS One* 2013; **8**: e59354.
45. Anderson, P., Carrillo-Galvez, A. B., Garcia-Perez, A. *et al.* CD105 (endoglin)-negative murine mesenchymal stromal cells define a new multipotent subpopulation with distinct differentiation and immunomodulatory capacities. *PLoS One* 2013; **8**: e76979.
46. Han, Z. C., Du, W. J., Han, Z. B. *et al.* New insights into the heterogeneity and functional diversity of human mesenchymal stem cells. *Biomed Mater Eng* 2017; **28**: S29-S45.
47. Lin, C. S., Xin, Z. C., Dai, J. *et al.* Commonly used mesenchymal stem cell markers and tracking labels: Limitations and challenges. *Histol Histopathol* 2013; **28**: 1109-1116.
48. Ryan, J. M., Barry, F. P., Murphy, J. M. *et al.* Mesenchymal stem cells avoid allogeneic rejection. *J Inflamm (Lond)* 2005; **2**: 8.
49. Di Nicola, M., Carlo-Stella, C., Magni, M. *et al.* Human bone marrow stromal cells suppress T-lymphocyte proliferation induced by cellular or nonspecific mitogenic stimuli. *Blood* 2002; **99**: 3838-3843.
50. Klyushnenkova, E., Mosca, J. D., Zernetkina, V. *et al.* T cell responses to allogeneic human mesenchymal stem cells: immunogenicity, tolerance, and suppression. *J Biomed Sci* 2005; **12**: 47-57.
51. Reinders, M. E. J., van Kooten, C., Rabelink, T. J. *et al.* Mesenchymal Stromal Cell Therapy for Solid Organ Transplantation. *Transplantation* 2018; **102**: 35-43.
52. Bernardo, M. E. & Fibbe, W. E. Mesenchymal stromal cells and hematopoietic stem cell transplantation. *Immunol Lett* 2015; **168**: 215-221.

53. Molendijk, I., Bonsing, B. A., Roelofs, H. *et al.* Allogeneic Bone Marrow-Derived Mesenchymal Stromal Cells Promote Healing of Refractory Perianal Fistulas in Patients With Crohn's Disease. *Gastroenterology* 2015; **149**: 918-927 e916.
54. Cakiroglu, F., Osbahr, J. W., Kramer, J. *et al.* Differences of cell surface marker expression between bone marrow- and kidney-derived murine mesenchymal stromal cells and fibroblasts. *Cell Mol Biol (Noisy-le-grand)* 2016; **62**: 11-17.
55. Haniffa, M. A., Collin, M. P., Buckley, C. D. *et al.* Mesenchymal stem cells: the fibroblasts' new clothes? *Haematol-Hematol J* 2009; **94**: 258-263.
56. Haniffa, M. A., Wang, X. N., Holtick, U. *et al.* Adult human fibroblasts are potent immunoregulatory cells and functionally equivalent to mesenchymal stem cells. *J Immunol* 2007; **179**: 1595-1604.
57. Alt, E., Yan, Y. S., Gehmert, S. *et al.* Fibroblasts share mesenchymal phenotypes with stem cells, but lack their differentiation and colony-forming potential. *Biol Cell* 2011; **103**: 197-208.
58. Sakaida, I., Terai, S., Yamamoto, N. *et al.* Transplantation of bone marrow cells reduces CCl4-induced liver fibrosis in mice. *Hepatology* 2004; **40**: 1304-1311.
59. Hu, C., Zhao, L., Duan, J. *et al.* Strategies to improve the efficiency of mesenchymal stem cell transplantation for reversal of liver fibrosis. *J Cell Mol Med* 2019; **23**: 1657-1670.
60. AlAhmari, L. S., AlShenaifi, J. Y., AlAnazi, R. A. *et al.* Autologous Bone Marrow-derived Cells in the Treatment of Liver Disease Patients. *Saudi J Gastroentero* 2015; **21**: 5-10.
61. Alfaifi, M., Eom, Y. W., Newsome, P. N. *et al.* Mesenchymal stromal cell therapy for liver diseases. *J Hepatol* 2018;
62. Barnhoorn, M., de Jonge-Muller, E., Molendijk, I. *et al.* Endoscopic Administration of Mesenchymal Stromal Cells Reduces Inflammation in Experimental Colitis. *Inflamm Bowel Dis* 2018; **24**: 1755-1767.
63. Fiore, E., Malvicini, M., Bayo, J. *et al.* Involvement of hepatic macrophages in the antifibrotic effect of IGF-I-overexpressing mesenchymal stromal cells. *Stem Cell Res Ther* 2016; **7**: 172.
64. Fiore, E. J., Bayo, J. M., Garcia, M. G. *et al.* Mesenchymal stromal cells engineered to produce IGF-I by recombinant adenovirus ameliorate liver fibrosis in mice. *Stem Cells Dev* 2015; **24**: 791-801.
65. Li, Q., Zhou, X., Shi, Y. *et al.* In vivo tracking and comparison of the therapeutic effects of MSCs and HSCs for liver injury. *PLoS One* 2013; **8**: e62363.
66. Eom, Y. W., Shim, K. Y. & Baik, S. K. Mesenchymal stem cell therapy for liver fibrosis. *Korean J Intern Med* 2015; **30**: 580-589.
67. Luo, X. Y., Meng, X. J., Cao, D. C. *et al.* Transplantation of bone marrow mesenchymal stromal cells attenuates liver fibrosis in mice by regulating macrophage subtypes. *Stem Cell Res Ther* 2019; **10**: 16.
68. Najimi, M., Berardis, S., El-Kehdy, H. *et al.* Human liver mesenchymal stem/progenitor cells inhibit hepatic stellate cell activation: in vitro and in vivo evaluation. *Stem Cell Res Ther* 2017; **8**: 131.
69. Shams, S., Mohsin, S., Nasir, G. A. *et al.* Mesenchymal Stem Cells Pretreated with HGF and FGF4 Can Reduce Liver Fibrosis in Mice. *Stem Cells Int* 2015;
70. Wang, J., Bian, C., Liao, L. *et al.* Inhibition of hepatic stellate cells proliferation by mesenchymal stem cells and the possible mechanisms. *Hepatol Res* 2009; **39**: 1219-1228.

71. Siegel, G., Kluba, T., Hermanutz-Klein, U. *et al.* Phenotype, donor age and gender affect function of human bone marrow-derived mesenchymal stromal cells. *Bmc Med* 2013; **11**: 146.
72. Berebichez-Fridman, R. & Montero-Olvera, P. R. Sources and Clinical Applications of Mesenchymal Stem Cells: State-of-the-art review. *Sultan Qaboos Univ Med J* 2018; **18**: e264-e277.
73. Niibe, K., Zhang, M., Nakazawa, K. *et al.* The potential of enriched mesenchymal stem cells with neural crest cell phenotypes as a cell source for regenerative dentistry. *Jpn Dent Sci Rev* 2017; **53**: 25-33.
74. Buhring, H. J., Tremel, S., Cerabona, F. *et al.* Phenotypic characterization of distinct human bone marrow-derived MSC subsets. *Ann N Y Acad Sci* 2009; **1176**: 124-134.
75. Tunon, M. J., Alvarez, M., Culebras, J. M. *et al.* An overview of animal models for investigating the pathogenesis and therapeutic strategies in acute hepatic failure. *World J Gastroentero* 2009; **15**: 3086-3098.
76. Weber, L. W. D., Boll, M. & Stampfl, A. Hepatotoxicity and mechanism of action of haloalkanes: Carbon tetrachloride as a toxicological model. *Crit Rev Toxicol* 2003; **33**: 105-136.
77. van der Helm, D., Groenewoud, A., de Jonge-Muller, E. S. M. *et al.* Mesenchymal stromal cells prevent progression of liver fibrosis in a novel zebrafish embryo model. *Sci Rep* 2018; **8**: 16005.
78. Goessling, W. & Sadler, K. C. Zebrafish: an important tool for liver disease research. *Gastroenterology* 2015; **149**: 1361-1377.
79. Lieschke, G. J. & Currie, P. D. Animal models of human disease: zebrafish swim into view. *Nat Rev Genet* 2007; **8**: 353-367.
80. MacRae, C. A. & Peterson, R. T. Zebrafish as tools for drug discovery. *Nat Rev Drug Discov* 2015; **14**: 721-731.
81. Howe, K., Clark, M. D., Torroja, C. F. *et al.* The zebrafish reference genome sequence and its relationship to the human genome. *Nature* 2013; **496**: 498-503.
82. Tsedensodnom, O., Vacaru, A. M., Howarth, D. L. *et al.* Ethanol metabolism and oxidative stress are required for unfolded protein response activation and steatosis in zebrafish with alcoholic liver disease. *Dis Model Mech* 2013; **6**: 1213-1226.
83. Howarth, D. L., Yin, C., Yeh, K. *et al.* Defining hepatic dysfunction parameters in two models of fatty liver disease in zebrafish larvae. *Zebrafish* 2013; **10**: 199-210.
84. Huang, M., Xu, J. & Shin, C. H. Development of an Ethanol-induced Fibrotic Liver Model in Zebrafish to Study Progenitor Cell-mediated Hepatocyte Regeneration. *J Vis Exp* 2016;
85. Ellis, J. L. & Yin, C. Histological Analyses of Acute Alcoholic Liver Injury in Zebrafish. *J Vis Exp* 2017;
86. Lin, J. N., Chang, L. L., Lai, C. H. *et al.* Development of an Animal Model for Alcoholic Liver Disease in Zebrafish. *Zebrafish* 2015; **12**: 271-280.
87. Amali, A. A., Rekha, R. D., Lin, C. J. *et al.* Thioacetamide induced liver damage in zebrafish embryo as a disease model for steatohepatitis. *J Biomed Sci* 2006; **13**: 225-232.
88. Rekha, R. D., Amali, A. A., Her, G. M. *et al.* Thioacetamide accelerates steatohepatitis, cirrhosis and HCC by expressing HCV core protein in transgenic zebrafish *Danio rerio*. *Toxicology* 2008; **243**: 11-22.

89. Zhang, Y., Xu, H., Chi, X. *et al.* High level of serum Cripto-1 in hepatocellular carcinoma, especially with hepatitis B virus infection. *Medicine (Baltimore)* 2018; **97**: e11781.
90. Strizzi, L., Bianco, C., Normanno, N. *et al.* Cripto-1: a multifunctional modulator during embryogenesis and oncogenesis. *Oncogene* 2005; **24**: 5731-5741.
91. Strizzi, L., Margaryan, N. V., Gilgur, A. *et al.* The significance of a Cripto-1-positive subpopulation of human melanoma cells exhibiting stem cell-like characteristics. *Cell Cycle* 2013; **12**: 1450-1456.
92. Lo, R. C., Leung, C. O., Chan, K. K. *et al.* Cripto-1 contributes to stemness in hepatocellular carcinoma by stabilizing Dishevelled-3 and activating Wnt/beta-catenin pathway. *Cell Death Differ* 2018; **25**: 1426-1441.
93. Zhang, Y., Mi, X., Song, Z. *et al.* Cripto-1 promotes resistance to drug-induced apoptosis by activating the TAK-1/NF-kappaB/survivin signaling pathway. *Biomed Pharmacother* 2018; **104**: 729-737.
94. Bray, F., Jemal, A., Grey, N. *et al.* Global cancer transitions according to the Human Development Index (2008-2030): a population-based study. *Lancet Oncol* 2012; **13**: 790-801.
95. El-Serag, H. B. & Rudolph, K. L. Hepatocellular carcinoma: epidemiology and molecular carcinogenesis. *Gastroenterology* 2007; **132**: 2557-2576.
96. Global Burden of Disease Liver Cancer, C., Akinyemiju, T., Abera, S. *et al.* The Burden of Primary Liver Cancer and Underlying Etiologies From 1990 to 2015 at the Global, Regional, and National Level: Results From the Global Burden of Disease Study 2015. *JAMA Oncol* 2017; **3**: 1683-1691.
97. Li, D., Kang, J., Golas, B. J. *et al.* Minimally invasive local therapies for liver cancer. *Cancer Biology & Medicine* 2014; **11**: 217-236.
98. European Association for the Study of the Liver. Electronic address, e. e. e. & European Association for the Study of the, L. EASL Clinical Practice Guidelines: Management of hepatocellular carcinoma. *J Hepatol* 2018; **69**: 182-236.
99. Wilhelm, S. M., Dumas, J., Adnane, L. *et al.* Regorafenib (BAY 73-4506): a new oral multikinase inhibitor of angiogenic, stromal and oncogenic receptor tyrosine kinases with potent preclinical antitumor activity. *Int J Cancer* 2011; **129**: 245-255.
100. Bruix, J., Raoul, J. L., Sherman, M. *et al.* Efficacy and safety of sorafenib in patients with advanced hepatocellular carcinoma: subanalyses of a phase III trial. *J Hepatol* 2012; **57**: 821-829.
101. Lersritwimanmaen, P. & Nimanong, S. Hepatocellular Carcinoma Surveillance: Benefit of Serum Alfa-fetoprotein in Real-world Practice. *Euroasian J Hepatogastroenterol* 2018; **8**: 83-87.
102. Behne, T. & Copur, M. S. Biomarkers for hepatocellular carcinoma. *Int J Hepatol.* 2012; **2012**: 7.
103. Sauzay, C., Petit, A., Bourgeois, A. M. *et al.* Alpha-foetoprotein (AFP): A multi-purpose marker in hepatocellular carcinoma. *Clin Chim Acta* 2016; **463**: 39-44.
104. Xu, C.-H., Sheng, Z.-H., Hu, H.-D. *et al.* Elevated expression of Cripto-1 correlates with poor prognosis in non-small cell lung cancer. *Tumor Biology* 2014; **35**: 8673-8678.
105. Cocciaferro, L., Miceli, V., Kang, K.-S. *et al.* Profiling cancer stem cells in androgen-responsive and refractory human prostate tumor cell lines. *Annals of the New York Academy of Sciences* 2009; **1155**: 257-262.

106. D'Antonio, A., Losito, S., Pignata, S. *et al.* Transforming growth factor alpha, amphiregulin and cripto-1 are frequently expressed in advanced human ovarian carcinomas. *Int J Oncol* 2002; **21**: 941-948.
107. Giorgio, E., Liguoro, A., D'Orsi, L. *et al.* Cripto haploinsufficiency affects in vivo colon tumor development. *International Journal of Oncology* 2014; **45**: 31-40.
108. Sun, C., Sun, L., Jiang, K. *et al.* NANOG promotes liver cancer cell invasion by inducing epithelial-mesenchymal transition through NODAL/SMAD3 signaling pathway. *The International Journal of Biochemistry & Cell Biology* 2013; **45**: 1099-1108.
109. Fujii, K., Yasui, W., Kuniyasu, H. *et al.* Expression of CRIPTO in human gall bladder lesions *The Journal of Pathology* 1996; **180**: 166-168.
110. Tysnes, B. B., Satran, H. A., Mork, S. J. *et al.* Age-dependent association between protein expression of the embryonic stem cell marker Cripto-1 and survival of glioblastoma patients. *Translational Oncology* 2013; **6**: 732-741.
111. Wang, J. H., Wei, W., Xu, J. *et al.* Elevated expression of Cripto-1 correlates with poor prognosis in hepatocellular carcinoma. *Oncotarget* 2015; **6**: 35116-35128.
112. Gray, P. C. & Vale, W. Cripto/GRP78 modulation of the TGF-beta pathway in development and oncogenesis. *FEBS Lett* 2012; **586**: 1836-1845.
113. Kelber, J. A., Panopoulos, A. D., Shani, G. *et al.* Blockade of Cripto binding to cell surface GRP78 inhibits oncogenic Cripto signaling via MAPK/PI3K and Smad2/3 pathways. *Oncogene* 2009; **28**: 2324-2336.
114. Sun, C., Sun, L., Jiang, K. *et al.* NANOG promotes liver cancer cell invasion by inducing epithelial-mesenchymal transition through NODAL/SMAD3 signaling pathway. *Int J Biochem Cell Biol* 2013; **45**: 1099-1108.
115. Klauzinska, M., Castro, N. P., Rangel, M. C. *et al.* The multifaceted role of the embryonic gene Cripto-1 in cancer, stem cells and epithelial-mesenchymal transition. *Semin Cancer Biol* 2014; **29**: 51-58.
116. Gray, P. C., Shani, G., Aung, K. *et al.* Cripto binds transforming growth factor beta (TGF-beta) and inhibits TGF-beta signaling. *Mol Cell Biol* 2006; **26**: 9268-9278.
117. Steelman, L. S., Chappell, W. H., Abrams, S. L. *et al.* Roles of the Raf/MEK/ERK and PI3K/PTEN/Akt/mTOR pathways in controlling growth and sensitivity to therapy-implications for cancer and aging. *Aging (Albany NY)* 2011; **3**: 192-222.
118. Suk, K. T., Yoon, J. H., Kim, M. Y. *et al.* Transplantation With Autologous Bone Marrow-Derived Mesenchymal Stem Cells for Alcoholic Cirrhosis: Phase 2 Trial. *Hepatology* 2016; **64**: 2185-2197.
119. Du, W., Li, X., Chi, Y. *et al.* VCAM-1+ placenta chorionic villi-derived mesenchymal stem cells display potent pro-angiogenic activity. *Stem Cell Res Ther* 2016; **7**: 49.

CHAPTER 2

2

Local but not systemic administration of mesenchymal stromal cells ameliorates fibrogenesis in regenerating livers

Danny van der Helm, Marieke. C. Barnhoorn, Eveline S.M. de Jonge-Muller, Ilse Molendijk, Luuk J.A.C. Hawinkels, Minneke J. Coenraad, Bart van Hoek*, Hein W. Verspaget*

*Joint senior authorship

Abstract

Background

Chronic liver injury leads to the accumulation of myofibroblasts resulting in increased collagen deposition and hepatic fibrogenesis. Treatments specifically targeting fibrogenesis are not yet available. Mesenchymal stromal cells (MSCs) are fibroblast-like stromal (stem) cells, which stimulate tissue regeneration and modulate immune responses. In the present study we assessed whether liver fibrosis and cirrhosis can be reversed by treatment with MSCs or fibroblasts concomitant to partial hepatectomy (pHx)-induced liver regeneration.

Methods

After carbon tetrachloride-induced fibrosis and cirrhosis, mice underwent a pHx and received either systemically or locally MSCs in one of the two remaining fibrotic/cirrhotic liver lobes. Eight days after treatment, liver fibrogenesis was evaluated by Sirius-red staining for collagen deposition.

Results

A significant reduction of collagen content in the locally treated lobes of the regenerated fibrotic and cirrhotic livers was observed in mice that received high dose MSCs. In the non-MSC-treated counterpart liver lobes no changes in collagen deposition were observed. Local fibroblast administration or intravenous administration of MSCs did not ameliorate fibrosis.

Conclusion

To conclude, local administration of MSCs after pHx, in contrast to fibroblasts, results in a dose-dependent on-site reduction of collagen deposition in mouse models for liver fibrosis and cirrhosis.

Introduction

The liver is an organ with multiple important roles in detoxification, metabolism, immune defence and homeostasis. External factors like viral hepatitis infection, chronic alcohol abuse, non-alcoholic steatohepatitis and metabolic- and cholestatic disease can cause chronic liver damage, leading to hepatic fibrogenesis. This process can eventually result in end-stage liver cirrhosis and liver failure. Fibrogenesis is the result of a complex cellular interplay between apoptotic hepatocytes, inflammatory cells, biliary epithelial cells, Kupffer cells and stellate cells¹⁻³. In this process, apoptotic hepatocytes are thought to induce the activation and increased proliferation of stellate cells and their subsequent differentiation into myofibroblast. These myofibroblasts play a central role in liver fibrosis and are responsible for the characteristic production of excessive amounts of extracellular matrix (ECM)¹⁻³.

To date, curing of the underlying disease is the only treatment for fibrosis. For instance, the case of sustained viral response to treatment for hepatitis C-virus, can lead to reversal of fibrogenesis^{3,4}. Therapeutic drugs or interventions which can specifically target fibrosis or the process of fibrogenesis are not yet available. Orthotopic liver transplantation (OLT) is the only available treatment for end-stage liver cirrhosis^{5,6}. As OLT is a major surgical intervention and medical undertaking with inherent complications and risks and is dependent on patient condition and donor availability, alternative strategies including hepatocyte transplantation and potential anti-fibrotic drugs are being explored⁷⁻⁹.

Mesenchymal stromal cells (MSCs) are fibroblast-like multipotent stromal (stem) cells which can be isolated from bone marrow, adipose tissue and umbilical cord. MSCs expand easily *in vitro* and are not rejected upon transplantation¹⁰⁻¹². Furthermore, MSCs are able to modulate inflammatory responses, and the repair and regeneration of damaged tissues. These characteristics make them attractive candidates for prevention and treatment of liver fibrosis where these specific processes need to be restored in order to reverse fibrogenesis¹¹⁻¹³. Currently, MSCs have been tested in clinical trials with promising, but also sometimes ineffective, results regarding the reversal of fibrosis, cirrhosis and end-stage liver disease¹⁴⁻¹⁶. Several working mechanisms of MSCs have been proposed, including their ability to differentiate into hepatocytes, to stimulate the protection and survival of liver resident cells, to inhibit the activation of stellate cells and to silence the myofibroblasts^{11,17-20}. However, the exact mechanisms of action of MSCs in reducing liver fibrosis are still unknown.

Previous studies in mice and zebrafish embryos showed that MSCs are able to prevent chemically induced hepatic fibrosis when administered simultaneously with the causative agent²¹⁻²⁴. Some other *in vivo* studies showed that MSCs are also effective to treat carbon tetrachloride (CCL4) established fibrosis¹⁵. MSCs are fibroblast-like cells with several functions and characteristics similar to fibroblasts. Some studies claim that fibroblasts, like MSCs, have the same capacity

to suppress the immune system and that they also play a role in tissue repair²⁵⁻²⁷. However, no studies have been reported comparing both cell types in relation to liver fibrosis.

The liver has a high regenerative capacity upon tissue damage, for example after resection or because of hepatotoxic substances^{4,17,28,29}. None of the published studies combined MSC therapy with this regenerative capacity of the liver. Therefore, we explored if the combination of the intrinsic regeneration capacities of the liver and the pro-regenerative and anti-inflammatory capacities of MSC therapy could ameliorate liver fibrogenesis.

As also mentioned by Hu et al, results from literature are difficult to compare as there are multiple differences in study design such as disease aetiology, disease stage and the administration route and dosage and source of MSCs, which possibly all could affect the outcome of these studies³⁰. Therefore, in the present study, for the first time, the effects of different administration routes of MSCs (local vs iv), different disease stages (fibrosis vs cirrhosis) and different MSC dosages were evaluated and compared in the same study. Furthermore, we compared the therapeutic potential of MSCs and fibroblasts in a novel treatment strategy where mice with CCL4-induced fibrosis and cirrhosis underwent a partial hepatectomy (pHx), as regeneration stimulus, and received concomitant cell therapy. We suggested that specifically administration of MSCs in regenerating fibrotic and cirrhotic livers would be able to ameliorate fibrogenesis.

Material and Methods

MSC and fibroblast isolation, culturing and characterisation

Bone marrow-derived MSCs and liver-derived fibroblasts were isolated from 10-week-old actin-GFP C57Bl/6Jico mice obtained from an LUMC breeding population³¹. In short, mice were killed by cervical dislocation and the liver, femur, tibia and humerus were collected. For MSC isolation, bones were cleaned from tissue and flushed with RPMI medium supplemented with 10% foetal calf serum (FCS; Gibco, Paisley, UK), 3 mmol/L L-glutamine (Invitrogen Corp., Paisley, UK), penicillin/streptomycin (P/S; Invitrogen Corp., Paisley, UK) and 2% Heparin (Pharmacy LUMC, Leiden, The Netherlands). Collected cells were cultured in α MEM culture medium (Lonza, BE12-169F) supplemented with 10% FCS, 3 mmol/L L-glutamine and P/S (complete culture medium). After 24, 48 and 72 hours non-adhering cells and cell debris were removed. To isolate fibroblasts, livers were cut in small parts and incubated with LiberaseTM LT (Roche, Basel, Switzerland) for 30 minutes at 37°C. Next, the cell suspension was washed and subsequently cultured in DMEM/F12 culture media supplemented with 10% foetal calf serum, P/S, HEPES buffer solution and gentamicin (both Gibco). Cultured cells were used until passage 8-10. Cells were monthly tested for mycoplasma contamination. Isolated cells were

characterized by the expression of membrane markers and their ability to differentiate into osteoblasts and adipocytes (Supplementary Material).

Fibrotic and cirrhotic mouse model

All mice received food and water ad libitum and were housed in individually ventilated cages. All animal experiments were approved by the animal ethics committee of the Leiden University Medical Center. For the fibrotic and cirrhotic models 6-week-old male C57Bl/6Jico mice (Charles River Laboratories, The Netherlands) were used. For fibrosis induction, mice received three intraperitoneal (ip) CCL4 injections (100 µg/kg body weight) per week for 6 weeks (Sigma-Aldrich Chemie BV, Zwijndrecht, The Netherlands) (Supplemental Figure 1A). For induction of cirrhosis, mice were treated for 11 weeks with two initial doses of 200 µg/kg body weight CCL4, followed by a twice weekly 150 µg/kg body weight CCL4 ip injection for 10 weeks (Supplemental Figure 1B). All CCL4 injections were diluted to an injection volume of 50 µL with mineral oil (Sigma-Aldrich Chemie BV, Zwijndrecht, The Netherlands). After 6 weeks (fibrosis) or 11 weeks (cirrhosis) a pHx was performed, as described previously by Anderson and Higgins³². In short, animals were anaesthetized and the two median and the left lateral lobes were ligated and removed (50%-70% of the liver, Supplemental Figure 1C). Next, mice were randomly divided into four groups and were locally treated with vehicle (saline), 1 x 10⁶ or 2 x 10⁶ MSCs or 2 x 10⁶ fibroblasts divided over five spots in one of the remaining liver lobes (lobe 5, Supplemental Figure 1C). The tail vein administration group received 1 x 10⁶ MSCs one day before and one day after pHx (2 x 10⁶ MSCs in total). This group received two injections of 1 x 10⁶ MSCs as higher systemic dosages led to too high numbers of animal loss. Two groups with fibrosis did not undergo pHx and received no further treatment or received local administration of 2 x 10⁶ MSCs. Eight days after pHx, the mice were killed and livers were resected, weighted and fixated for paraffin embedding and stored for protein isolation.

Transaminase levels

Blood from the tail vein was collected before the start of CCL4 administration, the day before pHx and 8 days after pHx (Supplemental Figure 1A,B). Alanine aminotransferase (ALT) and aspartate aminotransferase (AST) serum levels were measured with Reflotron equipment (Roche diagnostics GmbH, Mannheim, Germany) according to the manufacturers' instructions.

TNF-α measurement

Liver homogenates were made with a Potter-Elvehjem glass homogenizer at 4°C in Greenberger lysis buffer. Homogenates were centrifuged (15 minutes, 11 000 g, 4°C) and stored at -80°C. BCA Protein Assay Kit (Thermo Scientific Pierce, Etten-Leur, The Netherlands) was used to measure total protein content in the homogenates. TNF-α protein levels were measured using the Cytometric Bead Array System (BD Biosciences, San Diego, CA, USA) according to the manufacturer's instructions. Data analysis was performed with FlowJow software. TNF-α levels were corrected for the total amount of extracted protein.

Histological examination

Paraffin sections of 4 μm were cut, rehydrated and stained for 90 minutes with 1 g/L Sirius-red (Klinipath Sirius F3B) in picric acid (Klinipath) to visualize collagen deposition. Next, slides were cleared with 0.01 mol/L HCl, washed, dehydrated and mounted with Entellan (Merck KGaA, Darmstadt, Germany). Collagen deposition was quantified by taking 5-8 random images (10 \times magnifications) of Sirius-red stained sections with fixed microscopy settings. Subsequently, the amount of staining was quantified with ImageJ (ImageJ 1.47v, National Institutes of Health, USA) and the reduction of collagen content in the liver, relative to the resected pHx tissue, calculated.

Lobuli closure was used as a second measure of fibrosis and cirrhosis and was performed blindly by two independent observers. In short, the liver is organized in lobuli with a hexagonal figure consisting of six portal triads with one central vein in the middle. In a fibrotic liver the excessive collagen is secreted into the space between the portal triads and forms septa. When fibrogenesis is sustained for a longer period, the septa will grow and eventually bridge the space between the portal triads, which correlates with a more severe fibrosis and finally cirrhosis (Supplemental Figure 2 for lobuli closure scoring method).

Immunohistochemistry

For the staining of green fluorescent protein (GFP) and α -smooth muscle actin (α -SMA), paraffin-embedded tissue sections were rehydrated, and endogenous peroxidases were blocked with 0.3% H₂O₂/methanol followed by a 10-minutes boiling citrate antigen retrieval (pH6). Next, sections were blocked with 2% horse serum in PBS containing 0.1% Triton X-100 and 1% bovine serum albumin. Primary antibodies for GFP (Rockland, cat 600101215), and α -SMA (Progen, Heidelberg, Germany, cat 61001) were incubated overnight. The next day, slides were incubated with a peroxidase-labelled polymer (EnVision+, Dako Netherlands BV, Heverlee, Belgium) after which the staining was visualized with 3,3'-diaminobenzidine (DAB Fast Tablet, Sigma-Aldrich, St. Louis, MO). After nuclear counterstaining with haematoxylin, slides were dehydrated and mounted with Entellan.

Statistical Analysis

Student's *t* test was used to compare two groups. For comparison of three or more groups one-way ANOVA was used followed by Dunnett's multiple comparison tests. The results are presented as mean \pm standard error of the mean (SEM). Statistical tests were performed with GraphPad Prism software (GraphPad Software, version 5.01, San Diego, CA). *P* < 0.05 were considered as statistically significant.

Results

Characterization of MSCs and fibroblasts

Flow cytometry revealed that the MSCs were positive for the MSC membrane markers: CD29, CD105, CD106, SCA-1, CD44 and negative for haematopoietic marker CD45 and endothelial marker CD31 (Supplemental Figure 3A). Fibroblasts showed a similar expression pattern, except for SCA-1 that was not detected in the fibroblasts (Supplemental Figure 3B). Further characterization revealed that MSCs showed adipogenic and osteoblastic differentiation potential (Supplemental Figure 4). Fibroblasts were able to differentiate into adipocytes but did not differentiate into osteoblasts (Supplemental Figure 4). Taken together these data indicate that the MSCs fulfilled the criteria for MSCs, whereas the fibroblasts did not.

CCL4-induced liver fibrosis and cirrhosis in mice

For the present study, mouse models representing fibrotic and cirrhotic disease stage were generated by CCL4 administration. During the first 6 weeks of CCL4 treatment, cirrhotic mice had a significantly lower body weight compared to the fibrotic mice (Figure 1A). After the induction of fibrosis and cirrhosis three liver lobes were resected and used to evaluate the severity of fibrogenesis. TNF- α levels in the liver, as a marker for inflammation, were significantly higher in mice with cirrhosis compared to mice with fibrosis or a healthy liver (Figure 1B). Sirius-red staining of the resected fibrotic and cirrhotic liver tissue showed significantly increasing levels of collagen deposition and lobuli closure indicative for progressive fibrogenesis in these groups respectively (Figure 1C-E). Furthermore, morphological cell analysis of H&E staining of the tissues illustrated increased numbers of myofibroblasts and infiltrating lymphocytes in the septa between the portal triads in these respective groups (Figure 1C, white arrows). The day before pHx, aminotransferase levels were measured. Alanine transaminase and aspartate transaminase serum levels were increased upon CCL4 injury and reached higher levels in cirrhotic mice, compared to fibrotic or healthy mice respectively (Figure 1F,G). Because of the toxicity and prolonged exposure of CCL4, more mice had to be prematurely killed during the induction of cirrhosis (40%) compared to the induction of fibrosis (17%). In combination, these results indicate that mice in the cirrhosis group had more severe liver damage at time of pHx, compared to the mice in the fibrosis group. These observations represent the starting point for the MSCs treatment experiments.

Systemically administrated MSCs did not further improve the pHx initiated reversal of fibrosis

To address the potential of MSCs to reverse liver fibrosis, MSCs were systemically administered by tail vein injection. One group of CCL4-treated mice received MSCs iv One day prior to and 1 day after pHx (pHx + ivMSC), the other group had only a pHx and the last group received no treatment (natural recovery after CCL4). In the first 2 days after surgery, the mice in the pHx and pHx + ivMSC group seemed to lose slightly but not significantly more weight as

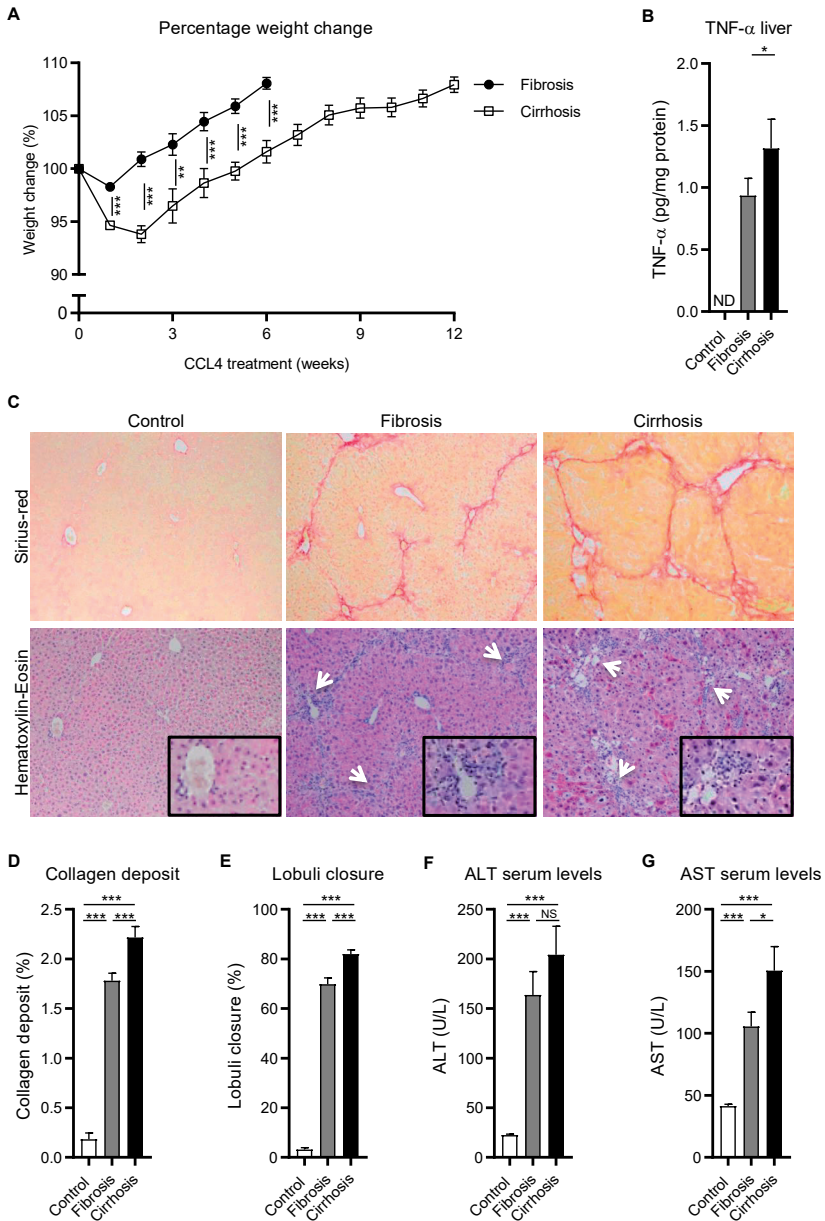


Figure 1. CCL4-induced liver fibrosis and cirrhosis in mice. A, Normalized body weight during the induction of fibrosis and cirrhosis (N = 25). B, TNF- α levels in healthy and resected liver tissues (N = 8). C, Sirius-red and Haematoxylin-eosin stained healthy, fibrotic and cirrhotic liver tissue (20x magnifications, inserts 40x magnifications). D, Quantified collagen deposit of Sirius-red stained sections (N = 25). E, Estimated lobuli closure of Sirius-red stained sections (N = 25). F and G, ALT and AST serum levels of healthy (N = 35), fibrotic (N = 30) and cirrhotic animals (N = 38). Data are expressed as mean \pm SEM. * $P \leq 0.05$, ** $P \leq 0.01$, *** $P \leq 0.001$. ALT, alanine aminotransferase; AST, aspartate aminotransferase; CCL4, carbon tetrachloride; ND, not detectable; NS, not significant

compared to the group that received no treatment (Figure 2A). After 8 days, no differences in body weights were observed. After regeneration, livers were collected, weighted and stained for collagen by Sirius-red staining. The pHx + ivMSC-treated mice had relatively smaller livers compared to the pHx group and to the no treatment group (Figure 2B). In order to compensate for the resected liver volume, the non-resected, remaining liver lobes had grown (lobes 4 and 5 in Supplemental Figure 1C, Figure 2C-E, white arrows). After regeneration, no differences in relative weights of these remaining liver lobes between the pHx and pHx + ivMSC groups were observed (Figure 2D). The remnant parts of the resected liver lobes remained small and did not regenerate (white arrowheads, Figure 2C,E).

The Sirius-red staining showed that the pHx significantly reduced the total collagen deposition, independently of the iv administered MSCs (72% and 73% reduction, Figure 2F,G). Scoring based on lobuli closure resulted in a corresponding trend towards less closure of the pHx (23%) and pHx + ivMSCs (29%) group compared to the no treatment (41%) group (Figure 2H).

Altogether, these data showed that only a pHx already leads to a considerable reduction in the collagen content of the regenerating livers and that the ivMSC treatment does not have an additional effect on this collagen reduction.

Local administration of MSCs during pHx reduces collagen content of regenerating livers in a fibrotic mouse model, whereas fibroblast administration does not

Next, we assessed whether local MSC therapy could enhance the effect of the pHx-induced collagen reduction. Therefore, MSCs were locally injected underneath the liver capsule in one of the remaining lobes after pHx (Supplemental Figure 1C). As a control, one group of mice received local MSC therapy without pHx. After pHx, the 1×10^6 and 2×10^6 MSC groups lost slightly but not significantly more weight compared to the vehicle control group (Figure 3A). Mice that received only local MSC therapy did not lose body weight after treatment. At the end of the experiment no differences in body weight and relative liver weight were observed and livers were fully regenerated in all groups (Figure 3A-C). The groups that received pHx showed bigger liver lobes compared to the corresponding lobes of the group that only received local MSC treatment (Figure 3C). In addition, no differences in serological ALT and AST levels were observed (Supplemental Figure 5A,B).

Sirius-red stained liver tissue showed that 2×10^6 MSC treatment without pHx had led to more reduction of collagen content compared to no treatment but less reduction compared to mice that received pHx + vehicle (Figure 2G and 3E). Furthermore, the reduction of collagen deposition in mice that received pHx and MSCs was related to the number of administered MSCs. Collagen reduction was higher in pHx + 2×10^6 MSC (80%)-treated animals compared to the pHx + 1×10^6 MSC (77%) and pHx + vehicle (71%) group respectively (Figure 3D,E).

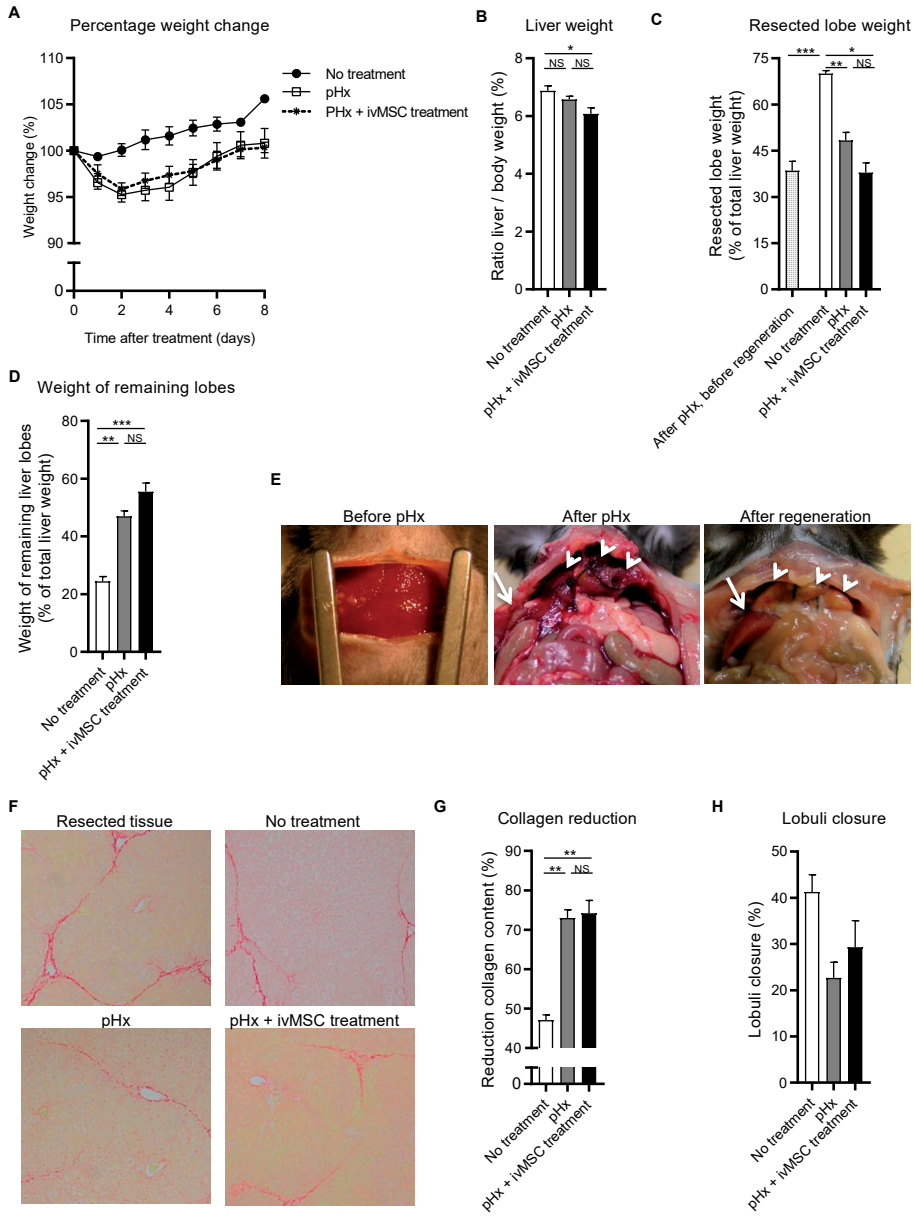


Figure 2. Systemically administrated MSCs did not further improve the pHx initiated reversal of fibrosis. Mice with liver fibrosis received no treatment, pHx or pHx + ivMSC (N = 6/9 per group). A, Normalized body weight during regeneration. Relative weights of (B) total liver, (C) remnant parts of the resected lobes and (D) remaining lobes after regeneration. E, Pictures of the liver before pHx, after pHx and after regeneration. Remnant and remaining lobes are indicated with white arrow heads and white arrows respectively. F, Sirius-red stained liver tissue (20x magnifications) (G) Reduction of Sirius-red staining relative to resected tissue. H, Estimated lobuli closure. Data are expressed as mean \pm SEM. * $P \leq 0.05$, ** $P \leq 0.01$, *** $P \leq 0.001$. MSCs, mesenchymal stromal cells; pHx, partial hepatectomy; NS, not significant

No differences in the reduction of collagen content in the non-treated liver lobes between the same three groups of mice were observed, suggesting an on-site effect of MSCs in this model. When pHx + vehicle and pHx + ivMSC treatment were compared to the pHx + local administration of 2×10^6 MSCs, we concluded that local administration of MSCs enhanced the pHx-induced reduction of collagen deposition (72%, 73% vs 80%, Figures 2G and 3E). No significant difference in lobuli closure was observed (Figure 3F).

Next, the ability of liver fibroblasts to modulate the regenerative process was examined. In this experiment, CCL4-treated mice underwent a pHx with or without local fibroblast treatment. At the end of the experiment no differences in body weight and relative liver weight were observed in mice which received fibroblasts compared to control mice which received vehicle (Figure 4A-C). Also Sirius-red staining in these fibroblast experiments did not show differences in collagen reduction or lobuli closure (Figure 4D,E). Overall, these results indicate that local injection with MSCs, in contrast to local injection with fibroblasts, seems to enhance the effect on collagen reduction of the pHx initiated liver regeneration.

Local MSC treatment reduced the amount of collagen deposition in a mouse model for liver cirrhosis

Subsequently, we evaluated if the observed therapeutic effect could also be reached in a more severe disease stage of fibrosis, that is, liver cirrhosis. After regeneration, slightly lower body weight was observed in the 1×10^6 MSC group compared to the other groups (Figure 5A). After killing, livers and the individually separated liver lobes showed no differences in relative weight between the different treatment groups (Figure 5B,C). Furthermore, TNF- α expression levels in the liver were below the detection limits in all samples (data not shown) and ALT and AST serum levels reached healthy baseline levels in all treatment groups (Supplemental Figure 5C,D).

Sirius-red stained tissue sections showed a significant relative reduction of collagen content in the locally treated liver lobe of the 2×10^6 MSC treatment group (82%) compared to pHx + vehicle control group (71%). The 1×10^6 MSC group reached an intermediate reduction of collagen deposition (76%, Figure 5D,E). More collagen reduction in the locally treated lobe (82%) vs the untreated counterpart (75%) in 2×10^6 MSC group was observed (Figure 5E). The untreated liver lobes showed no differences between the different treatment groups, again indicating a local effect of the MSCs. Furthermore, lobuli closure showed a trend towards less closure in the 2×10^6 MSC group, but this did not reach statistical significance. Also, no differences in lobuli closure between the untreated counterparts were observed further suggesting the importance of local MSC treatment (Figure 5F).

At the end of the experiment, locally administered GFP-expressing MSCs were traced at the injection site. Haematoxylin and eosin staining of regenerated liver tissue shows the well

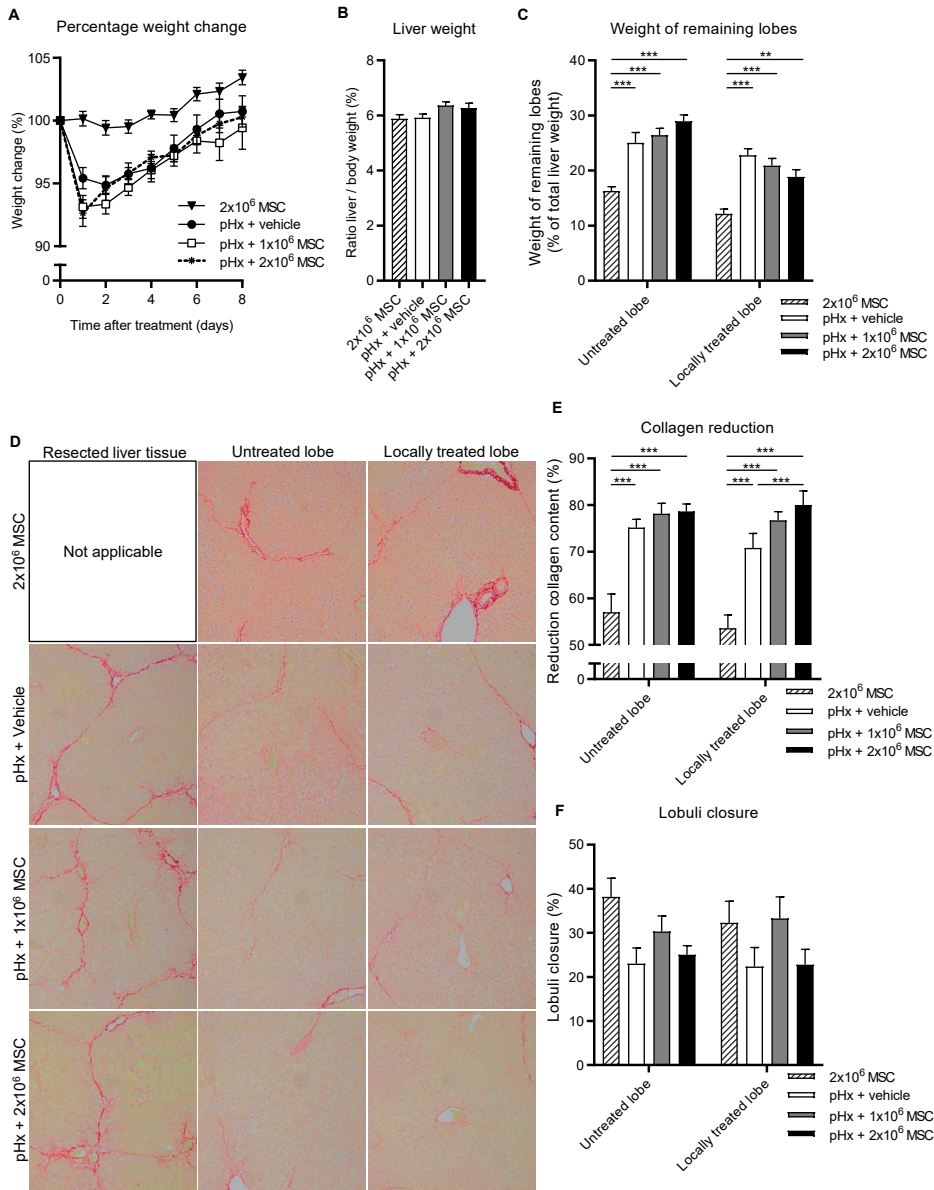


Figure 3. Local administration of MSCs during partial hepatectomy reduces collagen content of regenerating livers in a fibrotic mouse model. After induction of fibrosis mice received local 2×10^6 MSC treatment or underwent pHx and local treatment with vehicle, 1×10^6 or 2×10^6 MSCs (N = 15 per group). A, Normalized body weight during regeneration. B, Normalized liver weight and (C) relative weights of treated and untreated lobes as percentage liver after regeneration. D, Sirius-red stained sections of resected, untreated and treated remaining liver lobe tissue of the different treatment groups (20x magnifications). E, Reduction of Sirius-red staining relative to resected tissue. F, Estimated lobuli closure. Data are expressed as mean \pm SEM. $**P \leq 0.01$, $***P \leq 0.001$. MSCs, mesenchymal stromal cells; pHx, partial hepatectomy

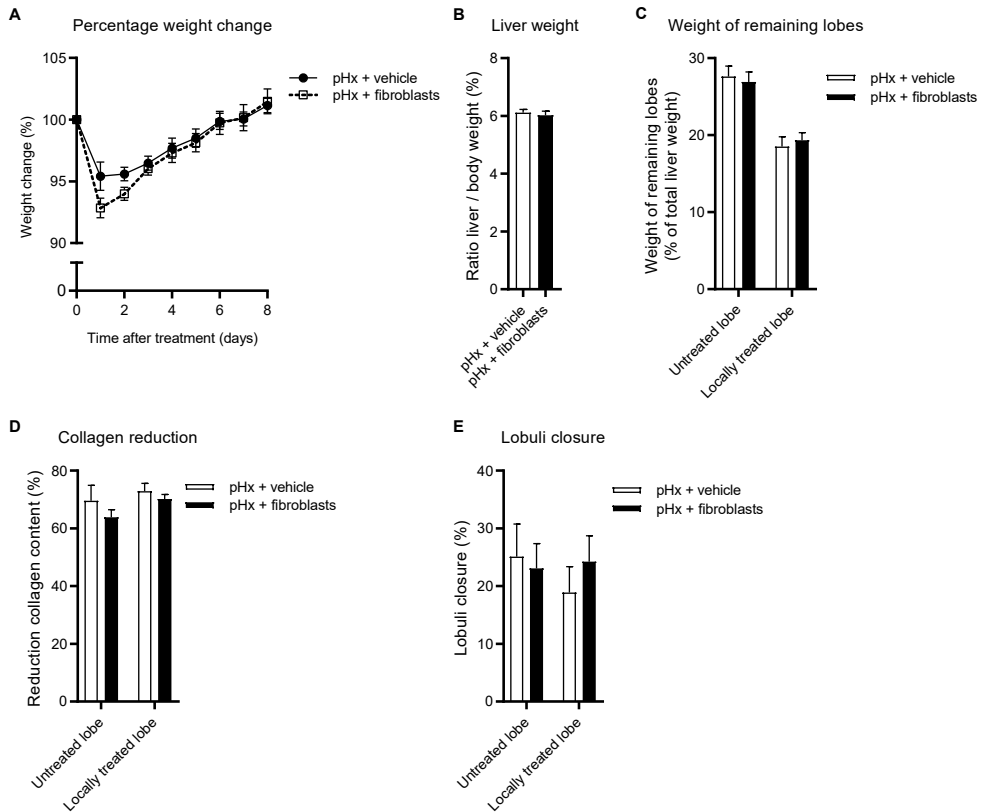


Figure 4. Fibroblasts are unable to resolve fibrosis in regeneration mouse livers. After fibrosis induction, mice underwent pHx and received local administration of vehicle or 2×10^6 fibroblasts ($N = 9$ group size). A, Normalized bodyweight during regeneration (B) Normalized liver weight and (C) relative treated and untreated lobe weights as percentage liver after regeneration (D) Reduction of Sirius-red staining relative to resected tissue. E, Estimated lobuli closure. Data are expressed as mean \pm SEM. pHx, partial hepatectomy; SEM, standard error of the mean

organized liver structure with hepatocyte plates. MSC regions were characterized by less well organized regions with few to no hepatocytes and multiple elongated, GFP- and α -SMA-positive cells, all indicative for MSCs (Figure 6, black arrows). MSCs were not observed outside these regions indicating that MSCs exert their anti-fibrotic or pro-regenerative effects from the injection site and do not migrate through the tissue. Altogether these results indicate an on-site dose-dependent effect of locally administered MSCs on collagen reduction in regenerating cirrhotic livers.

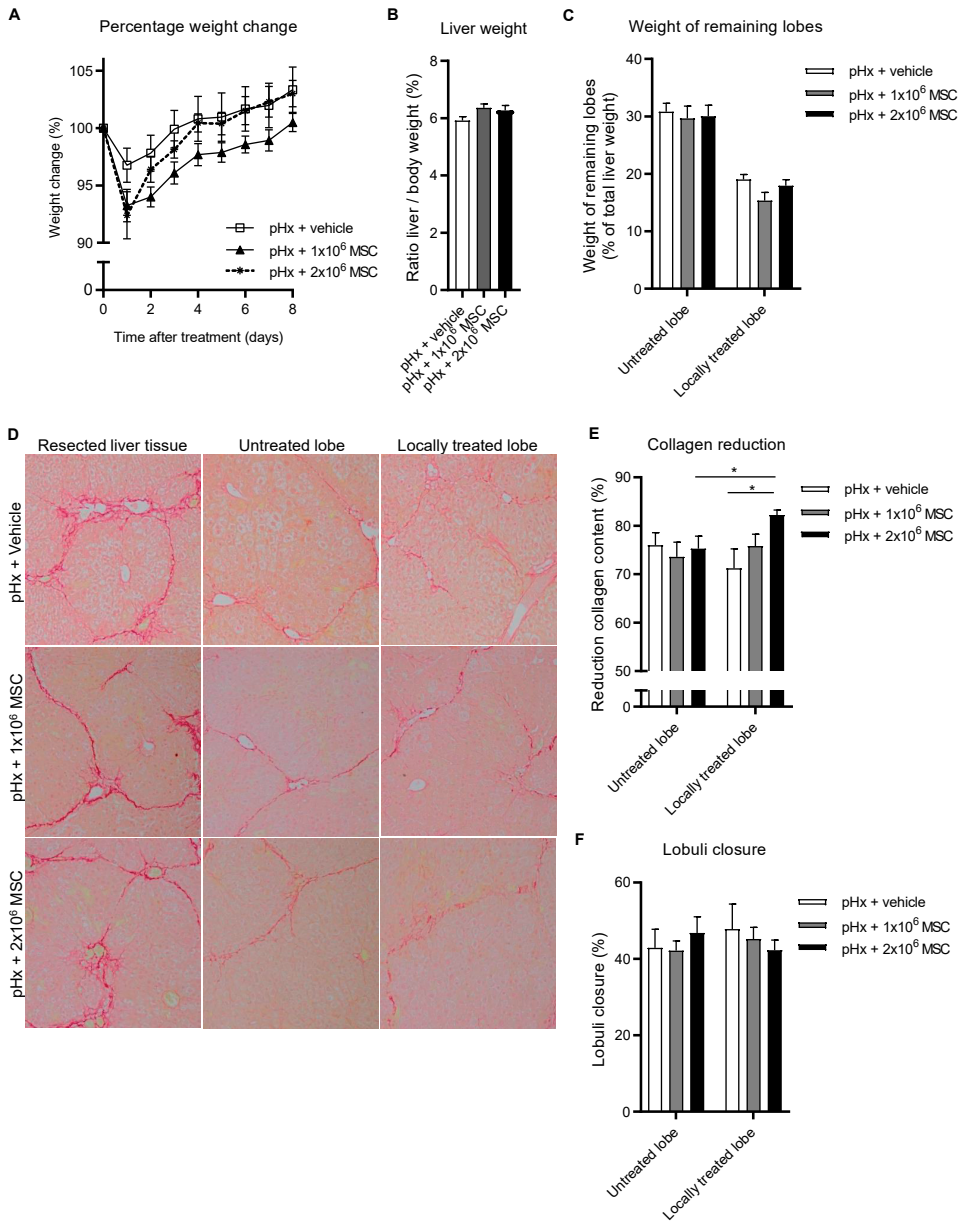


Figure 5. MSCs significantly decrease collagen deposition in a mouse model for liver cirrhosis. Mice with liver cirrhosis were treated by pHx and local administration of vehicle, or 1×10^6 or 2×10^6 MSCs (N = 8/10 group size). A, Normalized bodyweight during regeneration (B) Normalized liver weight and (C) relative treated and untreated lobe weights as percentage liver after regeneration (D) Sirius-red stained sections of resected, untreated and treated remaining liver lobe tissue of the different treatment groups (20x magnifications). E, Reduction of Sirius-red staining relative to resected tissue. F, Estimated lobuli closure. Data are expressed as mean \pm SEM. * $P < 0.05$. MSCs, mesenchymal stromal cells; pHx, partial hepatectomy

Discussion

In the present observational study, the therapeutic efficacy in counteracting liver fibrogenesis by MSC or fibroblast therapy was tested in regenerating livers of mice with fibrosis or cirrhosis. Different dosages and administration routes of MSCs were evaluated to find the optimal therapy. Our data showed that local MSC treatment in combination with a pHx, as regeneration stimulus, dose dependently reduces collagen content in both a fibrotic and in a cirrhotic mouse model, while local administration of liver fibroblasts and systemic intravenous MSC administration had no effect. The locally administered MSCs were traced at the injection site from where they are thought to exert their function and locally reduce the collagen content in the regenerating livers.

Various studies used the CCL4-based mouse models to evaluate potential therapeutic interventions, but they differ in the dose, frequency and duration of CCL4 administration, leading to differences in illness between studies and sometimes opposing results³³. In the present study, we established, described and compared chronic CCL4-induced mouse models for liver fibrosis and cirrhosis in detail. At time of pHx, cirrhotic mice as compared to fibrotic mice had more liver damage based on lobuli closure, collagen deposit, aminotransferase levels and TNF- α expression, indicating a more severe disease stage.

Several studies previously evaluated the ability of MSCs as potential treatment in fibrotic and cirrhotic animal models^{15,20,23,34}. In line with these earlier studies, our results showed increased reduction of collagen levels upon MSC treatment. However, none of these previous studies included the regenerative response initiated by a pHx. In the present study, we aimed to enlarge the effect of MSC treatment by stimulating liver regeneration by performing a pHx. Our results showed that a pHx as such already leads to a reduction of collagen content and improve the effect of local MSC treatment and vice versa.

Beneficial characteristics of MSCs for reversing fibrosis and improving liver function include their ability to differentiate into hepatocytes, to stimulate proliferation and survival of resident liver cells, their immunosuppressive capacity and their ability to silence the collagen-producing myofibroblasts^{11,17,18,20,34-36}. The precise working mechanisms are still unknown but probably are because of the combined action of these characteristics. In our study, an enhanced liver regeneration based on relative liver weights, in the mice treated with local MSC therapy, was not observed. These results indicate that the observed effect of local MSC treatment on relative collagen content is because of collagen reduction and not only to the regeneration of resident liver cells. Other studies have shown that the enhanced regeneration owing to MSC treatment could be observed at day 3¹⁷. We examined the livers at day 8, and one could argue that this might be too late to find differences in liver weights as all livers were already fully regenerated at this time-point.

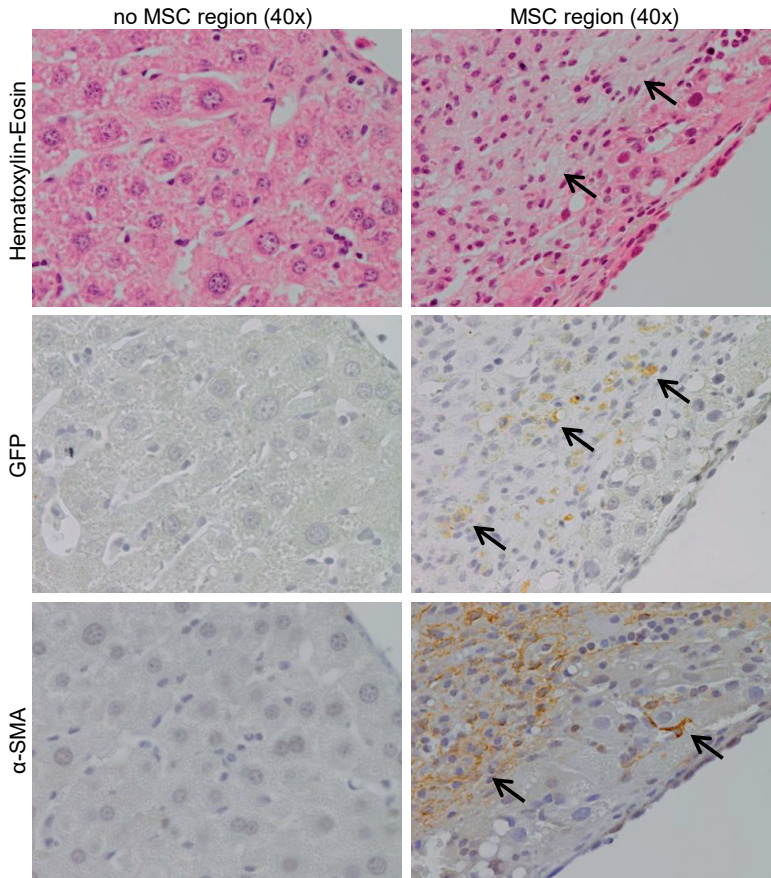


Figure 6. MSCs are traced in special organized regions. MSC regions and normal regions in regenerated liver tissue of cirrhotic mice treated with pHx + 2×10^6 MSC stained for Haematoxylin-eosin, GFP and α -SMA (40x magnifications, MSCs are indicated by the black arrows). GFP, green fluorescent protein; α -SMA, smooth muscle actin; MSCs, mesenchymal stromal cells; pHx, partial hepatectomy

In the present study, we did not find beneficial effects of iv administered MSCs. MSCs can easily get trapped in the lungs, which leads to fewer cells homing to the liver¹⁸. This might be a possible explanation for the absence of an effect of iv administered MSCs. In contrast to iv MSC administration, local MSC administration in the liver during pHx did lead to more pronounced reduction of collagen deposition. Locally MSC-treated lobes, when compared to the untreated counterparts, show a beneficial on-site effect of MSCs, whereas no remote effect of MSCs was observed in the untreated counterparts. To our knowledge this is the first study describing this on-site effect and could also further explain why the iv MSC treatment was ineffective. Particularly in the cirrhotic model the locally treated liver lobes of the pHx + 2×10^6 MSC group reached significantly more reduction in collagen content compared to the untreated counterparts, underlining the importance of the local administration of MSCs.

Thus, in general, a dose-response effect between untreated, pHx, pHx + 1×10^6 and pHx + 2×10^6 MSCs was observed in the fibrotic and cirrhotic models. Furthermore, as described in previous studies, we observed that local MSC treatment leads to more reduction of collagen but in addition we showed that this effect can be improved by initiating a regenerative response by pHx.

The present study also compared MSCs and fibroblasts in their ability to resolve fibrosis. Studies by Haniffa et al showed that MSCs are fibroblast-like cells with similar functions in immunosuppression and tissue repair²⁵. These studies, however, are not related to liver disease and focussed on basic mechanistic in vitro studies^{25,26,37}. We showed that MSCs and fibroblasts similarly express several membrane markers and both have adipogenic differentiation ability. In addition we found that MSCs, in contrast to fibroblasts, are positive for SCA-1 and are able to differentiate into osteoblasts. These differences are also described by Cakiroglu et al who also demonstrate that fibroblasts are negative for SCA-1³⁸. Furthermore, the present study revealed that MSCs but not the fibroblasts were able to reverse fibrogenesis in regenerating livers. These observations illustrate the unique phenotypical and functional features of MSCs. Fibroblasts may be considered as myofibroblast-like cells and, therefore, might be expected to severe the fibrosis. In the present study fibroblasts were, however, administered after the induction of fibrosis and were not exposed to activation stimuli and, therefore, probably remained inactivated. Furthermore, cells were injected during pHx which initiated liver regeneration. Altogether, this might explain why administration of fibroblasts did not lead to more severe fibrosis. The question remains how this local MSC treatment could reduce the collagen content in these regenerating livers. Hepatocyte differentiation of MSCs is one of the suggested working mechanisms of MSC therapy in literature^{15,16,39}. However, one could argue that MSC differentiation might affect the process of fibrogenesis. MSCs, which are differentiated into hepatocyte-like cells, are known to improve liver function but are less able to affect the resolution of fibrogenesis. Therefore, we speculate that hepatocyte differentiation is not the driving mechanism for the observed collagen reduction in the present study.

Parekkadan et al proposed that a reduction in proliferation of stellate cells and silencing of myofibroblasts was because of cytokines (IL-10, HGF, VEGF and IGF-1) secreted by MSCs leading to less ECM production in the liver^{20,40,41}. Previous results from our group, using the same murine MSCs, also showed expression of these pro-regenerative and anti-fibrotic cytokines^{24,42}. In literature, it was also suggested that the effect of MSC treatment depends on myofibroblast/MSC ratio, which might pose an explanation for the dose dependency²⁰. Altogether, it is highly suggestive that paracrine secretion of cytokines such as HGF and IGF-1 by the MSCs directly target the process of fibrogenesis and might explain the observed collagen reduction. However, further in-depth studies are needed to assess these suggested mechanisms.

Our study showed that different results between previous studies of MSC therapy might be explained by the use of different study designs. Variables like disease stage, MSC dosage, route of administration and even the local effect in the liver might explain these different and sometimes contradictory outcomes³⁰. For example, clinical studies mostly focus on systemic administration of MSCs. The present study showed that local MSC treatment had an on-site therapeutic effect while iv treatment was ineffective. Because of this finding, one could speculate that the effect of MSCs in patients could be enlarged when MSCs are locally administered at multiple injection sites over the liver combined with a trigger for regeneration by a pHx comparable as to the treatment of perianal fistulas in Crohns disease⁴³. The set-up of this observational study was to evaluate the effects of different study designs of MSC therapy on the reversal of fibrogenesis at the end of the regenerating process. In the present study, the most optimal MSC therapy was identified but owing to the observational nature of the study we did not assess the underlying working mechanisms. A follow-up study where mice are sacrificed at multiple time-points during the regeneration process is needed to unravel the underlying working mechanism of this novel MSC therapy. Possible effects on proliferation of endogenous liver cells need to be examined at an earlier time-point, because in the present study all the livers are already fully regenerated. Furthermore, as portal infusion is comparable to local administration one might speculate that portal infusion also has a functional effect that might be considered for clinical use. However, this administration route was not tested because it was impossible to perform a portal infusion of MSCs in mice.

In conclusion, our data show that local administration of MSCs in combination with pHx enhances reduction of relative collagen content in regenerating livers. This observation might potentially lead in the future to an attractive novel treatment strategy of patients with liver fibrosis and cirrhosis.

Acknowledgements

This work was supported by the Dutch Digestive Foundation (project number: WO 10-84). Furthermore, we thank the staff of the central animal facility of the LUMC for animal care.

Conflict of interest

The authors confirm that there are no conflicts of interest.

Data Availability Statement

The data that support the findings of this study are available from the corresponding author upon reasonable request.

Reference List

1. Bataller, R. & Brenner, D. A. Liver fibrosis. *J Clin Invest* 2005; **115**: 209-218.
2. Friedman, S. L. Mechanisms of hepatic fibrogenesis. *Gastroenterology* 2008; **134**: 1655-1669.
3. Lee, Y. A., Wallace, M. C. & Friedman, S. L. Pathobiology of Liver Fibrosis—A Translational Success Story (vol 64, pg 830, 2015). *Gut* 2015; **64**: 1337-1337.
4. Marcellin, P., Gane, E., Buti, M. *et al.* Regression of cirrhosis during treatment with tenofovir disoproxil fumarate for chronic hepatitis B: a 5-year open-label follow-up study. *Lancet* 2013; **381**: 468-475.
5. Liver, E. A. S. EASL Recommendations on Treatment of Hepatitis C 2016. *J Hepatol* 2017; **66**: 153-194.
6. Mathurin, P., Hadengue, A., Bataller, R. *et al.* EASL Clinical Practical Guidelines: Management of Alcoholic Liver Disease. *J Hepatol* 2012; **57**: 399-420.
7. Angaswamy, N., Tiriveedhi, V., Sarma, N. J. *et al.* Interplay between immune responses to HLA and non-HLA self-antigens in allograft rejection. *Hum Immunol* 2013; **74**: 1478-1485.
8. Lucidi, V., Gustot, T., Moreno, C. *et al.* Liver transplantation in the context of organ shortage: toward extension and restriction of indications considering recent clinical data and ethical framework. *Curr Opin Crit Care* 2015; **21**: 163-170.
9. Reddy, M. S., Rajalingam, R. & Rela, M. Liver transplantation in acute-on-chronic liver failure: lessons learnt from acute liver failure setting. *Hepatol Int* 2015; **9**: 508-513.
10. Gronthos, S., Zannettino, A. C. W., Hay, S. J. *et al.* Molecular and cellular characterisation of highly purified stromal stem cells derived from human bone marrow. *J Cell Sci* 2003; **116**: 1827-1835.
11. Parekkadan, B. & Milwid, J. M. Mesenchymal Stem Cells as Therapeutics. *Annu Rev Biomed Eng* 2010; **12**: 87-117.
12. Klyushnenkova, E., Mosca, J. D., Zernetkina, V. *et al.* T cell responses to allogeneic human mesenchymal stem cells: immunogenicity, tolerance, and suppression. *J Biomed Sci* 2005; **12**: 47-57.
13. Di Nicola, M., Carlo-Stella, C., Magni, M. *et al.* Human bone marrow stromal cells suppress T-lymphocyte proliferation induced by cellular or nonspecific mitogenic stimuli. *Blood* 2002; **99**: 3838-3843.
14. Suk, K. T., Yoon, J. H., Kim, M. Y. *et al.* Transplantation With Autologous Bone Marrow-Derived Mesenchymal Stem Cells for Alcoholic Cirrhosis: Phase 2 Trial. *Hepatology* 2016; **64**: 2185-2197.
15. Berardis, S., Dwisthi Sattwika, P., Najimi, M. *et al.* Use of mesenchymal stem cells to treat liver fibrosis: current situation and future prospects. *World J Gastroenterol* 2015; **21**: 742-758.
16. Alfaifi, M., Eom, Y. W., Newsome, P. N. *et al.* Mesenchymal stromal cell therapy for liver diseases. *J Hepatol* 2018;
17. Fouraschen, S. M. G., Pan, Q. W., de Ruiter, P. E. *et al.* Secreted Factors of Human Liver-Derived Mesenchymal Stem Cells Promote Liver Regeneration Early After Partial Hepatectomy. *Stem Cells Dev* 2012; **21**: 2410-2419.

18. Li, D. L., He, X. H., Zhang, S. A. *et al.* Bone Marrow-Derived Mesenchymal Stem Cells Promote Hepatic Regeneration after Partial Hepatectomy in Rats. *Pathobiology* 2013; **80**: 228-234.
19. Wang, J., Bian, C., Liao, L. *et al.* Inhibition of hepatic stellate cells proliferation by mesenchymal stem cells and the possible mechanisms. *Hepatol Res* 2009; **39**: 1219-1228.
20. Parekkadan, B., van Poll, D., Megeed, Z. *et al.* Immunomodulation of activated hepatic stellate cells by mesenchymal stem cells. *Biochem Bioph Res Co* 2007; **363**: 247-252.
21. Sakaida, I., Terai, S., Yamamoto, N. *et al.* Transplantation of bone marrow cells reduces CCl₄-induced liver fibrosis in mice. *Hepatology* 2004; **40**: 1304-1311.
22. Park, M., Kim, Y. H., Woo, S. Y. *et al.* Tonsil-derived Mesenchymal Stem Cells Ameliorate CCl₄-induced Liver Fibrosis in Mice via Autophagy Activation. *Sci Rep-Uk* 2015; **5**:
23. Parekkadan, B., van Poll, D., Sukanuma, K. *et al.* Mesenchymal stem cell-derived molecules reverse fulminant hepatic failure. *PLoS One* 2007; **2**: e941.
24. van der Helm, D., Groenewoud, A., de Jonge-Muller, E. S. M. *et al.* Mesenchymal stromal cells prevent progression of liver fibrosis in a novel zebrafish embryo model. *Sci Rep* 2018; **8**: 16005.
25. Haniffa, M. A., Collin, M. P., Buckley, C. D. *et al.* Mesenchymal stem cells: the fibroblasts' new clothes? *Haematol-Hematol J* 2009; **94**: 258-263.
26. Haniffa, M. A., Wang, X. N., Holtick, U. *et al.* Adult human fibroblasts are potent immunoregulatory cells and functionally equivalent to mesenchymal stem cells. *J Immunol* 2007; **179**: 1595-1604.
27. Alt, E., Yan, Y. S., Gehmert, S. *et al.* Fibroblasts share mesenchymal phenotypes with stem cells, but lack their differentiation and colony-forming potential. *Biol Cell* 2011; **103**: 197-208.
28. Lee, Y. A. & Friedman, S. L. Reversal, maintenance or progression: What happens to the liver after a virologic cure of hepatitis C? *Antivir Res* 2014; **107**: 23-30.
29. Tranchart, H., Catherine, L., Maitre, S. *et al.* Efficient Liver Regeneration following Temporary Portal Vein Embolization with Absorbable Gelatin Sponge Powder in Humans. *J Vasc Interv Radiol* 2015; **26**: 507-515.
30. Hu, C., Zhao, L., Duan, J. *et al.* Strategies to improve the efficiency of mesenchymal stem cell transplantation for reversal of liver fibrosis. *J Cell Mol Med* 2019; **23**: 1657-1670.
31. Okabe, M., Ikawa, M., Kominami, K. *et al.* 'Green mice' as a source of ubiquitous green cells. *FEBS Lett* 1997; **407**: 313-319.
32. GM Higgins, R. A. *Experimental pathology of the liver.* . Vol. 12 186-202 (1931).
33. Tunon, M. J., Alvarez, M., Culebras, J. M. *et al.* An overview of animal models for investigating the pathogenesis and therapeutic strategies in acute hepatic failure. *World J Gastroentero* 2009; **15**: 3086-3098.
34. van Poll, D., Parekkadan, B., Cho, C. H. *et al.* Mesenchymal stem cell-derived molecules directly modulate hepatocellular death and regeneration in vitro and in vivo. *Hepatology* 2008; **47**: 1634-1643.
35. Pournasr, B., Mohamadnejad, M., Bagheri, M. *et al.* In Vitro Differentiation of Human Bone Marrow Mesenchymal Stem Cells into Hepatocyte-like Cells. *Arch Iran Med* 2011; **14**: 244-249.

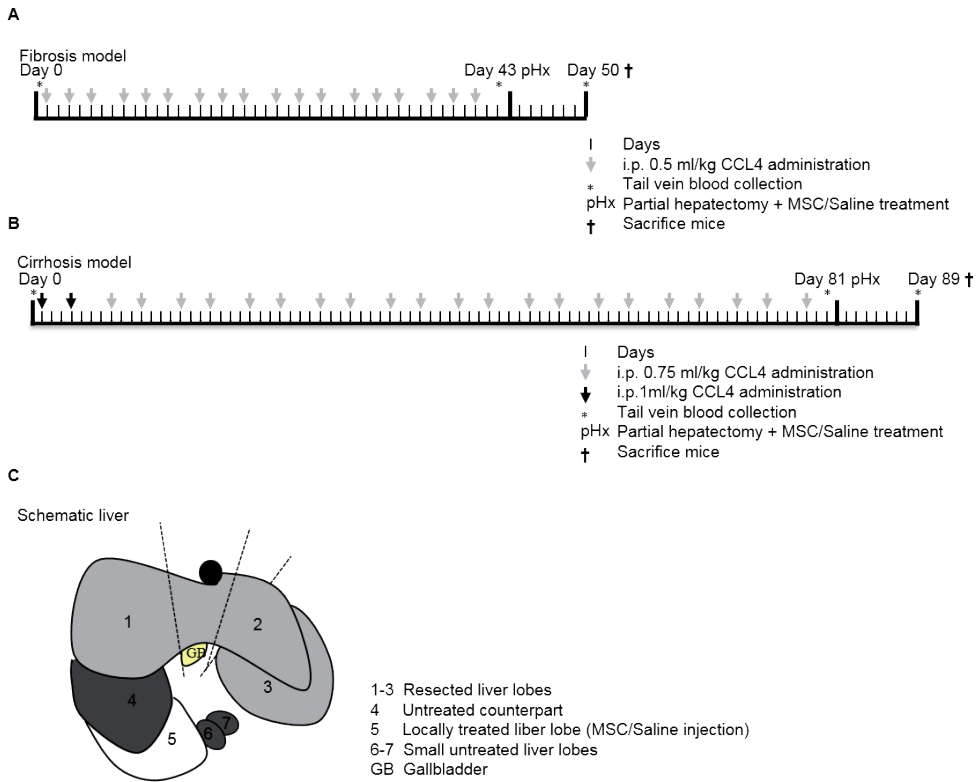
36. Snykers, S., Vanhaecke, T., Papeleu, P. *et al.* Sequential exposure to cytokines reflecting embryogenesis: The key for in vitro differentiation of adult bone marrow stem cells into functional hepatocyte-like cells. *Toxicol Sci* 2006; **94**: 330-341.
37. Haniffa, M. A., Wang, X. N., Holtick, U. *et al.* Mesenchymal stem cells and fibroblasts have similar immunoregulatory properties in vitro but distinct gene expression profiles: Implications for cellular therapy. *Blood* 2007; **110**: 573a-573a.
38. Cakiroglu, F., Osbahr, J. W., Kramer, J. *et al.* Differences of cell surface marker expression between bone marrow- and kidney-derived murine mesenchymal stromal cells and fibroblasts. *Cell Mol Biol (Noisy-le-grand)* 2016; **62**: 11-17.
39. El Baz, H., Demerdash, Z., Kamel, M. *et al.* Transplant of Hepatocytes, Undifferentiated Mesenchymal Stem Cells, and In Vitro Hepatocyte-Differentiated Mesenchymal Stem Cells in a Chronic Liver Failure Experimental Model: A Comparative Study. *Exp Clin Transplant* 2018; **16**: 81-89.
40. Pulavendran, S., Vignesh, J. & Rose, C. Differential anti-inflammatory and anti-fibrotic activity of transplanted mesenchymal vs. hematopoietic stem cells in carbon tetrachloride-induced liver injury in mice. *Int Immunopharmacol* 2010; **10**: 513-519.
41. Tanimoto, H., Terai, S., Taro, T. *et al.* Improvement of liver fibrosis by infusion of cultured cells derived from human bone marrow. *Cell Tissue Res* 2013; **354**: 717-728.
42. Barnhoorn, M., de Jonge-Muller, E., Molendijk, I. *et al.* Endoscopic Administration of Mesenchymal Stromal Cells Reduces Inflammation in Experimental Colitis. *Inflamm Bowel Dis* 2018; **24**: 1755-1767.
43. Molendijk, I., Bonsing, B. A., Roelofs, H. *et al.* Allogeneic Bone Marrow-Derived Mesenchymal Stromal Cells Promote Healing of Refractory Perianal Fistulas in Patients With Crohn's Disease. *Gastroenterology* 2015; **149**: 918-927 e916.

Supplementary files

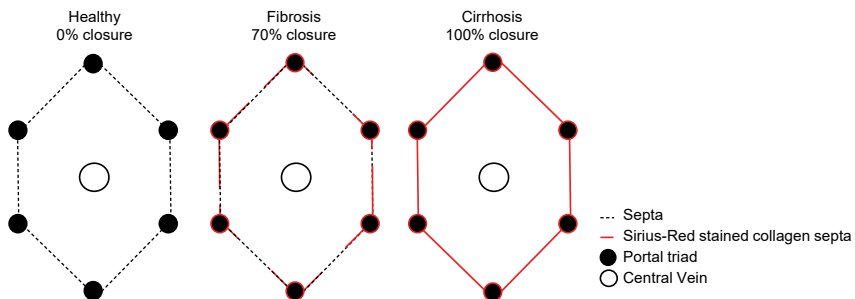
Supplementary material and methods

MSC and fibroblast characterisation

Flow cytometry was used to characterise the isolated cells. The isolated cells were incubated for 30 minutes with fluorescent conjugated antibodies: CD29-PE-Cy7, C45-PE, SCA-1-APC, CD31-APC (eBioscience, Vienna, Austria), CD44-APC, CD105-PE or CD106-PE (BD Pharmingen, San Diego, CA, USA). Next, the fluorescence was measured by LSR II flow cytometer (BD Biosciences, San Diego, CA, USA), with FACS-diva software (version 8.7.1., Tree Star Inc. Ashland, OR, USA). Data analysis was performed with FlowJow software (version 8.7.1., Tree Star Inc. Ashland, OR, USA). Furthermore, the ability of MSCs and fibroblasts to differentiate in to osteoblasts and adipocytes was tested. In short, MSCs and fibroblasts were cultured for 21 days with osteogenic or adipogenic differentiation medium. Osteogenic differentiation medium consists of complete medium supplemented with 10nM dexamethason, 50µg/ml ascorbic acid and 10mM β-glycerophosphate (all from Sigma-Aldrich Chemie BV, Zwijndrecht, The Netherlands). Adipogenic differentiation medium consists of complete medium supplemented with 1µM dexamethason, 5µM insulin, 100µM indomethacin and 0.5mM 3-isobutyl-1-methylxanthine (all from Sigma-Aldrich Chemie BV, Zwijndrecht, The Netherlands). Osteogenic differentiation was verified by alkaline phosphatase expression and calcium deposition confirmed by fast blue and alizarin red staining respectively (both Sigma-Aldrich Chemie BV, Zwijndrecht, The Netherlands). Adipogenic differentiation was verified by the formation of lipid droplets with an oil-red-o staining (Sigma-Aldrich Chemie BV, Zwijndrecht, The Netherlands).

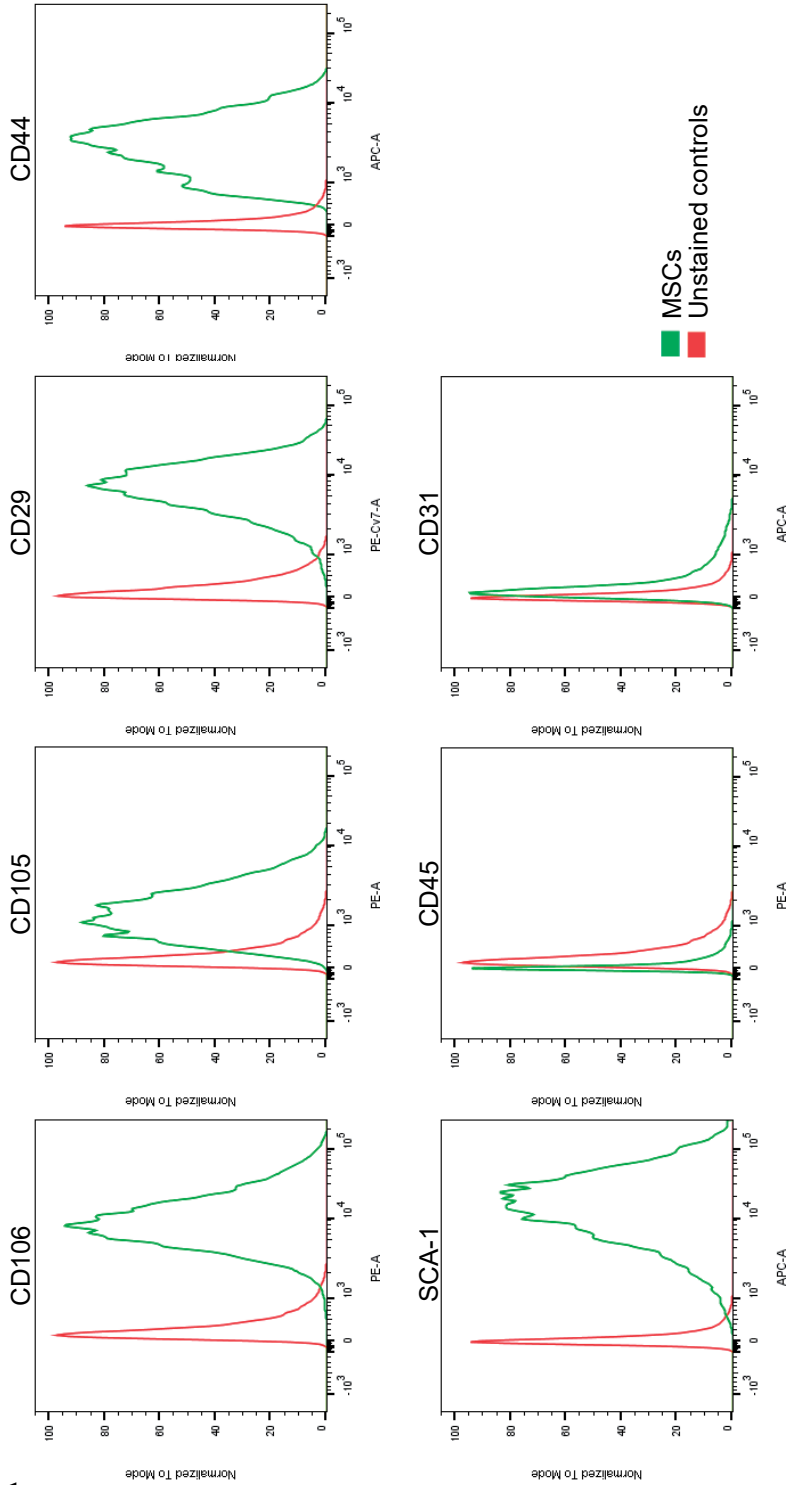


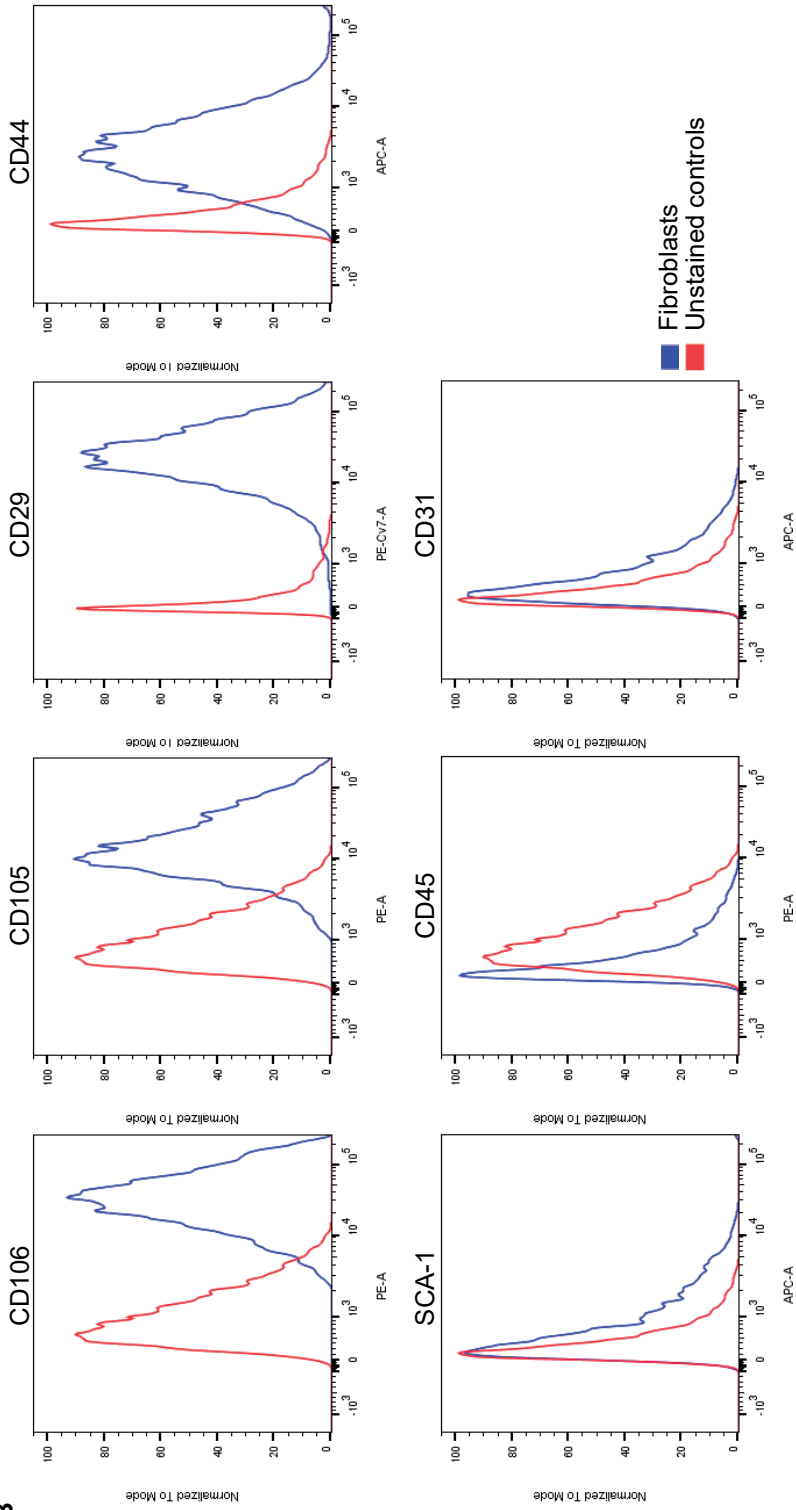
Supplemental Figure 1. Induction of fibrotic and cirrhotic mouse models. (A) Schematic overview of the induction of fibrosis. (B) Schematic overview of the induction of cirrhosis. (C) During partial hepatectomy, with concomitant local treatment, three lobes were resected (1-3). Lobe 4 was untreated and lobe 5 received vehicle, MSCs or fibroblasts.



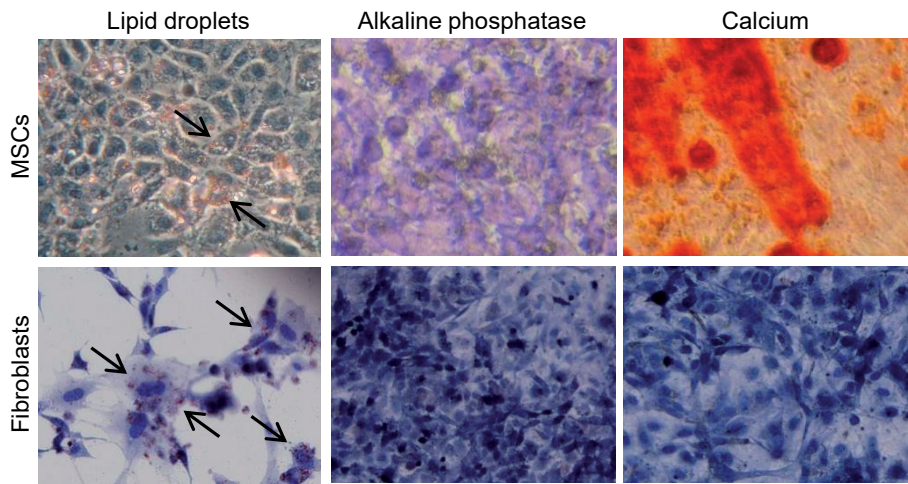
Supplemental Figure 2. Lobuli closure scoring method. Schematically overview and explanation of the lobuli closure score. (A) Typical healthy hexagonal liver structure (lobuli) consisting of 6 portal triads and 1 central vein. (B) Example of lobuli during fibrotic induction in which septa between the triads have begun to form (estimated closure is 70%). (C) Example of lobuli during cirrhotic induction in which bridging between the triads is observed (closure is 100%).

A

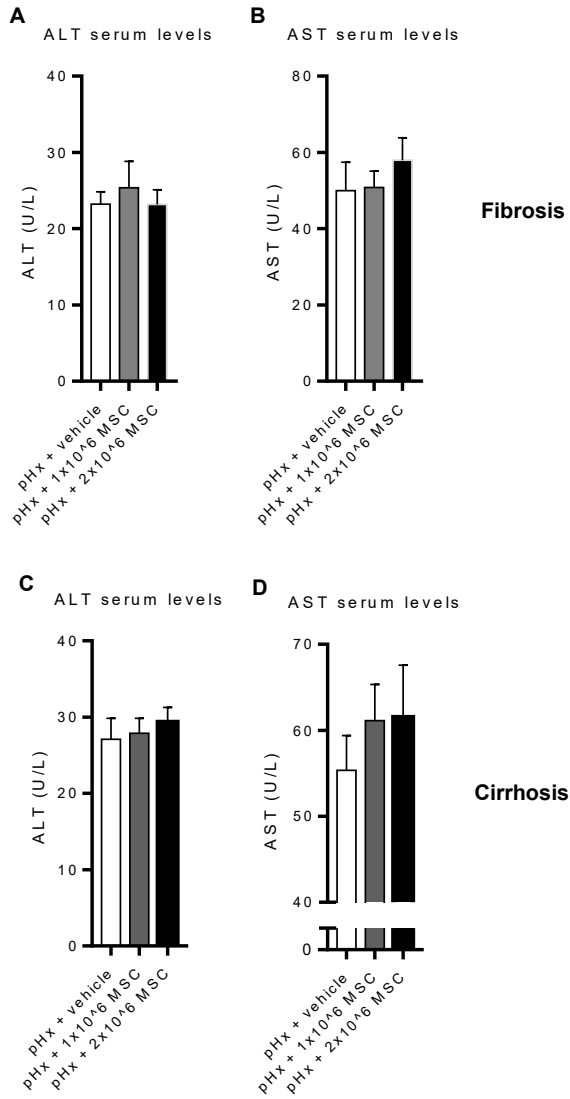


B

Supplemental Figure 3. MSC and fibroblast cell characterization. Bone marrow-derived and liver-derived fibroblast were isolated from 10 week old actin-GFP C57Bl/6jico mice. (A) MSCs and (B) Fibroblasts were characterized by flow cytometry for the presence or absence of CD106, CD105, CD29, CD44, SCA-1, CD45 and CD31 membrane proteins.



Supplemental Figure 4. Osteoblast and adipocyte cell differentiation. MSCs and Fibroblasts were isolated from the liver of 10 week old actin-GFP C57Bl/6Jico mice and characterized by adipocyte differentiation visualized by cytoplasmic lipid droplets (oil-red-o) staining (black arrows) and osteoblast differentiation visualized by upregulation of alkaline phosphatase (fast blue staining) and calcium deposit (Alizarin red staining).



Supplemental Figure 5. Aminotransferase levels after liver regeneration. After CCL4 induced fibrosis and cirrhosis, mice underwent partial hepatectomy and were divided in three groups which received a local treatment of vehicle, 1x10⁶ or 2x10⁶ MSCs. Eight days after treatment blood from the tail vein blood was collected. (A,B) ALT and AST serum levels of treated fibrotic mice. (C,D) ALT and AST serum levels of treated cirrhotic mice.

3

CHAPTER 3

VCAM-positive mesenchymal stromal cells are most instrumental in ameliorating experimental liver fibrogenesis

Danny van der Helm, Jayron J. Habibe, Marieke C. Barnhoorn, Eveline S.M. de Jonge-Muller, Minneke J. Coenraad, Bart van Hoek*, Hein W. Verspaget*

*Joint senior authorship

Abstract

Background

Liver fibrogenesis starts with apoptotic hepatocytes that induce proliferation of stellate cells and their subsequent differentiation into myofibroblasts. Myofibroblasts are the main source of extracellular matrix in fibrogenesis. Mesenchymal stromal cells (MSCs) are known to possess pro-regenerative and anti-inflammatory properties, but in relation to the reversal of fibrogenesis contradictory findings have been reported. The reported differences might partly be explained by the use of different subpopulations of MSCs. In the present study we compared the pro-regenerative and anti-fibrotic effects of four different subpopulations of MSCs, categorised on Endoglin (CD105) and VCAM (CD106) membrane expression.

Methods and Results

Proliferation, wound healing and trans-well migration experiments using damaged HepG2 cells showed that VCAM-positive MSC subpopulations have more pro-regenerative capacities compared to the VCAM-negative subpopulations. VCAM-positive MSC populations also expressed higher levels of migratory (SDF-1 and CXCR4) and anti-fibrotic (TGF- β 1, VEGF, HGF and IGF) genes. Furthermore, only VCAM-positive MSCs, independent of Endoglin expression, were able to reverse fibrogenesis in a mouse model for liver fibrosis.

Conclusion

To conclude, VCAM-positive subpopulations of MSCs are superior compared to VCAM-negative subpopulations in relation to their anti-fibrotic and pro-regenerative properties. Endoglin expression of MSCs does not have major functional implications regarding their antifibrogenic activity. These observations indicate that differences in subpopulations of MSCs have considerable functional impact that should be implicated in their functional assessment analyses.

Introduction

Liver fibrogenesis is becoming a serious health problem, since therapies specifically targeting this process and thereby preventing progression of fibrosis to cirrhosis are not yet available¹⁻⁴. Fibrogenesis in the liver is caused by injuring stimuli such as excessive alcohol intake, viral hepatitis, non-alcoholic steatohepatitis, autoimmune hepatitis or metabolic syndromes⁵⁻⁷. These injuries may lead to apoptosis of hepatocytes which leads to increased proliferation, activation and myofibroblast-differentiation of the stellate cells. These myofibroblasts are responsible for the excessive extracellular matrix deposition observed in fibrosis^{5,7}.

While removal of the injuring stimulus in some cases may reverse liver fibrogenesis, no medication directly targeting fibrogenesis is available. For example, In the case of hepatitis C infection, a sustained response to anti-viral treatment can lead to a regression of fibrosis⁸. For end-stage cirrhosis, an orthotopic liver transplantation (OLT) is the only curative treatment^{2,3}. OLT is a major intervention with associated risks and feasibility for its use depends on donor availability and patient condition⁹⁻¹¹. Therefore, new therapeutics or interventions specifically targeting the process of hepatic fibrogenesis are needed.

Recently, the use of mesenchymal stromal cells (MSCs) has been explored as a possible treatment for liver fibrosis^{12,13}. MSCs are pluripotent cells that can be isolated from various tissues, such as bone-marrow, umbilical cord and adipose tissue. Furthermore, MSCs are not rejected by the immune system upon transplantation and are known to be immuno-suppressive and able to stimulate the repair and regeneration of damaged tissue¹⁴⁻¹⁷. Several *in vivo* studies, including our own, have shown the potency of MSCs to inhibit the induction and to promote the reversal of fibrogenesis^{12,18-21}. MSCs have been used to successfully reverse liver fibrosis in patients with alcohol-related or viral-induced liver injury^{18,19}. Different working mechanisms of MSCs in the reversal of liver fibrosis have been proposed. These mechanisms include the capacity of MSCs to inhibit stellate cell proliferation and their subsequent activation and differentiation into myofibroblasts, but also the ability of MSCs to silence the myofibroblasts, and thereby directly target fibrogenesis²²⁻²⁴. Furthermore, it is suggested that MSCs can stimulate the proliferation and survival of hepatocytes²²⁻²⁶. Other proposed mechanisms include the immunomodulatory abilities of MSCs by -for example- inhibition of T-cell activation and stimulation of pro-inflammatory macrophages to an immunosuppressive phenotype^{22,27}.

Besides the positive results obtained from *in vivo* studies and clinical trials with MSC therapy for liver fibrosis, other studies have shown different and even contradictory results^{18,19,21,28}. Disease stage, timing of MSC administration, source of MSCs, dosage of MSCs and administration routes differ between the studies and may therefore account for the observed contradictory results^{21,28}. Another, less studied explanation is the use of different subpopulations of MSCs²⁸⁻³⁰. The current isolation methods for MSCs lead to a rather heterogeneous group of

cells³¹⁻³³. Most of the studies describe MSCs as cells that are able to differentiate *in vitro* into osteoblasts and adipocytes, express CD29, SCA-1 and CD44 on their membranes, and adhere to plastic^{14,28,31,33}. However, most studies are less consistent about the Endoglin (CD105) and vascular cell adhesion protein (VCAM, CD106) membrane expression of MSCs^{29,31,33-35}. VCAM-negative subpopulations are thought to have less regenerative and immunosuppressive properties as compared to VCAM-positive MSC subpopulations^{31,34,35}. Studies describing Endoglin-negative subpopulations reveal a more immunosuppressive phenotype compared to Endoglin-positive MSC subpopulations²⁹. Thus, in order to find the optimal treatment and to get reproducible results, it might be highly relevant to characterise the different MSC subpopulations and assess the functional implications. However, there are no studies focussing on the use of different subpopulations of MSCs in relation to the treatment of liver fibrosis. Therefore, in the present study we compared the pro-regenerative and anti-fibrotic abilities of four different subpopulations of MSCs, selected to be double-positive, double-negative, or single-positive for either Endoglin and VCAM. We hypothesized that different subpopulations of MSCs will lead to different experimental outcomes, which may explain the contradictory results in different studies.

Material and Methods

MSC isolation and culturing

Tg(s100a4-cre)1Egn mice (Jackson laboratory, Bar Harbor, USA) were crossed with Bl6-ROSA-LacZ reporter mice (LUMC breeding population) and their offspring was used for the isolation of MSCs following standard protocol³⁶. In short, mice were sacrificed by cervical dislocation and femur, tibia and humerus were collected and cleared from surrounding tissues. Bones were flushed with RPMI culture medium supplemented with, L-glutamine, penicillin/streptomycin (P/S; Invitrogen Corp., Paisley, UK), fetal calf serum (FCS; Gibco, Paisley, UK) and Heparin (Pharmacy AZL, Leiden, The Netherlands). Flushed bone-marrow was filtered and subsequently cultured in complete culture medium consisting of α MEM culture medium (Lonza, BE12-169F) supplemented with L-glutamine, P/S and FCS. Floating cells were removed by daily medium refreshment and growing MSC populations were obtained after a few weeks. Cells were used in passage 3-5 and monthly tested for mycoplasma contamination.

Identification and characterisation of MSC subpopulations

MSC subpopulations were identified and characterised by FACS analysis. MSCs were stained for CD29-PE-Cy5, SCA-1-APC, CD45-PE, CD31-APC (eBioscience, Vienna, Austria), CD44-APC, Endoglin-PE and VCAM-PE (BD Pharmingen, San Diego, CA, USA) and fluorescence was measured with LSR II flow cytometer (BD Biosciences, San Diego, CA, USA) with FACS diva software (version 8.7.1., Tree Star Inc. Ashland, OR, USA). Results were analysed using FlowJow analysis software (version 8.7.1., Tree Star Inc. Ashland, OR, USA). FACS analysis identified four

different subpopulations of MSCs: double-positive ($V^{\text{pos}}E^{\text{pos}}$ -MSC), double-negative ($V^{\text{neg}}E^{\text{neg}}$ -MSC), or single-positive for Endoglin or VCAM ($V^{\text{neg}}E^{\text{pos}}$ -MSC or $V^{\text{pos}}E^{\text{neg}}$ -MSC).

To test the ability of the identified MSC subpopulations to differentiate into osteoblasts and adipocytes, the MSCs were cultured for three weeks with adipocyte or osteoblast differentiation medium as previously described by our group³⁶. In short, adipogenic differentiation medium consists of complete culture medium supplemented with 1 μM dexamethason, 5 μM insulin, 100 μM indomethacin and 0.5 mM 3-isobutyl-1-methylxanthine (all from Sigma-Aldrich Chemie BV, Zwijndrecht, The Netherlands). Osteoblast differentiation medium consists of complete culture medium supplemented with 10 nM dexamethason, 50 $\mu\text{g}/\text{ml}$ ascorbic acid and 10 mM β -glycerophosphate (all from Sigma-Aldrich Chemie BV, Zwijndrecht, The Netherlands). After three weeks, fast blue staining for alkaline phosphatase expression and alizarin red staining for calcium deposition were used to verify osteogenic differentiation (Sigma-Aldrich Chemie BV, Zwijndrecht, The Netherlands). Adipogenic differentiation was confirmed by oil-red-o stained lipid droplets (Sigma-Aldrich Chemie BV, Zwijndrecht, The Netherlands).

Proliferation, trans-well migration and wound healing assays

Cell proliferation was measured with Promega MTS assay following manufactures' protocol (Promega, Madison, Wisconsin, USA). MSCs were plated in a 96 well plate and the next day (day 0) and at day 2, MTS was added and after 1 h of incubation the colour development was measured. To evaluate the ability of MSCs to influence HepG2 proliferation, 2 days conditioned MSC medium (FCS free) was added to HepG2 cells or wounded HepG2 cells (cross-sectional scratch injuries) and a MTS assay was performed at day 0 and 2.

For wound healing assays 500.000 HepG2 cells were plated on a coverslip in a 24 well plate. Next day, a wound was made, and medium replaced by MSC conditioned medium (FCS free) or 150.000 cells of the different MSC subpopulations. Images (10x magnification) were made at 0 h and 48 h and used to calculate the wound size.

Trans-well migration assays were used to study the migration capacity of the subpopulations of MSCs (8 μm , Thincert TM Greiner Bio-One 12 well, 665638). In all experiments 10.000 MSCs in FCS free αMEM culture medium were added to the upper compartment. Thereafter, migration to 1% FCS medium with or without HepG2 or wounded HepG2 cells (cross-sectional scratches) in the lower compartment was evaluated. After 24 h, migrated cells were visualized by crystal violet staining and counted subsequently.

RNA isolation, cDNA synthesis and quantitative Polymerase Chain Reaction (qPCR)

NucleoSpin RNA kit (Machery-Nagel GmbH, Düren, Germany) was used to isolate mRNA following manufactures' protocol. Next, cDNA was synthesized according to Promega standard

protocol (Promega, Madison, Wisconsin, USA). For qPCR a mix containing 1 nM primers, 5 μ l iQ SYBR Green supermix reagent and 4 μ l cDNA was used (Bio-Rad Laboratories, Berkeley, California, USA). CXCR4, stromal derived factor-1 (SDF-1), hepatocyte growth factor (HGF), vascular endothelial growth factor (VEGF), insulin-like growth factor (IGF), VCAM, Endoglin and transforming growth factor- β 1 (TGF- β 1) expression levels were measured and normalised to Glyceraldehyde 3-phosphate dehydrogenase (GAPDH), (Supplemental Table 1: Primer sequences).

Mouse model for liver fibrosis

All experiments were approved by the animal ethics committee of the Leiden University Medical Center. Mice were housed under 12 h day/night cycle and received food and water *ad libitum*. For the induction of liver fibrosis 6 week old male C57Bl/6J mice were used (Charles River Laboratories, The Netherlands). For a period of 6 weeks, mice received 3 intraperitoneal injections with carbon tetrachloride (CCL4, 0.5 ml/kg body weight) in mineral oil per week (Sigma-Aldrich Chemie BV, Zwijndrecht, The Netherlands). After these 6 weeks, mice underwent a partial hepatectomy where the three frontal lobes were removed³⁷. During surgery, one of the four different MSC subpopulations (2×10^6 cells) or vehicle control (NaCl) were locally injected in one of the two intact lateral lobes (N=10 mice per group). After 8 days, mice were sacrificed by cervical dislocation and livers were collected, weighed and stored in paraformaldehyde for paraffin embedding.

Histological examination of extracellular matrix

To evaluate the severity of fibrosis a Sirius-red staining was performed to visualize and subsequently quantify the amount of extracellular matrix (ECM). Fixed cell cultures and hydrated paraffin tissue sections were stained for 90 min with 1 g/L Sirius-red F3B in saturated picric acid (both Klinipath, Guildford, UK). Next, the cells or tissue sections were incubated for 10 min with 0.01 M HCL, dehydrated and mounted with Entellan (Merck KGaA, Darmstadt, Germany).

To quantify the amount of ECM in liver tissue, 5-8 random pictures (10x magnifications) with fixed microscopy settings were captured and thereafter analysed with ImageJ (ImageJ 1.47v, National Institutes of Health, USA). Subsequently, the reduction of collagen content in the regenerated liver tissue, relative to the resected pHx tissue was calculated. In addition, lobuli closure was used as a second score for the severity of fibrosis. More lobuli closure indicated a more severe degree of fibrosis.

Statistical Analysis

Statistical analysis was performed using GraphPad Prism software and P values lower than 0.05 were considered to be statistically significant (GraphPad Software, version 5.01, San

Diego, CA). To compare two or multiple groups Student's t-test or One-Way ANOVA test was used respectively. Results are presented as the means ± standard error of the mean (SEM).

Results

Identification and characterisation of VCAM/Endoglin subpopulations of MSCs

$V^{pos}E^{pos}$ -MSC, $V^{pos}E^{neg}$ -MSC, $V^{neg}E^{pos}$ -MSC, $V^{neg}E^{neg}$ -MSC subpopulations were identified and characterised by FACS analysis. All four subpopulations revealed to be positive for CD44, CD29 and SCA-1 expression (Figure 1A). Endothelial marker CD31 and haematopoietic marker CD45 were absent in all subpopulations (Figure 1A). Endoglin and VCAM expression as such were independent of each other (Figure 1A). QPCR measurements of mRNA expression of

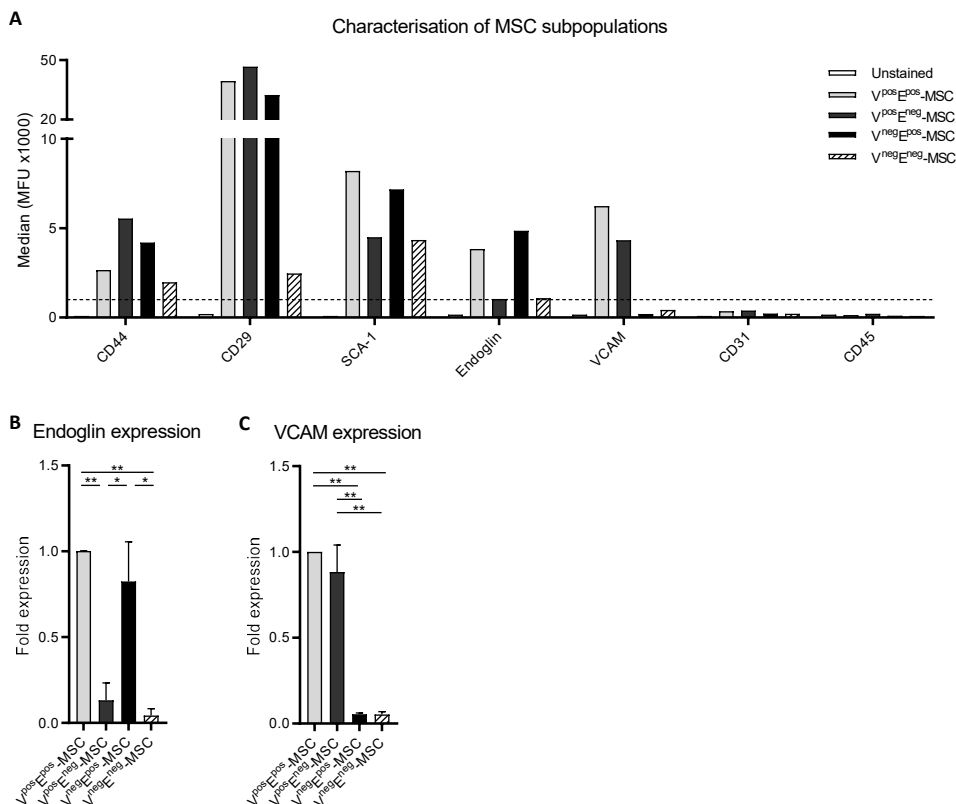


Figure 1. Identification and characterisation of VCAM/Endoglin subpopulations of MSCs. Identification and characterization of the different subpopulations of MSCs by membrane marker expression. (A) CD44, CD29, SCA-1, Endoglin, VCAM, CD31 and CD45 membrane expression measured by flow cytometry. RNA expression levels of (B) Endoglin and (C) VCAM were measured by qPCR and normalized to GAPDH. The qPCR data is represented as mean ± SEM of three independent experiments. * $p \leq 0.05$ ** $p \leq 0.01$

Endoglin and VCAM confirmed the protein results obtained from the FACS experiments (Figure 1B and C). To confirm that the subpopulations are indeed MSCs, osteoblast and adipocyte differentiation assays were performed. All four populations showed to be able to differentiate into adipocytes and osteoblasts (Figure 2). Some small differences in the extent of differentiation were observed. The $V^{\text{neg}}E^{\text{neg}}$ -MSC population showed less differentiation into osteoblasts, while the adipocyte differentiation was more pronounced in both Endoglin-negative subpopulations. These results indicate that the four identified subpopulations of cells can all be classified as classical MSCs.

Conditioned medium of the VCAM-positive MSC subpopulation enhances the survival and proliferation of damaged HepG2 cells

Proliferation and survival of endogenous liver cells are two proposed mechanisms of MSC treatment for liver fibrosis. The results of an *in vitro* assay using HepG2 cells as a model for

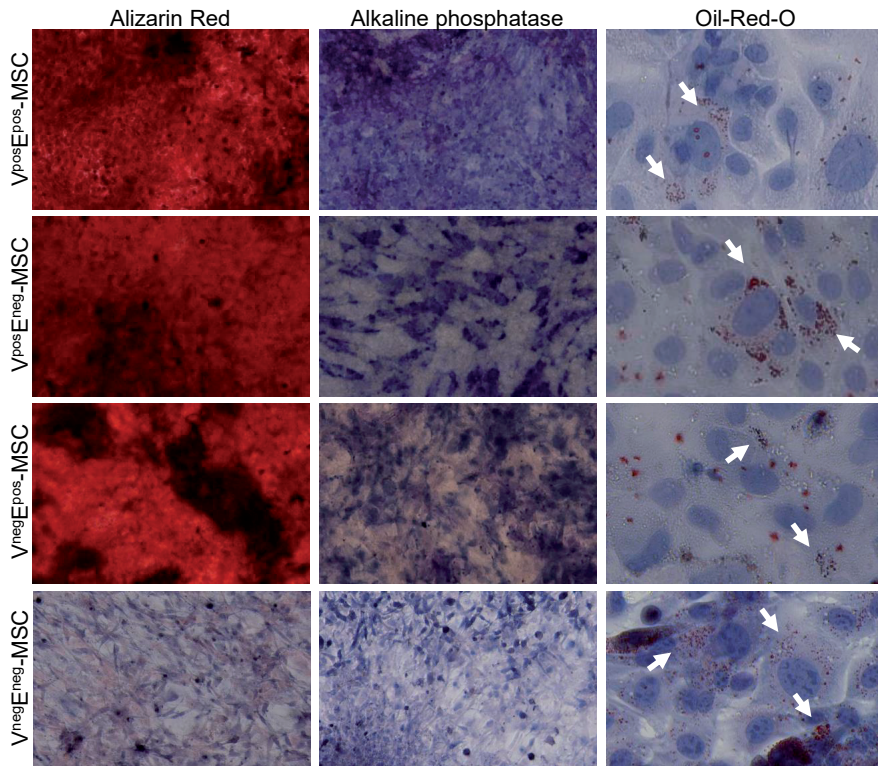


Figure 2. Osteoblast and adipocyte differentiation of MSC subpopulations. Characterisation of the isolated MSC subpopulations by osteoblast and adipocyte differentiation. Osteoblast differentiation was visualized by calcium deposit (Alizarin red staining), and alkaline phosphatase production (fast blue staining, 10x magnifications). Adipocyte differentiation was visualized by Oil-red-o stained cytoplasmic lipid droplets (indicated by the white arrows, 40x magnifications).

endogenous hepatocytes showed that incubation with conditioned medium of the four different MSC subpopulations did not affect basal proliferation of HepG2 cells (Figure 3A). When the HepG2 cells were challenged with injuring scratches, increased proliferation was observed when incubated with conditioned medium obtained from the VCAM positive populations compared to control (non-conditioned medium) and conditioned medium obtained from the VCAM-negative populations (Figure 3B). Next, the ability of MSCs to sense tissue damage and actively migrate to these damaged regions was evaluated. In a trans-well migration assay, the basal migration of the different populations from medium without FCS to medium with 1% FCS was tested. VCAM-positive MSCs showed significantly more migration compared to the VCAM-negative subpopulations (Figure 3C). Similar migration patterns were observed when

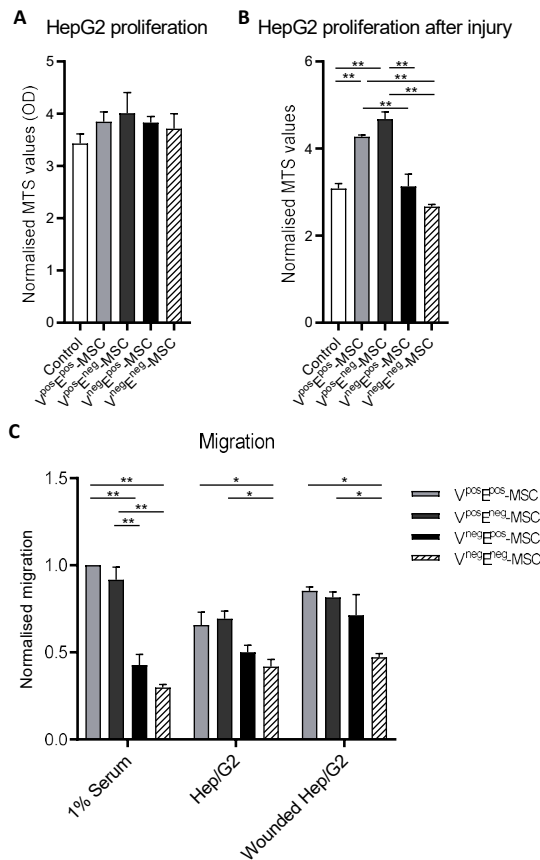


Figure 3. Conditioned medium of the VCAM-positive MSC subpopulation enhances the survival and proliferation of damaged HepG2 cells. The ability of the MSC subpopulations to affect HepG2 cell proliferation was measured by MTS proliferation assays. Proliferation of (A) HepG2 or (B) scratched HepG2 monolayers after 48 h of stimulation with conditioned medium of the different MSC subpopulations, normalized to baseline measurement. (C) In trans-well migration assays the migration to 1% serum, HepG2 or wounded HepG2 cells in 24 h was evaluated. Migrated cells were visualized with crystal violet staining, counted, and normalized to 1% serum initiated migration of the V^{pos}E^{pos}-MSC subpopulation. Graphs represented the mean ±SEM of three independent experiments. *p<0.05 **p<0.01

the MSC subpopulations migrated to HepG2 or wounded HepG2 cells (Figure 3C). Altogether these data indicate that VCAM-positive MSC subpopulations are more migratory and more able to stimulate proliferation upon injuring stimuli compared to the VCAM-negative MSC subpopulations.

VCAM-positive and VCAM-negative MSC subpopulations equally enhance HepG2 wound closure and form 2D lobuli-like structures

Wound closure assays were performed to study whether the four subpopulations of MSCs differently affect tissue regeneration. The results showed faster wound closure of the HepG2 cells after adding MSCs or MSC conditioned medium but no differences between the subpopulations were observed (Figure 4A and B). Proliferation assays showed that the $V^{\text{neg}}E^{\text{neg}}$ -MSC population proliferate faster compared to the other subtypes which showed equal proliferation rates (Figure 4C). Since the other subpopulations have a similar proliferation rate, this could not affect the results of the wound closure experiments. At the end of the wound closure experiments, hexagonal/lobuli-like structures were observed. Sirius-red staining of these cocultures co-localised with the observed hexagonal structures (Figure 4D). These observed structures are similar to those observed in *in vivo* livers. To study the exact location of the MSCs in these experiments GFP- $V^{\text{pos}}E^{\text{pos}}$ -MSCs were used. Results showed that GFP- $V^{\text{pos}}E^{\text{pos}}$ -MSCs co-localised with the hexagonal structures (Figure 4E, white arrow) and the wound opening (Figure 4E, area surrounded by the dashed line). Furthermore, the results showed that, although MSCs adhere in the wound area, the borders of HepG2 cells did grow towards each other and that the MSCs were excluded from the wounds. The finding that the MSC subpopulations lead to faster wound closure and the formation of liver-like structures implies that MSCs affect tissue regeneration.

VCAM-positive MSC subpopulations express a better pro-regenerative and migratory gene profile compared to VCAM-negative subpopulations

QPCRs were performed to assess whether differences in migration could be explained by different expression levels of genes involved in MSC migration. Results showed that VCAM-positive MSC subpopulations express higher levels of CXCR4 and SDF-1 compared to the VCAM-negative subpopulations (Figure 5A and B). Furthermore, expression levels of known anti-fibrotic and pro-regenerative genes (VEGF, TGF- β 1, IGF and HGF) were measured. VEGF expression was less affected by the VCAM profile (Figure 5C). TGF- β 1 and IGF were higher expressed in $V^{\text{pos}}E^{\text{neg}}$ -MSC population compared to the other three subpopulations (Figure 5D and E). $V^{\text{pos}}E^{\text{pos}}$ -MSCs showed the highest expression level of HGF (Figure 5F). Altogether these data indicate that VCAM-positive MSC subpopulations have a more pro-regenerative and migratory gene profile compared to the VCAM-negative MSC subpopulations.

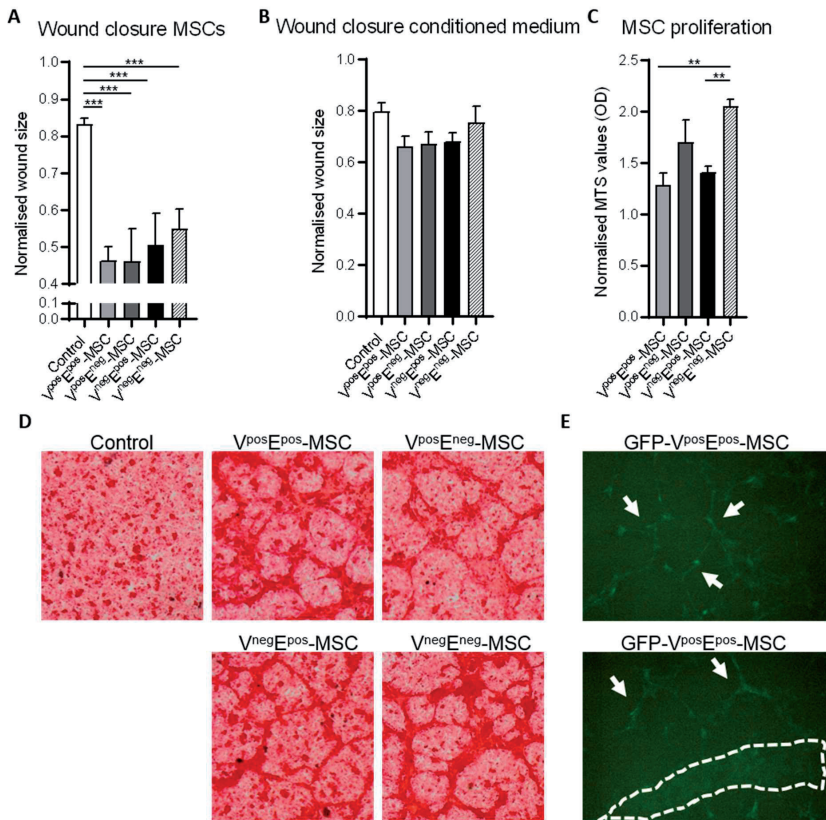


Figure 4. VCAM-positive and VCAM-negative MSC subpopulations equally enhance HepG2 wound closure and form 2D lobuli-like structures. HepG2 wound healing experiments were performed with (A) cells or (B) conditioned medium of the 4 different MSC subpopulations. The graphs are presenting wound closure after 48 h normalised to baseline. (C) Basal proliferation of the 4 different MSC subpopulations measured by a MTS assay. (D) Pictures of Sirius-red stained HepG2–MSC cocultures at the end of the wound healing experiments (10x magnifications). (E) Pictures of wound closure experiments with GFP expressing MSCs. MSCs colocalising with the lobuli-like structures are indicated by white arrows and the wound area is surrounded by a white dashed line. The data is represented as the mean \pm SEM (n=3). ** $p \leq 0.01$, *** $p \leq 0.001$

VCAM-positive but not VCAM-negative MSC subpopulations reverse fibrogenesis in regenerating mouse livers

To study the ability of the different MSC subpopulations to reverse fibrogenesis, an *in vivo* model for liver fibrosis was used. After 6 weeks of fibrosis induction with CCL4, mice underwent a partial hepatectomy as regeneration stimulus, and locally received one of the four subsets of MSCs or vehicle as control. During 8 days of regeneration no differences in body weights were observed, except for the last two days where the mice treated with the VCAM-negative MSCs had relative lower body weights (Figure 6A). Eight days after cell treatment, mice were sacrificed and livers collected and weighted. No differences in total liver weights were observed (Figure 6B). Liver lobes which were locally treated with the VCAM-negative subpopulations

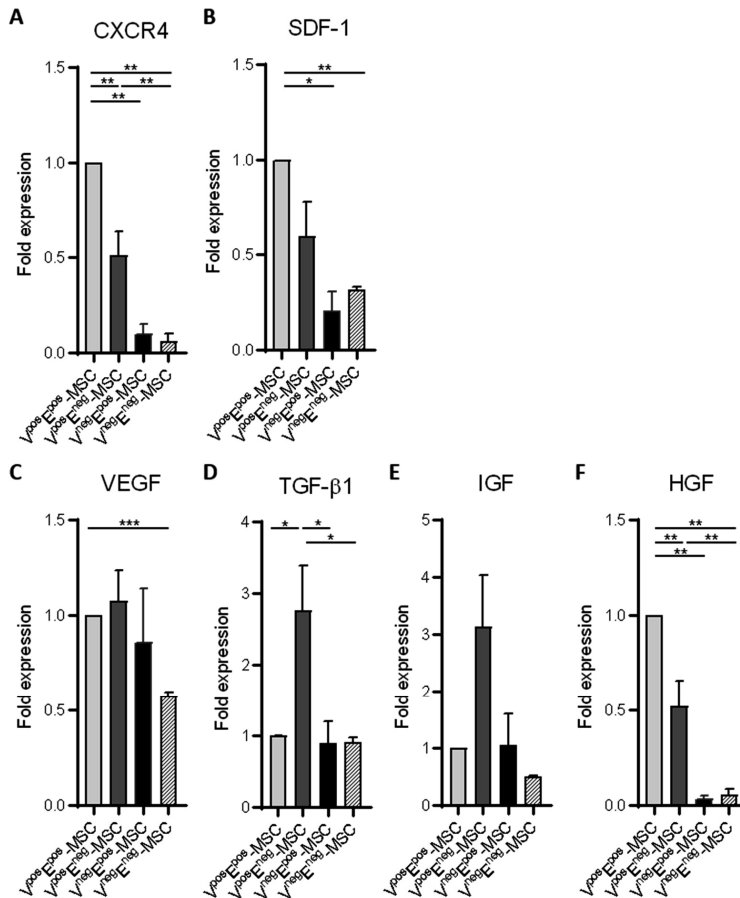


Figure 5. Basal pro-migratory and anti-fibrotic gene expression levels. QPCR analysis of pro-migratory and anti-fibrotic gene expression levels of the different MSC subpopulations. Expression levels of (A) CXCR4, (B) SDF-1, (C) VEGF, (D) TGF- β 1, (E) IGF and (F) HGF were measured and normalized to GAPDH. The graphs represent the mean of three independent experiments \pm SEM. * p <0.05, ** p <0.01, *** p <0.001

were significantly smaller compared to controls. The weights of the locally treated lobes of the groups receiving the VCAM-positive populations were not different compared to control (Figure 6C). Paraffin embedded liver sections were stained for Sirius-red to assess the degree of liver fibrosis. Results showed that local $V^{pos}E^{pos}$ -MSC treatment lead to more reduction in collagen content compared to mice treated with vehicle control or the VCAM-negative MSC populations (Figure 6D and E). Next, the tissues were also scored for lobuli closure, in which more closure indicates a more severe fibrosis. More closure was observed in the mice treated with the VCAM-negative subpopulations compared to control, while the mice treated with the VCAM-positive populations did not differ from controls (Figure 6F). $V^{pos}E^{pos}$ -MSCs showed, although not significantly, a trend towards less closure (Figure 6F). No significant differences in the weights, reduction of collagen or lobuli closure in the untreated counterpart liver lobes

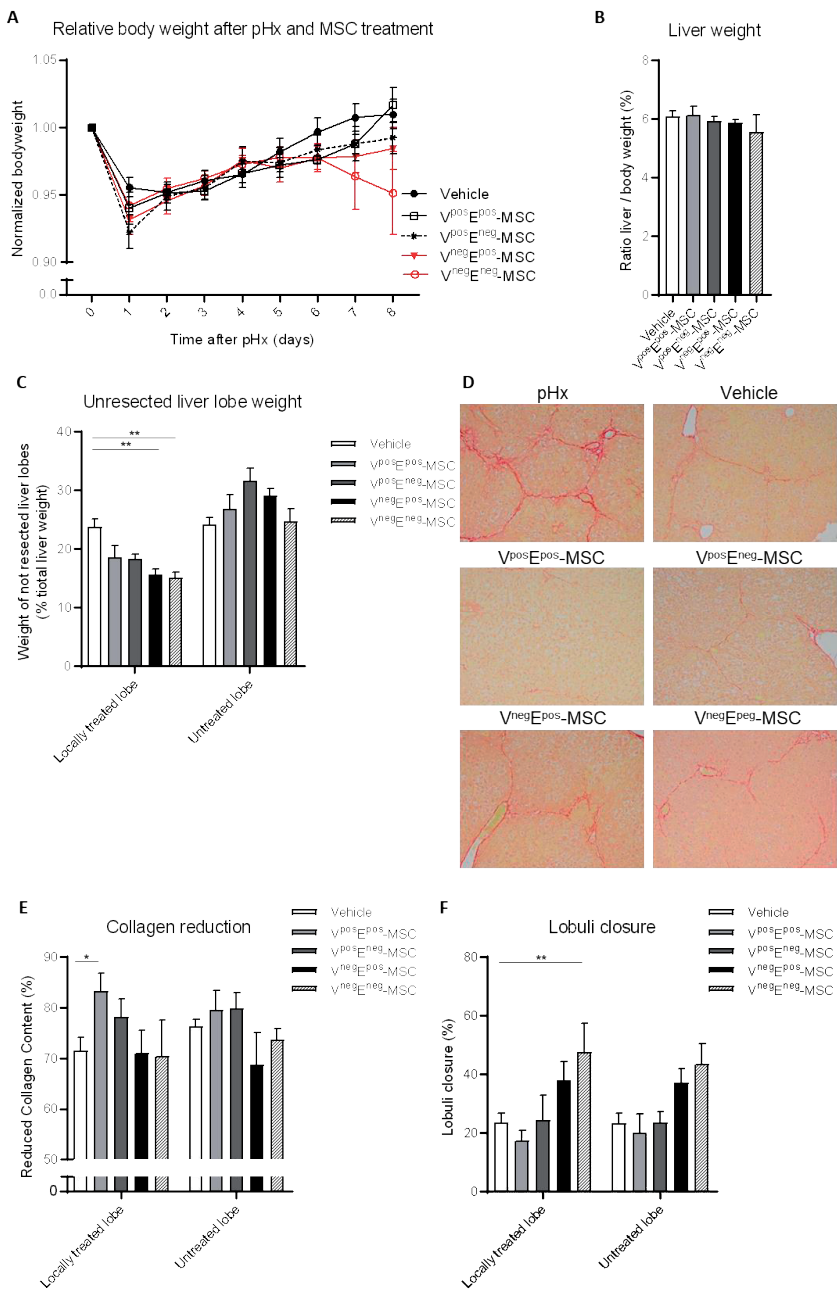


Figure 6. VCAM-positive MSC populations ameliorate fibrosis in regenerating mouse livers. After CCL4 induced fibrosis, mice underwent partial hepatectomy and received local treatment of vehicle, or one the MSC subpopulations in one of two remaining liver lobes (N=10 mice/group). (A) Relative body weight during regeneration. (B) Liver weight normalised to total body weight and (C) treated and untreated lobe weight as percentage liver after regeneration. (D) Representative pictures of Sirius-red stained sections of resected and locally treated liver lobes (10x magnifications). (E) Reduction of Sirius-red staining relative to resected tissue. (F) Estimated lobuli closure of Sirius-red stained sections. Data are expressed as mean ± SEM. *p<0.05, **p<0.01

were observed, which indicates a local effect of the MSC treatment (Figure 6C, E and F). These results showed that VCAM-positive subpopulations, independent of Endoglin expression, have the ability to locally ameliorate liver fibrosis in regenerating livers.

Discussion

The incidence and the progression of liver fibrosis to cirrhosis is an increasing health problem for which new interventions or therapeutics are needed^{4,38}. Extensive research is ongoing in order to find new treatments specifically targeting fibrogenesis. Currently, several studies have tested the application of MSC therapy as a new treatment strategy, and while some results were promising, other studies had negative outcomes^{12,18,19}. Explanations for these opposing effects could be variation in the study design, source of MSCs, dosage, route of administration and possibly the existence and use of different subpopulations of MSCs^{12,21,28}. So far, functional assessments of different subpopulations of MSCs in the reversal of liver fibrosis has not been studied. Therefore, in the present study, we compared the pro-regenerative and anti-fibrotic capacities of four different subpopulations of MSCs, selected for Endoglin and VCAM membrane marker expression. Results showed that VCAM-positive MSC subpopulations are more migratory and lead to more proliferation of damaged HepG2 cells compared to the VCAM-negative subpopulations. Furthermore, in a mouse model for liver fibrosis we showed that local MSC treatment with the VCAM-positive subpopulations in combination with a partial hepatectomy as regeneration stimulus, ameliorates fibrosis. The VCAM-negative subpopulations were not able to ameliorate fibrosis in this model. The contribution of Endoglin expression was found to be less relevant.

Studies of Li and Huang et al. have shown that MSCs could protect hepatocytes from apoptosis and are able to promote hepatocyte proliferation^{24,26}. The results of the present study were in line with these observations, and showed that conditioned medium of the VCAM-positive MSC populations led to more proliferation of the damaged HepG2 cells compared to control. However, the previous studies did not compare their results to a VCAM-negative subpopulation. Therefore, it is interesting that the current study showed that the conditioned medium of the VCAM-negative MSC populations lacked this property needed for enhanced liver regeneration.

The migration assays showed increased mobility of all tested subpopulations of MSCs to damaged HepG2 cells compared to healthy HepG2 cells. In all experiments, the VCAM-positive MSC subpopulations migrate more compared to VCAM-negative subpopulations. These results are in line with previous research of Gao et al. who also showed less migration of MSCs with altered VCAM expression³⁹. In contrast to the present study, they focused on Glioma cell- instead of hepatocyte- induced migration and used VCAM blocking antibodies instead of using different MSC populations. The SDF-1-CXCR4 gradient is a well-known pathway for

directed migration of MSCs²⁶. Several studies described that MSCs recognise tissue damage by higher SDF-1 concentrations in damaged tissue. The qPCR results of the present study showed higher expression of these genes in VCAM-positive compared to the VCAM-negative MSC subpopulations which might explain the faster migration of these cells as observed in our *in vitro* trans-well assays. Altogether, the current results indicate that properties of VCAM-positive MSCs are better suitable for the treatment of liver fibrosis as compared to the VCAM-negative MSC subpopulations.

Wound healing experiments with HepG2 cells showed faster wound closure upon MSC treatment, but surprisingly did not show differences between the different MSC subpopulations. Unexpectedly, the traced MSCs in these experiments formed hexagonal structures mimicking the structures observed in *in vivo* livers²⁴. We hypothesise that MSCs sense the old liver architecture and try to rebuild this structure. This 2D phenomenon has not been described before and further research is needed to study this architectural aspect in more detail.

Previous studies, including our own, showed that MSCs express proteins involved in tissue-regeneration (HGF, VEGF, IGF, and TGF- β 1)^{20,22,23,25,27,35,40}. HGF and IGF are thought to stimulate the survival and proliferation of liver-resident cells^{22,25,26,41}. Furthermore, HGF is known to inhibit stellate cell activation and is also able to silence activated myofibroblasts and thereby directly inhibiting the fibrogenic process^{19,23,25}. The present study showed higher expression levels of these genes in VCAM-positive subpopulations compared to the VCAM-negative subpopulations. These results are in line with earlier studies showing lower basal expression level of HGF, VEGF, and IGF in VCAM-negative MSC populations^{31,35}. However, these previous studies did not focus on fibrogenesis and therefore do not explain how their results might affect the potency of VCAM-positive or VCAM-negative MSCs to reverse fibrogenesis. Altogether these gene expression profiles might explain the results as observed in our current *in vitro* studies which showed that VCAM-positive populations protect and stimulate cell proliferation of damaged HepG2 cells. Furthermore, it could also explain the reduced collagen content observed in the mice treated with VCAM-positive MSC subpopulations.

The observed faster proliferation of wounded HepG2 cells *in vitro* was not observed *in vivo* where the weights of the regenerating livers were not affected by local MSC treatment. This might be explained by the time the livers were weighted (on day 8), since other studies observed differences in liver weight at an earlier stage⁴¹. Weighing on day 8 might have been too late to find differences in liver weight as all livers are already fully regenerated.

In the present study, no major functional differences between the V^{pos}E^{pos}-MSC and the V^{pos}E^{neg}-MSC populations were observed. Like Anderson et al., we found that the Endoglin-negative subpopulation was more prone to adipogenic differentiation compared to the Endoglin-positive subpopulations²⁹. Our results also showed that the V^{pos}E^{neg}-MSC population expresses higher

IGF and TGF- β 1 RNA levels. Fiore et al. described that IGF produced by MSCs could stimulate macrophage differentiation to an anti-inflammatory and anti-fibrotic phenotype²⁵. In our *in vivo* experiment we observed that V^{pos}E^{neg}-MSCs led to an intermediate reduction of collagen content compared to the control- or the V^{pos}E^{pos}-MSC-treated groups. One could speculate that the working mechanism of V^{pos}E^{pos}-MSCs is more HGF pathway related, directly targeting the stellate cells and myofibroblasts leading to a direct effect. On the other hand, as Anderson et al. suggested, it could be that V^{pos}E^{neg}-MSCs are working anti-inflammatory leading to an delayed, indirect, effect that might explain the observed intermediate result *in vivo*. Since the immunosuppressive capacity of MSCs was not in the scope of the present study we did not further evaluate this hypothesis.

Several studies have described the use of MSC treatment in relation to liver fibrosis in humans, rodents and zebrafish embryos^{12,18-20}. These studies showed contradictory results about the efficacy of MSC treatment on liver fibrosis. In the present study, we hypothesised that these observed differences might very well be due to the use of different subpopulations of MSCs. This hypothesis is strengthened by the present study, as we showed that mice treated with VCAM-positive MSC subpopulations showed a reduction in collagen content and less lobuli closure compared to mice treated with the VCAM-negative MSC subpopulations. Altogether, the present study showed that VCAM-positive MSCs subpopulations have advantageous properties for therapeutic interaction with regenerating fibrotic livers compared to VCAM-negative subpopulations indicating that patients with liver cirrhosis might benefit more from the treatment with VCAM-positive MSC subpopulations. Therefore, it is highly recommendable to include VCAM as a marker in the characterization panel of MSCs before use.

To conclude, VCAM-positive MSC subpopulations are more able to migrate and stimulate survival and proliferation of endogenous liver cells and contain a more pro-regenerative and anti-fibrotic RNA expression profile. Furthermore, the VCAM-positive population showed to be more effective in ameliorating fibrosis in an *in vivo* model for liver fibrosis and regeneration. Endoglin expression of MSCs have less functional implications regarding ameliorating liver fibrosis. These observations lead to the conclusion that the VCAM-positive subpopulation of MSCs is superior compared to the VCAM-negative population regarding their pro-regenerative and anti-fibrotic properties.

Acknowledgements

We thank the staff of the central animal facility of the LUMC for animal care.

Disclosure of conflicts of interest

The authors confirm that there are no conflicts of interest.

References

- 1 Byass, P. The global burden of liver disease: a challenge for methods and for public health. *Bmc Med* 2014; **12**:
- 2 Liver, E. A. S. EASL Recommendations on Treatment of Hepatitis C 2016. *J Hepatol* 2017; **66**: 153-194.
- 3 Mathurin, P., Hadengue, A., Bataller, R. *et al.* EASL Clinical Practical Guidelines: Management of Alcoholic Liver Disease. *J Hepatol* 2012; **57**: 399-420.
- 4 Marcellin, P. & Kutala, B. K. Liver diseases: A major, neglected global public health problem requiring urgent actions and large-scale screening. *Liver Int* 2018; **38**: 2-6.
- 5 Friedman, S. L. Mechanisms of hepatic fibrogenesis. *Gastroenterology* 2008; **134**: 1655-1669.
- 6 Lee, Y. A., Wallace, M. C. & Friedman, S. L. Pathobiology of Liver Fibrosis—A Translational Success Story (vol 64, pg 830, 2015). *Gut* 2015; **64**: 1337-1337.
- 7 Bataller, R. & Brenner, D. A. Liver fibrosis. *J Clin Invest* 2005; **115**: 209-218.
- 8 Marcellin, P., Gane, E., Buti, M. *et al.* Regression of cirrhosis during treatment with tenofovir disoproxil fumarate for chronic hepatitis B: a 5-year open-label follow-up study. *Lancet* 2013; **381**: 468-475.
- 9 Angaswamy, N., Tiriveedhi, V., Sarma, N. J. *et al.* Interplay between immune responses to HLA and non-HLA self-antigens in allograft rejection. *Hum Immunol* 2013; **74**: 1478-1485.
- 10 Lucidi, V., Gustot, T., Moreno, C. *et al.* Liver transplantation in the context of organ shortage: toward extension and restriction of indications considering recent clinical data and ethical framework. *Curr Opin Crit Care* 2015; **21**: 163-170.
- 11 Reddy, M. S., Rajalingam, R. & Rela, M. Liver transplantation in acute-on-chronic liver failure: lessons learnt from acute liver failure setting. *Hepatol Int* 2015; **9**: 508-513.
- 12 Berardis, S., Dwisthi Sattwika, P., Najimi, M. *et al.* Use of mesenchymal stem cells to treat liver fibrosis: current situation and future prospects. *World J Gastroenterol* 2015; **21**: 742-758.
- 13 Amer, M. E. M., El-Sayed, S. Z., Abou El-Kheir, W. *et al.* Clinical and laboratory evaluation of patients with end-stage liver cell failure injected with bone marrow-derived hepatocyte-like cells. *Eur J Gastroen Hepat* 2011; **23**: 936-941.
- 14 Gronthos, S., Zannettino, A. C. W., Hay, S. J. *et al.* Molecular and cellular characterisation of highly purified stromal stem cells derived from human bone marrow. *J Cell Sci* 2003; **116**: 1827-1835.
- 15 Parekkadan, B. & Milwid, J. M. Mesenchymal Stem Cells as Therapeutics. *Annu Rev Biomed Eng* 2010; **12**: 87-117.
- 16 Klyushnenkova, E., Mosca, J. D., Zernetkina, V. *et al.* T cell responses to allogeneic human mesenchymal stem cells: immunogenicity, tolerance, and suppression. *J Biomed Sci* 2005; **12**: 47-57.
- 17 Di Nicola, M., Carlo-Stella, C., Magni, M. *et al.* Human bone marrow stromal cells suppress T-lymphocyte proliferation induced by cellular or nonspecific mitogenic stimuli. *Blood* 2002; **99**: 3838-3843.

- 18 AlAhmari, L. S., AlShenaifi, J. Y., AlAnazi, R. A. *et al.* Autologous Bone Marrow-derived Cells in the Treatment of Liver Disease Patients. *Saudi J Gastroentero* 2015; **21**: 5-10.
- 19 Alfaihi, M., Eom, Y. W., Newsome, P. N. *et al.* Mesenchymal stromal cell therapy for liver diseases. *J Hepatol* 2018;
- 20 van der Helm, D., Groenewoud, A., de Jonge-Muller, E. S. M. *et al.* Mesenchymal stromal cells prevent progression of liver fibrosis in a novel zebrafish embryo model. *Sci Rep* 2018; **8**: 16005.
- 21 van der Helm, D., Barnhoorn, M. C., de Jonge-Muller, E. S. M. *et al.* Local but not systemic administration of mesenchymal stromal cells ameliorates fibrogenesis in regenerating livers. *J Cell Mol Med* 2019;
- 22 Fiore, E., Malvicini, M., Bayo, J. *et al.* Involvement of hepatic macrophages in the antifibrotic effect of IGF-I-overexpressing mesenchymal stromal cells. *Stem Cell Res Ther* 2016; **7**: 172.
- 23 Najimi, M., Berardis, S., El-Kehdy, H. *et al.* Human liver mesenchymal stem/progenitor cells inhibit hepatic stellate cell activation: in vitro and in vivo evaluation. *Stem Cell Res Ther* 2017; **8**: 131.
- 24 Huang, B., Cheng, X., Wang, H. *et al.* Mesenchymal stem cells and their secreted molecules predominantly ameliorate fulminant hepatic failure and chronic liver fibrosis in mice respectively. *J Transl Med* 2016; **14**: 45.
- 25 Fiore, E. J., Bayo, J. M., Garcia, M. G. *et al.* Mesenchymal stromal cells engineered to produce IGF-I by recombinant adenovirus ameliorate liver fibrosis in mice. *Stem Cells Dev* 2015; **24**: 791-801.
- 26 Li, Q., Zhou, X., Shi, Y. *et al.* In vivo tracking and comparison of the therapeutic effects of MSCs and HSCs for liver injury. *PLoS One* 2013; **8**: e62363.
- 27 Deng, Y., Zhang, Y., Ye, L. *et al.* Umbilical Cord-derived Mesenchymal Stem Cells Instruct Monocytes Towards an IL10-producing Phenotype by Secreting IL6 and HGF. *Sci Rep* 2016; **6**: 37566.
- 28 Siegel, G., Kluba, T., Hermanutz-Klein, U. *et al.* Phenotype, donor age and gender affect function of human bone marrow-derived mesenchymal stromal cells. *Bmc Med* 2013; **11**: 146.
- 29 Anderson, P., Carrillo-Galvez, A. B., Garcia-Perez, A. *et al.* CD105 (endoglin)-negative murine mesenchymal stromal cells define a new multipotent subpopulation with distinct differentiation and immunomodulatory capacities. *PLoS One* 2013; **8**: e76979.
- 30 Morikawa, S., Mabuchi, Y., Kubota, Y. *et al.* Prospective identification, isolation, and systemic transplantation of multipotent mesenchymal stem cells in murine bone marrow. *J Exp Med* 2009; **206**: 2483-2496.
- 31 Han, Z. C., Du, W. J., Han, Z. B. *et al.* New insights into the heterogeneity and functional diversity of human mesenchymal stem cells. *Biomed Mater Eng* 2017; **28**: S29-S45.
- 32 Niibe, K., Zhang, M., Nakazawa, K. *et al.* The potential of enriched mesenchymal stem cells with neural crest cell phenotypes as a cell source for regenerative dentistry. *Jpn Dent Sci Rev* 2017; **53**: 25-33.
- 33 Buhring, H. J., Tremel, S., Cerabona, F. *et al.* Phenotypic characterization of distinct human bone marrow-derived MSC subsets. *Ann N Y Acad Sci* 2009; **1176**: 124-134.
- 34 Yang, Z. X., Han, Z. B., Ji, Y. R. *et al.* CD106 identifies a subpopulation of mesenchymal stem cells with unique immunomodulatory properties. *PLoS One* 2013; **8**: e59354.

- 35 Du, W., Li, X., Chi, Y. *et al.* VCAM-1+ placenta chorionic villi-derived mesenchymal stem cells display potent pro-angiogenic activity. *Stem Cell Res Ther* 2016; **7**: 49.
- 36 Molendijk, I., Barnhoorn, M. C., de Jonge-Muller, E. S. *et al.* Intraluminal Injection of Mesenchymal Stromal Cells in Spheroids Attenuates Experimental Colitis. *J Crohns Colitis* 2016; **10**: 953-964.
- 37 GM Higgins, R. A. *Experimental pathology of the liver.* . Vol. 12 186-202 (1931).
- 38 Blachier, M., Leleu, H., Peck-Radosavljevic, M. *et al.* The burden of liver disease in Europe: a review of available epidemiological data. *J Hepatol* 2013; **58**: 593-608.
- 39 Gao, Z., Cheng, P., Xue, Y. *et al.* Vascular endothelial growth factor participates in modulating the C6 glioma-induced migration of rat bone marrow-derived mesenchymal stem cells and upregulates their vascular cell adhesion molecule-1 expression. *Exp Ther Med* 2012; **4**: 993-998.
- 40 Barnhoorn, M., de Jonge-Muller, E., Molendijk, I. *et al.* Endoscopic Administration of Mesenchymal Stromal Cells Reduces Inflammation in Experimental Colitis. *Inflamm Bowel Dis* 2018; **24**: 1755-1767.
- 41 Fouraschen, S. M. G., Pan, Q. W., de Ruiter, P. E. *et al.* Secreted Factors of Human Liver-Derived Mesenchymal Stem Cells Promote Liver Regeneration Early After Partial Hepatectomy. *Stem Cells Dev* 2012; **21**: 2410-2419.

Supplementary files

Supplemental table 1: Primer sequences

Gene	Abbreviation	Forward	Reverse
<i>Hepatocyte growth factor</i>	HGF	AAGAGTGGCATCAAATGCCAG	CTGGATTGCTTGTGAAACACC
<i>Vascular endothelial growth factor</i>	VEGF	CACAGCAGATGTGAATGCAG	TTTACACGTCTGCGGATCTT
<i>Insulin-like growth factor</i>	IGF	CTACAAAAGCAGCCCGCTCT	CTTCTGAGTCTTGGGCATGTCA
<i>Transforming growth factor-β1</i>	TGF- β 1	CAACAATTCCTGGCGTTACC	TGCTGTCACAAGAGCAGTGA
<i>Stromal derived factor 1</i>	SDF-1	GAAAGGAAGGAGGGTGGCAG	TCCCCGTCTTCTCGAGTGT
<i>CXCR4</i>	CXCR4	TTACCCCGATAGCCTGTGGA	GCAGGACGAGACCCACCAT
<i>Vascular cell adhesion protein</i>	VCAM	TGCCGAGCTAAATTACACATTG	CCTTGTGGAGGGATGTACAGA
<i>Glyceraldehyde 3-phosphate dehydrogenase</i>	GAPDH	AACCTTGGCATTGTGGAAGG	ACACATTGGGGGTAGGAACA

CHAPTER 4



Mesenchymal stromal cells prevent progression of liver fibrosis in a novel zebrafish embryo model

Danny van der Helm, Arwin Groenewoud, Eveline S.M. de Jonge-Muller, Marieke C. Barnhoorn, Mark J.A. Schoonderwoerd, Minneke J. Coenraad, Luuk J.A.C. Hawinkels, Ewa B. Snaar-Jagalska, Bart van Hoek*, Hein W. Verspaget*

*Joint senior authorship

Abstract

Background

Chronic liver damage leads to the onset of fibrogenesis. Rodent models for liver fibrosis have been widely used, but are less suitable for screening purposes. Therefore the aim of our study was to design a novel model for liver fibrosis in zebrafish embryos, suitable for high throughput screening. Furthermore, we evaluated the efficacy of mesenchymal stromal cells (MSCs) to inhibit the fibrotic process and thereby the applicability of this model to evaluate therapeutic responses.

Methods

Zebrafish embryos were exposed to TAA or CCL4 and mRNA levels of fibrosis-related genes (Collagen-1 α 1, Hand-2, and Acta-2) and tissue damage-related genes (TGF- β and SDF-1a, SDF-1b) were determined, while Sirius-red staining was used to estimate collagen deposition. Three days after start of TAA exposure, MSCs were injected after which the fibrotic response was determined.

Results

In contrast to CCL4, TAA resulted in an upregulation of the fibrosis-related genes, increased extracellular matrix deposition and decreased liver sizes suggesting the onset of fibrosis. The applicability of this model to evaluate therapeutic responses was shown by local treatment with MSCs which resulted in decreased expression of the fibrosis-related RNA markers.

Conclusion

In conclusion, TAA induces liver fibrosis in zebrafish embryos, thereby providing a promising model for future mechanistic and therapeutic studies.

Introduction

The liver is a vital organ with distinct functions like detoxification, metabolism and immune defence. Chronic exposure of the liver to injuring circumstances, like viral hepatitis infection, chronic alcohol abuse, steatohepatitis and cholestatic disease results to apoptotic hepatocytes and subsequent stellate cell activation which differentiate into myofibroblasts¹⁻³. These myofibroblasts are the main source of progressive deposition of extracellular matrix (ECM) components, which leads to fibrogenesis¹⁻³.

To understand the pathogenesis and investigate novel therapeutic interventions diverse model systems for fibrogenesis have been used. These include *in vivo* mouse and rat models, mostly based on the well-known carbon tetrachloride (CCL4) or thioacetamide (TAA) induced liver fibrosis. Both compounds are metabolised by the hepatocytes into hepatotoxic metabolites leading to apoptosis of these cells and subsequently activation and proliferation of stellate cells^{4,5}. These mouse models have been proven valuable, but are expensive and time consuming, as it takes 6 and 12 weeks to induce a chronic fibrosis or cirrhosis, respectively. Furthermore, administration of the toxic compounds in mice may cause acute toxicity, sometimes leading to death of the mice. Finally, using the CCL4 method non-liver related side effects like intraperitoneal adhesions have been reported⁴. These drawbacks make these models less attractive for high throughput compound screening.

Zebrafish embryos are often used to perform high throughput drug screens⁶. Beneficial characteristics of zebrafish embryos as model organisms include the convenience to house these small-sized animals, the short generation time, ease of embryo accessibility, low costs and transparency of the organism in the early development⁷⁻⁹. With respect to liver physiology, the zebrafish shows a 70% similarity to the human liver, including the same cell types as observed in the human liver (e.g., hepatocytes, stellate cells, biliary cells and endothelial cells)^{7,10}. In mature zebrafish, TAA or ethanol dissolved in aquarium water has been reported to induce liver fibrosis with similar mechanism as observed in humans¹¹⁻¹³. This makes zebrafish embryos an attractive model for liver fibrosis and to screen new therapeutic compounds in a high throughput screening fashion.

A limited number of studies have reported on models of liver fibrosis in zebrafish embryos. Addition of ethanol in aquarium water shows an acute fibrotic response in zebrafish embryos, characterised by increased collagen and Hand-2 (stellate cell proliferation marker) protein levels¹⁴⁻¹⁷. However, fibrotic effects of the hepatotoxic compounds CCL4 and TAA has not been investigated. In the present study we aim to translate the widely used CCL4 and TAA mouse models for liver fibrosis to zebrafish embryos in order to obtain a new model which is suitable for high throughput studies and show its applicability to study therapeutic effects.

Liver fibrosis is one of the most prevalent diseases in the western world and no real treatment for end-stage cirrhosis, besides liver transplantation, exists^{18–20}. Novel treatments to reverse fibrogenesis are needed. Promising results regarding the effect on fibrogenesis have been obtained from *in vivo* experimental and clinical studies using mesenchymal stromal cells (MSCs)^{21–25}. MSCs are stromal cells which can be easily isolated from various tissue sources, expanded in culture and are not rejected after transplantation^{23,26,27}. Positive functional characteristics of MSCs are their ability to modulate the immune system and their role in the repair and regeneration of damaged tissue^{23,28}. In relation to liver fibrosis several animal studies already showed that MSCs can inhibit and reverse the fibrotic process^{24,25,29,30}. Supposed mechanisms for this effect include improvement of hepatocyte survival, inhibition of stellate cell activation, and proliferation and silencing of myofibroblasts^{24,25,29,31,32}. MSCs and fibroblasts are both stromal cells with overlapping functions in the organisation of extracellular matrix. However, studies comparing both cell types side by side are limited. Therefore, we established a new high throughput zebrafish embryo model for liver fibrosis and evaluated its applicability to test potential new therapeutics by testing the ability of injected MSCs and fibroblasts to reduce the induction of liver fibrosis.

Material and Methods

Induction of liver fibrosis in zebrafish embryos

Housing and experiments were done according to the Dutch guidelines for the care and use of laboratory animals and approved by the animal welfare committee of the Leiden University. Carbon tetrachloride (CCL4) and thioacetamide (TAA) were used to induce liver fibrosis in liver-fatty-acid-binding-protein (LFABP)-GFP zebrafish embryos from the Leiden University breeding facility, which only express GFP in the liver⁴². For the CCL4 model, zebrafish embryos were injected in the yolk sack once [2 days post fertilization (dpf)] or twice (2dpf and 4dpf) with 0.25 M CCL4 diluted in mineral oil or mineral oil control (Sigma-Aldrich Chemie BV, Zwijndrecht, The Netherlands) (Supplemental Figure 1A,B). Different volumes (1 nl, 5 nl and 10 nl) of 0.25 M CCL4 were evaluated. Injections were done on tricaine mesylate (Sigma-Aldrich) tranquilized embryos, fixed to an agar coated plate with use of a microinjector (20 psi, PV820 Pneumatic PicoPump, World Precision Instruments) using needles pulled from borosilicate capillaries (O.D. 1.0 mm × I.D. 0.78 mm, Science products, Hofheim, Germany) and Leica MS55 stereo microscope visualization⁴³.

For the TAA model, 2dpf zebrafish embryos were treated by adding TAA for 6 days in the egg water (water with 60 µg/ml instant ocean, sea salt). Different concentrations of TAA were tested (0.0075%, 0.015%, 0.03%, 0.06%, 0.12%, 0.24%) to evaluate the induction of fibrosis (Supplemental Figure 1C).

At the end of the experiment, the embryos were imaged, fixated in 4% buffered paraformaldehyde for paraffin embedding or stored in PAXgene blood RNA solution (PreAnalytiX, Hombrechtikon, Switzerland) for RNA isolation. Furthermore, embryos were imaged by bright field and GFP fluorescent microscopy (2x magnification, Olympus IX53) to image the total embryo and the liver, respectively. Embryo and liver size were quantified using ImageJ analysis software (ImageJ 1.47v, National Institutes of Health, USA).

MSC and fibroblast cell culture and treatment

MSCs were isolated from the bone marrow of 8–10 week old male mT/mG C57Bl/6Jico mice obtained from an LUMC breeding population. These mice express red fluorescence protein (RFP) in all cells⁴⁴. Mice were sacrificed by cervical dislocation, femur and tibia were collected. Subsequently, bones were flushed with RPMI cell culture medium supplemented with 10% fetal calf serum (FCS; Gibco, 3mM L-glutamine (Invitrogen Corp., Paisley, UK), penicillin/streptomycin (Pen/Strep; Invitrogen Corp., Paisley, UK) and 2% Heparin (Pharmacy AZL). Isolated cells were cultured in α MEM culture medium (Lonza) supplemented with 10% FCS, 3mM L-glutamine and P/S. Non-adhering cells were removed by refreshing the media after 24, 48 and 72 h. GFP expressing colon fibroblasts were isolated from GFP-actin male mice and cultured in DMEM/F12 culture media supplemented with Pen/Strep and 10% FCS.

Approximately 100 MSCs or fibroblasts in 1 nl polyvinylpyrrolidone (PVP) or PVP only as a control were injected in closest proximity to the liver at 5dpf of 0.06% TAA treated or healthy zebrafish embryos. After cell therapy, TAA treatment was continued until the end of the experiment (Supplemental Figure 1D). At the end of the experiment, the embryos were imaged and subsequently fixated in 4% paraformaldehyde for paraffin embedding and stored in PAXgene RNA storage solution for RNA isolation.

Phenotypical and functional characterization of MSCs

To characterize the bone marrow derived MSCs, cells were incubated with fluorescent conjugated antibodies: CD29-PE-Cy7, C45-PE-Cy-7, SCA-1-PE-Cy-7, CD31-APC (eBioscience, Vienna, Austria), CD44-APC, CD105-BV786 or CD106-V450 (BD Pharmingen, San Diego, CA, USA). LSR II flow cytometer (BD Biosciences, San Diego, CA, USA), with FACS-diva software (version 8.7.1, Tree Star Inc. Ashland, OR, USA) were used to measure the fluorescence intensity. FlowJow software (version 8.7.1., Tree Star Inc. Ashland, OR, USA) was used for data analysis. Functional characterization was done by testing the ability of MSCs to differentiate in osteoblasts and adipocytes. Experiments were performed as earlier described by our group⁴⁵. In short, MSCs were cultured with osteogenic or adipogenic differentiation medium. Osteogenic differentiation medium consists of complete medium with 10 nM dexamethason, 50 μ g/ml ascorbic acid and 10 mM β -glycerophosphate (all from Sigma-Aldrich Chemie BV, Zwijndrecht, The Netherlands). Adipogenic differentiation medium consists of complete medium with 1 μ M dexamethason, 5 μ M insulin, 100 μ M indomethacin and 0.5 mM 3-isobutyl-

1-methylxanthine (all from Sigma-Aldrich Chemie BV, Zwijndrecht, The Netherlands). After 21 days, differentiation was verified by fast blue staining for alkaline phosphatase expression and Alizarin red for calcium deposition (both Sigma-Aldrich Chemie BV, Zwijndrecht, The Netherlands). Oil-red-O staining was used to visualize lipid droplets and used as a marker for adipogenic differentiation.

Histological examination

Paraffin sections of 4 μm were cut, hydrated and stained with Sirius-red and Hematoxylin-Eosin (H&E) solutions. For Sirius-red staining, sections were incubated for 90 min with 1 g/L Sirius-red F3B in picric acid (both Klinipath) and subsequently incubated for 10 min with 0.01 M HCl. H&E staining was performed by 5 min incubation with Hematoxylin solution (Mayer, Merck) followed by a 10 min wash with tap water and a 30 seconds Eosin staining (Sigma). After the staining slides were dehydrated and mounted with Entellan (Merck KGaA).

Immunohistochemistry

In order to detect the fibroblasts and MSCs in the zebrafish embryos, sections were stained for mouse specific Vimentin. In short, sections were hydrated and endogenous peroxidases were blocked by 20 min incubation with 0.3% H₂O₂/methanol at room temperature (RT). Next, antigen retrieval was performed by boiling the section for 10 min in citrate buffer (0.1 M, pH6.0), cooled down and incubated overnight with a rabbit anti mouse Vimentin antibody at 4 °C (Cell signalling). Subsequently, slides were incubated for 1 h with a secondary goat anti rabbit-HRP conjugated antibody followed by a 10 min incubation with 3,3'-diaminobenzidine (DAB Fast Tablet, Sigma-Aldrich, St. Louis, MO). Nuclear counterstaining was performed with Hematoxylin after which the sections were dehydrated and mounted with Entellan.

RNA isolation, cDNA synthesis and Quantitative polymerase chain reaction (qPCR)

Zebrafish embryos (N = 25) were dissolved for 2 days at 4 °C in PAXgene Blood RNA solution (PreAnalytiX). mRNA from the total embryo lysates, MSCs and fibroblasts was isolated with NucleoSpin RNA kit (Machery-Nagel GmbH, Düren, Germany). cDNA was synthesised with 1 μg RNA incubated with M-MLV transcriptase, dNTPS, random primers and RNasin ribonuclease inhibitor according to manufacturers' protocol (Promega, Madison, Wisconsin, USA). Quantative PCR was performed with a mix consisting of 1 nl cDNA, 1 nM primer and 5 μl iQ SYBR Green supermix reagent (Bio-Rad Laboratories, Berkeley, California, USA). In mRNA samples of the zebrafish embryos, expression levels of fibrosis- (Colagen-1 α 1, Hand-2, Acta-2), inflammatory- (TGF- β , SDF-1a, SDF-1b) and liver function genes (group-specific component, alpha-1 antitrypsin and serum amyloid A) were evaluated and normalised to ribosomal protection protein (RPP), which was used as reference gene. mRNA expression of pro-regenerative and fibrogenesis inhibitory genes (HGF, VEGF, IGF-1, TGF- β and SDF-1)

in the cultured MSCs and fibroblasts levels was measured and normalised to GAPDH, which was used as reference gene (Supplemental Table 1: primer sequences).

Statistical Analysis

GraphPad Prism software was used for statistical analysis and p-values lower than 0.05 were considered to be statistically significant (GraphPad Software, version 5.01, San Diego, CA). One-Way ANOVA test was used to compare 3 or more groups. Two groups comparisons were performed with Student's t-test. Results are displayed as the means \pm standard error of the mean (SEM). All data shown are from two or three independent experiments, using group sizes of 25–50 embryos.

4

Results

CCL4 administration does not induce liver fibrosis in zebrafish embryos

Due to the hydrophobic characteristic of CCL4, this compound could not be dissolved in the egg water and was therefore injected in the yolk sac of the zebrafish embryo. To find the optimal dose, 0.25 M CCL4 was 1 (2dpf) or 2 times (2 and 4dpf) injected to the yolk sac of the embryo. Survival analysis of the CCL4 treated embryos indicated toxic effects at higher volumes/doses. A single injection of 10 nl CCL4 did lead to phenotypic toxic effects (like oedema in heart cavity or malformations) and was lethal for all embryos within 2 days after administration. Embryos receiving two CCL4 injections resulted in 40–50% survival regardless of the injected volume (Figure 1A). In these groups no phenotypic toxic effects were observed. Furthermore, CCL4 administration did not lead to differences in embryo and liver sizes compared to the control groups (Figure 1B). When analysing extracellular matrix deposition by Sirius-red staining, no structures of collagen deposition were observed (data not shown). Furthermore expression of the fibrosis-related genes (collagen-1 α 1, Acta-2 and Hand-2) (Figure 1C–E) was not affected. Also the inflammation and damage (TGF- β , SDF-1a, SDF-1b) or liver function (GC or α 1AT) related mRNA expression levels were not consistently affected (Figure 1F–K). Only the acute phase protein SAA was significantly upregulated in all groups compared to the control embryos (Figure 1J). These data indicate an acute toxic effect of CCL4 injection without signs of induction of liver fibrosis.

TAA treatment induces liver fibrosis in zebrafish embryos

TAA is a hydrophilic compound which can be easily dissolved in egg water. After analysing increasing doses of TAA, we observed that treatment with 0.24% and 0.48% TAA induced an acute toxic effect with oedema in the heart cavity and all embryos died within 2 to 4 days after start of the treatment (Figure 2A). None of the other groups showed any signs of toxicity, also the total embryo size was not affected (data not shown). Liver size relative to total embryo, however, was smaller in all groups that received TAA, except for the lowest concentration

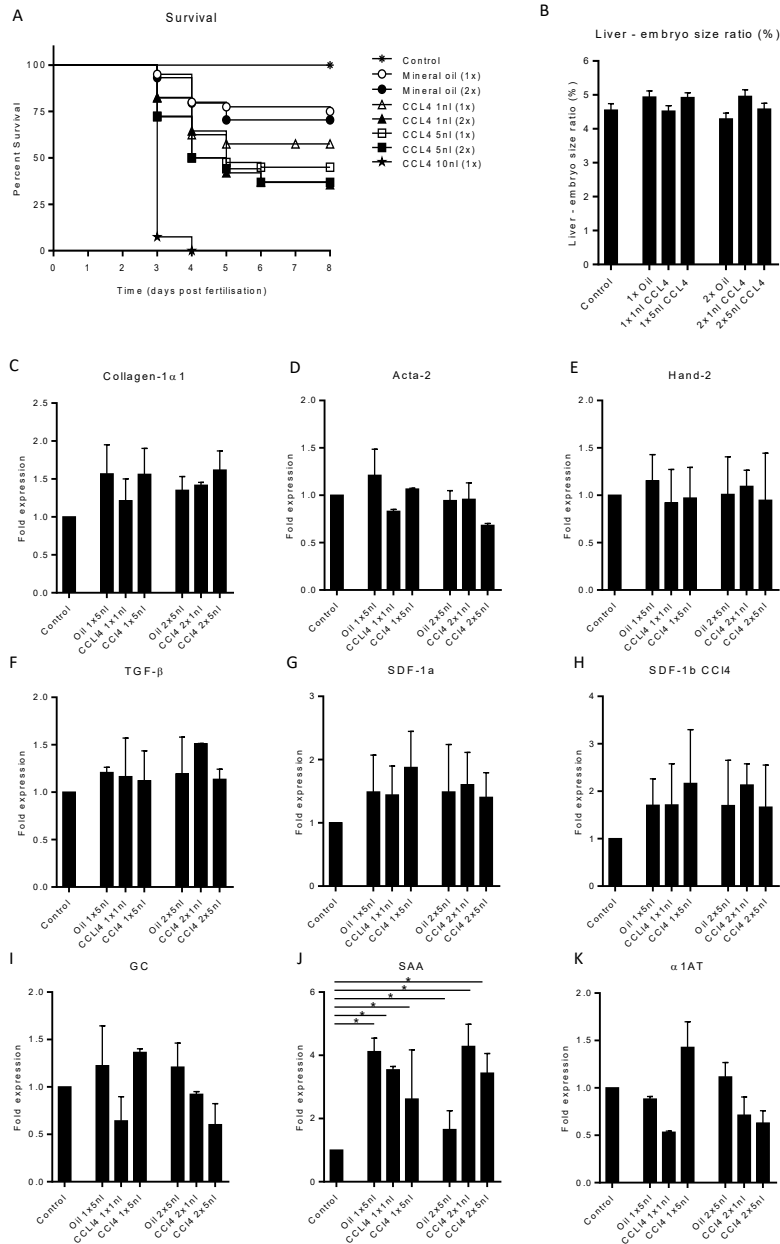


Figure 1. CCL4 administration does not induce liver fibrosis in de zebrafish embryos. Zebrafish embryos (2dpf) were injected in the yolk sac with various volumes and frequencies of 0.25M CCL4 or mineral oil as a control. (A) Survival of the embryos during CCL4 treatment (N = 50 embryos, \pm SEM). (B) At 8dpf the embryos were imaged to measure the sizes of the liver and total embryo in order to calculate the liver to embryo size ratio (N = 50 embryos). (C–K) Quantitative PCR for mRNA expression of fibrotic, tissue damage and liver function related genes after CCL4 administration. Expression levels of Collagen1 α 1, Acta-2, Hand-2, TGF β , SDF β , SDF-1a, SDF-1b, GC, SAA and α 1AT are normalized to RPP and to healthy control embryos. The graphs represent values of three independent experiments (n = 3, \pm SEM). *p \leq 0.05.

indicating an TAA effect on the liver (Figure 2B). To analyse collagen deposition a Sirius-red staining was performed. This analysis revealed subtle structures of collagen deposition between the hepatocytes in the 0.03%, 0.06% and 0.12% TAA treated embryos (Figure 2C). Also the cells and total liver architecture seemed to be disturbed in the higher doses compared to control and lower dosages (0.0075% and 0.015% TAA). These results indicate an effect of TAA treatment on the liver and a possible onset of fibrogenesis in the 0.03%, 0.06% and 0.12% TAA treatment groups.

Furthermore, qPCR analysis showed increased expression of collagen mRNA levels in the 0.06% and 0.12% TAA groups (Figure 3A). Acta-2 and Hand-2 expression levels were higher in the 0.06% TAA treated group compared to the other groups (Figure 3B,C). Furthermore,

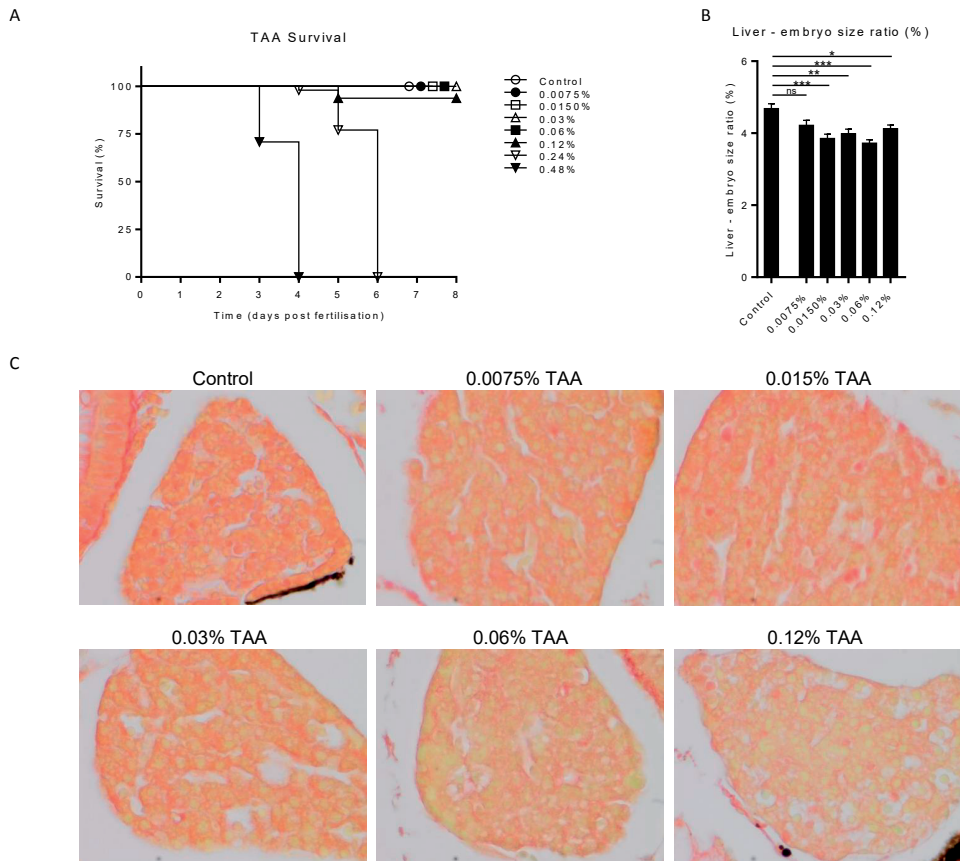


Figure 2. Thioacetamide titration in zebrafish embryos. Zebrafish embryos (2dpf) were treated until 8dpf with different concentrations of TAA in egg water. (A) Survival of the embryos during TAA treatment (N = 50 embryos). (B) At 8dpf the embryos were imaged to measure the sizes of the liver and total embryo in order to calculate the liver to embryo size ratio (N = 2, \pm SEM). (C) Sirius-red stained section of TAA treated zebrafish embryo livers (8dpf, 400x magnification). * $p \leq **p \leq 0.01$, *** $p \leq 0.001$.

the tissue damage/inflammatory genes, TGF- β , SDF-1a, SDF-1b, show a trend toward higher expression levels in the 0.06% TAA treated group (Figure 3D–F). The liver function related genes, GC and SAA showed a similar trend. No significant effect on α 1AT RNA level was observed (Figure 3G–I). To study these expression levels more locally, head, trunk (including the liver) and tail of the embryos were separated and RNA was isolated. Observed expression levels of fibrotic, inflammatory/damage and liver function related genes in the trunk reveal a similar trend as the expression levels found in whole embryo RNA isolations. Furthermore, this

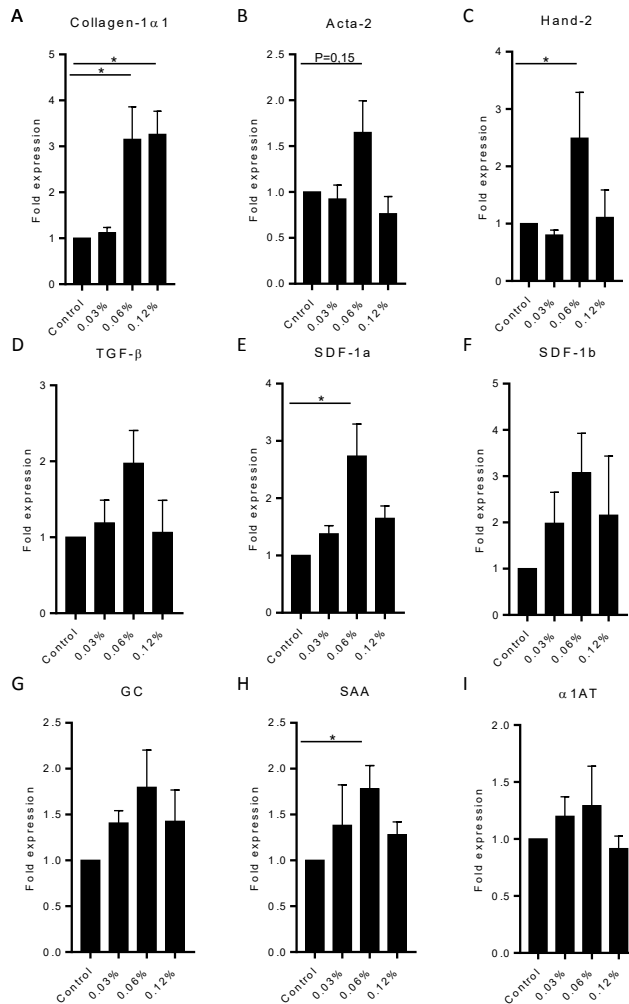


Figure 3. RNA expression levels after TAA treatment. Quantitative PCR for mRNA expression of fibrotic, tissue damage and liver function genes after TAA treatment (8dpf). (A–I) Expression levels of Collagen1 α 1, Acta-2, Hand-2, TGF- β , SDF-1a, SDF1-b, GC, SAA and α 1AT are normalized to RPP and to healthy control embryos. The graphs represent values of three independent experiments ($n = 3$, \pm SEM). * $p \leq 0.05$.

effect was not observed in pooled head and tail RNA samples of 0.06% TAA treated embryos (Figure 4A–I). Altogether these data indicate an consistent induction of liver fibrosis in the 0.06% TAA treatment group, as shown by increased expression of fibrosis related genes and increased deposition of collagen.

MSCs ameliorate TAA induced fibrosis in zebrafish embryos

To study if therapeutic interventions can be tested in this model, MSCs and fibroblast were used. First, the MSCs were phenotypical and functionally characterized. MSCs were positive for the membrane MSC markers CD29, CD44, CD105, CD106 and SCA-1 and negative for the hematopoietic marker CD45 and endothelial marker CD31 (Supplemental Figure 2A). To analyze their multipotency differentiation assays followed by fast blue, alizarin-red and oil-red-o staining were performed. Positive staining for osteogenic markers, and presence of

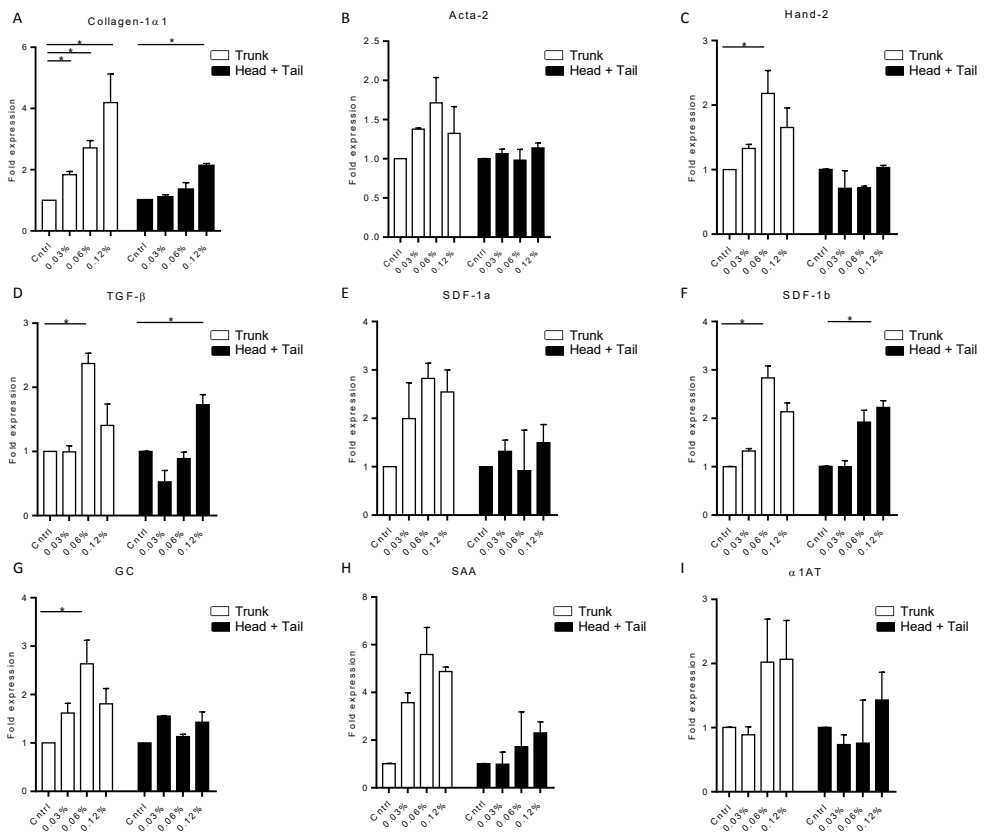


Figure 4. Gene expression changes in the trunk region compared to head and tail pools Quantitative PCR for mRNA expression of fibrotic, tissue damage and liver function genes after TAA treatment. The trunk region was compared to het pooled head and tail RNA expression levels. (A–I) Expression levels of Collagen1 α 1, Acta-2, Hand-2, TGF- β , SDF-1a, SDF1-b, GC, SAA and α 1AT are normalized to RPP and to healthy control embryos. The graphs represent values of three independent experiments (n = 3, \pm SEM). *p \leq 0.05.

lipid droplets in the adipogenic differentiation medium showed that the MSCs can undergo osteogenic- and adipogenic differentiation (Supplemental Figure 2B). Based on the expressed membrane markers and the ability to differentiate into different lineages these cells were defined as MSCs.

MSCs, fibroblasts or a solvent control (PVP), were injected 3 days after the start of 0.06% TAA treatment (5dpf), in close proximity to the liver. MSCs expressing the RFP construct could be detected in 7 out of 8 of the embryos (87.5%) at the end of the experiment in the TAA treated group. Surprisingly, MSCs injected in control embryos could be traced in only 2 out of 8 embryos (25%). Traced MSCs were observed around the injection area and further cell migration to, for example, the tail, was not observed (Figure 5A). In concordance, mouse specific Vimentin staining also revealed that both MSCs and fibroblasts could be traced until the end of the experiment (Figure 5B).

Treatment with either MSCs or fibroblasts both abolished the effect of TAA treatment on liver size (Figure 6A), compared to control. MSC treatment in embryos with liver fibrosis consistently reduced the RNA expression levels of collagen and TGF- β compared to embryos without MSC treatment (Figure 6B,E). Acta-2 and Hand-2 expression were also downregulated, although this did not reach statistical significance (Figure 6C,D). Fibroblast or PVP solvent control administration resulted in an intermediate reduction of these genes. No changes in SDF-1a and SDF-1b expression levels were observed after MSC treatment. Expression levels

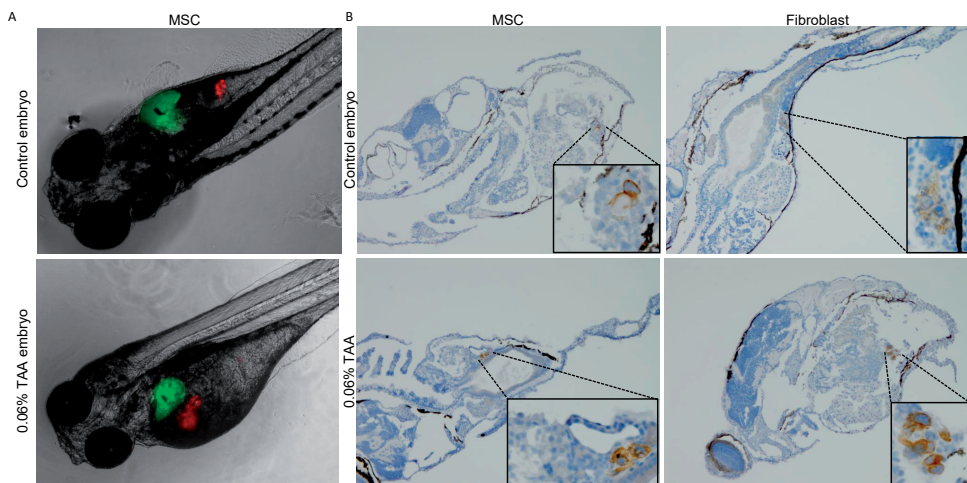


Figure 5. MSC and fibroblast tracing at 8dpf. During fibrotic induction (5dpf) with 0.06% TAA fibroblasts and MSCs were injected in close proximity to the liver. (A) Representative fluorescence images of zebrafish after MSC administration (8dpf) liver (green) and MSCs (red) (20x magnification). (B) Representative Vimentin stained section of fibroblast or MSC treated embryos (20x magnification).

of GC and α 1AT upon MSC treatment revealed a trend towards normal levels (Figure 6H,J). SAA expression levels were non-significantly elevated upon MSC administration (Figure 6I). Sirius-red staining for collagen deposition revealed a normalised liver architecture with less collagen structures after MSC or fibroblast administration (Figure 6K).

To evaluate how MSCs could potentially prevent progression of liver fibrosis, qPCR analysis on cultured cells was performed to determine if growth factors, which have been described to stimulate tissue regeneration and inhibit fibrogenesis, were expressed. Results showed that cultured MSCs express HGF, IGF-1, VEGF, TGF β and SDF-1, all important factors in tissue regeneration and reversing fibrosis (Figure 7). Fibroblasts had lower expression levels of these

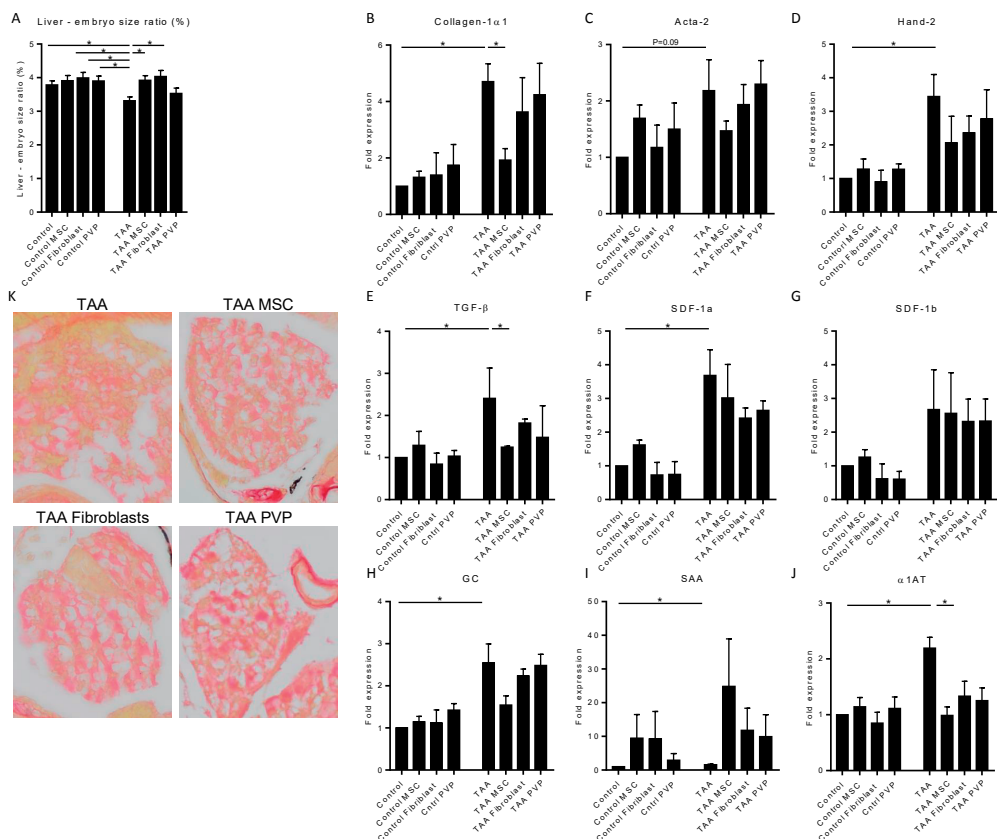


Figure 6. MSCs prevent the progression of liver fibrosis in zebrafish embryos. Quantitative PCR for mRNA expression of fibrotic, tissue damage and liver function genes after TAA treatment and MSC, Fibroblast or PVP injections. (A) At 8dpf the embryos were imaged to measure the sizes of the liver and total embryo in order to calculate the liver to embryo size ratio (N = 2, \pm SEM). (B–J) Expression levels of Collagen1 α 1, Acta-2, Hand-2, TGF- β , SDF-1a, SDF1-b, GC, SAA and α 1AT are normalized to RPP and to healthy control embryos. The graphs represent values of three independent experiments (n = 3, \pm SEM). *p \leq 0.05.

genes, except for SDF-1. Unfortunately analysis of the expression levels of these genes in the zebrafish embryo was not possible. The low number of cells injected resulted in expression levels below the detection limit of the qPCR.

Altogether these results indicate that MSCs ameliorate TAA-induced liver fibrosis in zebrafish embryos and show the applicability to use this model to test new therapeutic interventions for liver fibrosis.

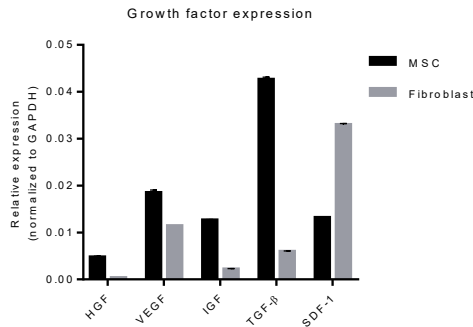


Figure 7. Pro-regenerative and fibrosis inhibitory gene expression levels in cultured MSCs and fibroblasts. Quantitative PCR for mRNA expression of pro-regenerative and fibrosis inhibitory genes in cultured MSCs and fibroblasts. Expression levels of HGF, VEGF, IGF-1, TGF- β and SDF-1 are normalized to GAPDH. The graphs represent values of two independent experiments (n = 2, \pm SEM).

Discussion

Cirrhosis mostly evolves when the liver is chronically challenged by harmful impulses like alcohol or hepatitis viruses. Treatment is limited to the removal of the harmful stimuli or a liver transplantation^{19,20}. Although many studies already have been done no real new therapeutic strategies to counter fibrogenesis have emerged yet. In most of these studies mice and rats were used as animal models which, are although valuable, are not suitable for high throughput screening. Our current study shows that zebrafish embryos can be used as a robust and reliable novel model system for liver fibrosis. We found that 0.06% TAA treatment induced liver fibrosis, characterized by increased RNA expression of collagen, Hand-2 and Acta-2, smaller liver sizes and collagen deposition. Applicability to analyse novel therapeutic interventions was shown by the administration MSCs and fibroblasts as potential novel cell therapies. Results showed that MSCs, in contrast to fibroblasts, were able to considerably prevent the progression of TAA-induced liver fibrosis in the zebrafish embryos.

Chronic intraperitoneal administration of CCL4 is a frequently used model to induce liver fibrosis in mice and rats. Due to the long time to induce fibrosis, the costs and workload

these models are not suitable for high throughput screening^{7,8}. Based on the results from the present study, CCL4 is not capable of inducing fibrosis in zebrafish embryos in non-toxic dosages. No structures of collagen deposition or upregulation of fibrotic, inflammation or damage related genes were observed in CCL4 injected embryos. Altogether this indicates that CCL4 yolk sac injections do not lead to liver fibrosis in zebrafish embryos.

Next, we studied the ability of different concentrations of TAA dissolved in egg water to induce liver fibrosis. Survival and liver size measurements reveal a toxic effect to the embryos since the two highest dosages of TAA (0.24% and 0.48%) were lethal and showed oedema in the heart cavity. Lower dosages of TAA were not lethal and led to smaller liver sizes after 6 days of treatment. The shrinkage of the liver is a well-known feature of fibrotic livers in animals and humans. Amali and Huang *et al.*, like us, also observed this liver shrinkage when zebrafish embryos were treated with TAA or ethanol, respectively^{12,16}. However, the TAA study of Amali *et al.* focused on a model for steatosis but did not evaluate the induction of fibrosis. In the present study we focused on the ability and mechanisms of TAA to induce fibrogenesis.

Sirius-red staining, showed structures of collagen deposition in the livers of the 0.03, 0.06 and 0.12% TAA treatment groups but looked different compared to the structures observed in fibrotic mouse and human livers¹¹. This difference can be due to the well-known different cell organisation within the liver of the fish compared to humans. The zebrafish liver does not have the typical lobular architecture of the liver of human and mice consisting of 6 portal triads (location of stellate cells) surrounding the hepatocytes and one central vein in the middle. These veins, arteries, bile ducts, hepatocytes and stellate cells are less well organised in the zebrafish⁷. These fundamental architectural differences could be the reason that the collagen structures found upon TAA treatment looked different compared to the septa-like structures found in fibrotic livers of human and mice.

Our data show that collagen RNA expression was also upregulated in 0.06% and 0.12% TAA treated embryos. These results are in line with several other studies with mouse and adult zebrafish which also show increased expression of collagen RNA levels^{11,13}. Surprisingly the fibrotic (Hand-2, Acta-2) and inflammatory/damage (TGF- β , SDF-1a and SDF-1b) related genes were only upregulated in the 0.06% TAA treatment group. We can speculate that the 0.12% TAA treatment was too toxic and induced another type of damage next to the induction of fibrosis. The increased expression levels of Hand-2 and Acta-2 (fish homologue of α -smooth muscle actin) indicates stellate cell proliferation, activation and, differentiation to myofibroblasts, which are responsible for the secretion of collagen^{7,13-15}. This is a well-known and highly preserved mechanism of fibrogenesis in human and rodents and starts by the apoptosis of hepatocytes which initiates the activation of stellate cells. Research of Howarth *et al.* and other studies also observed increased expression levels of these fibrosis-related genes in adult fish livers upon ethanol treatment¹⁵. These data indicate that the mechanism of fibrogenesis

in zebrafish embryos is highly similar to that in mice, rats and humans. Altogether these data showed that 6 day treatment of zebrafish embryos with 0.06% TAA induces liver fibrosis. The low labour intensiveness, cushiness and low costs of this TAA based model make it suitable for high throughput drug screening.

In the second part of our study we tested the applicability of this novel TAA model to screen for new therapeutics by testing the abilities of MSCs and fibroblasts to modulate the fibrotic process. Sakaida *et al.* published one of the first articles describing reduced CCL4 induced liver fibrosis in mice upon MSC treatment³³. Over time more data were published on reduced liver damage with MSC treatment^{25,29,30,32,34,35}. Until the present study, zebrafish embryos were never used to test the applicability of MSCs as treatment or preventive therapy for liver fibrosis. Our results show that local MSC treatment in our novel zebrafish embryo model can prevent the progression of fibrosis since after administration no collagen structures in the liver were observed and all the fibrotic-, inflammatory/damage- and liver function related- genes normalised. In addition, fibroblast and MSC treatment also abolished the TAA induced shrinkage of the liver. This could be due to the secreted growth factors like hepatocyte growth factor (HGF) and the survival stimulating factors of the MSCs on hepatocytes^{24,35}. Administration of fibroblasts showed less modulation of this fibrotic process than with MSCs.

MSCs are known to play a role in cell survival, tissue regeneration and immune suppression^{23,28}. Immune suppression cannot be the main working mechanism in the amelioration of fibrosis in zebrafish embryos since the T-cells are generated at 8dpf and are thus not present during the experimental period³⁶⁻³⁸. It could be that MSCs inhibit the proliferation of stellate cells indicated by the down-regulation of Hand-2 RNA levels. This event is also described by Najimi *et al.* who observed this MSC guided inhibition of stellate cell proliferation in mice^{24,25}. In addition, it could be that MSCs prevent stellate cell activation or silence the activated stellate cells indicated by the downregulation of Acta-2 RNA levels. Previous studies suggest that there is a reduction in proliferation and silencing of myofibroblasts due to cytokines (IL-10, HGF, VEGF and IGF-1) secreted by MSCs leading to less ECM production in the liver^{23,25,30,35,39}.

In line with these studies we showed that MSCs in culture express HGF, IGF, VEGF and TGF β , which are all important in tissue regeneration and are also described to be important in reversing fibrosis. Fibroblasts had lower expression levels of these cytokines providing a potential explanation for the observed specific effect of MSCs, although additional studies would be required to explore this further.

Xenogenic or xenograft models in general always have some limitations since there are differences between species, which theoretically could lead to different experimental outcomes or hamper translation to humans^{40,41}. This could also be the case for the present novel zebrafish model where we evaluated cellular therapeutic interventions to prevent progression

of fibrosis. To illustrate its applicability we used mouse MSCs as proof of principle. Previous studies have shown that both mouse and human MSCs can reduce fibrosis in mouse models for liver fibrosis^{24,25,29,31,32,35,39}. We think that the preserved pathogenesis of liver fibrosis in the zebrafish embryos (e.g., stellate cell activation, collagen deposition), we observed and its applicability to be used as a test model using mouse MSCs, makes it a valuable model for high throughput testing novel preventive or therapeutic interventions for liver fibrosis. Of course further investigations are required to validate this model and explore other applications.

Altogether our results indicate that mouse MSCs seem to have the same effect in zebrafish embryos and could also have the same working mechanism on liver fibrosis as observed in mouse models. This suggests the usefulness of this novel TAA induced zebrafish fibrosis model for drug screening.

In conclusion, TAA can induce liver fibrosis in zebrafish embryos. This probably acts through mechanisms similar to man and mice, thereby providing a promising and rapid model for future mechanistic and therapeutic studies on liver fibrosis, like we showed by the administration of MSCs. We showed that MSCs seem to prevent progression of liver fibrogenesis in this novel zebrafish embryo model. Therefore MSCs may be a promising novel therapy for patients with increased liver fibrogenesis.

Acknowledgements

We thank the staff of the central zebrafish animal facility of the Gorleaus Laboratories of Leiden University for maintaining the zebrafish population.

Additional information

Competing Interests: The authors declare no competing interests.

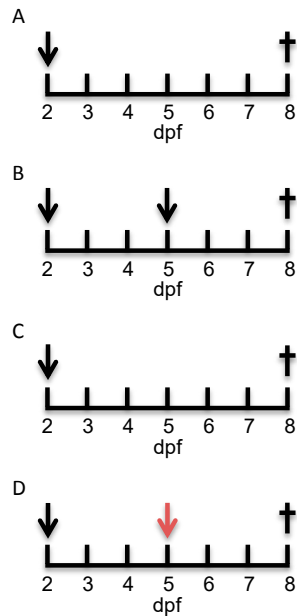
References

1. Bataller, R. & Brenner, D. A. Liver fibrosis. *J Clin Invest* 2005; **115**: 209-218.
2. Friedman, S. L. Mechanisms of hepatic fibrogenesis. *Gastroenterology* 2008; **134**: 1655-1669.
3. Lee, Y. A., Wallace, M. C. & Friedman, S. L. Pathobiology of Liver Fibrosis—A Translational Success Story (vol 64, pg 830, 2015). *Gut* 2015; **64**: 1337-1337.
4. Tunon, M. J., Alvarez, M., Culebras, J. M. *et al.* An overview of animal models for investigating the pathogenesis and therapeutic strategies in acute hepatic failure. *World J Gastroentero* 2009; **15**: 3086-3098.
5. Weber, L. W. D., Boll, M. & Stampfl, A. Hepatotoxicity and mechanism of action of haloalkanes: Carbon tetrachloride as a toxicological model. *Crit Rev Toxicol* 2003; **33**: 105-136.
6. MacRae, C. A. & Peterson, R. T. Zebrafish as tools for drug discovery. *Nat Rev Drug Discov* 2015; **14**: 721-731.
7. Goessling, W. & Sadler, K. C. Zebrafish: an important tool for liver disease research. *Gastroenterology* 2015; **149**: 1361-1377.
8. Lieschke, G. J. & Currie, P. D. Animal models of human disease: zebrafish swim into view. *Nat Rev Genet* 2007; **8**: 353-367.
9. Yin, C., Evason, K. J., Maher, J. J. *et al.* The basic helix-loop-helix transcription factor, heart and neural crest derivatives expressed transcript 2, marks hepatic stellate cells in zebrafish: analysis of stellate cell entry into the developing liver. *Hepatology* 2012; **56**: 1958-1970.
10. Howe, K., Clark, M. D., Torroja, C. F. *et al.* The zebrafish reference genome sequence and its relationship to the human genome. *Nature* 2013; **496**: 498-503.
11. Lin, J. N., Chang, L. L., Lai, C. H. *et al.* Development of an Animal Model for Alcoholic Liver Disease in Zebrafish. *Zebrafish* 2015; **12**: 271-280.
12. Amali, A. A., Rekha, R. D., Lin, C. J. *et al.* Thioacetamide induced liver damage in zebrafish embryo as a disease model for steatohepatitis. *J Biomed Sci* 2006; **13**: 225-232.
13. Rekha, R. D., Amali, A. A., Her, G. M. *et al.* Thioacetamide accelerates steatohepatitis, cirrhosis and HCC by expressing HCV core protein in transgenic zebrafish *Danio rerio*. *Toxicology* 2008; **243**: 11-22.
14. Tsedensodnom, O., Vacaru, A. M., Howarth, D. L. *et al.* Ethanol metabolism and oxidative stress are required for unfolded protein response activation and steatosis in zebrafish with alcoholic liver disease. *Dis Model Mech* 2013; **6**: 1213-1226.
15. Howarth, D. L., Yin, C., Yeh, K. *et al.* Defining hepatic dysfunction parameters in two models of fatty liver disease in zebrafish larvae. *Zebrafish* 2013; **10**: 199-210.
16. Huang, M., Xu, J. & Shin, C. H. Development of an Ethanol-induced Fibrotic Liver Model in Zebrafish to Study Progenitor Cell-mediated Hepatocyte Regeneration. *J Vis Exp* 2016;
17. Ellis, J. L. & Yin, C. Histological Analyses of Acute Alcoholic Liver Injury in Zebrafish. *J Vis Exp* 2017;
18. Byass, P. The global burden of liver disease: a challenge for methods and for public health. *Bmc Med* 2014; **12**:

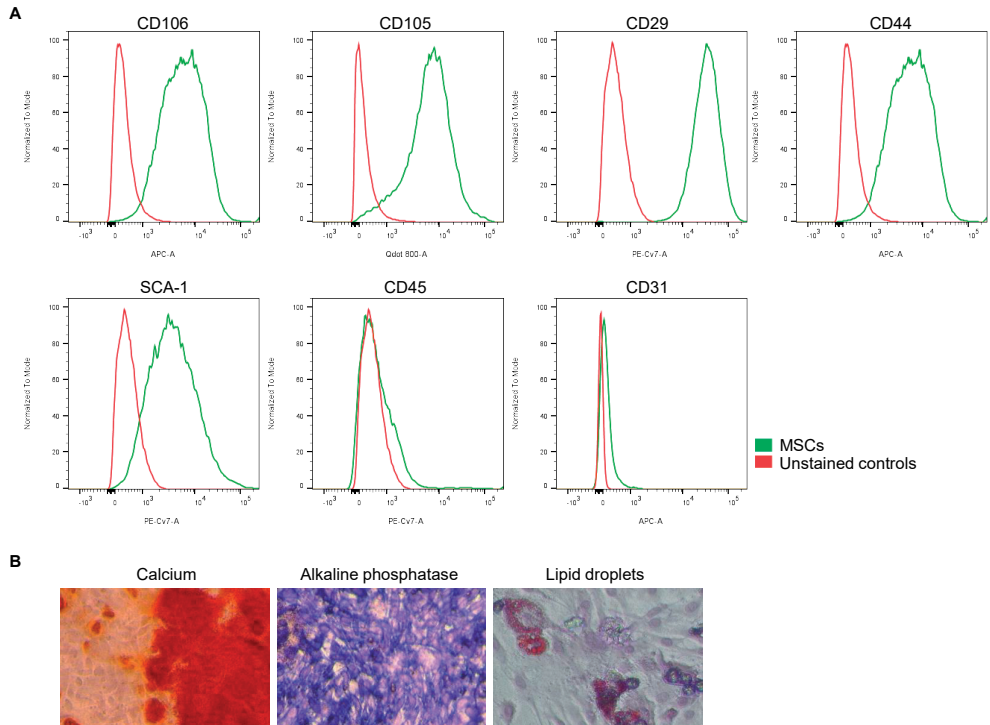
19. Liver, E. A. S. EASL Recommendations on Treatment of Hepatitis C 2016. *J Hepatol* 2017; **66**: 153-194.
20. Mathurin, P., Hadengue, A., Bataller, R. *et al.* EASL Clinical Practical Guidelines: Management of Alcoholic Liver Disease. *J Hepatol* 2012; **57**: 399-420.
21. Suk, K. T., Yoon, J. H., Kim, M. Y. *et al.* Transplantation With Autologous Bone Marrow-Derived Mesenchymal Stem Cells for Alcoholic Cirrhosis: Phase 2 Trial. *Hepatology* 2016; **64**: 2185-2197.
22. Amer, M. E. M., El-Sayed, S. Z., Abou El-Kheir, W. *et al.* Clinical and laboratory evaluation of patients with end-stage liver cell failure injected with bone marrow-derived hepatocyte-like cells. *Eur J Gastroen Hepat* 2011; **23**: 936-941.
23. Alfaifi, M., Eom, Y. W., Newsome, P. N. *et al.* Mesenchymal stromal cell therapy for liver diseases. *J Hepatol* 2018;
24. Huang, B., Cheng, X., Wang, H. *et al.* Mesenchymal stem cells and their secreted molecules predominantly ameliorate fulminant hepatic failure and chronic liver fibrosis in mice respectively. *J Transl Med* 2016; **14**: 45.
25. Najimi, M., Berardis, S., El-Kehdy, H. *et al.* Human liver mesenchymal stem/progenitor cells inhibit hepatic stellate cell activation: in vitro and in vivo evaluation. *Stem Cell Res Ther* 2017; **8**: 131.
26. Gronthos, S., Zannettino, A. C. W., Hay, S. J. *et al.* Molecular and cellular characterisation of highly purified stromal stem cells derived from human bone marrow. *J Cell Sci* 2003; **116**: 1827-1835.
27. Klyushnenkova, E., Mosca, J. D., Zernetkina, V. *et al.* T cell responses to allogeneic human mesenchymal stem cells: immunogenicity, tolerance, and suppression. *J Biomed Sci* 2005; **12**: 47-57.
28. Berardis, S., Dwisthi Sattwika, P., Najimi, M. *et al.* Use of mesenchymal stem cells to treat liver fibrosis: current situation and future prospects. *World J Gastroenterol* 2015; **21**: 742-758.
29. Park, M., Kim, Y. H., Woo, S. Y. *et al.* Tonsil-derived Mesenchymal Stem Cells Ameliorate CCl₄-induced Liver Fibrosis in Mice via Autophagy Activation. *Sci Rep-Uk* 2015; **5**:
30. Deng, Y., Zhang, Y., Ye, L. *et al.* Umbilical Cord-derived Mesenchymal Stem Cells Instruct Monocytes Towards an IL10-producing Phenotype by Secreting IL6 and HGF. *Sci Rep* 2016; **6**: 37566.
31. Li, Q., Zhou, X., Shi, Y. *et al.* In vivo tracking and comparison of the therapeutic effects of MSCs and HSCs for liver injury. *PLoS One* 2013; **8**: e62363.
32. Jang, Y. O., Kim, M. Y., Cho, M. Y. *et al.* Effect of bone marrow-derived mesenchymal stem cells on hepatic fibrosis in a thioacetamide-induced cirrhotic rat model. *BMC Gastroenterol* 2014; **14**: 198.
33. Sakaida, I., Terai, S., Yamamoto, N. *et al.* Transplantation of bone marrow cells reduces CCl₄-induced liver fibrosis in mice. *Hepatology* 2004; **40**: 1304-1311.
34. Mouiseddine, M., Francois, S., Souidi, M. *et al.* Intravenous human mesenchymal stem cells transplantation in NOD/SCID mice preserve liver integrity of irradiation damage. *Methods Mol Biol* 2012; **826**: 179-188.
35. Sun, Y., Wang, Y., Zhou, L. *et al.* Spheroid-cultured human umbilical cord-derived mesenchymal stem cells attenuate hepatic ischemia-reperfusion injury in rats. *Sci Rep* 2018; **8**: 2518.
36. Danilova, N., Hohman, V. S., Sacher, F. *et al.* T cells and the thymus in developing zebrafish. *Dev Comp Immunol* 2004; **28**: 755-767.

37. Willett, C. E., Cortes, A., Zuasti, A. *et al.* Early hematopoiesis and developing lymphoid organs in the zebrafish. *Dev Dyn* 1999; **214**: 323-336.
38. Willett, C. E., Kawasaki, H., Amemiya, C. T. *et al.* Ikaros expression as a marker for lymphoid progenitors during zebrafish development. *Dev Dyn* 2001; **222**: 694-698.
39. Fiore, E. J., Bayo, J. M., Garcia, M. G. *et al.* Mesenchymal stromal cells engineered to produce IGF-I by recombinant adenovirus ameliorate liver fibrosis in mice. *Stem Cells Dev* 2015; **24**: 791-801.
40. Konantz, M., Balci, T. B., Hartwig, U. F. *et al.* Zebrafish xenografts as a tool for in vivo studies on human cancer. *Ann N Y Acad Sci* 2012; **1266**: 124-137.
41. Reichert, D., Friedrichs, J., Ritter, S. *et al.* Phenotypic, Morphological and Adhesive Differences of Human Hematopoietic Progenitor Cells Cultured on Murine versus Human Mesenchymal Stromal Cells. *Sci Rep* 2015; **5**: 15680.
42. Her, G. M., Chiang, C. C., Chen, W. Y. *et al.* In vivo studies of liver-type fatty acid binding protein (L-FABP) gene expression in liver of transgenic zebrafish (*Danio rerio*). *FEBS Lett* 2003; **538**: 125-133.
43. Cianciolo Cosentino, C., Roman, B. L., Drummond, I. A. *et al.* Intravenous microinjections of zebrafish larvae to study acute kidney injury. *J Vis Exp* 2010;
44. Muzumdar, M. D., Tasic, B., Miyamichi, K. *et al.* A global double-fluorescent Cre reporter mouse. *Genesis* 2007; **45**: 593-605.
45. Molendijk, I., Barnhoorn, M. C., de Jonge-Muller, E. S. *et al.* Intraluminal Injection of Mesenchymal Stromal Cells in Spheroids Attenuates Experimental Colitis. *J Crohns Colitis* 2016; **10**: 953-964.

Supplementary files



Supplemental Figure 1. Schematically treatment scheme for CCL4 and TAA and administration. CCL4 was one (A) or two (B) time injected in the yolk sac of zebrafish embryos (black arrows). Embryos were sacrificed 8dpf (cross). (C) TAA was dissolved at day 1 (black arrow) in the egg water of 2dpf zebrafish embryos. Embryos were kept in this water until 8dpf. Embryos were sacrificed 8dpf (cross). (D) TAA treated (black arrow) or control zebrafish were injected at 5dpf (red arrow) with MSCs, fibroblasts or PVP. Embryos were sacrificed 8dpf (cross).



Supplemental Figure 2. Phenotypal and functional characterization of MSCs. MSCs were isolated from bone marrow of 8-10 week old C57Bl/6Jico mice. MSCs were characterised by membrane markers and osteoblast and adipocyte differentiation. (A) CD29, CD44, SCA-1, CD105, CD106, CD45 and CD31 membrane markers were measured by flow cytometry. (B) Osteoblast differentiation was visualised by upregulation of alkaline phosphatase (fast blue staining) and calcium deposit (Alizarin red staining). Adipocyte differentiation was visualised by cytoplasmic lipid droplets (oil-red-o) staining.

Supplemental table 1: Primer sequences

Gene	Abbreviation	Forward	Reverse
Zebrafish			
α 1-antitrypsine	α 1AT	CATGTTGGGTCACAGTCAGG	CGATTCAGGCTTGGAGAA
ACTA-2	ACTA-2	TTGTGCTGGACTCTGGTGAT	GGCCAAGTCCAAACGCATAA
Collagen-1 α 1	Col-1 α 1	CTTTTGCTCACAGGGCCTTT	AAGACTGCATGCATCACAGC
Vitamin D-binding protein	GC	ACTCTCCATTCCTCCCAAGCAT	TAGCGAAGTGAAGCCAGACA
HAND-2	HAND-2	CCTTCAAAGCGGAATTCAAA	CAGATGGCCTCATTTCGTCT
Ribosomal Protection protein	RPP	CTGAACATCTCGCCCTTCTC	TAGCCGATCTGCAGACACAC
Serum amyloid A	SAA	CGTGCCTACCAGCATATGAA	CAGCATCTGAATTGCCTCTG
Stromal derived factor 1a	SDF-1a	CGCCATTCATGCACCGATTTC	GGTGGGCTGTCAGATTTCCTTGTC
Stromal derived factor -1b	SDF-1B	CGCCTTCTGGAGCCAGAGA	AGAGATTCTCCGCTGTCCTCC
Transforming growth factor- β	TGF- β	CCTTGCTTGTGGACAGTTT	AATCCGCTTCTTCTCACCA
Mouse			
<i>Hepatocyte growth factor</i>	HGF	AAGAGTGGCATCAAATGCCAG	CTGGATTGCTTGTGAAACACC
<i>Vascular endothelial growth factor</i>	VEGF	CACAGCAGATGTGAATGCAG	TTTACACGTCTGCGGATCTT
<i>Insulin-like growth factor</i>	IGF	CTACAAAAGCAGCCCGCTCT	CTTCTGAGTCTTGGGCATGTCA
<i>Transforming growth factor-β</i>	TGF- β	CAACAATTCTGGCGTTACC	TGCTGTACAAGAGCAGTGA
<i>Stromal derived factor 1</i>	SDF-1	GAAAGGAAGGAGGGTGGCAG	TCCCCGTCTTCTCGAGTGT
<i>Glyceraldehyde 3-phosphate dehydrogenase</i>	GAPDH	AACCTTGGCATTGTGGAAGG	ACACATTGGGGGTAGGAACA

CHAPTER 5

5

Local and systemic elevated Cripto levels during liver fibrogenesis

Danny van der Helm*, Sofia Karkampouna*, Arwin Groenewoud, Ewa B. Snaar-Jagalska, Bart van Hoek, Hein W. Verspaget, Marianna Kruithof-de Julio#, Minneke J. Coenraad#

*These authors contributed equally to this work

#Joint senior authorship

Abstract

Background

CRIPTO-1 is an (onco)foetal protein that is silenced postnatally and often re-expressed in neoplastic processes. Cell survival and cell proliferation are some of the processes stimulated by CRIPTO-1, which are also known to be important during liver regeneration and fibrogenesis. In the present study we assessed whether CRIPTO-1 is (re-)expressed during liver fibrogenesis.

Methods

Liver tissues of patients with cirrhosis and of experimental liver fibrosis in zebrafish embryos and mice, induced with thioacetamide or carbon tetrachloride, respectively, were evaluated for CRIPTO-1 expression. Immuno-histochemical staining and qPCR for collagen, α -SMA and CRIPTO-1 were performed to determine their expression levels. In addition, CRIPTO-1 levels were assessed in pre- and post-liver transplantation (LT) plasma samples of patients treated for end-stage liver cirrhosis.

Results

CRIPTO-1 was expressed in hepatocytes of humans, zebrafish embryos and mice during fibrogenesis. In humans, CRIPTO-1 expression was positively correlated with the MELD score for end-stage liver disease. Furthermore, patients with end-stage liver cirrhosis showed elevated CRIPTO-1 levels in plasma, which had decreased one year after LT.

Conclusion

Multiple species show enhanced CRIPTO-1 during fibrogenesis and elevated CRIPTO-1 plasma levels in humans with cirrhosis normalize after LT. Altogether, these results are indicative for a functional role of CRIPTO-1 in fibrogenesis which warrant further mechanistic studies.

Introduction

CRIPTO-1 (Teratocarcinoma-Derived Growth Factor 1; TGDF1) is a GPI-anchored signalling protein and member of the epidermal growth factor-CRIPTO/frl/cryptic (EGF-CFC) family, with diverse functions in embryogenesis and as regulator of stemness¹⁻³. CRIPTO-1 is silenced postnatally and often re-expressed in neoplasms of breast, lung, prostate, ovarian, bladder, colon, skin, and brain, where it is thought to be involved in cancer progression and metastasis^{2,4-12}. Recently, CRIPTO-1 expression was found to be associated with poor overall survival and faster tumour recurrence in patients with hepatocellular carcinoma (HCC), but the underlying mechanism(s) are still largely unknown^{3,13}. Suggested mechanisms include CRIPTO-1 involvement in both the classical canonical and the non-canonical signalling pathways, leading to faster proliferation and onset of epithelial to mesenchymal transition of tumour cells^{3,14}. Previous research of our group showed that HCCs with high CRIPTO-1 expression show a poorer response to Sorafenib, an oral multi-kinase inhibitor^{14,15}. Furthermore, we observed in an experimental model that administration of CRIPTO-1 inhibitors sensitize HCCs for Sorafenib treatment¹⁴.

HCC mostly evolve in a background of cirrhosis, which may be caused by chronic exposure of the liver to damaging factors such as alcohol and viral hepatitis B or C (HBV, HCV)¹⁶. These factors may lead to damaged and apoptotic hepatocytes, which are thought to activate stellate cells. Subsequently, stellate cells differentiate into myofibroblasts and produce excessive amounts of extracellular matrix components (ECM) as observed in fibrogenesis¹⁷⁻¹⁹. Chronic fibrogenesis leads to fibrosis, cirrhosis and eventually increases the risk of HCC development. This pathophysiological mechanism and course of the disease are highly conserved between species including human, rat, mouse and zebrafish^{17,20,21}.

Fibrosis, cirrhosis and HCC are major health problems, HCC being the third most frequent cause of cancer-related death, with a lack of effective antifibrotic treatment options²²⁻²⁴. Withdrawal of the injuring stimulus is the only current treatment for liver fibrosis, which in some cases leads to the resolution of fibrogenesis²⁵. For end-stage liver cirrhosis, liver transplantation (LT) is still the only curative treatment option of which feasibility depends on patient condition and donor availability, but LT is still a major surgical intervention with substantial risks²⁶⁻²⁸. Therefore, therapies directly targeting fibrogenesis are needed. Better understanding of the pathological mechanisms underlying the fibrosis-cirrhosis-HCC disease cascade could lead to identification of new biomarkers to monitor the disease and may also lead to new targets for the development of alternative treatment strategies.

CRIPTO-1 is a cancer stem cell marker known to maintain stemness as well as to support cell survival and cell proliferation^{3,15}. These latter processes are also important during fibrogenesis, regeneration and repair of liver tissue²⁹⁻³¹. In a previous study, we showed CRIPTO-1 to be highly expressed in HCC and associated with resistance to Sorafenib treatment. Coincidentally,

we observed a relatively high CRIPTO-1 expression in a majority of the cirrhotic liver tissues¹⁴. Given that CRIPTO-1 is not expressed in liver tissue of healthy adults, we wondered what this CRIPTO-1 re-expression implies for the fibrogenic cascade in the liver. Therefore, in the present study we assessed whether CRIPTO-1 is expressed during liver fibrogenesis in different species and whether this was related with the severity of the disease. CRIPTO-1 expression was evaluated in liver tissue of humans with cirrhosis and in validated zebrafish embryo- and mouse-models for liver fibrogenesis. Furthermore, we also assessed whether enhanced liver CRIPTO-1 was reflected in circulating blood levels of patients with cirrhosis and whether these levels were affected by removing the fibrogenic liver by LT. CRIPTO-1 expression in different species and a correlation with disease stage, could imply a functional role for CRIPTO-1 in the fibrosis–cirrhosis–HCC cascade rendering it a potential interesting marker for disease monitoring or even as a treatment target.

Material and Methods

Patients and controls

All experiments with human specimens were approved by the ethical research committee of the Leiden University Medical Center (LUMC, protocol number: B15.006). Materials were used in compliance with the rules prescribed by the regulations of the LUMC Liver diseases Biobank and with a signed informed consent of the donors. CRIPTO-1 plasma levels were measured in paired pre- and post-LT plasma samples from patients with alcoholic liver disease (ALD, N=25) or viral hepatitis (N=20) related cirrhosis, with plasma from healthy volunteers (N=16) as controls. Post-LT samples were collected and stored at 1 year after LT. Exclusion criteria for this study were the presence of HCC, a combined etiology of cirrhosis, death or re-LT within one year after LT and the development of serious adverse events after LT, such as Tacrolimus induced renal insufficiency (Table 1: patient characteristics). For mRNA-qPCR and (immuno)-histochemical analysis, control tissue (N=5) and alcohol- or viral hepatitis-induced fibrotic/cirrhotic liver tissue (N=19) were obtained from the tissue collections of the LUMC Liver diseases Biobank and Pathology department. These tissues were not from the same patients from which the above mentioned plasma samples were available. The liver tissues were obtained during LT, resection of colorectal cancer-derived liver metastasis, or HCC resection. Clinical data were extracted from the database, including laboratory assessments and clinical MELD (Model for End-Stage Liver Disease) scores, a scoring system for assessing liver function impairment in cirrhosis and risk of short-term mortality.

Table 1: Patient characteristics. Data presented as median (range) for continuous variables and percentage (number) for categorized variables.

Variable	Healthy controls (N=16)	Pre-LT (N=45)	Post-LT (N=45)
Gender (male), % (n)	50% (8)		78% (35)
Age (median, range)	29 (23-65)		54 (42-69)
Aetiology			
Alcoholic liver disease			25
Viral Hepatitis			20
Blood (median, range)			
AST (U/L)		72 (24-517)	27 (11-240)
ALT (U/L)		37 (15-360)	25 (8-401)
INR		1.2 (1-2.4)	1.0 (0.9-2.4)
ALP (U/L)		130 (50-555)	88 (47-487)
Creatinin ($\mu\text{mol/L}$)		92 (34-171)	111 (68-204)
γGT (U/L)		43 (7-374)	39 (9-1395)
Sodium (mmol/L)		138 (124-156)	142 (134-148)
Bilirubin ($\mu\text{mol/L}$)		46 (5-593)	12 (5-29)
Platelet count ($10^9/\text{L}$)		72 (30-142)	144 (93-243)
CRIPTO-1 plasma (pg/ml)	0 (0-818)	1381 (0-12108)	357 (0-5314)
Clinical scores			
MELD		15 (8-33)	10 (6-18)

LT = Liver Transplantation, ALD = Alcoholic Liver Disease, AST = Aspartate aminotransferase, ALT = Alanine aminotransferase, INR = International Normalized Ratio, ALP = Alkaline phosphatase, γGT : gamma-glutamyltransferase, MELD = Model for End-Stage Liver Disease

Mouse and zebrafish embryo models for liver fibrosis

All animal experiments were performed in compliance with the guidelines for animal care and approved by the LUMC Animal Care Committee. Mice received food and water *ad libitum* and were housed under 12h day/night cycle. Liver fibrosis was induced in 6 week old male C57Bl/6Jico mice (Charles River Laboratories, The Netherlands) as described previously³². For a period of 11 weeks, mice received 2 intraperitoneal injections per week with carbon tetrachloride (CCL4) in mineral oil (Sigma-Aldrich Chemie BV, Zwijndrecht, The Netherlands). The first week, mice received 2 initiating higher dosages of CCL4 of 1 ml/kg. The following 10 weeks a maintenance dose of 0.75 ml/kg was given twice weekly. At the end of 11th week, mice were sacrificed and livers collected and subsequently fixated with 4% paraformaldehyde for paraffin embedding and stored in isobutyl for RNA isolation.

Liver-fatty-acid-binding-protein (LFABP)-GFP zebrafish embryos were used for the induction of fibrosis with thioacetamide (TAA) as previous described by our group^{21,33}. In short, 2 days post fertilisation (dpf) old zebrafish embryos were maintained for 6 days in egg water (water with 60 $\mu\text{g/ml}$ instant ocean, sea salt) supplemented with 0.06% TAA (Sigma-Aldrich Chemie

BV, Zwijndrecht, The Netherlands). After the induction of fibrosis, the embryos were collected and stored in PAXgene blood RNA solution (PreAnalytiX, Hombrechtikon, Switzerland) for RNA isolation.

Histological examination of fibrosis

To evaluate the severity of fibrosis in human and mouse liver tissue, a Sirius-red staining was performed to visualize the amount of collagen deposition. Paraffin sections (4 μm) were hydrated and subsequently stained for 90 min with 1 g/L Sirius-red F3B in saturated picric acid (both Klinipath). Next, the sections were incubated for 10 min with 0.01 M HCL, dehydrated and mounted with Entellan (Merck KGaA, Darmstadt, Germany). Fixed microscope settings were used to capture 5-8 representative images (10x magnifications) which were subsequently used to quantify the amount of staining with ImageJ software (ImageJ 1.47v, National Institutes of Health, USA). With fixed threshold settings, based on control tissues, positive pixels were measured and the respective percentage to the total image calculated and defined as the positive area.

Immuno-histochemical staining, imaging and quantification

Immuno-histochemical stainings were performed to evaluate the expression of CRIPTO-1 and α -smooth muscle actin (α -SMA) in fibrotic and control human and mouse liver tissue. Paraffin tissue sections (4 μm) were hydrated and endogenous peroxidases blocked with 0.3% H_2O_2 /methanol (20 min). Antigen retrieval was performed by 10 min boiling in citrate buffer (0.1 M, pH 6.0). After cooling down, primary antibodies detecting mouse- and human-CRIPTO-1 (both kindly provided by Dr Gray Clayton Foundation Laboratories for Peptide Biology, The Salk Institute for Biological Studies, La Jolla, California, USA) and anti- α -SMA (A2547, clone 1A4; Sigma, Buchs, Switzerland) were added and incubated overnight. Next day, mouse- and human-CRIPTO-1 staining was visualised with Alexa fluor 647 secondary antibody and mouse- α -SMA staining with Alexa fluor 488 secondary antibody. In addition a nuclei DAPI staining was performed (Sigma). Representative pictures were captured using a confocal microscope (Leica Biosystems BV, Amsterdam, The Netherlands) and 40x 1.4NA oil-immersion objective with fixed microscope and software settings. Human- α -SMA staining was visualised by 1h incubation with a secondary goat anti-rabbit-HRP conjugated antibody followed by a 10 min incubation with 3,3'-diaminobenzidine (DAB Fast Tablet, Sigma-Aldrich, St. Louis, MO). Nuclear counterstaining was performed with hematoxylin after which the sections were dehydrated and mounted with Entellan. Subsequently, 5-10 representative pictures were captured and used for quantification. The amount of DAB or fluorescent staining in the representative pictures was quantified with ImageJ software. For the CRIPTO-1 staining, the positive area was measured with fixed threshold settings, based on control tissues, and defined as a percentage of positive pixels compared to the total pixels within the hepatocyte regions, regions such as the vessels, bile ducts and the septa with ECM were excluded from the analysis. For the α -SMA stainings, whole images were used to quantify the positive area.

RNA isolation, cDNA synthesis and quantitative Polymerase Chain Reaction (qPCR)

Mouse and human liver tissues were homogenised with UltraTurrax homogenizer (T25 basic, IKA) and TRIpure reagent (Roche). Subsequently, mRNA was isolated following TRIpure RNA isolation protocol. Per experiment, 20 zebrafish embryos were pooled and homogenised by 48h incubation with PAXgene Blood RNA solution at 4°C and next RNA was isolated with NucleoSpin RNA kit (Machery-Nagel GmbH, Düren, Germany). Promega standard protocol was used to synthesise cDNA from 1 µg RNA (Promega, Madison, Wisconsin, USA). CRIPTO-1, collagen-1α1 and α-SMA expression in human and mouse samples and CRIPTO-1, collagen-1α1 and Acta-2 expression in zebrafish embryos samples were measured by qPCR analysis. QPCR reaction mixtures consisted of 5 µl iQ SYBR Green supermix reagent (Bio-Rad Laboratories, Berkeley, California, USA, 1708886), 1 nM primers and 4 µl cDNA. Results were normalised to β-actin for mouse and human samples and to ribosomal protection protein for zebrafish embryo samples (Supplemental table 1: primer sequences).

Plasma CRIPTO-1 measurements

CRIPTO-1 levels in plasma were measured using ELISA, performed according to manufacturer's protocol (R&D systems, Minneapolis, Canada, DY145).

Statistical Analysis

IBM SPSS statistics software (SPSS Inc. Chicago, IL USA, version 23) was used to perform Spearman tests for correlations. GraphPad Prism software (GraphPad Software, version 5.01, San Diego, CA) was used to perform Student's t-test for the comparison between 2 groups. P-values lower than 0.05 were considered to be statistically significant. The data in the graphs are presented as means ± standard error of the mean (SEM).

Results

CRIPTO-1 expression in patients with end-stage liver cirrhosis correlates with the laboratory MELD score

The presence of liver fibrosis was evaluated by Sirius-red stained collagen-1α1 deposition and α-SMA stained activated stellate cells. Liver tissue of patients with cirrhosis showed significantly more Sirius-red and α-SMA staining compared to control tissue (which validated the clinical indication of cirrhosis, Figure 1A and B). CRIPTO-1 expression in these tissues was mainly observed in the hepatocytes and was clearly more present in the cirrhotic tissue as compared to control tissue, with 16 out 19 (84.2%) cirrhotic livers above the highest level in control livers (Figure 1A and B). Furthermore, the results showed a positive correlation between the amount of CRIPTO-1 staining and the laboratory MELD scores of the patients (correlation coefficient: 0.577, P<0.003). No significant correlations between the CRIPTO-1

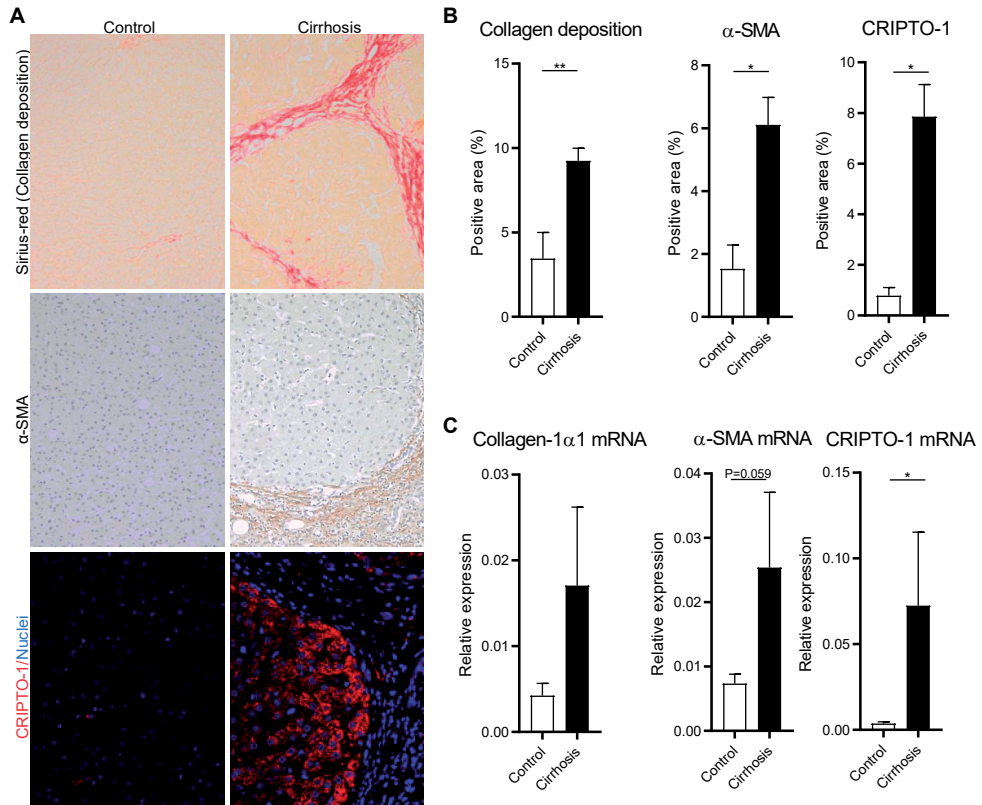


Figure 1. CRIPTO-1 expression in patients with end-stage liver cirrhosis. Liver tissue samples of patients with ALD or viral induced liver cirrhosis (N=19) and controls (N=5) were randomly selected to evaluate CRIPTO-1 expression. (A) Representative pictures of control and cirrhotic liver tissue stained for collagen deposition (Sirius-Red), α-SMA and CRIPTO-1 (CRIPTO-1 in Red, Nuclei in Blue, 100x magnifications). (B) Quantification of Sirius-red, α-SMA and CRIPTO-1 staining (mean±SEM). (C) mRNA expression levels of collagen-1α1, α-SMA and CRIPTO-1 normalized to β-actin (mean±SEM). *p<0.05 **p<0.01

and Sirius-red or α-SMA staining were observed (data not shown). QPCR analysis also showed elevated collagen-1α1, α-SMA and CRIPTO-1 mRNA expression levels in cirrhotic liver tissue compared to control liver tissue (Figure 1C). Altogether, these results indicate that livers of patients with cirrhosis express higher levels of CRIPTO-1 compared to control liver tissue and that the amount of CRIPTO-1 staining is correlated to the MELD score.

CRIPTO-1 expression is upregulated in liver tissue of mice and zebrafish embryos with chemically-induced fibrosis

To study whether expression of CRIPTO-1 in liver fibrogenesis also occurs in other species, we evaluated CRIPTO-1 expression in two *in vivo* models: a CCL4 induced mouse model for liver fibrosis and in our recently described TAA-induced zebrafish embryo model for liver fibrosis. In the mouse model, liver fibrosis was confirmed by Sirius-red and α-SMA staining

of the paraffin embedded liver tissue (Figure 2A). Quantification of the Sirius-red and α -SMA staining revealed more collagen deposition and activated stellate cells in the livers of mice with fibrosis compared to healthy control animals (Figure 2B). Similar as observed in humans (Figure 1), CRIPTO-1 staining was more pronounced in the liver tissues of mice with fibrosis and mainly observed in the hepatocytes (Figure 2A and B). These findings were further supported by qPCR analysis, which also showed higher collagen-1 α 1, α -SMA and CRIPTO-1 mRNA expression in the livers of mice with liver fibrosis compared to the healthy control livers (Figure 2C).

In addition, we evaluated CRIPTO-1 expression in our TAA-induced zebrafish embryo model for liver fibrosis²¹. QPCR measurements showed increased expression levels of collagen-1 α 1 and Acta-2 (the zebrafish homologue for α -SMA) after TAA treatment which indicates the onset of liver fibrogenesis (Figure 3). In this model, CRIPTO-1 mRNA expression was also higher in embryos with liver fibrosis as compared to healthy control embryos (Figure 3). Thus, both

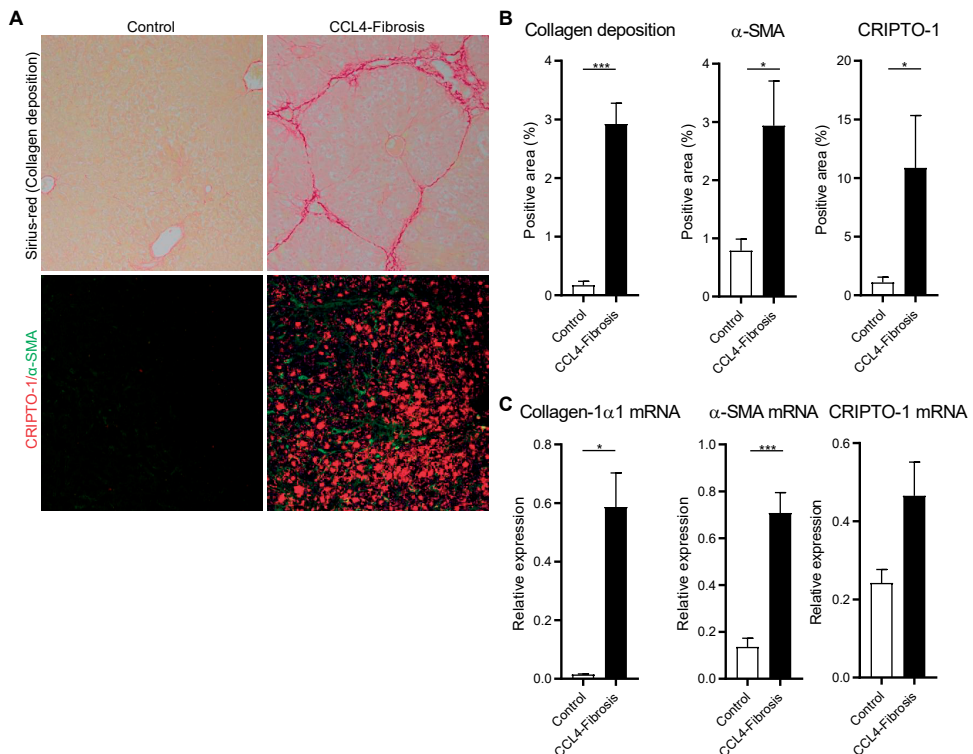


Figure 2. CRIPTO-1 is upregulated in a CCL4 based mouse model for liver fibrogenesis. Mice received chronic administration of CCL4 to induce liver fibrosis. (A) Representative pictures of healthy control and fibrogenic liver tissue stained for collagen deposition (Sirius-Red) or duo-stained for α -SMA (green) and CRIPTO-1 (red) (100x magnifications). (B) Quantification of Sirius-Red, α -SMA and CRIPTO-1 staining (N=8 mice, mean \pm SEM). (C) mRNA expression levels of collagen-1 α 1, α -SMA and CRIPTO-1 normalized to β -actin (N=8 mice, mean \pm SEM). * p \leq 0.05 *** p \leq 0.001

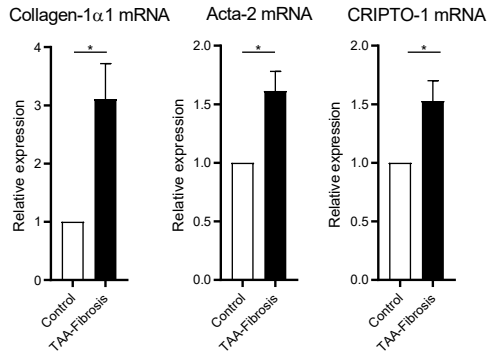


Figure 3. Elevated CRIPTO-1 levels in a zebrafish embryo model for liver fibrogenesis. Collagen-1α1, Acta-2 and CRIPTO-1 mRNA levels normalised to ribosomal protection protein in control zebrafish embryos and embryos with TAA-induced fibrosis. The graphs represent values of three independent experiments (mean±SEM). *p<0.05

in vivo models show similar results as observed in the experiments with human materials where CRIPTO-1 expression was higher in livers of patients with cirrhosis.

CRIPTO-1 level in plasma decreases after liver transplantation

ELISAs were performed to study whether CRIPTO-1 is reflected in blood of patients with liver cirrhosis. CRIPTO-1 was detected in 31 out of 45 plasma samples of patients with end-stage cirrhosis and only in 2 out of the 16 controls (Chi-square 15.1; p<0.001). The mean CRIPTO-1 level in these detectable samples (3070 pg/ml) was significantly (P=0.03) higher in the end-stage liver cirrhosis group compared to that of the healthy controls (653 pg/ml). In this sub-cohort, the laboratory MELD scores did not correlate with the CRIPTO-1 levels in the blood (correlation coefficient: 0.151, P=0.310).

One year after LT, CRIPTO-1 levels had decreased in all 31 patients as compared to their initial level before transplantation (Figure 4). Furthermore, on average a significant decrease of CRIPTO-1 in post- versus pre-LT plasma samples was observed (Table 1, Figure 4). A significant decrease in plasma CRIPTO-1 was also observed when the ALD and viral-induced cirrhosis cohorts were analysed separately (Supplemental Figure 1A and B). Altogether these data indicate that CRIPTO-1 level in plasma decreases significantly once the cirrhotic liver has been replaced by a healthy donor liver. The mean post-LT plasma level of CRIPTO-1 (1044 pg/ml) did not differ (P=0.6) from the healthy controls (653 pg/mL). However, the frequency of detectable CRIPTO-1 levels between these groups was very different (27/31 for patients versus 2/16 for controls, Chi-square 24.9; p<0.0001).

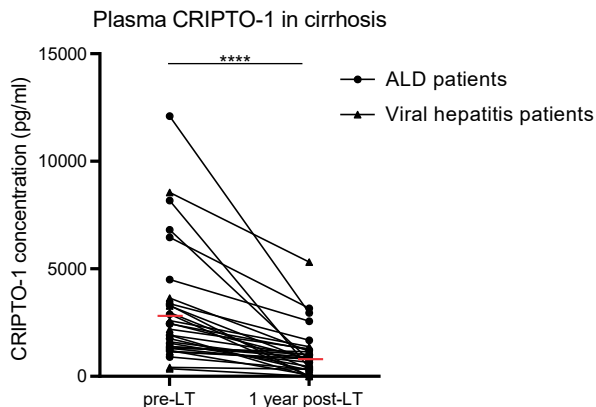


Figure 4. CRIPTO-1 levels in plasma decrease after liver transplantation. CRIPTO-1 levels in and pre- and post-LT paired plasma samples of patients suffering from ALD or viral induced cirrhosis (N=31). Mean group levels are indicated by a red line. *** $p \leq 0.001$

Discussion

Liver fibrosis, cirrhosis and hepatocellular carcinoma are major health problems, and treatments which specifically targeting fibrogenesis and thereby preventing progression of the disease are still not available²²⁻²⁴. Identification of novel biomarkers in the fibrosis-cirrhosis-HCC cascade could lead to improved monitoring of the course of the disease or even provide alternative targets of treatment. In the present study, we assessed whether CRIPTO-1 is expressed in liver tissue of humans, mice and zebrafish embryos during fibrogenesis. We found that CRIPTO-1 is expressed in hepatocytes of patients with liver cirrhosis and that these expression levels positively correlate with the MELD scoring system for end-stage liver diseases^{34,35}. In mouse- and zebrafish embryo-models for liver fibrosis, we observed the same phenomenon, indicative for a general and well preserved role of CRIPTO-1 during fibrogenesis. In addition, we observed elevated CRIPTO-1 levels in the plasma of patients with end-stage liver disease, as a reflection of the liver CRIPTO-1 accumulation, which decreased 1 year after orthotopic liver transplantation.

The observed CRIPTO-1 expression in hepatocytes of human cirrhotic liver tissue is in line with the findings of our previous HCC study where we showed that CRIPTO-1 was highly expressed in HCC tumors, and associated with Sorafenib resistance¹⁴. In the present study, we specifically investigated CRIPTO-1 expression in a larger cohort of non-HCC cirrhosis, i.e. ALD and hepatitis B or C associated cirrhosis, to extend our previous findings. Interestingly, we found a statistically significant correlation between the amount of CRIPTO-1 protein staining and the laboratory MELD score, which illustrates that the CRIPTO-1 expression is related to the severity of the disease. Surprisingly, no correlation between the CRIPTO-1 and Sirius-red or

α -SMA staining was observed. This finding might be explained by the observation that these proteins are expressed by different cell types (hepatocytes vs stellate cells/myofibroblasts). Altogether, our data indicates that CRIPTO-1 expression could be a hepatocyte specific marker for the severity of liver fibrogenesis, similar to collagen and α -SMA for the stellate cells in a fibrotic liver.

Since blood samples are easier to obtain than liver biopsies, we also determined CRIPTO-1 levels in plasma samples of patients with ALD or viral hepatitis related end-stage liver cirrhosis to assess whether this might reflect the CRIPTO-1 accumulation in the liver. Most (69%) of the measured plasma samples showed elevated CRIPTO-1 levels prior to LT which decreased after the patients underwent LT. This observation is in line with recent findings of Zhang et al. who also observed enhanced CRIPTO-1 levels in serum of patients with HCV- and HBV-induced cirrhosis³⁶. In concordance with the present study, they found undetectable CRIPTO-1 levels in some of the serum samples obtained from patients with cirrhosis. The reason for these undetectable CRIPTO-1 levels is unknown but in the present study it is unrelated to the disease stage (data not shown). In contrast to protein quantification of the liver tissue, CRIPTO-1 plasma levels did not correlate with the MELD score. This discrepancy might be related to the use of unpaired plasma-tissue samples, i.e. from different patients. A prospective study to evaluate individual liver-plasma CRIPTO-1 expression and correlation to MELD score needs to be performed to elucidate this potential relationship. Nevertheless, we observed decreased CRIPTO-1 plasma levels after LT in all samples from the patients that had detectable levels pre-LT. This finding strengthens our hypothesis that CRIPTO-1 is expressed during fibrogenesis since the elevated plasma levels decrease after removal of the fibrogenic source by the LT.

Our descriptive observations on the elevated CRIPTO-1 expression in the fibrogenic cascade does not provide information on the mechanism(s) which cause this increase. The liver is well-known for its regenerative capacity upon tissue injury²⁹⁻³¹. Perhaps CRIPTO-1 is re-expressed as a response to cellular injury in order to survive the injuring stimuli and to promote the proliferation of hepatocytes. Research of Zhang et al. indeed showed that challenging HepG2 cells with harmful stimuli will lead to the upregulation of CRIPTO-1 which initiates apoptotic resistance and increased proliferation¹⁵. Altogether, this would suggest that CRIPTO-1 has an inducible function and can be activated by external liver injuring stimuli.

To conclude, CRIPTO-1 is known to be expressed only during embryogenesis and oncogenesis. We showed, however, that CRIPTO-1 is also expressed during fibrogenesis in livers of humans, mice and zebrafish embryos, indicative of a well preserved role for this growth factor protein in the pathology of hepatic fibrogenesis. Furthermore, CRIPTO-1 protein expression in liver tissue of humans was found to be correlated with the laboratory MELD score and elevated plasma CRIPTO-1 levels normalized after liver transplantation. Altogether the observations

from this study warrants further research to disentangle whether CRIPTO-1 has a functionally relevant role in liver fibrogenesis.

Acknowledgements

We thank the staffs of the central animal facility of the LUMC and the central zebrafish animal facility of the Gorleaus Laboratories for animal care and for maintaining the zebrafish population.

Disclosure of conflicts of interest

The authors confirm that there are no conflicts of interest.

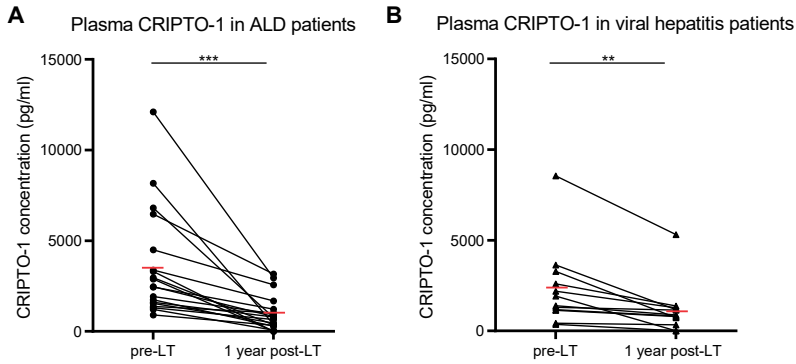
References

1. Strizzi, L., Bianco, C., Normanno, N. *et al.* Cripto-1: a multifunctional modulator during embryogenesis and oncogenesis. *Oncogene* 2005; **24**: 5731-5741.
2. Strizzi, L., Margaryan, N. V., Gilgur, A. *et al.* The significance of a Cripto-1-positive subpopulation of human melanoma cells exhibiting stem cell-like characteristics. *Cell Cycle* 2013; **12**: 1450-1456.
3. Lo, R. C., Leung, C. O., Chan, K. K. *et al.* Cripto-1 contributes to stemness in hepatocellular carcinoma by stabilizing Dishevelled-3 and activating Wnt/beta-catenin pathway. *Cell Death Differ* 2018; **25**: 1426-1441.
4. Spike, Benjamin T., Kelber, Jonathan A., Booker, E. *et al.* CRIPTO/GRP78 signaling maintains fetal and adult mammary stem cells ex vivo. *Stem Cell Reports* 2014; **2**: 427-439.
5. Xu, C.-H., Sheng, Z.-H., Hu, H.-D. *et al.* Elevated expression of Cripto-1 correlates with poor prognosis in non-small cell lung cancer. *Tumor Biol.* 2014; **35**: 8673-8678.
6. Cocciaferro, L., Miceli, V., Kang, K.-S. *et al.* Profiling cancer stem cells in androgen-responsive and refractory human prostate tumor cell lines. *Annals of the New York Academy of Sciences* 2009; **1155**: 257-262.
7. Terry, S., El-Sayed, I. Y., Destouches, D. *et al.* CRIPTO overexpression promotes mesenchymal differentiation in prostate carcinoma cells through parallel regulation of AKT and FGFR activities. *Oncotarget* 2015; **6**: 11994-12008.
8. D'Antonio, A., Losito, S., Pignata, S. *et al.* Transforming growth factor alpha, amphiregulin and cripto-1 are frequently expressed in advanced human ovarian carcinomas. *International journal of oncology* 2002; **21**: 941-948.
9. Fujii, K., Yasui, W., Kuniyasu, H. *et al.* Expression of CRIPTO in human gall bladder lesions *The Journal of Pathology* 1996; **180**: 166-168.
10. Giorgio, E., Liguoro, A., D'Orsi, L. *et al.* Cripto haploinsufficiency affects in vivo colon tumor development. *International journal of oncology* 2014; **45**: 31-40.
11. Sun, C., Sun, L., Jiang, K. *et al.* NANOG promotes liver cancer cell invasion by inducing epithelial-mesenchymal transition through NODAL/SMAD3 signaling pathway. *The International Journal of Biochemistry & Cell Biology* 2013; **45**: 1099-1108.
12. Tysnes, B. B., Satran, H. A., Mork, S. J. *et al.* Age-dependent association between protein expression of the embryonic stem cell marker Cripto-1 and survival of glioblastoma patients. *Translational Oncology* 2013; **6**: 732-741.
13. Wang, J. H., Wei, W., Xu, J. *et al.* Elevated expression of Cripto-1 correlates with poor prognosis in hepatocellular carcinoma. *Oncotarget* 2015; **6**: 35116-35128.
14. Karkampouna, S., van der Helm, D., Gray, P. C. *et al.* CRIPTO promotes an aggressive tumour phenotype and resistance to treatment in hepatocellular carcinoma. *J Pathol* 2018; **245**: 297-310.
15. Zhang, Y., Mi, X., Song, Z. *et al.* Cripto-1 promotes resistance to drug-induced apoptosis by activating the TAK-1/NF-kappaB/survivin signaling pathway. *Biomed Pharmacother* 2018; **104**: 729-737.
16. El-Serag, H. B. & Rudolph, K. L. Hepatocellular carcinoma: epidemiology and molecular carcinogenesis. *Gastroenterology* 2007; **132**: 2557-2576.

17. Friedman, S. L. Mechanisms of hepatic fibrogenesis. *Gastroenterology* 2008; **134**: 1655-1669.
18. Bataller, R. & Brenner, D. A. Liver fibrosis. *J Clin Invest* 2005; **115**: 209-218.
19. Lee, Y. A., Wallace, M. C. & Friedman, S. L. Pathobiology of Liver Fibrosis—A Translational Success Story (vol 64, pg 830, 2015). *Gut* 2015; **64**: 1337-1337.
20. Tunon, M. J., Alvarez, M., Culebras, J. M. *et al.* An overview of animal models for investigating the pathogenesis and therapeutic strategies in acute hepatic failure. *World J Gastroentero* 2009; **15**: 3086-3098.
21. van der Helm, D., Groenewoud, A., de Jonge-Muller, E. S. M. *et al.* Mesenchymal stromal cells prevent progression of liver fibrosis in a novel zebrafish embryo model. *Sci Rep* 2018; **8**: 16005.
22. Byass, P. The global burden of liver disease: a challenge for methods and for public health. *Bmc Med* 2014; **12**:
23. Liver, E. A. S. EASL Recommendations on Treatment of Hepatitis C 2016. *J Hepatol* 2017; **66**: 153-194.
24. Mathurin, P., Hadengue, A., Bataller, R. *et al.* EASL Clinical Practical Guidelines: Management of Alcoholic Liver Disease. *J Hepatol* 2012; **57**: 399-420.
25. Lee, Y. A. & Friedman, S. L. Reversal, maintenance or progression: What happens to the liver after a virologic cure of hepatitis C? *Antivir Res* 2014; **107**: 23-30.
26. Angaswamy, N., Tiriveedhi, V., Sarma, N. J. *et al.* Interplay between immune responses to HLA and non-HLA self-antigens in allograft rejection. *Hum Immunol* 2013; **74**: 1478-1485.
27. Lucidi, V., Gustot, T., Moreno, C. *et al.* Liver transplantation in the context of organ shortage: toward extension and restriction of indications considering recent clinical data and ethical framework. *Curr Opin Crit Care* 2015; **21**: 163-170.
28. Mesens, N., Crawford, A. D., Menke, A. *et al.* Are zebrafish larvae suitable for assessing the hepatotoxicity potential of drug candidates? *J Appl Toxicol* 2015; **35**: 1017-1029.
29. Fausto, N. & Campbell, J. S. The role of hepatocytes and oval cells in liver regeneration and repopulation. *Mech Dev* 2003; **120**: 117-130.
30. Fausto, N., Campbell, J. S. & Riehle, K. J. Liver regeneration. *Hepatology* 2006; **43**: S45-53.
31. Gilgenkrantz, H. & Collin de l'Hortet, A. Understanding Liver Regeneration: From Mechanisms to Regenerative Medicine. *Am J Pathol* 2018; **188**: 1316-1327.
32. van der Helm, D., Barnhoorn, M. C., de Jonge-Muller, E. S. M. *et al.* Local but not systemic administration of mesenchymal stromal cells ameliorates fibrogenesis in regenerating livers. *J Cell Mol Med* 2019;
33. Her, G. M., Chiang, C. C., Chen, W. Y. *et al.* In vivo studies of liver-type fatty acid binding protein (L-FABP) gene expression in liver of transgenic zebrafish (*Danio rerio*). *FEBS Lett* 2003; **538**: 125-133.
34. Sebastiani, G., Castera, L., Halfon, P. *et al.* The impact of liver disease aetiology and the stages of hepatic fibrosis on the performance of non-invasive fibrosis biomarkers: an international study of 2411 cases. *Aliment Pharmacol Ther* 2011; **34**: 1202-1216.
35. Afify, S. M., Tabll, A., Nawara, H. M. *et al.* Five Fibrosis Biomarkers Together with Serum Ferritin Level to Diagnose Liver Fibrosis and Cirrhosis. *Clin Lab* 2018; **64**: 1685-1693.

36. Zhang, Y., Xu, H., Chi, X. *et al.* High level of serum Cripto-1 in hepatocellular carcinoma, especially with hepatitis B virus infection. *Medicine (Baltimore)* 2018; **97**: e11781.

Supplementary files



Supplemental figure 1. CRIPTO-1 levels in aetiological sub-cohorts. CRIPTO-1 levels in pre- and post-LT paired plasma samples of patients suffering from (A) ALD (N=19) or (B) viral (N=12) induced liver cirrhosis. Mean group levels are indicated by a red line. ** $p < 0.01$ *** $p < 0.001$

Supplemental table 1: Primer sequences

Gene	Forward	Reversed
Human		
<i>α-smooth muscle actin</i>	TTGCCTGATGGGCAAGTGAT	GTGGTTTCATGGATGCCAGC
<i>Collagen-1α1</i>	GGAACCTGGGGCAAGACAGT	GAGGGAACCAAGATTGGGGTG
<i>CRIPTO-1</i>	CACGATGTGCGCAAAGAGAA	TGACCGTGCCAGCATTTACA
<i>β-actin</i>	AATGTCGCGGAGGACTTTGATTGC	GGATGGCAAGGGACTTCCTGTAAA
Mouse		
<i>α-smooth muscle actin</i>	GTCCCAGACATCAGGGAGTAA	TCGGATACTTCAGCGTCAGGA
<i>Collagen-1α1</i>	GTGGAAACCCGAGCCCTGCC	TCCCTTGGGTCCCTCGAGCGC
<i>CRIPTO-1</i>	CGCCAGCTAGCATAAAAGTG	CCCAAGAAGTGTTCCCTGTG
<i>β-actin</i>	GGGGTGTTGAAGGTCTCAA	AGAAAATCTGGCACCCC
Zebrafish		
<i>Acta-2</i>	TTGTGCTGGACTCTGGTGAT	GGCCAAGTCCAAACGCATAA
<i>Collagen-1α1</i>	CTTTTGCTCACAGGGCCTTT	AAGACTGCATGCATCACAGC
<i>CRIPTO-1</i>	GGCTCCCTCAGAACACTGTC	CGTTCAACAGGGGAGATCAT
<i>Ribosomal protection protein</i>	CTGAACATCTGCCCTTCTC	TAGCCGATCTGCAGACACAC

CHAPTER 6



CRIPTO promotes an aggressive tumour phenotype and resistance to treatment in hepatocellular carcinoma

Danny van der Helm*, Sofia Karkampouna*, Peter C. Gray, Lanpeng Chen, Irena Klima, Joël Grosjean, Mark C. Burgmans, Arantza Farina-Sarasqueta, Ewa B. Snaar-Jagalska, Deborah M. Stroka, Luigi Terracciano, Bart van Hoek, Alexander F. Schaapherder, Susan Osanto, George N. Thalmann, Hein W. Verspaget, Minneke J. Coenraad, Marianna Kruithof-de Julio

*These authors contributed equally to this work

Abstract

Background and Aim

Hepatocellular carcinoma (HCC) is the third leading cause of cancer-related death worldwide. Despite increasing treatment options for this disease, prognosis remains poor. CRIPTO (TDGF1) protein is expressed at high levels in several human tumours and promotes oncogenic phenotype. Its expression has been correlated to poor prognosis in HCC. In this study, we aimed to elucidate the basis for the effects of CRIPTO in HCC.

Methods

We investigated CRIPTO expression levels in three cohorts of clinical cirrhotic and HCC specimens. We addressed the role of CRIPTO in hepatic tumourigenesis using Cre-loxP-controlled lentiviral vectors expressing CRIPTO in cell line-derived xenografts. Responses to standard treatments (sorafenib, doxorubicin) were assessed directly on xenograft-derived ex vivo tumour slices. CRIPTO-overexpressing patient-derived xenografts were established and used for ex vivo drug response assays. The effects of sorafenib and doxorubicin treatment in combination with a CRIPTO pathway inhibitor were tested in ex vivo cultures of xenograft models and 3D cultures.

Results

CRIPTO protein was found highly expressed in human cirrhosis and hepatocellular carcinoma specimens but not in those of healthy participants. Stable overexpression of CRIPTO in human HepG2 cells caused epithelial-to-mesenchymal transition, increased expression of cancer stem cell markers, and enhanced cell proliferation and migration. HepG2-CRIPTO cells formed tumours when injected into immune-compromised mice, whereas HepG2 cells lacking stable CRIPTO overexpression did not. High-level CRIPTO expression in xenograft models was associated with resistance to sorafenib, which could be modulated using a CRIPTO pathway inhibitor in ex vivo tumour slices.

Conclusion

Our data suggest that a subgroup of CRIPTO-expressing HCC patients may benefit from a combinatorial treatment scheme and that sorafenib resistance may be circumvented by inhibition of the CRIPTO pathway.

Introduction

Hepatocellular carcinoma (HCC) is the third leading cause of cancer-related death worldwide¹. In the majority of cases, HCC arises on a background of cirrhosis, which may be caused by chronic exposure to damaging factors, such as chronic alcohol abuse, hepatitis B or C, and various other chronic liver diseases². The invasive and metastatic potential of HCCs is an important factor causing poor prognosis of affected patients. Treatment options include resection of the tumour, liver transplantation, minimal invasive image-guided oncologic therapies such as local ablation, and transarterial therapies for the early and intermediate tumour stages³.

Targeted systemic treatments available for advanced stage tumours or tumours progressing after locoregional therapies are the tyrosine kinase inhibitors (TKIs) sorafenib (first-line)⁴ and regorafenib (second-line). Sorafenib is a tyrosine kinase (VEGFR, PDGFR, RAF) inhibitor which delays HCC progression and metastatic spread but is effective in only a minority of patients and has severe side effects⁴⁻⁷. Recently, it was shown that nivolumab, a programmed cell death protein-1 (PD-1) checkpoint inhibitor, induces durable objective responses in patients with advanced stage HCC⁸. Due to a lack of biomarkers, it remains a challenge to estimate the disease progression or responsiveness to therapies⁴. In addition to the high number of non-responders to systemic therapy, there is a high percentage of HCC patients who relapse after surgical resection or minimal invasive oncological therapies. The prognosis of HCC is often dismal, with a significant risk of tumour recurrence or insufficient response to therapies due to non-specificity of the treatments⁹. Circulating α -fetoprotein (AFP) levels have been explored as biomarkers in HCC¹⁰. However, detection of high levels of AFP cannot be used for diagnosis or prognosis as it does not predict tumour size, stage, or HCC progression, and is absent in 30% of HCC cases¹⁰. Elucidation of the basic mechanisms behind the invasive and migration properties of HCCs and the identification of markers that can predict therapeutic response and the likelihood of recurrence are needed to identify suitable personalized treatments. For example, identification of sorafenib responders versus non-responders based on biomarker expression and functional *ex vivo* assay would allow better treatment selection.

CRIPTO (teratocarcinoma-derived growth factor 1; TDGF1) is a GPI-anchored signalling protein and atypical member of the transforming growth factor (TGF) gene family¹¹⁻¹³. CRIPTO has multiple binding partners and signalling functions^{14,15}. It enables the signalling of a subset of TGF- β superfamily ligands, including NODAL¹⁶, that require a co-receptor (CRIPTO or Cryptic) to bind and assemble their type I and type II signalling receptors¹⁷. CRIPTO also inhibits other TGF- β superfamily ligands and attenuates cytotstatic TGF- β 1 signalling¹². In addition, CRIPTO can act independently of the TGF- β pathway as a secreted factor that activates c-src/MAPK/Akt signalling, a pathway that is oncogenically mutated in liver cancer¹⁸. Notably, each of these CRIPTO signaling functions was shown to depend on CRIPTO binding to cell surface glucose regulated protein 78 kDa (GRP78)¹⁹. GRP78 is strongly induced by endoplasmic reticulum (ER)

stress and, like CRIPTO, plays key roles in embryogenesis, stem cell regulation, and tumour progression²⁰. In addition to its physiological roles in stem cells and embryogenesis, CRIPTO is an oncofetal protein that is silenced postnatally. Re-expression is often associated with pathological conditions such as neoplasia of the breast, prostate, ovarian, bladder, colon, skin, lung, and brain^{21–29}. Recently, CRIPTO expression was correlated to poor survival and tumour recurrence in HCC patients³⁰. Moreover, liver-specific deletion of GRP78 promoted maintenance of tissue homeostasis and played a protective role during ER-stress response, while elevated GRP78 levels were associated with HCC progression^{31–33}.

In this study, we investigated CRIPTO expression in HCC aiming to elucidate the effects of the CRIPTO pathway while also exploring its potential use as a therapeutic target. We identified a potential role for CRIPTO in therapy resistance to sorafenib, suggesting that combination treatment with an inhibitor of the CRIPTO pathway might induce a beneficial response in selected patient groups.

Materials and methods

Human specimens

Aetiopathological heterogeneity in tumours was taken into account during the selection of HCC patient material; in this study, we assessed specimens from HCV infection-driven HCC (HCC-HCV, N= 4) and alcoholic liver disease-driven HCC (HCC-ALD, N= 4). Non-cirrhotic hepatitis C (HCV) tissues (N= 5) were selected as controls. Selection of tissues was performed in agreement with the ‘code of good practice’. Written informed consent was obtained from each patient included in the study. The study protocol conforms to the ethical guidelines of the 1975 Declaration of Helsinki as reflected in a priori approval by the institution’s Human Research Committee (B15.006/SH/sh, biobank METC MDL/009/NV/nv). Tissue microarrays (TMAs) used were from the Pathology Department of University Hospital Basel (N= 234 tissue samples including 33 HCC–adjacent tissue matched pairs) and a commercially available TMA (BC03117; US Biomax, Rockville, MD, USA; N= 69 tissue samples including seven HCC–adjacent tissue matched pairs).

Animal models

Animal protocols were approved by the Committee for Animal Experimentation and the Veterinary authorities of the Canton of Bern, Switzerland (BE55/16). Mice received food and water *ad libitum* and were housed in individually ventilated cages. NOD.Cg-Prkdc^{scid} Il2rg^{tm1Wjl}/SzJ (NSG) mice were injected subcutaneously with 0.5×10^6 HepG2-CRIPTO ($n=4$) or HepG2-MOCK ($n=3$) cells in Matrigel (354234; Corning, Kaiserslautern, Germany). Tumour growth was monitored weekly. At week 12, mice were sacrificed and tumours collected for further analysis.

Patient-derived xenograft (PDX)

A tumour needle biopsy from an anonymized advancedstage HCC patient was subcutaneously implanted in NSG mice and routinely passaged *in vivo*. A zebrafish line [Tg(fli1:GFP)j114] was handled and maintained according to local animal welfare regulations to standard protocols (<http://www.ZFIN.org>). Two days post-fertilization (dpf), dechorionated zebrafish embryos were anaesthetized and injected with approximately 200 HepG2-MOCK or HepG2-CRIPTO cells fluorescently labelled as described previously³⁴. Two days after injection, the embryos were imaged and clumps of cells (foci) counted. Zebrafish embryos (including non-injected controls) were maintained at 33 °C, to compromise between the optimal temperature requirements for fish and mammalian cells. Data are representative of/from at least two independent and blind experiments with ≥ 30 embryos per group. Foci were counted using Leica Application Suite X software (version 1.1.0.12420; Leica Biosystems BV, Amsterdam, The Netherlands).

Ex vivo tumour tissue culture and organoid generation

Tissues from HCC PDX or HepG2-CRIPTO-derived tumours were maintained in *ex vivo* cultures. Tissue slices (150–200 μm) were cultured using Transwell plates with an attached nitrocellulose membrane (Thin-Cert #662640 inserts for 24-well plates, 0.4 μm pore size; Greiner Bio-One, Kremsmünster, Austria) that allowed contact of the tissue with the growth medium but not the plastic in a manner that prevented alteration of the tissue^{35,36}. Culture plates were placed in a sealed container saturated with oxygen, 40–50%, at 37 °C. Cultures were maintained for 7 days. Organoids were derived from the bulk of PDX tumours similarly to previously developed methods^{37,38}. Single cell suspensions were obtained by enzymatic homogenization of the tissue by collagenase type II (Gibco, St-Sulpice VD, Switzerland) (5 mg/ml) and Accutase (Sigma, Buchs, Switzerland), followed by red blood cell lysis. Organoids were maintained in low attachment plates (Corning, Wiesbaden, Germany) in defined media (supplementary material, Table S1). Tumour slices and organoids were incubated for 7 and 2 days, respectively, with dimethyl sulphoxide (DMSO, 0.1%), DMSO plus Control-Fc antibody (2 $\mu\text{g}/\text{ml}$), sorafenib (1 μM), doxorubicin (1 $\mu\text{g}/\text{ml}$), and GRP78 N20 blocking peptide (sc1050P, 2 $\mu\text{g}/\text{ml}$; Santa Cruz, LabForce, Muttenz, Switzerland). After treatment, tissues were processed for histology.

Cell lines and CRIPTO overexpression

The HepG2 cell line was maintained in Dulbecco's Modified Eagle medium (DMEM) supplemented with 10% fetal calf serum (FCS; Gibco) and 1% penicillin/streptomycin (P/S; Invitrogen, Paisley, UK). Lentiviral pTomo-mock³⁹ and pTomo-CRIPTO constructs (provided by Dr P Gray; sequence from ref 12) were used for HepG2 cell transduction. Selection of positive clones was based on red fluorescent protein (RFP)-based cell sorting (FACS). Activation of CRIPTO transcription was induced by lentivirus-CRE transduction, which switched off RFP expression and induced green fluorescent protein (GFP) expression. Further information is provided in the supplementary material, supplementary materials and methods.

Results

CRIPTO promotes a proliferative and mesenchymal phenotype in *in vitro* HCC cells

CRIPTO has been shown to play an important role in tumour development and progression in various cancer types; however, its role in hepatic pathologies, such as in HCC, remains understudied.

Firstly, we studied the functional effects of CRIPTO *in vitro*, by stable overexpression of CRIPTO in HepG2, an HCC-derived cell line with low tumourigenicity *in vivo*⁴⁰. We used a lentiviral red-to-green pTOMO-CRIPTO construct in which CRE recombinase activity excises a floxed RFP cassette, which turns on CRIPTO expression and increases expression of GFP³⁹. A pTOMO-MOCK lentivirus lacking the CRIPTO insert was used to generate a control cell line (HepG2-MOCK). HepG2-CRIPTO cells transduced with pTOMO-CRIPTO and CRE virus lacked RFP expression and had GFP expression as predicted (Figure 1A). HepG2-MOCK cells were also generated in the presence of viral-mediated CRE and maintained expression of RFP and weak GFP upon transduction, whereas non-transduced cells (HepG2) showed no fluorochrome (Figure 1A). CRIPTO overexpression in the HepG2-CRIPTO cells was confirmed at both the mRNA (Figure 1B) and the protein level (supplementary material, Supplemental Figure 1A). The mRNA levels of *NODAL* and *GRP78*, encoding CRIPTO interaction partners, were both induced in HepG2-CRIPTO cells (Figure 1C, D). *GRP78* protein levels were reduced (supplementary material, Supplemental Figure 1B) and phosphorylated AKT (pAKT) levels were increased, indicating downstream pathway activation (supplementary material, Supplemental Figure 1C) in HepG2-CRIPTO cells. PCNA protein level differences were minor (supplementary material, Supplemental Figure 1D). HepG2-CRIPTO cells acquired a more mesenchymal phenotype relative to control cells (HepG2 WT and HepG2-MOCK), as indicated by the downregulation of *E-CADHERIN* (Figure 1E) and upregulation of EMT markers such as *VIMENTIN (VIM)*, *ZEB-1*, *ZEB-2*, *TWIST1*, and *SNAIL-2* (Figure 1F–J). HepG2-CRIPTO cells exhibited higher expression of the cancer stem cell (CSC) markers *BMI1* and *CD44* than control cells (Figure 1L, M). EPCAM levels were also higher in HepG2-CRIPTO cells, although this difference did not reach statistical significance (Figure 1K). Additional stemness marker expression was assessed at the mRNA level: *GLI-1*, α *INTEGRIN (ITGAV)*, β *INTEGRIN (ITGB3)*, *ALDH1A1*, *SOX2*, and *CD24* (supplementary material, Supplemental Figure 2A–F). HepG2 CRIPTO cells also had a higher proliferation rate (Figure 1N), enhanced migration (Figure 1O), and wound closure properties (Figure 1P) compared with control cells, in line with EMT-associated gene expression (Figure 1E–J).

CRIPTO overexpression induces pro-tumourigenic *in vivo* effects

We investigated possible effects of CRIPTO on the cancer phenotype *in vivo*. HepG2-CRIPTO and HepG2-MOCK cells were implanted subcutaneously in Matrigel plugs in immunodeficient mice. Tumour formation was observed at 5 weeks post-implantation; HepG2-MOCK cells formed

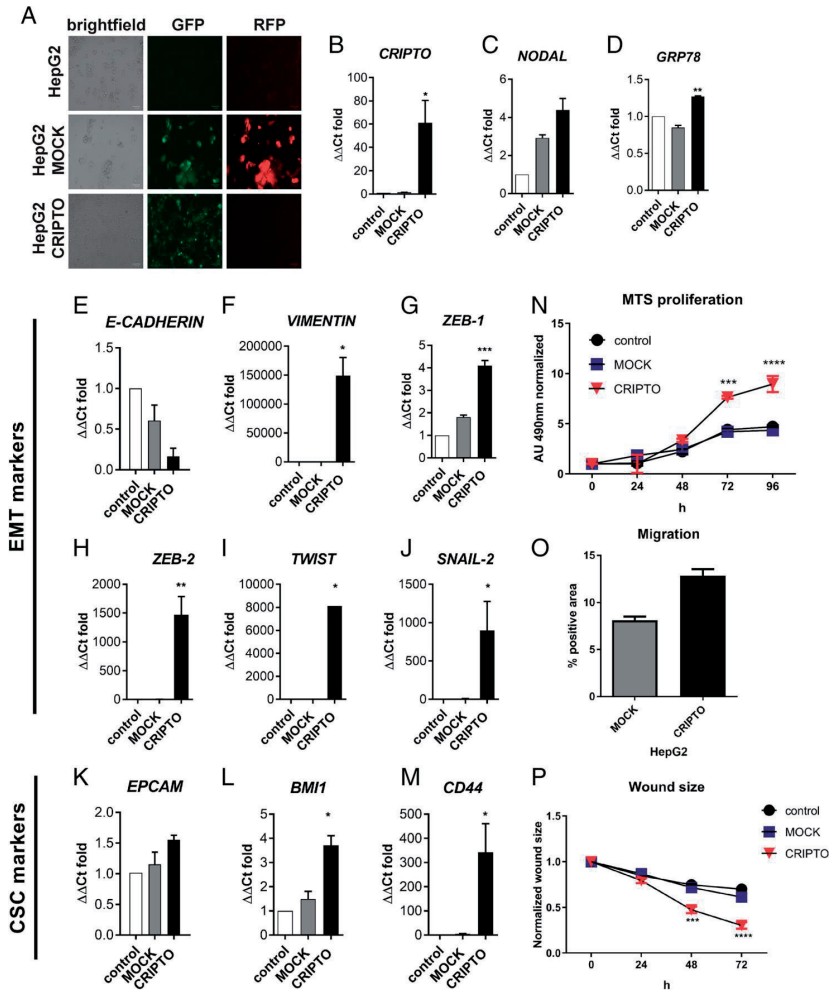


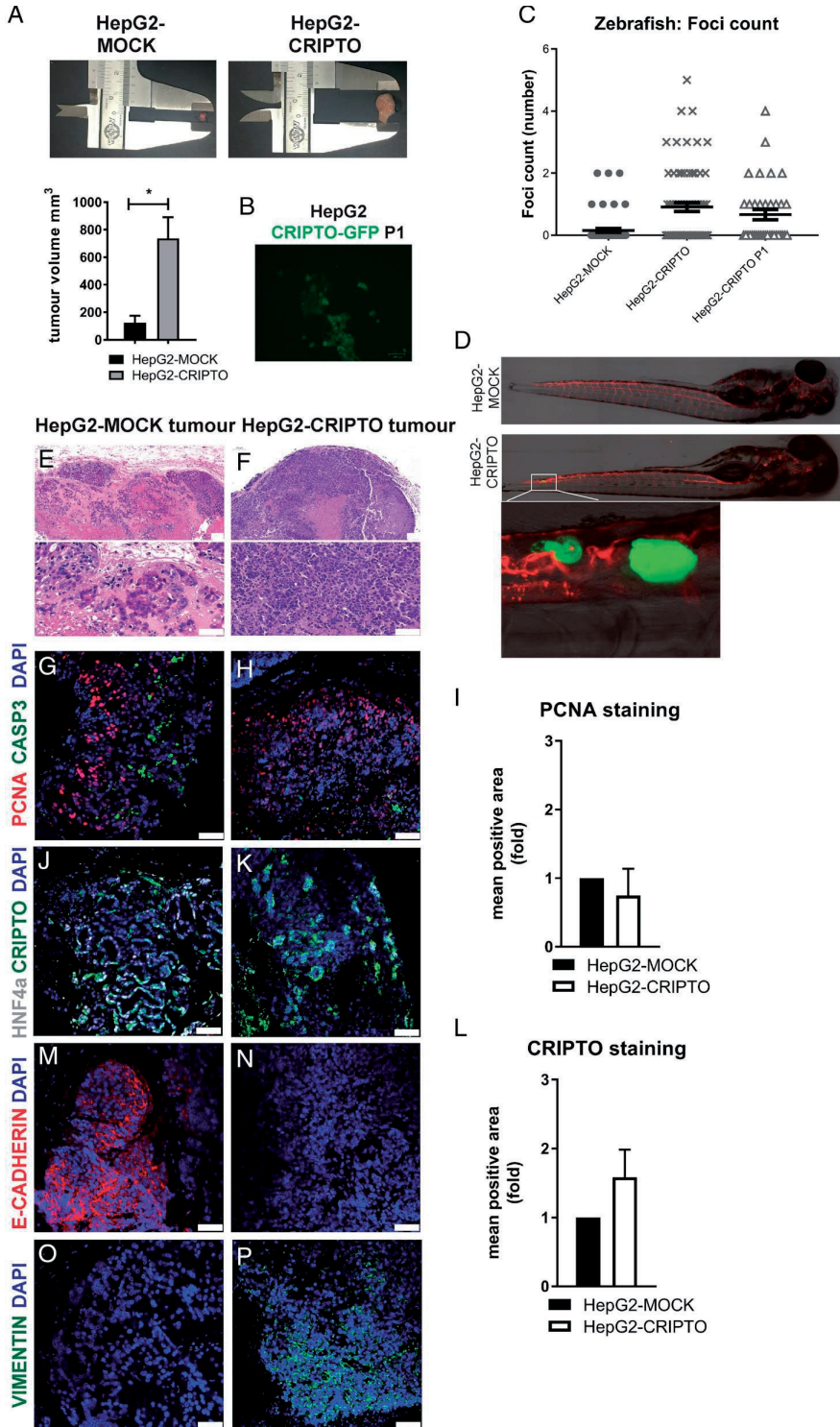
Figure 1. In vitro effects of stable overexpression of CRIPTO in HepG2 cells. (A) Cell morphology of wild-type HepG2 cells; control, stably overexpressing pTomo MOCK construct (MOCK, GFP+, RFP+); and stably overexpressing CRIPTO (CRIPTO, GFP+). Both cell lines were transfected with pTOMO and CRE lentivirus. (B–D) RT-qPCR for mRNA expression of CRIPTO-associated members of the NODAL and GRP78 pathways in (B) *CRIPTO* (*TGDF1*), (C) *NODAL*, and (D) *GRP78* mRNA expression ($n=3$, \pm SEM). Values were normalized to *ACTB* and to control sample ($\Delta\Delta$ Ct fold expression). (E–J) Levels of mRNA expression of epithelial-to-mesenchymal (EMT) markers in control, MOCK, and overexpressing CRIPTO HepG2 cells were assessed by RT-qPCR. (E) *E-CADHERIN* (*CDH1*); (F) *VIMENTIN* (*VIM*); (G) *ZEB-1*; (H) *ZEB-2*; (I) *TWIST1*; (J) *SNAIL-2*. Unpaired *t*-test; * $p < 0.05$. (K–M) mRNA expression levels of cancer stem cell (CSC) markers. (K) *EPCAM*; (L) *BMI1*; (M) *CD44*. All values were normalized to *ACTB* and to control sample ($\Delta\Delta$ Ct fold expression); $n=3$; \pm SEM. Unpaired *t*-test; * $p < 0.05$. (N) Metabolic activity MTS assay (24, 48, 72, 96 h) was performed in control, MOCK, and CRIPTO-overexpressing HepG2 cells. Accumulation of MTS was measured based on the absorbance at 490 nm. Values were normalized to the basal measurements at 0 h after cell seeding. The graph represents values for three independent experiments ($n=3$). Error bars indicate \pm SEM. Two-way ANOVA; *** $p < 0.001$; **** $p < 0.0001$. (O) Transwell migration assay of MOCK and CRIPTO-overexpressing HepG2 cells. Quantification of percentage positive area of migrated cells (crystal violet cell dye) was performed in two independent experiments. Error bars indicate \pm SEM. (P) Cell motility was assessed in wound healing (scratch) assay. Wound size was quantified in a time-dependent manner (0, 24, 48, and 72 h) in three independent experiments. Data were normalized to the 0 h time point; error bars indicate \pm SEM. Unpaired *t*-test; * $p < 0.05$.

Table 1. Clinical parameters of the specimens used from the LUMC cohort for mRNA analysis. The list corresponds to Figure 6A. n.a. = not applicable

qPCR cases	LUMC (N =15)
Gender, male, N (%)	11 (73.3%)
Age (range), years	72 (59–74.5)
Control (no underlying liver disease)	8 (53.3%)
Adjacent and HCC matched samples	
Fibrosis–cirrhosis (yes), N (%)	7 (46.6%)
HCC, N (%)	7 (46.6%)
T1 (N)	5
T2 (N)	1
T3 (N)	1
T4 (N)	n.a.

smaller tumours compared with the HepG2-CRIPTO-bearing mice (Figure 2A). We isolated single cells from the HepG2-CRIPTO tumour tissues and selected CRIPTO-transduced cells based on GFP expression (HepG2-CRIPTO-p1) (Figure 2B). The single cells were then injected into the duct of Cuvier of 2 dpf zebrafish embryos along with the parental HepG2-CRIPTO and HepG2-MOCK lines (Figure 2C, D) in order to determine their potential to migrate and generate tumour foci *in vivo*. HepG2-CRIPTO and HepG2-CRIPTO-p1 both showed significantly more foci at 6 dpf relative to HepG2-MOCK (Figure 2C). Histological analysis of HepG2-MOCK and HepG2-CRIPTO tumour tissues, grown as subcutaneous xenografts in mice, showed different morphological structures (Figure 2E, F); only HepG2-CRIPTO tumours resembled HCC morphology. Both tumours showed similar levels of proliferation (PCNA) (Figure 2G–I) and HNF4a liver marker expression (Figure 2J, K); however, different levels of CRIPTO were observed (Figure 2L). HepG2-MOCK xenograft tumours were distinguished by staining for the epithelial marker E-CADHERIN (Figure 2M) and absence of mesenchymal VIMENTIN expression

Figure 2. In vivo tumour formation is induced by overexpression of CRIPTO. (A) Subcutaneous tumour growth of HepG2-MOCK and HepG2-CRIPTO cells in immunocompromised mice. Tumour volumes at endpoint were calculated with calliper measurement and using the formula $V = (L \times W \times W)/2$. Average values from HepG2-MOCK (N= 3) and HepG2-CRIPTO (N= 4) are shown. Error bars indicate \pm SEM. Unpaired *t*-test; **p* <0.05. (B–D) GFP-positive HepG2-CRIPTO cells (p1) from the tumours were collected and injected in zebrafish to monitor cell migration and tumour growth (C, D) along with HepG2-MOCK and HepG2-CRIPTO cells. (E, F) Haematoxylin and eosin staining representative of the HepG2-MOCK and HepG2-CRIPTO tumours. Scale bars: 100 μ m (top); 50 μ m (bottom). (G–I) Immunofluorescence for PCNA (red) and cleaved caspase-3 (green) in HepG2-MOCK (G) and HepG2-CRIPTO (H) tumour sections. Scale bars: 50 μ m. (I) Quantification of PCNA-positive area normalized to nuclei surface area and represented as fold change over the HepG2-MOCK samples. (J, K) Immunofluorescence for HNF4a (grey) and CRIPTO (green) in HepG2-MOCK and HepG2-CRIPTO tumour sections. Scale bars: 50 μ m. (L) Quantification of CRIPTO expression (positive stained area normalized to nuclei surface area); fold change HepG2-MOCK values. (M, N) Immunofluorescence for the epithelial marker E-CADHERIN (red) in HepG2-MOCK and HepG2-CRIPTO tumour sections. Scale bars: 50 μ m. (O, P). Immunofluorescence for the mesenchymal marker VIMENTIN (green) in HepG2-MOCK and HepG2-CRIPTO tumour sections. Scale bars: 50 μ m.



(Figure 2O), in contrast to the HepG2-CRIPTO tumours, which were E-CADHERIN-negative (Figure 2N) and had VIMENTIN-positive areas (Figure 2P).

HepG2-CRIPTO tumours were cultured *ex vivo* for 7 days, during which they were treated with doxorubicin or sorafenib – two compounds that are currently widely used in clinical practice for HCC treatment – in the setting of transarterial chemoembolization and oral therapy, respectively. Based on H&E staining, both treatments (Figure 3C, D) led to tissue damage compared with the untreated and vehicle (DMSO) groups (Figure 3A, B). Immunofluorescence analysis of proliferating cells (PCNA+; proliferating cell nuclear antigen-positive) indicated that doxorubicin treatment had a negative impact on tissue viability, exhibited by the absence of PCNA+ cells (Figure 3G, T). Sorafenib treatment showed areas of sustained proliferation (Figure 3H, T).

The gene expression profiles of tumours treated *ex vivo* with doxorubicin and sorafenib showed reduced CRIPTO expression (Figure 3I) in both conditions compared with control groups. However, CRIPTO expression was higher in the sorafenib condition than in the doxorubicin condition (Figure 3I). *GRP78* levels (Figure 3J) were not affected, compared with the vehicle control. *EPCAM* and *E-CADHERIN (CDH1)* levels were also reduced following doxorubicin and sorafenib treatment (Figure 3K, N), while *CD44* was increased significantly in both drug treatments (Figure 3M). Interestingly, only sorafenib induced expression of the stem cell marker *BMI1* (Figure 3L) and the EMT-associated genes *VIM* and *TWIST1* (Figure 3O, P). Expression of the liver cancer stem cell marker *CD24* was significantly decreased upon sorafenib treatment (supplementary material, Supplemental Figure 2G). The induction of mesenchymal (*VIM*, *TWIST1*) and stem cell markers (*CD44*, *BMI1*) by sorafenib in the HepG2-CRIPTO tumour slices may indicate an acquired aggressiveness due to CRIPTO-related activation of a resistance mechanism to sorafenib. To understand whether sorafenib resistance pre-exists in the HepG2 or is linked to CRIPTO overexpression, we assessed the proliferation rate of the HepG2 parental, control MOCK, and HepG2-CRIPTO cell lines in response to different sorafenib or doxorubicin concentrations. Proliferation, as assessed using an MTS assay, was reduced in the doxorubicin and sorafenib-treated HepG2, HepG2-MOCK, and HepG2-CRIPTO cell lines. Interestingly, HepG2 and HepG2-MOCK cells proliferated less in the presence of sorafenib (1 μ M) compared with HepG2-CRIPTO (Figure 3Q–S, 96h).

CRIPTO may confer sorafenib resistance

To further investigate the role of CRIPTO in HCC, we established a patient-derived xenograft (PDX) from a needle biopsy obtained from a CRIPTO-expressing advanced cancer stage HCC prior to patient treatment with sorafenib (Figure 4A, B, original tumour and PDX1). The PDX tissue (PDX2 and PDX3 tumours) maintained both HNF4a and CRIPTO expression over time (Figure 4A, B), showing persistent proliferation (Figure 4C, D) and minimal apoptosis (Figure 4C, E) and HCC morphology (Figure 4F, G).

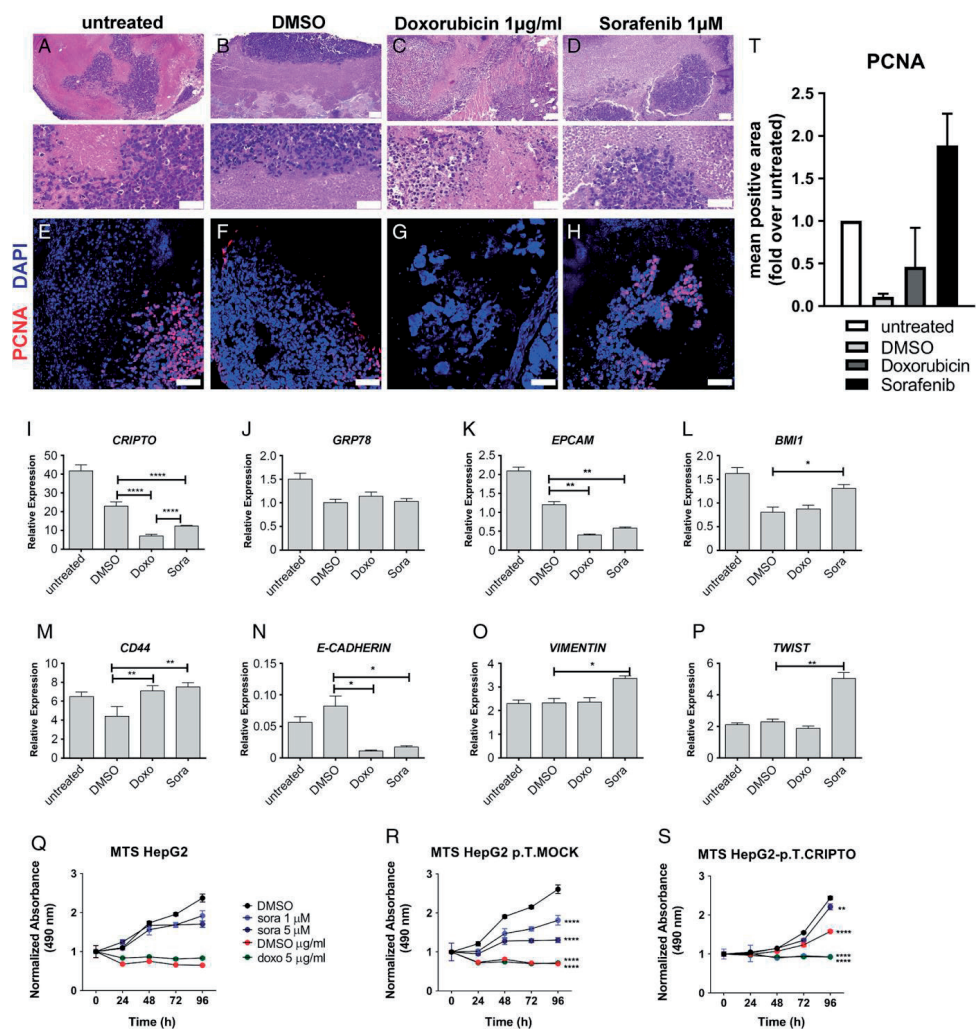


Figure 3. Ex vivo drug response to doxorubicin and sorafenib treatments indicates differential proliferation. EMT and CSC marker expression in CRIPTOhigh tumour slices *ex vivo*. (A–D) *Ex vivo* culture of HepG2-CRIPTO tumour slices; H&E staining of untreated part (A), DMSO vehicle (B), doxorubicin (1 µg/ml) (C), and sorafenib (1 µM) (D) treated. Scale bars: 100 µm (top); 50 µm (bottom). (E–H) Immunofluorescence of PCNA (red) staining on *ex vivo* cultured tissue parts; untreated part (E), DMSO vehicle (F), doxorubicin (G), and sorafenib (H) treated. DAPI marks the nuclei (blue). Scale bars: 50 µm. (I–P) Levels of mRNA for (I) *CRIPTO*, (J) *GRP78*, (K) *EPCAM*, (L) *BMI1*, (M) *CD44*, (N) *E-CADHERIN*, (O) *VIMENTIN*, and (P) *TWIST1* in HepG2-CRIPTO tumours (untreated) exposed to vehicle (DMSO), doxorubicin (1 µg/ml) (C), and sorafenib (1 µM). Unpaired *t*-test; **p* < 0.05; ***p* < 0.01. (Q–S) Metabolic activity MTS assay (24, 48, 72, 96 h) was performed in control (Q), MOCK- (R) and CRIPTO-overexpressing HepG2 cells (S). Cells were exposed to sorafenib (1 or 5 µM) and doxorubicin (1 or 5 µg/ml). Values are normalized to the basal measurements at 0 h after cell seeding. Graph represents values for three independent experiments (*n*=3). Error bars indicate ±SEM. Two-way ANOVA; ****p* < 0.001; *****p* < 0.0001. (T) Quantification of immunofluorescence staining. Mean percentage of PCNA-positive area, normalized to the nuclei (DAPI-positive area). Error bars indicate ±SD.

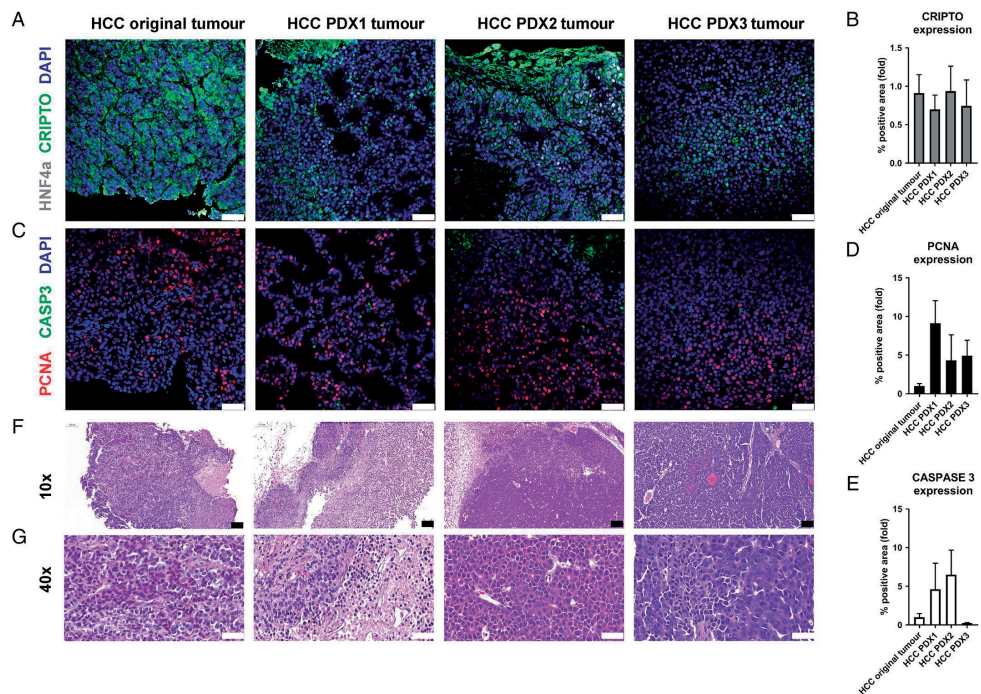


Figure 4. Establishment of CRIPTO-positive patient-derived xenograft model. (A) Immunofluorescence staining for HNF4a (grey) and CRIPTO (green) expression in an HCC tumour sample (left), HCC PDX first passage (PDX1), second passage (PDX2, centre), and third passage (PDX3, right). (B) Quantification of CRIPTO immunofluorescence staining in the PDX tumours represented as fold change the original tumour tissue expression values. Error bars indicate \pm SEM. (C) Immunofluorescence staining for PCNA (red) and cleaved CASP3 (green) expression in an HCC tumour sample (left), HCC PDX first passage (PDX1), second passage (PDX2, centre), and third passage (PDX3, right). (D) Quantification of PCNA and (E) cleaved CASPASE 3 (CASP3) immunofluorescence staining in the PDX tumours represented as fold change over the original tumour tissue expression values. Error bars indicate \pm SEM. (F, G) H&E staining at 10 \times (F) and at 40 \times objective (G) magnification; HCC tumour sample (left), HCC PDX first passage (PDX1), HCC PDX second passage (PDX2, centre) and third passage (PDX3, right). Scale bars 50: panels A, C and G. Scale bars 100: panel F.

To address whether CRIPTO inhibition increases tumour responsiveness to sorafenib, we employed an *ex vivo* tissue slice culture system. Tumour slices and organoids derived from the PDX (from three different passages) were treated with sorafenib; N20 (GRP78 blocking peptide), which blocks CRIPTO/GRP78 binding and CRIPTO signalling; or both in combination. Treatment with N20 blocking peptide inhibited AKT signalling activity, as shown by increased FOXO-luc activity (supplementary material, Supplemental Figure 1E).

H&E staining showed necrotic regions in all treatments in various degrees (Figure 5C–F) compared with the original and untreated condition, respectively (Figure 5A, B). Proliferation (PCNA levels) was affected in both single and combination treatments (Figure 5G–M). However, treatment with sorafenib and N20 in combination reduced cell proliferation (Figure 5L, M)

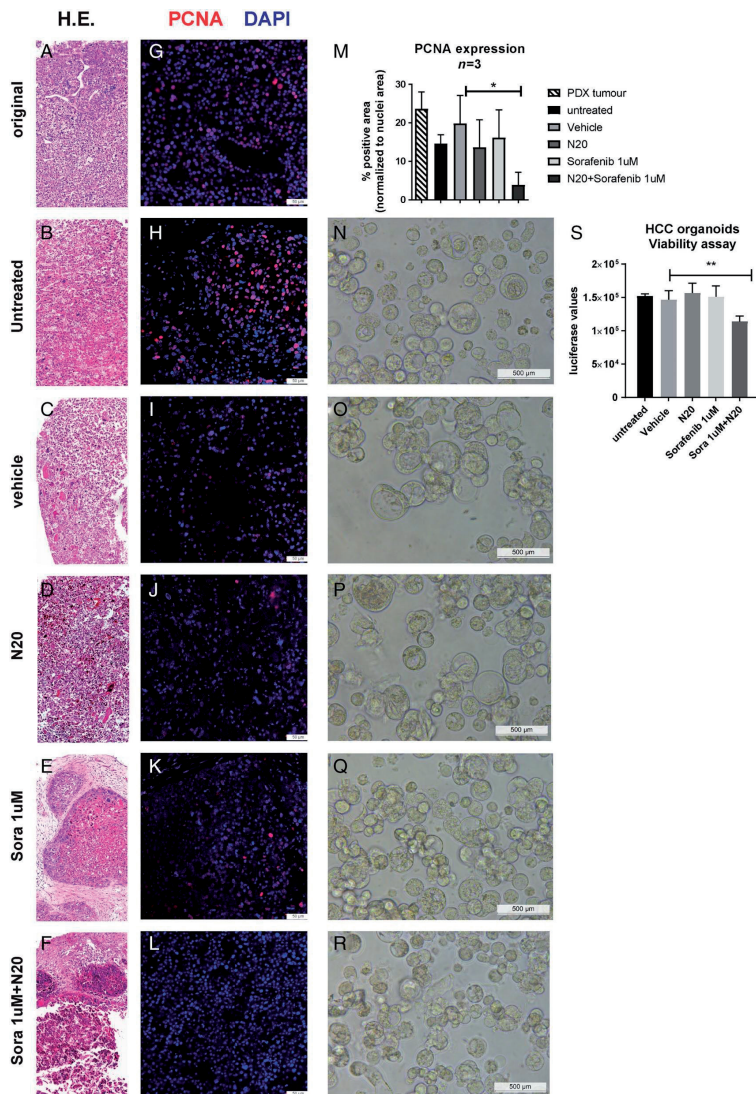


Figure 5. Sorafenib resistance may be circumvented by CRIPTO pathway inhibitor in an ex vivo culture model of HCC PDX. (A–F) *Ex vivo* tissue culture of HCC tumour tissue slices from PDX4 of the established PDX. Drug treatments were performed during the 7 days of *ex vivo* cultures. (A) Original tissue (non-cultured); (B) untreated; (C) vehicle (DMSO 0.1%) plus Control-Fc (2 µg/ml); (D) N20 blocking peptide (2 µg/ml); (E) sorafenib (1 µM); (F) sorafenib (1 µM) plus N20 (2 µg/ml). (G–L) Immunofluorescence staining for PCNA (red) and cleaved caspase-3 (green) expression. DAPI: nuclear dye. (G) Original tissue (non-cultured); (H) untreated, (I) vehicle (DMSO 0.1%) plus Control-Fc (2 µg/ml); (J) N20 blocking peptide (2 µg/ml); (K) sorafenib (1 µM); (L) sorafenib (1 µM) plus N20 (2 µg/ml). (M) Quantification of PCNA immunofluorescence staining. Mean percentage of PCNA-positive area, normalized to the nuclei (DAPI-positive area). Error bars indicate ±SEM; $n=3$ independent experiments. Paired t -test; $*p < 0.05$. (N–R) Bright-field images showing the morphology of organoids derived from the HCC PDX after 48 h of culture (N, untreated), and after treatments with (O) DMSO plus Control-Fc, (P) N20 (2 µg/ml), (Q) sorafenib (1 µM) or (R) sorafenib (1 µM) plus N20 (2 µg/ml). (S) CellTiter Glo viability luciferase-based assay measuring ATP content in organoids derived from HCC PDX tumour. Organoids were treated with DMSO plus Control-Fc, N20 (2 µg/ml), sorafenib (1 µM) or sorafenib (1 µM) plus N20 (2 µg/ml) for 48 h. Error bars indicate ±SD. Ordinary one-way ANOVA; $**p < 0.01$.

to a greater extent than treatment with either of the single compounds alone. In organoid cultures derived from the PDX tumour tissue, viability, measured by CellTiterGlo assay, was also significantly reduced in the combination treatment (Figure 5N–S), indicating a higher susceptibility of sorafenib-resistant cells when CRIPTO-GRP78 signalling was blocked.

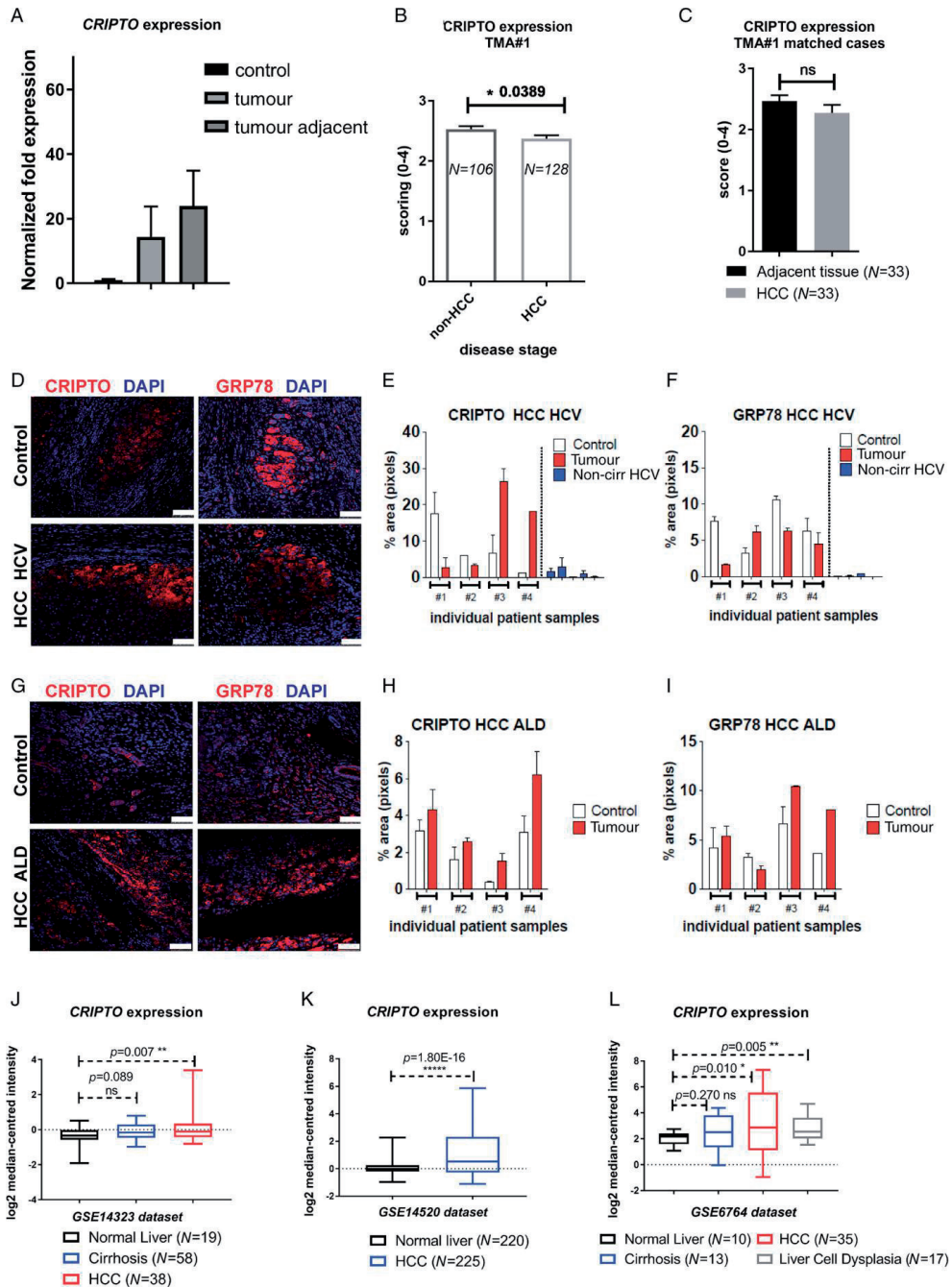
CRIPTO expression in human HCC

Expression of CRIPTO is present in embryonic tissues and becomes silenced in postnatal tissues. Reactivation of CRIPTO in adult tissues has been associated with various cancer types and thus far, only one study has investigated the role of CRIPTO in hepatic malignancy. Considering the low expression of CRIPTO at mRNA level and the absence of protein levels in human liver tissues (both obtained from <http://www.proteinatlas.org>), the role of CRIPTO in homeostatic and pathological liver conditions merits further investigation.

We determined the transcript levels of *CRIPTO* (*TDGF1*) in normal human liver, tumour, and tumour-adjacent tissues by RT-qPCR. Expression was low to undetectable in normal samples ($N= 8$) compared with both tumour ($N= 7$, Table 1) and tumour-adjacent ($N= 7$, cirrhotic, Table 1) tissues, which showed similar levels, indicating that increased *CRIPTO* expression is possibly associated with pre-existing chronic liver disease.

To better understand the expression pattern of CRIPTO in disease states, we determined the protein expression in a tissue microarray (TMA Basel university cohort, 234 tissue samples) by immunohistochemistry and found that HCC tissue ($N= 128$) had significantly ($p=0.0389$) less CRIPTO expression than non-HCC tissue ($N= 106$) (Figure 6B and Table 2). The non-HCC cases reflect unpaired, tumour-adjacent tissues from fibrosis, cirrhosis, and low-grade and

Figure 6. Expression of CRIPTO and its signalling partner GRP78 in human HCC liver tissues. (A) *CRIPTO* mRNA levels in tissue from healthy liver tissues ($N= 8$), tumour ($N= 7$), and tumour-adjacent tissue ($N= 7$) matched cases; values are normalized to the average of the control samples ($\Delta\Delta Ct$ fold). (B) CRIPTO staining scoring in tissue microarray (TMA#1) samples; non-HCC ($N= 106$) versus HCC cases ($N= 128$). (C) CRIPTO protein expression in the cohort of 19 matched (tumour versus tumour-adjacent tissue) cases of TMA#1. (D–F) Representative immunofluorescence images of CRIPTO and GRP78 staining in human liver sections from HCV-derived HCC tissue (HCV infection-driven) and adjacent non-tumour control tissue from the same patient. Nuclei are stained with TO-PRO-3 (blue). Scale bars: 75 μm . Quantification of protein expression of CRIPTO (E) and GRP78 (F), determined by immunofluorescence in HCC HCV tumour (Tumour) or adjacent non-tumour tissue (Control) from the same patient ($N= 4$). Liver tissue from patients with HCV infection but absence of fibrosis (non-cirrhotic HCV, $N= 4$) was used for comparison. The percentage of positive pixel area was the average from two to four focal areas per section. Each bar represents values from each patient. Error bars indicate $\pm SD$. (G–I) Representative immunofluorescence images of CRIPTO and GRP78 protein expression in human liver sections from alcoholic liver disease (ALD)-derived HCC tissue and adjacent non-tumour control tissue from the same patient. Nuclei are stained with TO-PRO-3 (blue). Scale bars: 75 μm . Quantification of (H) CRIPTO and (I) GRP78 protein expression as assessed by immunofluorescence in tumour HCC ALD (Tumour) and adjacent non-tumour tissue (Control) from the same patient ($N= 4$). The percentage of positive area (pixels) was the average from two to four focal areas per section. Each bar represents values from each patient. Error bars indicate $\pm SD$. (J–L) Transcript levels for *CRIPTO* in liver tissues from normal, cirrhosis, HCC, and liver dysplasia conditions. Data were obtained from three distinct publicly available datasets (GSE14323⁴², GSE14520⁴³, and GSE6764⁴¹), accessed through the OncoPrint database (<https://www.oncoPrint.org>). Statistical analysis and P values were obtained from the OncoPrint plots.



high-grade dysplastic nodule cases (supplementary material, Supplemental Figure 3A), thus not healthy liver tissues. Within this TMA, we also analysed paired, matched cases of tumour and adjacent non-tumour tissue ($N=33$) corresponding to the same patients and found that the CRIPTO levels were similar in both cases (Figure 6C and Table 3). A second TMA (US Biomax) was used for the validation of these results and we confirmed CRIPTO expression in both tumour-adjacent cirrhotic tissues and tumour (HCC) tissue, as in the first TMA (supplementary material, Supplemental Figure 3B, and Tables 2 and 3).

Table 2. Baseline characteristics of patients (staining samples). Patient samples correspond to Figure 6B and supplementary material, Supplemental Figure 3A (TMA Basel); Figure 6D–I (LUMC); and supplementary material, Supplemental Figure 3B (TMA US Biomax). Median (IQR). n.a. = not applicable. Only the cases with known clinical background are included in this table

Staining cases	LUMC (N =13)	TMA Basel (N =163)	TMA US Biomax (N =62)
<i>Cohort with clinical background, N (%)</i>	13 (100%)	76 (46.6%)	62 (100%)
<i>Gender, male, N (%)</i>	13 (100%)	58 (35.6%)	52 (83.9%)
<i>Age (range), years</i>	54 (47–63)	76 (67–80)	53 (45–59)
<i>Fibrosis–cirrhosis Yes/undefined, N (%)</i>	8 (61.5%)/n.a.	38 (23.3%)/9 (5.5%)	62 (100%)/n.a.
<i>Patients with HCC, N (%)</i>	8 (61.5%)	46 (28.2%)	48 (77.4%)
<i>T1</i>	1	15	1
<i>T2</i>	5	12	18
<i>T3</i>	2	18	25
<i>T4</i>	n.a.	1	4
<i>Unknown clinical background</i>	n.a.	87 (53.4%)	n.a.
<i>Patients with HCC, N (%)</i>	n.a.	82 (50.3%)	n.a.
<i>Fibrosis–cirrhosis Yes/undefined, N (%)</i>	n.a.	49 (30.1%)/10 (6.1%)	n.a.

Table 3. Baseline characteristics. Patient samples correspond to the matched tumour versus tumour-adjacent tissues of Figure 1A–F (LUMC); Figure 1H (TMA Basel); and supplementary material, Supplemental Figure 3 (TMA US Biomax). Median (IQR). n.a. = not applicable

Matched cases	LUMC (N =8)	TMA Basel (N =33)	TMA US Biomax (N =7)
<i>Gender (male), N (%)</i>	8 (100%)	26 (78.8%)	6 (85.7%)
<i>Age (range), years</i>	56.5 (51–63)	77 (68–80.5)	52 (48–54)
<i>Fibrosis–cirrhosis Yes/undefined, N (%)</i>	8 (100%)	27 (81.8%)/6(18.1%)	7 (100%)
<i>Patients with HCC, N (%)</i>			
<i>T1</i>	1 (12.5%)	11 (33.3%)	n.a.
<i>T2</i>	5 (62.5%)	7 (21.2%)	2 (28.6%)
<i>T3</i>	2 (25%)	15 (45.5%)	4 (57.1%)
<i>T4</i>	n.a.	n.a.	1 (14.3%)

Next, we evaluated CRIPTO and GRP78 expression by immunofluorescent staining in tumours of resected human livers from HCC and adjacent cirrhotic (non-tumour) tissues ($N= 8$) and in non-cirrhotic tissues ($N= 5$, HCV infection). Clinical and tumour characteristics are shown in Table 2 (all cases) and Table 3 (matched cases). CRIPTO expression was detected at higher levels in the tumour than in adjacent cirrhotic non-tumour tissue in two out of four patients with HCV-related disease (Figure 6D, E) and in two out of four ALD-related HCC patients ($N= 4$) (Figure 6G, H). In non-cirrhotic HCV samples, we observed that expression levels of CRIPTO were lower than those of the tumour-adjacent groups (Figure 6E).

The CRIPTO binding and signalling partner GRP78 was expressed in a similar pattern with CRIPTO in hepatocytes. Quantification indicated that higher GRP78 expression in tumour tissue, as compared with adjacent non-tumorous tissue, was detected in one HCV-related (Figure 6D, F) and two ALD-related HCC patients (Figure 6G, I). In matched cases in all three TMA datasets that we have analysed here, we detected CRIPTO expression in HCC specimens both in the tumour and in the tumour-adjacent tissue – however, at different levels – and identified three subgroups of CRIPTO-expressing HCCs (Table 4).

Given the low expression of *CRIPTO* in non-cirrhotic samples (Figure 6A, E) and the high expression already in tumour-adjacent cirrhotic tissue, we accessed the transcript levels of *CRIPTO* in three microarray datasets^{41–43} (publicly available data from the Oncomine database, <https://www.oncomine.org>). Comparison among normal liver, cirrhosis, HCC, and liver cell dysplasia indicated that HCC cases had statistically significantly higher *CRIPTO* mRNA levels versus normal liver tissues in all datasets (Figure 6J–L; $p \leq 0.01$). Cirrhotic cases showed non-significant changes (Figure 6J, L), while liver cell dysplasia showed significantly higher levels versus normal liver expression levels (Figure 6L).

The data above highlight that in individual HCC cases, evaluation of the tumour-adjacent tissue is informative but cannot be considered as control. CRIPTO expression is upregulated in many cases of pathological conditions (cirrhosis, dysplasia); thus, absolute expression levels of CRIPTO in liver tissues should be compared with reference levels from healthy tissues, and not cirrhotic, tumour-adjacent counterparts.

Table 4. Comparison of CRIPTO expression in the different cohorts of tumour versus tumour-adjacent tissue (matched cases)

Matched tissue samples	LUMC (N =8)	TMA Basel (N =33)	TMA US Biomax (N =7)
<i>Cripto tumour < Cripto adjacent tissue, N (%)</i>	2 (25%)	16 (48.5%)	5 (71.4%)
<i>Cripto tumour=Cripto adjacent tissue, N (%)</i>	0 (0%)	8 (24.2%)	1 (14.3%)
<i>Cripto tumour > Cripto adjacent tissue, N (%)</i>	6 (75%)	9 (27.3%)	1 (14.3%)

Discussion

CRIPTO is a cell surface protein that regulates signaling of TGF- β superfamily ligands and also has EGF-like activity. It is a small glycosylphosphatidylinositol (GPI)-anchored cell surface/secreted oncoprotein that plays important roles in regulating stem cell differentiation, embryogenesis, tissue growth, and remodeling¹⁴. The tumour-promoting role of CRIPTO has been documented in multiple malignancies, including those characterized by osteotropism in their metastatic stage, such as breast and prostate cancer^{25,44,45}. Recently, higher CRIPTO expression was detected in a cohort of HCC patients (49.8%, $N=205$), and which correlated with poor prognosis³⁰.

We showed that CRIPTO expression in tumours was mainly detected in areas lining the stromal compartment. This is not surprising given its role in promoting EMT, which we and other groups have shown for other cancer types⁴⁶. The CRIPTO-positive tumour cells adjacent to the stroma may enter the circulation and be responsible for metastatic spread. However, further studies are necessary to corroborate this hypothesis.

Interestingly, in the TMAs (Basel and US Biomax) that we analysed, CRIPTO protein expression was higher in the non-tumour tissue than in tumour tissue. The same trend was observed in a smaller cohort of adjacent and tumour tissue in matched cases of the TMAs, although the number of available matched pairs in the present study may be too small to draw firm conclusions.

Given the fact that the non-tumour tissues have a cirrhotic background and CRIPTO is not expressed during homeostasis, it could be speculated that CRIPTO correlates to disease progression^{30,40}. Moreover, it should be noted that tissue sections (cores) available in the TMAs have a small size, without information of the exact location of where it was derived from within the tumour tissue. The LUMC cohort of matched cases contained large tissue areas derived from a histopathologically confirmed area (tumour, tumour-adjacent), as evaluated by a certified pathologist. It needs to be emphasized that HCCs are heterogeneous tumours and therefore the results of this study should be validated in larger numbers of matched larger tissue sections. Using a transcriptomic approach, we showed that *CRIPTO* mRNA expression is progressively elevated in pathological hepatic conditions such as HCC and liver cell dysplasia compared with normal state, as assessed in three distinct datasets (Oncomine).

In line with the human data, stable overexpression of CRIPTO in HepG2 cells led to a more aggressive tumour phenotype *in vitro*, *ex vivo* and *in vivo* characterized by EMT, mesenchymal phenotype, as well as stem cell characteristics as determined by histology and transcript level alterations. Our data support the notion that CRIPTO plays a role in cirrhosis as well as

tumour initiation and aggressiveness by increasing cellular plasticity and stem cell properties similar to what we have also shown recently for prostate cancer³⁴.

Elevated CRIPTO levels in both HCC and the cirrhotic, potentially premalignant, state suggest that targeted inhibition of CRIPTO could be beneficial in combination with chemical compounds currently used in clinical practice. Doxorubicin is a single-agent drug that has been the most studied chemotherapy agent for advanced HCC⁴⁷. Despite initial studies showing high response rates, subsequent studies showed only a small survival advantage. It is currently widely used for trans-arterial chemoembolization. The development of combination therapy using molecularly targeting drugs such as sorafenib might be useful for the prevention of early HCC metastasis. Given that sorafenib is the standard of care in advanced stage HCC but provides only a 3-month median survival benefit in advanced stage HCC⁴⁶ and no survival benefit in combination with doxorubicin (clinical trial phase III NCT01015833⁴⁸), we explored the possible role of CRIPTO in sorafenib resistance. A low dose of sorafenib did not affect the proliferation of HepG2-CRIPTO cells. These results suggest that CRIPTO causes a differential drug response and refractoriness to sorafenib. This possibility was supported by our finding that HepG2-CRIPTO tumours cultured *ex vivo* possessed areas of proliferating cells following sorafenib treatment.

PDX tissue slices cultured *ex vivo* showed no sensitivity to sorafenib. However, the combination treatment with the N20 peptide, which blocks CRIPTO signalling, showed a significant reduction of proliferation and no effect on apoptosis. This suggests that it might be beneficial to employ a combination of treatments that target either CRIPTO directly or one of its downstream signalling mediators, e.g. ERK and AKT pathways, in order to achieve an inhibition of proliferation in the HCC tumour cells. Similarly, organoids derived from the PDX tumour tissue, treated in the same conditions as the *ex vivo* cultures, showed a reduction in viability when treated with both N20 and sorafenib. This suggests that inhibition of CRIPTO/GRP78 signalling specifically enhances the response to sorafenib. Mechanistically, this effect can be explained by the fact that PI3K/AKT kinase, which is downstream of CRIPTO/GRP78, is also involved in the acquisition of resistance after long exposure to sorafenib⁴⁹, while inhibition of AKT may resensitize tumour cells⁵⁰. CRIPTO has been implicated in therapy resistance in lung cancer, with studies showing that high CRIPTO expression correlates with lower sensitivity to treatment with EGFR kinase inhibitors^{51,52}. Modulation of CRIPTO expression or downstream (SRC, AKT) signalling reverses the resistance to EGFR inhibitors⁵².

The results presented in this study show that CRIPTO signalling increases proliferation and seems to be required for tumour progression, as suggested for both prostate and breast cancer. Our findings suggest that blocking CRIPTO signalling may have therapeutic benefit in combination with existing therapies for HCC.

Acknowledgements

We thank all the members of the Kruithof-de Julio laboratory for critical feedback and specifically we would like to thank Dr Eugenio Zoni for manuscript revision. This work was supported by private funding to M. Kruithof-de Julio and S. Karkampouna.

References

1. Bray F, Jemal A, Grey N, *et al.* Global cancer transitions according to the Human Development Index (2008–2030): a population-based study. *Lancet Oncol* 2012; 13: 790–801.
2. El-Serag HB, Rudolph KL. Hepatocellular carcinoma: epidemiology and molecular carcinogenesis. *Gastroenterology* 2007; 132: 2557–2576.
3. Li D, Kang J, Golas BJ, *et al.* Minimally invasive local therapies for liver cancer. *Cancer Biol Med* 2014; 11: 217–236.
4. European Association for the Study of the Liver, European Organisation for Research and Treatment of Cancer. EASL–EORTC clinical practice guidelines: management of hepatocellular carcinoma. *J Hepatol* 2012; 56: 908–943.
5. Llovet JM, Ricci S, Mazzaferro V, *et al.* Sorafenib in advanced hepatocellular carcinoma. *N Engl J Med* 2008; 359: 378–390.
6. Rahimi RS, Trotter JF. Liver transplantation for hepatocellular carcinoma: outcomes and treatment options for recurrence. *Ann Gastroenterol* 2015; 28: 323–330.
7. Wilhelm SM, Dumas J, Adnane L, *et al.* Regorafenib (BAY73-4506): a new oral multikinase inhibitor of angiogenic, stromal and oncogenic receptor tyrosine kinases with potent preclinical antitumor activity. *Int J Cancer* 2011; 129: 245–255.
8. El-Khoueiry AB, Sangro B, Yau T, *et al.* Nivolumab in patients with advanced hepatocellular carcinoma (CheckMate 040): an open-label, non-comparative, phase 1/2 dose escalation and expansion trial. *Lancet* 2017; 389: 2492–2502.
9. Bruix J, Reig M, Sherman M. Evidence-based diagnosis, staging, and treatment of patients with hepatocellular carcinoma. *Gastroenterology* 2016; 150: 835–853.
10. Behne T, Copur MS. Biomarkers for hepatocellular carcinoma. *Int J Hepatol* 2012; 2012: 7.
11. Gray PC, Harrison CA, Vale W. Cripto forms a complex with activin and type II activin receptors and can block activin signaling. *Proc Natl Acad Sci U S A* 2003; 100: 5193–5198.
12. Gray PC, Shani G, Aung K, *et al.* Cripto binds transforming growth factor β (TGF- β) and inhibits TGF- β signaling. *Mol Cell Biol* 2006; 26: 9268–9278.
13. Gray PC, Vale W. Cripto/GRP78 modulation of the TGF- β pathway in development and oncogenesis. *FEBS Lett* 2012; 586: 1836–1845.
14. Klauzinska M, Castro NP, Rangel MC, *et al.* The multifaceted role of the embryonic gene Cripto-1 in cancer, stem cells and epithelial–mesenchymal transition. *Semin Cancer Biol* 2014; 29: 51–58.
15. Bianco C, Strizzi L, Rehman A, *et al.* A Nodal- and ALK4-independent signaling pathway activated by Cripto-1 through Glypican-1 and c-Src. *Cancer Res* 2003; 63: 1192–1197.
16. Yeo C-Y, Whitman M. Nodal signals to Smads through Criptodependent and Cripto-independent mechanisms. *Mol Cell* 2001; 7: 949–957.
17. Kruihof-de Julio M, Alvarez MJ, Galli A, *et al.* Regulation of extra-embryonic endoderm stem cell differentiation by Nodal and Cripto signaling. *Development* 2011; 138: 3885–3895.

18. Steelman LS, Chappell WH, Abrams SL, *et al.* Roles of the Raf/MEK/ERK and PI3K/PTEN/Akt/mTOR pathways in controlling growth and sensitivity to therapy – implications for cancer and aging. *Aging (Albany NY)* 2011; 3: 192–222.
19. Kelber JA, Panopoulos AD, Shani G, *et al.* Blockade of Cripto binding to cell surface GRP78 inhibits oncogenic Cripto signaling via MAPK/PI3K and Smad2/3 pathways. *Oncogene* 2009; 28: 2324–2336.
20. Lee AS. Glucose-regulated proteins in cancer: molecular mechanisms and therapeutic potential. *Nat Rev Cancer* 2014; 14: 263–276.
21. Sun C, Sun L, Jiang K, *et al.* NANOG promotes liver cancer cell invasion by inducing epithelial–mesenchymal transition through NODAL/SMAD3 signaling pathway. *Int J Biochem Cell Biol* 2013; 45: 1099–1108.
22. Spike BT, Kelber JA, Booker E, *et al.* CRIPTO/GRP78 signaling maintains fetal and adult mammary stem cells *ex vivo*. *Stem Cell Reports* 2014; 2: 427–439.
23. Xu C-H, Sheng Z-H, Hu H-D, *et al.* Elevated expression of Cripto-1 correlates with poor prognosis in non-small cell lung cancer. *Tumour Biol* 2014; 35: 8673–8678.
24. Coccidiferro L, Miceli V, Kang K-S, *et al.* Profiling cancer stem cells in androgen-responsive and refractory human prostate tumor cell lines. *Ann N Y Acad Sci* 2009; 1155: 257–262.
25. Terry S, El-Sayed IY, Destouches D, *et al.* CRIPTO overexpression promotes mesenchymal differentiation in prostate carcinoma cells through parallel regulation of AKT and FGFR activities. *Oncotarget* 2015; 6: 11994–12008.
26. D'Antonio A, Losito S, Pignata S, *et al.* Transforming growth factor alpha, amphiregulin and cripto-1 are frequently expressed in advanced human ovarian carcinomas. *Int J Oncol* 2002; 21: 941–948.
27. Fujii K, Yasui W, Kuniyasu H, *et al.* Expression of CRIPTO in human gall bladder lesions *J Pathol* 1996; 180: 166–168.
28. Giorgio E, Liguoro A, D'Orsi L, *et al.* Cripto haploinsufficiency affects *in vivo* colon tumor development. *Int J Oncol* 2014; 45: 31–40.
29. Strizzi L, Margaryan NV, Gilgur A, *et al.* The significance of a Cripto-1-positive subpopulation of human melanoma cells exhibiting stem cell-like characteristics. *Cell Cycle* 2013; 12: 1450–1456.
30. Wang JH, Wei W, Xu J, *et al.* Elevated expression of Cripto-1 correlates with poor prognosis in hepatocellular carcinoma. *Oncotarget* 2015; 6: 35116–35128.
31. Ji C, Kaplowitz N, Lau MY, *et al.* Liver-specific loss of GRP78 perturbs the global unfolded protein response and exacerbates a spectrum of acute and chronic liver diseases. *Hepatology* 2011; 54: 229–239.
32. Kuo T-C, Chiang P-C, Yu C-C, *et al.* A unique P-glycoprotein interacting agent displays anticancer activity against hepatocellular carcinoma through inhibition of GRP78 and mTOR pathways. *Biochem Pharmacol* 2011; 81: 1136–1144.
33. Chen W-T, Zhu G, Pfaffenbach K, *et al.* GRP78 as a regulator of liver steatosis and cancer progression mediated by loss of the tumor suppressor PTEN. *Oncogene* 2014; 33: 4997–5005.
34. Zoni E, Chen L, Karkampouna S, *et al.* CRIPTO and its signaling partner GRP78 drive the metastatic phenotype in human osteotropic prostate cancer. *Oncogene* 2017; 36: 4739–4749.

35. Karkampouna S, Kloen P, Obdeijn MC, *et al.* Human Dupuytren's *ex vivo* culture for the study of myofibroblasts and extracellular matrix interactions. *J Vis Exp* 2015; (98): 52534.
36. Karkampouna S, Kruithof BP, Kloen P, *et al.* Novel *ex vivo* culture method for the study of Dupuytren's disease: effects of TGFbeta type 1 receptor modulation by antisense oligonucleotides. *Mol Ther Nucleic Acids* 2014; 3: e142.
37. Michalopoulos GK, Bowen WC, Mulè K, *et al.* Histological organization in hepatocyte organoid cultures. *Am J Pathol* 2001; 159: 1877–1887.
38. Huch M, Dorrell C, Boj SF, *et al.* *In vitro* expansion of single Lgr5+ liver stem cells induced by Wnt-driven regeneration. *Nature* 2013; 494: 247–250.
39. Marumoto T, Tashiro A, Friedmann-Morvinski D, *et al.* Development of a novel mouse glioma model using lentiviral vectors. *Nat Med* 2009; 15: 110–116.
40. Friess H, Yamanaka Y, Buchler M, *et al.* Cripto, a member of the epidermal growth factor family, is over-expressed in human pancreatic cancer and chronic pancreatitis. *Int J Cancer* 1994; 56: 668–674.
41. Wurmbach E, Chen YB, Khitrov G, *et al.* Genome-wide molecular profiles of HCV-induced dysplasia and hepatocellular carcinoma. *Hepatology* 2007; 45: 938–947.
42. Mas VR, Maluf DG, Archer KJ, *et al.* Genes involved in viral carcinogenesis and tumor initiation in hepatitis C virus-induced hepatocellular carcinoma. *Mol Med* 2009; 15: 85–94.
43. Roessler S, Jia HL, Budhu A, *et al.* A unique metastasis gene signature enables prediction of tumor relapse in early-stage hepatocellular carcinoma patients. *Cancer Res* 2010; 70: 10202–10212.
44. Castro NP, Fedorova-Abrams ND, Merchant AS, *et al.* Cripto-1 as a novel therapeutic target for triple negative breast cancer. *Oncotarget* 2015; 6: 11910–11929.
45. de Castro NP, Rangel MC, Nagaoka T, *et al.* Cripto-1: an embryonic gene that promotes tumorigenesis. *Future Oncol* 2010; 6: 1127–1142.
46. Rangel MC, Karasawa H, Castro NP, *et al.* Role of Cripto-1 during epithelial-to-mesenchymal transition in development and cancer. *Am J Pathol* 2012; 180: 2188–2200.
47. Wrzesinski SH, Taddei TH, Strazzabosco M. Systemic therapy in hepatocellular carcinoma. *Clin Liver Dis* 2011; 15: 423–441.
48. Abou-Alfa GK, Johnson P, Knox JJ, *et al.* Doxorubicin plus sorafenib vs doxorubicin alone in patients with advanced hepatocellular carcinoma: a randomized trial. *JAMA* 2010; 304: 2154–2160.
49. Chen KF, Chen HL, Tai WT, *et al.* Activation of phosphatidylinositol 3-kinase/Akt signaling pathway mediates acquired resistance to sorafenib in hepatocellular carcinoma cells. *J Pharmacol Exp Ther* 2011; 337: 155–161.
50. Zhai B, Hu F, Jiang X, *et al.* Inhibition of Akt reverses the acquired resistance to sorafenib by switching protective autophagy to autophagic cell death in hepatocellular carcinoma. *Mol Cancer Ther* 2014; 13: 1589–1598.
51. Zhang H, Zhang B, Gao L, *et al.* Clinical significance of cripto-1 expression in lung adenocarcinoma. *Oncotarget* 2017; 8: 79087–79098.
52. Park K-S, Raffeld M, Moon YW, *et al.* CRIPTO1 expression in EGFR-mutant NSCLC elicits intrinsic EGFR-inhibitor resistance. *J Clin Invest* 2014; 124: 3003–3015.

- *53. Zoni E, van der Horst G, van de Merbel AF, *et al.* miR-25 modulates invasiveness and dissemination of human prostate cancer cells via regulation of α v- and α 6-integrin expression. *Cancer Res* 2015; 75: 2326–2336.
- *54. Karkampouna S, Goumans MJ, Ten Dijke P, *et al.* Inhibition of TGF β type I receptor activity facilitates liver regeneration upon acute CCl₄ intoxication in mice. *Arch Toxicol* 2016; 90: 347–357.
- *55. Brunet A, Bonni A, Zigmond MJ, *et al.* Akt promotes cell survival by phosphorylating and inhibiting a Forkhead transcription factor. *Cell* 1999; 96: 857–868.

*Cited only in supplementary material.

Supplementary files

Supplementary materials and methods

RNA isolation, RT-PCR, and quantitative PCR (qPCR)

RNA was isolated using an UltraTurrax homogenizer (T25 basic, IKA, Staufen, Germany) and directly processed according to the TRIpure RNA extraction protocol (Qiagen, Hombrechtikon, Switzerland). Total RNA (0.5 µg) was used for first-strand cDNA synthesis using a RevertAid H Minus first-strand cDNA synthesis kit (Fermentas, LuBio Science, Lucerne, Switzerland). For qPCR, ten-fold diluted cDNA was amplified in a CFX Real Time Detection system (Bio-Rad, Cressier, Switzerland) using SYBR Green Supermix reagent (Bio-Rad). Expression levels were normalized to the transcript of *ACTB*. Primer sequences are indicated in the supplementary material, Table S2.

Migration, measurement of metabolic rate (MTS), and wound-healing assay

Transwell cell migration and aqueous soluble tetrazolium/formazan (Cell Titer Aqueous One solution MTS assay; Promega, Dübendorf, Switzerland) metabolic activity/proliferation assays were performed as described in previous studies⁵³. For the wound-healing assay, 500 000 cells per well of a 24-well plate were seeded. After 24 h, the wound was made and the culture medium was refreshed. Subsequently, pictures were taken (4x objective magnification) at 0, 24, 48, and 76 h time points. The size of the wound was measured using ImageJ software and normalized to the time-zero width.

Microscopy and image analysis

Confocal microscopy was performed using a Leica TC-SP5 (Leica Biosystems BV, Amsterdam, The Netherlands) microscope with a 40x 1.4 NA oil-immersion objective. Series of Z stacks were collected and reassembled in ImageJ software (<http://rsbweb.nih.gov/ij>). Mean fluorescence-positive areas were calculated in ImageJ software using a threshold to select the root boundary and measuring the percentage of positive surface inside the intensity defined by the threshold. For quantification of immunofluorescence signals (LUMC cohort), staining experiments were performed on all samples simultaneously to reduce technical variation and imaged using identical exposure and recording settings. Scoring of the immunohistochemistry of the US Biomax and the Basel TMAs was done by a pathologist, in a blind manner, without any prior information on the clinical and pathological data. The homogeneous staining pattern of the tumour cells was assessed by the pathologist. According to this staining, the tissue received a score of 0 (no staining), 1 (low intensity), 2 (medium intensity), 3 (high intensity) or 4 (strong intensity).

Statistical analysis

Statistical analysis was performed using GraphPad Prism 5.0 software (GraphPad Software, San Diego, CA, USA) and two-way ANOVA tests. Data are presented as mean \pm SEM or median and interquartile range (IQR) for non-normally distributed variables. Statistically significant differences are indicated with asterisks (* $p < 0.05$, ** $p < 0.01$, *** $p < 0.001$, **** $p < 0.0001$). For qPCR analysis, experiments were repeated at least three times as technical replicates for each sample (different cDNA preparations using the RNA of HepG2 cells or patient tissues) and the average value was calculated. For quantification of the immunofluorescence signal of the stained sections, multiple fields of view were imaged, quantified, and averaged.

Immunofluorescence and immunohistochemistry

Tissues were fixed in 4% paraformaldehyde solution overnight, washed in phosphate buffer saline (PBS), processed for paraffin embedding, and serial paraffin sections of 4 μm were prepared. For antigen retrieval, sections were boiled for 10–30 min in antigen unmasking solution (Vector Labs, Adipogen AG, Liestal, Switzerland) and incubated in 3% H_2O_2 for endogenous peroxidase inactivation. Sections were blocked with 1% bovine serum albumin in PBS + Tween 20 (0.1%, v/v) and subsequently incubated with primary antibodies diluted in the blocking solution, overnight at 4°C. The primary antibodies and dilutions used were as follows: anti-CRIPTO, 1:2000 and anti-GRP78, 1:1000 (kindly provided by Dr Peter Gray), anti- α SMA, 1:500 (A2547, clone 1A4; Sigma, Buchs, Switzerland), anti-PCNA, 1:500 (P8825, clone PC 10; Sigma), anti-cleaved CASPASE 3, 1:500 (9661; Cell Signaling, BioConcept Allschwil, Switzerland), and anti-HNF4a, 1:100 (sc-6556, clone C19; Santa Cruz, LabForce, Muttenz, Switzerland). The following day, sections were incubated with secondary antibodies labelled with Alexa Fluor 488, 555, or 647 (Invitrogen/Molecular Probes, Zurich, Switzerland; 1:250 in PBS + 0.1% Tween 20). Detection of CRIPTO and GRP78 was enhanced using tyramide amplification (Invitrogen/Molecular Probes) as described previously⁵⁴. Sections were counterstained with TO-PRO-3 (Invitrogen/Molecular Probes) or DAPI solution (Sigma) for visualization of nuclei, and mounted using Prolong G mounting medium (Invitrogen/Molecular Probes). For CRIPTO immunohistochemistry, the TMA samples were deparaffinized and antigen retrieval was performed by boiling (microwave, 240 W) in 10 mM Tris–HCl containing 1 mM EDTA (pH 9.0) buffer for 30 min. Endogenous peroxidases were blocked using 3% H_2O_2 –15 mM NaN_3 for 5 min at room temperature. Sections were blocked with swine serum and incubated with primary anti-CRIPTO antibody [diluted 1:1000 in 0.5% swine serum in antibody diluent buffer (DAKO)]. Secondary anti-rabbit HRP was used (Envision system) for 30 min at room temperature. Signal was developed using AEC substrate (Sigma #A6926, 20 mg) diluted in 10% DMN, 10% imidazole buffer, and 0.02% H_2O_2 .

Reporter assays

To assess AKT pathway activation, the FOXO-luc reporter assay was used. The FOXO-luc construct (Addgene, #1789) contains the promoter response element of the Forkhead box

transcription factor gene *FOXO3* (FKHRL), which controls the expression of luciferase [55]. When AKT is active, it phosphorylates FOXO3 and blocks downstream FOXO transcription activation. Thus, FOXO-luc activation occurs when AKT is inactive. HepG2-CRIPTO cells were transfected with 500 ng of FOXO plasmid and 5 ng of *Renilla* plasmid in 24-well plates using DharmaFect I reagent (ratio to DNA 4:1) in OptiMem medium. After 16 h, cells were treated with vehicle (10% DMSO) plus IgG (2 µg/ml, R&D goat IgG), 20% FCS, sorafenib (1 µM), GRP78 antibody (2 µg/ml, A-10 Abcam), and N20 blocking peptide (2 µg/ml, Santa Cruz). Cells were lysed after 6 h of treatment with 100 µl of passive cells lysis (Promega). Lysates (10 µl) were transferred into opaque 96-well plates in triplicate per sample. Luciferase buffer (LAR-II, 25 µl) was added to the lysates and luciferase activity was measured after 10 min. An equal amount of STOP&Glo reagent was added and *Renilla* firefly activity was measured after 10 min. Values were normalized to cell lysis buffer as a control and to the *Renilla* counts. Mean fold-change values were calculated over the DMSO/IgG control.

Western immunoblotting

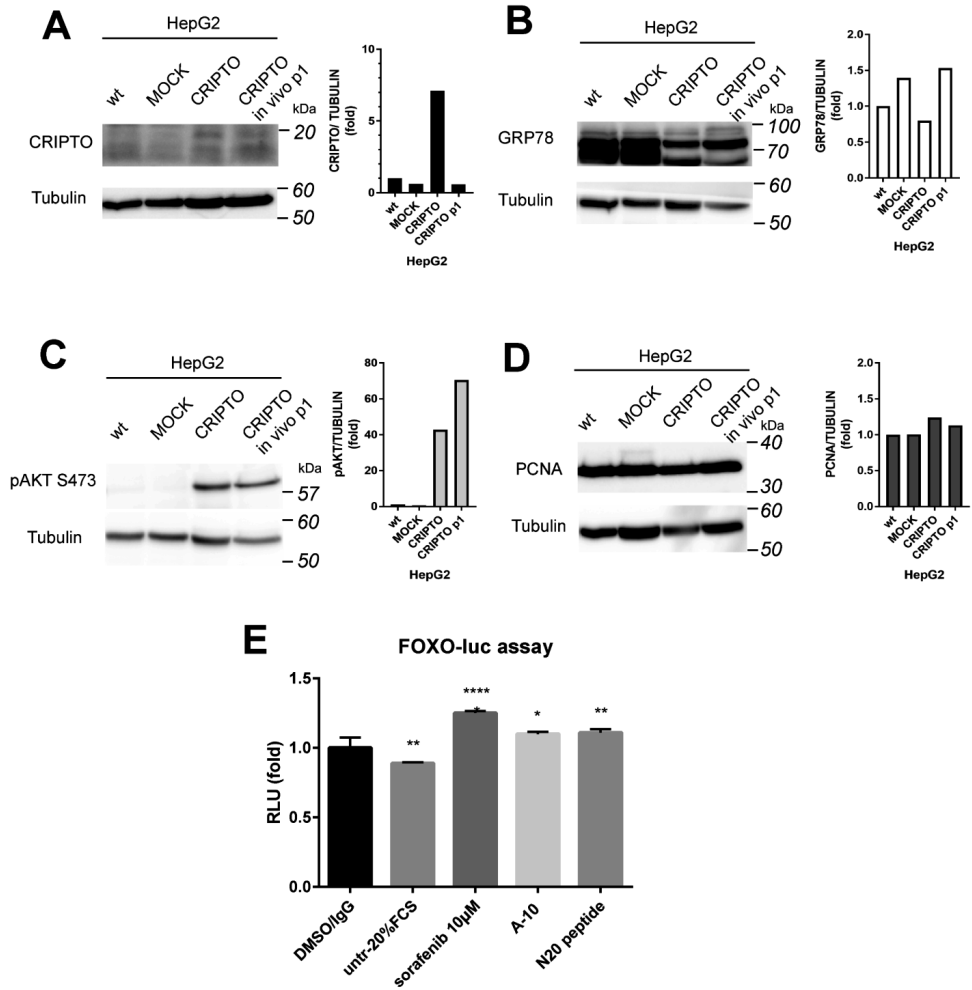
Cells were lysed in cold RIPA lysis buffer [10 mM Tris (pH 8.0), 140 mM NaCl, 1% Triton-X 100, 0.1% C₂₄H₃₉NaO₄, 1 mM EDTA (pH 8.0), 0.1% SDS, 1 mM EGTA plus complete protease inhibitors; Roche] using a cell scraper. Lysates were passed through a 26-gauge needle. Following a centrifugation step (15 min, 4000 rpm, 4°C) to remove debris, the protein extract was collected (supernatant). Protein content was quantified using a DC protein assay (Bio-Rad) using serial dilutions of BSA in tissue lysis buffer. A total of 30 µg was diluted in 4' Laemmli buffer, separated by SDS-PAGE, and transferred to PVDF membranes. The following primary antibodies were used in 5% bovine serum albumin diluted in TBS + 0.1% Tween 20: anti-PCNA, 1:5000 (P8825, clone PC 10; Sigma) anti-CRIPTO, 1:1000 and anti-GRP78, 1:1000 (kindly provided by Dr Peter Gray), tubulin, 1:3000 (T8578, clone 2G10; Sigma), and anti-pAKT (S473), 1:1000 (9271S, Cell Signaling). Appropriate secondary HRP antibodies (Promega) were used and detected by chemiluminescence (Bio-Rad).

Supplementary Table S1. Organoid media composition

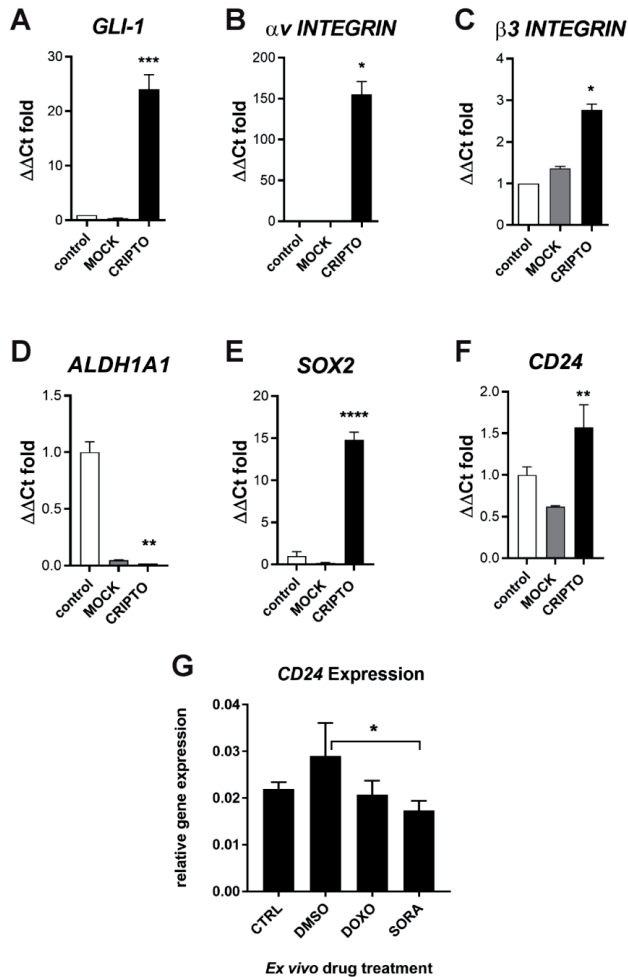
	Final concentration
<i>Advanced DMEM/F12 (supplemented with PenStrep, GlutaMAX, HEPES, and primocin)</i>	
<i>FCS</i>	5%
<i>Y-27632</i>	10 μ M
<i>A83-01</i>	500 nM
<i>SB202190</i>	10 μ M
<i>R-spondin</i>	500 ng/ml
<i>Noggin</i>	100 ng/ml
<i>B27</i>	1'
<i>N-acetyl-cysteine</i>	1.25 mM
<i>Nicotinamide</i>	10 mM
<i>EGF</i>	50 ng/ml
<i>FGF10</i>	10 ng/ml
<i>Wnt3A</i>	100 ng/ml
<i>HGF</i>	50 ng/ml

Supplementary Table S2. Primer sequences used in this study

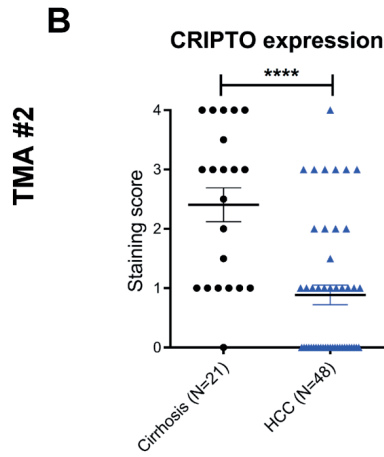
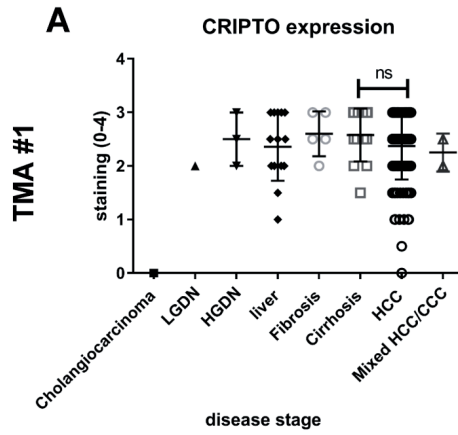
Primer	Forward	Reverse
<i>ALDH1A1 (human)</i>	TGGCTTATCAGCAGGAGTGT	GCAATTCACCCACACTGTTC
<i>ALK4 (human)</i>	GCTCGAAGATGCAATTCTGG	TTGGCATACCAACACTCTCG
<i>αv INTEGRIN (human)</i>	GCTGGACTGTGGAGAAGAC	AAGTGAGGTTCCAGGGCATTTC
<i>β-actin (human)</i>	AATGTCGCGGAGGACTTTGATTGC	GGATGGCAAGGGACTTCTGTAAA
<i>β-actin (mouse)</i>	GGGGTGTGAAGGTCTCAAA	AGAAAATCTGGCACCCC
<i>BMI-1 (human)</i>	TCATCCTTCTGCTGATGCTG	CCGATCCAATCTGTTCTGGT
<i>β3 INTEGRIN (human)</i>	GTCTGCCACAGCAGTGACTT	CTTGATAGCGGACACAGGAGA
<i>CD24 (human)</i>	TACCCACGCAGATTATT	AGAGTGAGACCACGAAGA
<i>CD44 (human)</i>	TGGCACCCGCTATGTCAG	GTAGCAGGGATTCTGTCTG
<i>Cripto (mouse)</i>	CGCCAGCTAGCATAAAAGTG	CCCAAGAAGTGTCCCTGTG
<i>CRIPTO (human)</i>	CACGATGTGCGCAAAGAGAA	TGACCGTGCCAGCATTACA
<i>E-CADHERIN (human)</i>	TTGACGCCGAGAGCTACAC	GACCGGTGCAATCTTCAAA
<i>EPCAM (mouse)</i>	AGGGGCGATCCAGAACAACG	ATGGTCGTAGGGGCTTTCTC
<i>GLI-1 (human)</i>	CTGGTGGCTTTCATCAACTCTC	GGTACACAGGGCTGGACTC
<i>GRP78 (human)</i>	GAACGTCTGATTGGCGATGC	TCAACCACCTTGAACGGCAA
<i>LEFTY (human)</i>	CGAGTGGCTGCGCTCCGCGA	CGAGGCACAGCTGCACTTCTGCACC
<i>N-CADHERIN (human)</i>	CAGACCGACCCAACAGCAAC	GCAGCAACAGTAAGGACAAACATC
<i>NANOG (human)</i>	AATACCTCAGCCTCCAGCAGATG	TGCGTCACACCATTGCTATTCTTC
<i>NODAL (human)</i>	CTTCTCCTTCTGAGCCAACAAGAGG	GGTGACCTGGGACAAAGTGACAGTG
<i>OCT4 (human)</i>	GAGAACCGAGTGAGAGGCAACC	CATAGTCGCTGCTTGATCGCTTG
<i>SNAIL-2 (human)</i>	TGTGTGGACTACCGCTGC	TCCGGAAAGAGGAGAGAGG
<i>SOX2 (human)</i>	CAGGAGTTGTCAAGGCAGAGA	CGCCGCCGATGATTGTTATTA
<i>TWIST (human)</i>	GCCGGAGACCTAGATGTCATT	TTTTAAAAGTGCGCCCCACG
<i>VIMENTIN (human)</i>	CCAAACCTTTTCTCCCTGAACC	CGTGATGCTGAGAAGTTTCGTTGA
<i>ZEB-1(human)</i>	CCATATTGAGCTGTTGCCGC	GCCCTTCTTTCTGTGTCA
<i>ZEB-2 (human)</i>	GACCTGGCAGTGAAGGAAAA	GGCACTGCAGAAACACAGA



Supplemental Figure 1. *In vitro* characterisation of CRIPTO downstream pathway activation. (A–D) Western blotting and corresponding quantifications for CRIPTO (A), GRP78 (B), phosphorylated AKT (pAKT) (C), and PCNA (D) in HepG2, HepG2-MOCK, HepG2-CRIPTO cells, and HepG2-CRIPTO cells after *in vivo* passaging. Tubulin was used to assess equal protein loading. (E) Reporter FOXO assay for AKT pathway activation determination in the HepG2-CRIPTO cells.



Supplemental Figure 2. Expression of stem cell markers in CRIPTO-overexpressing cells. (A–F) mRNA expression of stem cell markers in HepG2 (control), HepG2-MOCK, and HepG2-CRIPTO cell lines: (A) *GLI1*, (B) αv *INTEGRIN* (*ITGAV*), (C) β3 *INTEGRIN* (*ITGB3*), (D) *ALDH1A1*, (E) *SOX2*, (F) *CD24*. (G) mRNA levels of *CD24* after *ex vivo* culture of HepG2-CRIPTO tumour slices after treatment with vehicle (DMSO), doxorubicin (DOXO) or sorafenib (SORA). CTRL: no treatment control. Error bars indicate \pm SD. * $p < 0.05$.



Supplemental Figure 3. CRIPTO staining in HCC versus non-HCC cases of two TMAs. CRIPTO staining scoring after pathologist's evaluation of (A) TMA (Basel) with HCC and non-HCC cases (tumour-adjacent tissues from fibrosis, cirrhosis, cholangiocarcinoma, and low-grade and high-grade dysplastic nodule cases) and (B) TMA (US Biomax) containing cirrhosis and HCC cases. Error bars indicate \pm SEM. **** $p < 0.0001$.

7

CHAPTER 7

General Discussion

General Discussion

Liver fibrogenesis is the underlying process that leads to the onset and progression of the fibrosis-cirrhosis-hepatocellular carcinoma (HCC) cascade^{1,2}. This process is initiated by etiological factors that damage and destroy hepatocytes, and subsequently triggers the activation of the hepatic stellate cells. These activated stellate cells proliferate and differentiate into myofibroblasts which start to produce high levels of extracellular matrix (ECM)³⁻⁶. While effective treatments for some of the underlying etiological factors that trigger fibrogenesis, like viral hepatitis, become increasingly available, treatments which specifically target the process of fibrogenesis and thereby prevent progression of the disease cascade are not yet available^{1,2,7-9}. Mesenchymal stromal cells (MSCs) are thought to stimulate tissue regeneration as well as to modulate inflammatory responses¹⁰⁻¹⁵. These features make MSCs an attractive tool for the resolution of liver fibrosis where these specific processes need to be restored. In that context, MSCs are thought to support survival of liver cells and directly target fibrogenesis by silencing the myofibroblasts and by inhibiting the activation and proliferation of stellate cells¹⁶⁻²². Currently, MSCs have been tested in clinical trials with promising, but also sometimes disappointing, results regarding the reversal of fibrosis and cirrhosis^{14,23-25}. In the present thesis several studies are described which addressed the different aspects, which might shed light on the potential cause(s) of these sometimes even contradictory results. Furthermore, a novel treatment strategy is proposed where the beneficial features of MSCs are combined with the innate regenerative ability of the liver^{26,27}.

Study design might be an important factor for effective MSC therapy

MSC therapy for liver fibrogenesis is still in its infancy and an optimal and standardised treatment protocol is not available yet. The use of diverse protocols makes it difficult to compare and explain the contradictory findings observed in literature. Variables in study design which might have led to different study outcomes include the route of administration (local vs systemic), dosage of MSCs, disease stage (fibrosis vs cirrhosis), trigger for regeneration (e.g. partial hepatectomy), and possibly the existence and use of different subpopulations of MSCs^{28,29}. In the *in vivo* experiments of **chapter 2** we observed that a partial hepatectomy effectively reduces the fibrotic stage of fibrosis. This phenomenon has not been described before and it would be of interest to verify these outcomes in patients.

Furthermore, our *in vivo* studies also showed that local administration of MSCs had a smaller effect than the regenerative response after partial hepatectomy. However, when these two approaches were combined, this reinforced the effectivity of both therapies. This additional effect of MSC administration was not observed after systemic infusion, indicating the importance of local administration²⁶. MSCs, when injected intravenously (i.v.), can easily get trapped in the lungs, which leads to fewer, if any, cells homing to the liver, which in turn might very well be the possible explanation for the ineffectiveness of this route of administration of MSCs in

reverting liver fibrosis³⁰. After local administration, the MSCs did not migrate from the injection sites and were only effective in that part of the diseased liver. Nevertheless, our study is the first describing an on-site effect of MSC therapy on fibrogenesis and gives further reasoning to the ineffectiveness of i.v. MSC treatment.

Due to the limitations in time and of the mouse model for liver fibrosis, we did not assess the potency of portal- or liver artery-infusion of MSCs. Nevertheless, since portal- and liver artery-infusions are local administration routes one might expect similar results as observed for the local treatment in the present studies. CCL4-mouse models for liver fibrosis are frequently used to study potential therapeutic interventions. However, the severity of the induced disease is rather diverse between studies and this might potentially affect study outcomes^{31,32}. We showed that the described combination therapy (partial hepatectomy plus local MSC administration) effectively resolved both fibrosis and cirrhosis, illustrating that the disease stage is less relevant for the functionality of the described therapy (**chapter 2**). Furthermore, a dose-dependent response in the resolution of fibrosis between 1×10^6 and 2×10^6 MSCs treated mice was observed, which suggests that the effectiveness of therapy is related to the dose of MSCs. As suggested in the studies of Parekkadan et al., this observation could be explained by the myofibroblast/MSC ratio²². For example, in **chapters 3 and 4** we described that MSCs express HGF, which is thought to directly target and subsequently silence the myofibroblasts. When this hypothesis is true, one could imagine that higher dosages of MSCs lead to more expression of HGF and consequently induce a larger therapeutic effect. In relation to the treatment of fibrosis in patients, a therapy could be considered consisting of both a trigger for regeneration, by partial hepatectomy, and multiple local MSC injections. This approach is comparable to the successful treatment of perianal fistulas in Crohn's disease by our group, where fistulas received a trigger for regeneration by curettage of the fistula tract and subsequently local MSC administration at multiple injection sites³³.

MSC subpopulations differently affect the resolution of fibrosis

Most researchers are not familiar with the existence of multiple subpopulations of MSCs and as a result all kinds of (mixed)populations have been used, which might contribute to the different and even contradictory findings between various studies. Only a few studies assessed the possible existence of multiple subpopulations of MSCs³⁴⁻³⁶. This might be caused by the lack of more precise criteria for the identification and characterisation of these cells and results in a rather heterogenous population of cells being identified as MSCs³⁶. Most of the studies describe mouse-derived MSCs as cells that adhere to plastic and are able to differentiate into osteoblast, chondrocytes and adipocytes. Furthermore, CD29, CD44 and SCA-1 need to be expressed on their membranes but CD45 (haematopoietic marker) and CD31 (endothelial marker) should be absent^{37,38}. However, these criteria embrace different subpopulations of MSCs as identified by their VCAM (CD106) and/or Endoglin (CD105) expression^{34,35}. Until recently, only a few studies have shown different functional capacities of these MSC

subpopulations^{34,35,39,40}. Furthermore, there are no studies focusing on the use of different subpopulations of MSCs in relation to the treatment of liver fibrosis. Therefore, as described in **chapter 3**, we selected MSCs double-positive, double-negative, or single-positive for either Endoglin and VCAM and evaluated their antifibrotic and pro-regenerative capacity. More cell proliferation and survival of damaged HepG2 cells was observed when exposed to VCAM-positive subpopulations compared to the VCAM-negative MSC subpopulations. In addition, in line with the studies of Du et al.³⁹, we observed that VCAM-positive subpopulations are more migratory than the VCAM-negative MSC subpopulations. We used the CCL4 mouse-model and optimized MSC therapy from **chapter 2** to evaluate the therapeutic potential of the described subpopulations. The results showed that VCAM-positive but not the VCAM-negative MSC subpopulations successfully reduce fibrosis, regardless of their Endoglin expression (**chapter 3**). However, the Endoglin-negative subset of the VCAM-positive subpopulations revealed an intermediate collagen reduction, which was less than for the double positive population but more than in the VCAM-negative populations ($V^{neg}E^{pos}$, $V^{neg}E^{neg}$).

Previous studies, including those of our own group, showed that MSCs express pro-regenerative and antifibrotic cytokines (HGF, VEGF, IGF-1, and TGF- β 1)^{19,20,22,41-47}. In the study of **chapter 3** a higher expression level of HGF and IGF-1 was found in the VCAM-positive subpopulations compared to the VCAM-negative populations. Previous studies of Han and Du et al., observed the same phenomena, however, these studies were not related to liver fibrosis^{36,39}. The different expression levels of HGF and IGF-1 might very well clarify the results of our studies, since these genes are known to support tissue-regeneration and directly inhibit fibrogenesis by stimulation of cell survival, cell proliferation, inhibition of stellate cell activation, and silencing of myofibroblasts^{16,19,20,24,39,42,43,48}. Anderson et al. pointed out that the $V^{pos}E^{neg}$ population are more immunosuppressive compared to the $V^{pos}E^{pos}$ population³⁴. In line with this statement, we observed higher IGF-1 and TGF- β 1 expression levels in the $V^{pos}E^{neg}$ subpopulation compared to the other subpopulations. These genes are thought to stimulate macrophage differentiation to an anti-inflammatory and antifibrotic phenotype and thereby contribute to the resolution of fibrosis⁴³.

These different gene-profiles might thus also explain the intermediate results as observed for the $V^{pos}E^{neg}$ subpopulation in the *in vivo* experiments. It might very well be that the double positive subpopulation directly targets fibrogenesis by the HGF-mediated mechanisms and that the $V^{pos}E^{neg}$ subpopulation exposes an indirect and delayed anti-inflammatory pathway mediated effect. Further studies are needed to substantiate these observations since the immunosuppressive capacities of MSCs were not evaluated in our studies. In conclusion, our research showed that VCAM-positive MSC subpopulations have advantageous properties for therapeutic interaction with regenerating fibrotic livers compared to VCAM-negative subpopulations, indicating that patients with liver cirrhosis might benefit more from the treatment with VCAM-positive MSC subpopulations. Therefore, in the context of the

resolution of fibrosis it is highly recommended to include VCAM as a selection marker in the characterization panel of MSCs before use.

In addition to the existing subpopulations, previous studies claimed that MSCs are fibroblast-like cells with similar functions in immunosuppression and tissue repair⁴⁹. However, these studies were not related to liver diseases and focussed on basic mechanistic *in vitro* studies⁴⁹⁻⁵¹. In our studies fibroblasts, in contrast to MSCs, were found to be ineffective in resolving fibrogenesis *in vivo* (**chapter 2 and 4**)^{26,27}. These observations could very well be correlated to the observed lower expression levels of antifibrotic genes (HGF, VEGF, IGF-1 and TGF- β) in fibroblasts compared to MSCs^{13,19}. Overall, our observations illustrate the unique phenotypical and functional features of MSCs compared to fibroblasts.

MSCs also reverse fibrosis in a novel TAA-induced zebrafish embryo model for liver fibrosis

Liver fibrosis and cirrhosis in rodent models are most frequently induced by administration of hepatotoxic compounds, such as CCL4 and TAA^{31,32}. These models, however, are relative expensive, have a long induction period (6-12 weeks) and have a relatively high work load; they are therefore less attractive for high throughput compound screening^{52,53}. To generate a model for liver fibrosis suitable for this purpose, we attempted to translate the widely used CCL4 and TAA models to zebrafish embryos. The experiments illustrated that TAA, in contrast to CCL4, induces fibrogenesis with similar mechanisms as observed in man and rodents (**chapter 4**)²⁷. After 6 days of TAA treatment, increased collagen-1 α 1, Hand-2 and Acta-2 (the fish homologue of α -smooth muscle actin) expression levels were observed, which is indicative for the proliferation and activation of stellate cells and their subsequent differentiation into myofibroblasts, all illustrative for fibrogenesis^{52,54-56}. Furthermore, this model also showed smaller liver sizes and increased collagen deposition.

However, the characteristic collagen-filled septa structures as observed in the livers of humans and rodents with liver fibrosis were not observed in our zebrafish embryo model⁵⁷. This difference is very likely due to the different liver architecture between these species. Although, the livers of zebrafish embryos are constructed with the same cells as in humans, these livers are less well organised and miss the typical hexagonal cell organisation⁵². These fundamental differences might very well be the reason for the diffuse collagen deposition as observed in the livers of the zebrafish embryos in our model⁵². Furthermore, similar findings in RNA expression profiles and collagen deposition were observed in the livers of adult zebrafish upon ethanol treatment⁵⁶.

The applicability of this model system to analyse novel therapeutic interventions was shown by the administration of MSCs and fibroblasts as potential novel cell therapies for fibrosis. In concordance with our mouse studies (**chapter 2 and 3**) we observed that MSCs, in contrast to

fibroblasts, were able to considerably prevent the progression of TAA-induced liver fibrosis in the zebrafish embryos^{26,27}. One of the limitations of our model, however, is that the immune-system of zebrafish embryos is not fully developed. Therefore, compounds that intervene in the immunological pathways during fibrogenesis cannot be tested in this model. Although we have shown the pathological similarities between species and the robustness of our model, newly discovered compounds for the reversal of fibrogenesis identified by this model still need further testing in rodent models. This second step is crucial since the rodent models have a higher resemblance to man and contain a functioning immune-system. Furthermore, the pharmacokinetic and pharmacodynamic differences between rodents and man are better understood. Zebrafish embryos are known to resist higher dosages of certain compounds than rodents and man, which illustrates the difficulty to translate the dosages between these species. Altogether, our observations indicate that TAA induces liver fibrogenesis in zebrafish embryos through mechanisms that are highly comparable to the pathogenesis of liver fibrosis in humans. The proven induction of fibrogenesis together with the low labour intensiveness, cushioniness and low costs of this model provide researchers with a rapid model for future mechanistic and therapeutic studies on liver fibrosis suitable for high throughput screening purposes.

Cripto-1: a new player in the pathological pathway of fibrogenesis

As previously alluded to, Cripto-1 (Cripto) is an oncofetal protein and known to stimulate multiple processes including cell differentiation, cell survival and cell proliferation⁵⁸⁻⁶¹. These features are also involved in liver regeneration and fibrogenesis and Cripto was speculated to be also important during liver fibrogenesis⁶²⁻⁶⁴. This idea was encouraged by the study of Zhang et al. which showed elevated Cripto levels in blood of patients with viral hepatitis induced cirrhosis⁶⁵. In concordance with that study, we also observed elevated Cripto levels in plasma of patients with ALD- or HCV-induced cirrhosis. However, in addition, these elevated levels were found to normalise one year after removing the fibrosed source by liver transplantation (**chapter 5**). Furthermore, for the first time, human-, mouse-, and zebrafish embryo-livers were all found to express Cripto during fibrogenesis, which is indicative for a well preserved role for Cripto in the pathology of hepatic fibrogenesis⁶⁶. In humans, Cripto protein expression in liver tissue positively correlated with the clinical laboratory MELD score for liver disease. Surprisingly, this correlation was not observed between Cripto levels in the blood and the MELD score. Further studies with paired blood- and tissue-samples from patients are needed to verify whether Cripto tissue-expression is reflected by Cripto levels in the blood. These studies might also help to clarify the undetectable Cripto levels as observed in a minority of the tested plasma samples (**chapter 5**). The specific role of Cripto in liver fibrogenesis is still elusive. Based on literature it is known that NANOG is expressed in hepatocytes during fibrogenesis. NANOG is a regulator of Cripto expression, which could thus contribute to the Cripto expression during liver fibrogenesis⁶⁶⁻⁶⁸.

Another possible explanation might be related to the well-known regenerative capacity of the liver upon tissue injury⁶²⁻⁶⁴. Recently Zhang et al., observed upregulated Cripto levels in damaged HepG2 cells stimulating the survival and proliferation of the injured cells⁶¹. One might speculate that Cripto is re-expressed during fibrogenesis in order to survive the injuring stimuli and support tissue regeneration. The studies on Cripto of the present thesis are indicative for an active involvement of Cripto, but further research is required to disentangle whether Cripto has a functionally relevant role in liver fibrogenesis. Such studies might contribute to the identification of new leads for antifibrotic therapy.

Surprisingly, the studies of Kim and Yun et al. both showed increased expression of HGF and VEGF when MSCs were stimulated with Cripto^{69,70}. These cytokines are known to have a direct antifibrotic and pro-regenerative effect (e.g., inhibition of the activation and proliferation of stellate cells, inactivation of myofibroblasts and stimulation of hepatocyte survival) and therefore Cripto expression in fibrogenic livers might be the missing link to unravel the working mechanism for MSC treatment of liver fibrosis. In this mechanism, Cripto expressed by the fibrogenic livers may stimulate the MSCs to perform their antifibrotic function by -for example- increasing their HGF and VEGF production (Figure 1)^{13,19}.

Cripto expression promotes resistance to treatment in HCC

Cripto expression in HCC is correlated to faster tumour recurrence and poor patient survival, but the precise working mechanism(s) are still unknown^{60,71}. Suggested mechanisms include Cripto involvement in pathways leading to faster proliferation and onset of epithelial to mesenchymal transition (EMT) of tumour cells^{60,66}. The function of Cripto in fibrogenesis might be different than in HCC or one could speculate that the cells expressing Cripto in fibrogenesis are more likely to become oncogenic. Further research is needed to verify this hypothesis.

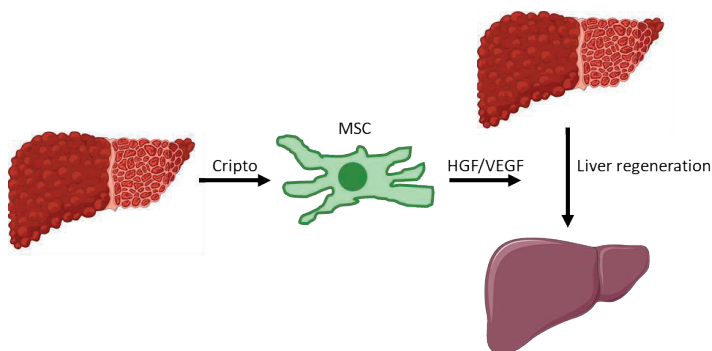


Figure 1. Cripto as one of the driving factors in effective MSC therapy. Cripto expressed by the fibrogenic livers may stimulate the administered MSCs to perform their antifibrotic function by increasing their HGF and VEGF production. These cytokines are known to silence fibrogenesis and to stimulate normal liver regeneration.

Our study revealed that Cripto expression induced an EMT gene profile, with increased proliferation and faster migration of HepG2 tumour cells (**chapter 6**). Furthermore, the PDX mouse model showed that HCCs with high Cripto expression respond less to conventional end-stage systemic therapies such as Sorafenib and that administration of Cripto inhibitors was found to sensitize Cripto-expressing HCCs for Sorafenib treatment^{61,66}. However, these observations were based on one PDX tumour and one HepG2 *in vitro* study, thus additional studies to verify these outcomes in a larger cohort are needed.

Not all HCCs express high levels of Cripto and expression sometimes is lower, as observed in non-tumour cirrhotic liver tissues (**Chapter 5 and 6**). This finding illustrates that Cripto expression levels in tissues are less suitable to use as a biomarker for the diagnosis of HCC. Nevertheless, our observations are suggestive for the existence of a more aggressive subgroup of HCCs or HCC cells recognised by their high Cripto expression. Further research is needed, but these findings at least indicate that patients with a high Cripto-expressing HCC may not benefit from Sorafenib treatment.

Perspectives for the future

MSCs possess pro-regenerative, antifibrotic and anti-inflammatory properties. The studies in this thesis particularly focussed on the regenerative and antifibrotic capacities of MSCs in relation to the resolution of fibrogenesis. To further assess these aspects a follow-up study in which mice are sacrificed at multiple timepoints during the regeneration process is needed to unravel the underlying working mechanism of the proposed novel MSC therapy. Possible MSC-initiated effects on proliferation of endogenous liver cells need to be examined at an earlier time point, since in the described studies all the livers were already fully regenerated at the time of examination. Furthermore, the exact cross-talk between the administered MSCs and the fibrotic liver environment needs to be elucidated further. In **chapter 2** we showed that locally administered MSCs form specific regions and did not migrate. In the future it might be possible to select these MSC regions for RNA isolation and subsequent RNA profiling²⁶. Another, more indirect approach would be to isolate and profile RNA from MSCs that are incubated with homogenates derived from fibrotic or cirrhotic livers. These experiments might lead to more knowledge of the cross-talk between MSCs and their environment, but might also identify mediators secreted by MSCs important for the resolution of fibrosis. This approach may lead to a cocktail of specific mediators, which possibly may be used for the treatment of fibrosis and cirrhosis instead of using the living MSCs themselves. For example, most of the suggested working mechanisms of MSC therapy are based on HGF and IGF-1 expression. For other diseases, such as amyotrophic lateral sclerosis (ALS) and vocal fold scar, HGF infusion has been demonstrated to be safe⁷²⁻⁷⁴. With use of the high throughput zebrafish embryo model for liver fibrosis, as described in **chapter 4**, it would be of interest to administer HGF, IGF-1 or newly discovered mediators to assess their therapeutic effect²⁷.

The characterisation panel of membrane-markers of MSCs differs between studies, which can lead to the use of different subpopulations of MSCs^{36,40}. We showed that different subpopulations of MSCs have a different impact with regard to the reversal of liver fibrogenesis (**chapter 3**). Therefore, it is highly recommendable to study the different subpopulations of MSCs and design different characterisation panels of membrane-markers which are tuned for purpose. For example, based on the present thesis we would suggest to add VCAM as a marker for MSCs for the resolution of liver fibrosis. However, for other purposes it might very well be better to use a different subpopulation of MSCs.

In the coming years more clinical trials, testing the efficacy of different MSC therapies for liver diseases, will be finalised (see clinicaltrials.gov). The results of these trials will lead to more knowledge regarding the effectiveness of MSC therapy. The University of Utah, for example, started a study to evaluate the potential of hepatic artery injection of autologous bone marrow-derived MSCs in patients with alcoholic liver cirrhosis. Another trial performed by the Xijing Hospital of Digestive Diseases is evaluating the effect of systemic (i.v.) administration of MSCs in patients with decompensated liver cirrhosis. These trials are using different administration strategies (portal-/local- and systemic intravenous-administration), and it would be interesting to compare those studies regarding MSC subpopulations and to assess whether the local administration is more effective compared to systemic treatment, as suggested by our studies. Unfortunately, these studies are using different doses of MSCs which might also affect their outcomes.

In **chapter 5 and 6** of the present thesis we observed that hepatocytes express Cripto during fibrogenesis and that Cripto is also involved in the progression and metastasis of HCC. Further research is needed to unravel the pathophysiological role of Cripto in fibrogenesis. Elucidation of the function of Cripto could possibly lead to new insights into fibrogenesis and might lead to alternative therapies for the resolution of fibrogenesis. HCC with high Cripto expression was found to be resistant to Sorafenib therapy, therefore a combination therapy of Sorafenib and Cripto inhibitors is advocated (**chapter 6**)⁶⁶. However, in relation to this proposed treatment the safety of Cripto inhibitors needs to be assessed first. Meanwhile one could reconsider to prescribe Sorafenib to patients with high Cripto-expressing HCCs. Furthermore, it would be of interest to study whether Cripto plasma levels correlate with tissue expression and are able to predict the aggressiveness of HCCs. This would provide clinicians with a relatively easy tool to distinguish Cripto high- and Cripto-low tumours as more or less aggressive, which can be of help to decide on the most optimal treatment.

Finally, it is anticipated that the rapid evolvement of our understanding of fibrogenesis, MSC functionality, regeneration and oncogenesis will lead to novel therapies for liver disease in the near future.

References

1. Lozano, R., Naghavi, M., Foreman, K. et al. Global and regional mortality from 235 causes of death for 20 age groups in 1990 and 2010: a systematic analysis for the Global Burden of Disease Study 2010. *Lancet* 2012; 380: 2095-2128.
2. Blachier, M., Leleu, H., Peck-Radosavljevic, M. et al. The burden of liver disease in Europe: a review of available epidemiological data. *J Hepatol* 2013; 58: 593-608.
3. Friedman, S. L. Mechanisms of hepatic fibrogenesis. *Gastroenterology* 2008; 134: 1655-1669.
4. Bataller, R. & Brenner, D. A. Liver fibrosis. *J Clin Invest* 2005; 115: 209-218.
5. Lee, Y. A., Wallace, M. C. & Friedman, S. L. Pathobiology of Liver Fibrosis—A Translational Success Story (vol 64, pg 830, 2015). *Gut* 2015; 64: 1337-1337.
6. Higashi, T., Friedman, S. L. & Hoshida, Y. Hepatic stellate cells as key target in liver fibrosis. *Adv Drug Deliv Rev* 2017; 121: 27-42.
7. Byass, P. The global burden of liver disease: a challenge for methods and for public health. *Bmc Med* 2014; 12:
8. Liver, E. A. S. EASL Recommendations on Treatment of Hepatitis C 2016. *J Hepatol* 2017; 66: 153-194.
9. Mathurin, P., Hadengue, A., Bataller, R. et al. EASL Clinical Practical Guidelines: Management of Alcoholic Liver Disease. *J Hepatol* 2012; 57: 399-420.
10. Gronthos, S., Zannettino, A. C. W., Hay, S. J. et al. Molecular and cellular characterisation of highly purified stromal stem cells derived from human bone marrow. *J Cell Sci* 2003; 116: 1827-1835.
11. Parekkadan, B. & Milwid, J. M. Mesenchymal Stem Cells as Therapeutics. *Annu Rev Biomed Eng* 2010; 12: 87-117.
12. Klyushnenkova, E., Mosca, J. D., Zernetkina, V. et al. T cell responses to allogeneic human mesenchymal stem cells: immunogenicity, tolerance, and suppression. *J Biomed Sci* 2005; 12: 47-57.
13. Alfaifi, M., Eom, Y. W., Newsome, P. N. et al. Mesenchymal stromal cell therapy for liver diseases. *J Hepatol* 2018; 68: 1272-1285.
14. Berardis, S., Dwisthi Sattwika, P., Najimi, M. et al. Use of mesenchymal stem cells to treat liver fibrosis: current situation and future prospects. *World J Gastroenterol* 2015; 21: 742-758.
15. Di Nicola, M., Carlo-Stella, C., Magni, M. et al. Human bone marrow stromal cells suppress T-lymphocyte proliferation induced by cellular or nonspecific mitogenic stimuli. *Blood* 2002; 99: 3838-3843.
16. Li, Q., Zhou, X., Shi, Y. et al. In vivo tracking and comparison of the therapeutic effects of MSCs and HSCs for liver injury. *PLoS One* 2013; 8: e62363.
17. Park, M., Kim, Y. H., Woo, S. Y. et al. Tonsil-derived Mesenchymal Stem Cells Ameliorate CCl4-induced Liver Fibrosis in Mice via Autophagy Activation. *Sci Rep-Uk* 2015; 5:
18. Jang, Y. O., Kim, M. Y., Cho, M. Y. et al. Effect of bone marrow-derived mesenchymal stem cells on hepatic fibrosis in a thioacetamide-induced cirrhotic rat model. *BMC Gastroenterol* 2014; 14: 198.

19. Najimi, M., Berardis, S., El-Kehdy, H. et al. Human liver mesenchymal stem/progenitor cells inhibit hepatic stellate cell activation: in vitro and in vivo evaluation. *Stem Cell Res Ther* 2017; 8: 131.
20. Huang, B., Cheng, X., Wang, H. et al. Mesenchymal stem cells and their secreted molecules predominantly ameliorate fulminant hepatic failure and chronic liver fibrosis in mice respectively. *J Transl Med* 2016; 14: 45.
21. van Poll, D., Parekkadan, B., Cho, C. H. et al. Mesenchymal stem cell-derived molecules directly modulate hepatocellular death and regeneration in vitro and in vivo. *Hepatology* 2008; 47: 1634-1643.
22. Parekkadan, B., van Poll, D., Megeed, Z. et al. Immunomodulation of activated hepatic stellate cells by mesenchymal stem cells. *Biochem Bioph Res Co* 2007; 363: 247-252.
23. Suk, K. T., Yoon, J. H., Kim, M. Y. et al. Transplantation With Autologous Bone Marrow-Derived Mesenchymal Stem Cells for Alcoholic Cirrhosis: Phase 2 Trial. *Hepatology* 2016; 64: 2185-2197.
24. Alfaifi, M., Eom, Y. W., Newsome, P. N. et al. Mesenchymal stromal cell therapy for liver diseases. *J Hepatol* 2018;
25. AlAhmari, L. S., AlShenaifi, J. Y., AlAnazi, R. A. et al. Autologous Bone Marrow-derived Cells in the Treatment of Liver Disease Patients. *Saudi J Gastroentero* 2015; 21: 5-10.
26. van der Helm, D., Barnhoorn, M. C., de Jonge-Muller, E. S. M. et al. Local but not systemic administration of mesenchymal stromal cells ameliorates fibrogenesis in regenerating livers. *J Cell Mol Med* 2019;
27. van der Helm, D., Groenewoud, A., de Jonge-Muller, E. S. M. et al. Mesenchymal stromal cells prevent progression of liver fibrosis in a novel zebrafish embryo model. *Sci Rep* 2018; 8: 16005.
28. Siegel, G., Kluba, T., Hermanutz-Klein, U. et al. Phenotype, donor age and gender affect function of human bone marrow-derived mesenchymal stromal cells. *Bmc Med* 2013; 11: 146.
29. Hu, C., Zhao, L., Duan, J. et al. Strategies to improve the efficiency of mesenchymal stem cell transplantation for reversal of liver fibrosis. *J Cell Mol Med* 2019; 23: 1657-1670.
30. Li, D. L., He, X. H., Zhang, S. A. et al. Bone Marrow-Derived Mesenchymal Stem Cells Promote Hepatic Regeneration after Partial Hepatectomy in Rats. *Pathobiology* 2013; 80: 228-234.
31. Tunon, M. J., Alvarez, M., Culebras, J. M. et al. An overview of animal models for investigating the pathogenesis and therapeutic strategies in acute hepatic failure. *World J Gastroentero* 2009; 15: 3086-3098.
32. Weber, L. W. D., Boll, M. & Stampfl, A. Hepatotoxicity and mechanism of action of haloalkanes: Carbon tetrachloride as a toxicological model. *Crit Rev Toxicol* 2003; 33: 105-136.
33. Molendijk, I., Bonsing, B. A., Roelofs, H. et al. Allogeneic Bone Marrow-Derived Mesenchymal Stromal Cells Promote Healing of Refractory Perianal Fistulas in Patients With Crohn's Disease. *Gastroenterology* 2015; 149: 918-927 e916.
34. Anderson, P., Carrillo-Galvez, A. B., Garcia-Perez, A. et al. CD105 (endoglin)-negative murine mesenchymal stromal cells define a new multipotent subpopulation with distinct differentiation and immunomodulatory capacities. *PLoS One* 2013; 8: e76979.
35. Yang, Z. X., Han, Z. B., Ji, Y. R. et al. CD106 identifies a subpopulation of mesenchymal stem cells with unique immunomodulatory properties. *PLoS One* 2013; 8: e59354.

36. Han, Z. C., Du, W. J., Han, Z. B. et al. New insights into the heterogeneity and functional diversity of human mesenchymal stem cells. *Biomed Mater Eng* 2017; 28: S29-S45.
37. Li, H., Ghazanfari, R., Zacharaki, D. et al. Isolation and characterization of primary bone marrow mesenchymal stromal cells. *Ann N Y Acad Sci* 2016; 1370: 109-118.
38. Morikawa, S., Mabuchi, Y., Kubota, Y. et al. Prospective identification, isolation, and systemic transplantation of multipotent mesenchymal stem cells in murine bone marrow. *J Exp Med* 2009; 206: 2483-2496.
39. Du, W., Li, X., Chi, Y. et al. VCAM-1+ placenta chorionic villi-derived mesenchymal stem cells display potent pro-angiogenic activity. *Stem Cell Res Ther* 2016; 7: 49.
40. Buhring, H. J., Tremel, S., Cerabona, F. et al. Phenotypic characterization of distinct human bone marrow-derived MSC subsets. *Ann N Y Acad Sci* 2009; 1176: 124-134.
41. Barnhoorn, M., de Jonge-Muller, E., Molendijk, I. et al. Endoscopic Administration of Mesenchymal Stromal Cells Reduces Inflammation in Experimental Colitis. *Inflamm Bowel Dis* 2018; 24: 1755-1767.
42. Fiore, E., Malvicini, M., Bayo, J. et al. Involvement of hepatic macrophages in the antifibrotic effect of IGF-I-overexpressing mesenchymal stromal cells. *Stem Cell Res Ther* 2016; 7: 172.
43. Fiore, E. J., Bayo, J. M., Garcia, M. G. et al. Mesenchymal stromal cells engineered to produce IGF-I by recombinant adenovirus ameliorate liver fibrosis in mice. *Stem Cells Dev* 2015; 24: 791-801.
44. Deng, Y., Zhang, Y., Ye, L. et al. Umbilical Cord-derived Mesenchymal Stem Cells Instruct Monocytes Towards an IL10-producing Phenotype by Secreting IL6 and HGF. *Sci Rep* 2016; 6: 37566.
45. Pulavendran, S., Vignesh, J. & Rose, C. Differential anti-inflammatory and anti-fibrotic activity of transplanted mesenchymal vs. hematopoietic stem cells in carbon tetrachloride-induced liver injury in mice. *Int Immunopharmacol* 2010; 10: 513-519.
46. Tanimoto, H., Terai, S., Taro, T. et al. Improvement of liver fibrosis by infusion of cultured cells derived from human bone marrow. *Cell Tissue Res* 2013; 354: 717-728.
47. Sun, Y., Wang, Y., Zhou, L. et al. Spheroid-cultured human umbilical cord-derived mesenchymal stem cells attenuate hepatic ischemia-reperfusion injury in rats. *Sci Rep* 2018; 8: 2518.
48. Fouraschen, S. M. G., Pan, Q. W., de Ruiter, P. E. et al. Secreted Factors of Human Liver-Derived Mesenchymal Stem Cells Promote Liver Regeneration Early After Partial Hepatectomy. *Stem Cells Dev* 2012; 21: 2410-2419.
49. Haniffa, M. A., Collin, M. P., Buckley, C. D. et al. Mesenchymal stem cells: the fibroblasts' new clothes? *Haematol-Hematol J* 2009; 94: 258-263.
50. Haniffa, M. A., Wang, X. N., Holtick, U. et al. Adult human fibroblasts are potent immunoregulatory cells and functionally equivalent to mesenchymal stem cells. *J Immunol* 2007; 179: 1595-1604.
51. Haniffa, M. A., Wang, X. N., Holtick, U. et al. Mesenchymal stem cells and fibroblasts have similar immunoregulatory properties in vitro but distinct gene expression profiles: Implications for cellular therapy. *Blood* 2007; 110: 573a-573a.
52. Goessling, W. & Sadler, K. C. Zebrafish: an important tool for liver disease research. *Gastroenterology* 2015; 149: 1361-1377.

53. Lieschke, G. J. & Currie, P. D. Animal models of human disease: zebrafish swim into view. *Nat Rev Genet* 2007; 8: 353-367.
54. Rekha, R. D., Amali, A. A., Her, G. M. et al. Thioacetamide accelerates steatohepatitis, cirrhosis and HCC by expressing HCV core protein in transgenic zebrafish *Danio rerio*. *Toxicology* 2008; 243: 11-22.
55. Tsedensodnom, O., Vacaru, A. M., Howarth, D. L. et al. Ethanol metabolism and oxidative stress are required for unfolded protein response activation and steatosis in zebrafish with alcoholic liver disease. *Dis Model Mech* 2013; 6: 1213-1226.
56. Howarth, D. L., Yin, C., Yeh, K. et al. Defining hepatic dysfunction parameters in two models of fatty liver disease in zebrafish larvae. *Zebrafish* 2013; 10: 199-210.
57. Lin, J. N., Chang, L. L., Lai, C. H. et al. Development of an Animal Model for Alcoholic Liver Disease in Zebrafish. *Zebrafish* 2015; 12: 271-280.
58. Strizzi, L., Bianco, C., Normanno, N. et al. Cripto-1: a multifunctional modulator during embryogenesis and oncogenesis. *Oncogene* 2005; 24: 5731-5741.
59. Strizzi, L., Margaryan, N. V., Gilgur, A. et al. The significance of a Cripto-1-positive subpopulation of human melanoma cells exhibiting stem cell-like characteristics. *Cell Cycle* 2013; 12: 1450-1456.
60. Lo, R. C., Leung, C. O., Chan, K. K. et al. Cripto-1 contributes to stemness in hepatocellular carcinoma by stabilizing Dishevelled-3 and activating Wnt/beta-catenin pathway. *Cell Death Differ* 2018; 25: 1426-1441.
61. Zhang, Y., Mi, X., Song, Z. et al. Cripto-1 promotes resistance to drug-induced apoptosis by activating the TAK-1/NF-kappaB/survivin signaling pathway. *Biomed Pharmacother* 2018; 104: 729-737.
62. Fausto, N. & Campbell, J. S. The role of hepatocytes and oval cells in liver regeneration and repopulation. *Mech Dev* 2003; 120: 117-130.
63. Fausto, N., Campbell, J. S. & Riehle, K. J. Liver regeneration. *Hepatology* 2006; 43: S45-53.
64. Gilgenkrantz, H. & Collin de l'Hortet, A. Understanding Liver Regeneration: From Mechanisms to Regenerative Medicine. *Am J Pathol* 2018; 188: 1316-1327.
65. Zhang, Y., Xu, H., Chi, X. et al. High level of serum Cripto-1 in hepatocellular carcinoma, especially with hepatitis B virus infection. *Medicine (Baltimore)* 2018; 97: e11781.
66. Karkampouna, S., van der Helm, D., Gray, P. C. et al. CRIPTO promotes an aggressive tumour phenotype and resistance to treatment in hepatocellular carcinoma. *J Pathol* 2018; 245: 297-310.
67. Toraih, E. A., Fawzy, M. S., El-Falouji, A. I. et al. Stemness-related transcriptional factors and homing gene expression profiles in hepatic differentiation and cancer. *Mol Med* 2016; 22: 653-663.
68. Bi, W. R., Jin, C. X., Xu, G. T. et al. Bone morphogenetic protein-7 regulates Snail signaling in carbon tetrachloride-induced fibrosis in the rat liver. *Exp Ther Med* 2012; 4: 1022-1026.
69. Kim, S., Yoon, Y. M., Han, Y. S. et al. Administration of Cripto in GRP78 overexpressed human MSCs enhances stem cell viability and angiogenesis during human MSC transplantation therapy. *Cell Prolif* 2018; 51: e12463.
70. Yun, S., Yun, C. W., Lee, J. H. et al. Cripto Enhances Proliferation and Survival of Mesenchymal Stem Cells by Up-Regulating JAK2/STAT3 Pathway in a GRP78-Dependent Manner. *Biomol Ther (Seoul)* 2018; 26: 464-473.

71. Wang, J. H., Wei, W., Xu, J. et al. Elevated expression of Cripto-1 correlates with poor prognosis in hepatocellular carcinoma. *Oncotarget* 2015; 6: 35116-35128.
72. Warita, H., Kato, M., Asada, R. et al. Safety, Tolerability, and Pharmacodynamics of Intrathecal Injection of Recombinant Human HGF (KP-100) in Subjects With Amyotrophic Lateral Sclerosis: A Phase I Trial. *J Clin Pharmacol* 2019; 59: 677-687.
73. Hirano, S., Kawamoto, A., Tateya, I. et al. A phase I/II exploratory clinical trial for intracordal injection of recombinant hepatocyte growth factor for vocal fold scar and sulcus. *J Tissue Eng Regen Med* 2018; 12: 1031-1038.
74. Powell, R. J., Goodney, P., Mendelsohn, F. O. et al. Safety and efficacy of patient specific intramuscular injection of HGF plasmid gene therapy on limb perfusion and wound healing in patients with ischemic lower extremity ulceration: results of the HGF-0205 trial. *J Vasc Surg* 2010; 52: 1525-1530.



Appendix

Nederlandse samenvatting

Leverfibrogenese is een ziekteproces dat in de volksmond beter bekend staat als “verlittekening van de lever”. Dit proces wordt in gang gezet als de lever gedurende een langere periode schade ondervindt. Deze beschadigingen kunnen door verschillende factoren worden veroorzaakt. De meest bekende oorzaken zijn onder andere de hepatitis B- en C-virussen, overmatige alcoholconsumptie, genetische afwijkingen, galwegproblematiek en obesitas. Ondanks de verschillende aard van deze oorzaken, activeren zij allemaal hetzelfde ziektemechanisme. Door de genoemde factoren raken de levercellen beschadigd en ondergaan een vorm van celdood, apoptose genaamd. Ter verdediging gaan de gezonde cellen van de lever delen om de dode cellen te vervangen. Dit proces van leverregeneratie zorgt ervoor dat de lever na geleden schade kan herstellen. Naast deze regeneratie vindt ook de fibrogenese (vorming van littekenweefsel) plaats.

Door de dode levercellen worden in de lever de zogenaamde stellaatcellen geactiveerd. Deze cellen gaan vervolgens delen en differentiëren/veranderen in myofibroblasten. Het zijn deze myofibroblasten die in de leverfibrose het littekenweefsel produceren. Bij kortdurende schade wordt dit proces vrij snel weer stilgelegd en wordt het littekenweefsel weer opgeruimd, zoals bij een wondje op de huid bijvoorbeeld. Echter, als een lever chronische (langdurige) schade ondervindt heeft deze geen tijd om tussen de schades door te herstellen en zo ontstaat er leverfibrose. Zolang de fibrogenese voortduurt stapelt het littekenweefsel zich op en zal de lever gaan verstijven. Door deze verstijving kan het bloed minder goed door de lever stromen, wat tot verhoogde druk in de poortader en aders van de buik (portale hypertensie) kan leiden. Ook kunnen er mogelijk ontstekingsprocessen en/of galstuwingsplaatsen gaan vinden welke tot nog meer celdood kunnen leiden. Vervolgens zal het ziekteproces in een neerwaartse spiraal terechtkomen, waarbij de lever zelf niet meer kan herstellen. Als dit proces langere tijd aanhoudt ontstaat levercirrose, een hobbelige lever, bestaand uit een netwerk van bindweefsel/littekenweefsel, waartussen door regeneratie ontstane knobbels van leverweefsel liggen. Geleidelijk kan de lever zijn functie niet meer naar behoren uitoefenen en ontstaat er een eindstadium, leverfalen genaamd. Naarmate de leverfibrogenese langer blijft bestaan, wordt de kans ook groter dat er zich kwaadaardige levertumoren (primaire leverkanker, oftewel hepatocellulair carcinoom) ontwikkelen.

Een van de grootste risico's van leverfibrose is dat dit vaak aanwezig is zonder dat een patiënt er al last van heeft. Dit geeft de ziekte de kans om langere tijd door te woekeren, waardoor het vaak pas in een vergevorderd stadium ontdekt wordt. Tot op heden bestaat de behandeling van leverfibrose en cirrose uit het wegnemen van de oorzaken van de ziekte, zoals het stoppen met de consumptie van alcohol of behandeling van de virale infectie. In enkele gevallen kan dit tot omkering en genezing van de fibrose leiden, maar in sommige gevallen ontkomt men

niet aan een levertransplantatie of zal de patiënt aan de leverziekte overlijden. Ondanks het voortschrijden van de techniek blijft een levertransplantatie een grote operatie met risico's en 15% tot 20% van de mensen op de wachtlijst overlijdt door het gebrek aan orgaandonoren. Therapieën die direct aangrijpen op het proces van fibrogenese en dit remmen, tegengaan of omkeren zijn in ontwikkeling, maar nog niet geregistreerd of beschikbaar.

Wetenschappelijk onderzoek heeft aangetoond dat mesenchymale (stromale) stamcellen (MSCs) het herstel en de regeneratie van organen kunnen stimuleren. Deze MSCs bevinden zich in vele weefsels, zoals beenmerg, vet en de navelstreng, en kunnen relatief makkelijk geïsoleerd en tot grote hoeveelheden opgekweekt worden. Onderzoeken hebben ook laten zien dat MSCs van gezonde donoren veilig bij patiënten toegediend kunnen worden. Dit wetende zouden MSCs dus ook een mogelijke toepassing in de behandeling van leverfibrose en cirrose kunnen hebben.

In ons onderzoek met muismodellen voor leverfibrose en cirrose toonden we aan dat lokale toediening (direct in de lever) van MSCs tot een vermindering van de fibrose leidt, zoals beschreven in **hoofdstuk 2** van dit proefschrift. In tegenstelling tot de lokale toediening werd gevonden dat intraveneuze toediening (via de bloedvaten) van MSCs geen effect had. Ook observeerden we, na een operatieve verwijdering van ongeveer 70% van het aangedane fibrotische leverweefsel (partiële leverresectie), een aangroei van gezonder leverweefsel door regeneratie. Deze bevindingen motiveerden ons om de partiële leverresectie met de lokale toediening van MSCs te combineren als mogelijke behandeling bij leverfibrose. De uitkomsten van deze experimenten lieten zien dat deze samenvoeging het resultaat van beide interventies versterkte en tot een grotere vermindering van fibrose en cirrose in het muismodel leidde.

MSCs worden gekenmerkt door hun vermogen om tot bot, kraakbeen en vetweefsel te differentiëren. Daarnaast worden de cellen ook getypeerd door de aan- en afwezigheid van specifieke eiwitten op het celmembraan (omhulsel van de cel). Met inachtneming van deze karakteristieken bleek dat MSCs niet altijd zowel VCAM als Endoglin op het membraan tot expressie brachten. Mogelijke verschillen tussen subpopulaties van MSCs, op basis van deze kenmerken, met betrekking tot de toepassing in de behandeling van leverfibrose werden verder onderzocht, als beschreven in **hoofdstuk 3**. Voor deze studie selecteerden we, op basis van VCAM en Endoglin expressie, vier verschillende subpopulaties van MSCs (1: VCAM-positief + Endoglin-positief, 2: VCAM-positief + Endoglin-negatief, 3: VCAM-negatief + Endoglin-positief en 4: VCAM-negatief + Endoglin-negatief). Vervolgens werd bestudeerd of deze cellen een verschillend therapeutisch effect in de vermindering van leverfibrose hadden. In ons model voor leverfibrose ondergingen muizen een partiële leverresectie en vervolgens werden de verschillende MSC subpopulaties lokaal toegediend. Uit dit onderzoek kwam naar voren dat de MSCs die VCAM tot expressie brachten, subtypen 1 en 2, tot een grotere vermindering van het littekenweefsel in de lever leidden dan de VCAM-negatieve MSCs, subtypen 3 en 4.

Interessant genoeg vertoonden deze laatste cellen zelfs helemaal geen therapeutisch effect. Celkweek modellen onderbouwden de resultaten uit het proefdiermodel en lieten zien dat de VCAM-positieve MSCs tot een versnelde celdeling van de levercellen leidden en daarnaast ook de levercellen tegen celdood beschermden. De productie van Hepatocyt-groefactor (HGF) door MSCs wordt gezien als één van de drijvende krachten achter het bovenstaande therapeutisch effect van MSCs in leverfibrose. Toen we de mate van HGF productie van de 4 genoemde MSC-subpopulaties met elkaar vergeleken bleek dat de VCAM-positieve MSCs de hoogste HGF-expressie hadden. Deze bevinding zou een mogelijke verklaring voor de resultaten uit het proefdiermodel kunnen zijn. Op basis van de resultaten van dit onderzoek is ons advies om alleen VCAM-positieve MSCs voor de behandeling van leverfibrose te gebruiken.

Proefdieren zijn van wezenlijk belang voor het bestuderen van verschillende ziekten en de ontwikkeling van nieuwe behandelingen. Uiteraard is de Nederlandse en Europese wetgeving zo ingericht dat mogelijk leed van de proefdieren tot een minimum beperkt blijft. In de muismodellen voor het onderzoek uit dit proefschrift werd leverfibrose opgewekt door chronische toediening van CCL4. Voor de fibrose of cirrose moesten de muizen relatief lang (6-12 weken) met dit stofje geïnjecteerd worden. De inductie van leverfibrose of cirrose is dus een lange, tijdrovende en kostbare periode waarin de muizen veel aangerakt en geïnjecteerd worden. Dit bracht ons op het idee om een ander proefdiermodel voor leverfibrose met minimaal dierenleed te ontwikkelen, dat bovendien goedkoper en makkelijk hanteerbaar is. Zebravis embryo's worden al in vele onderzoeken gebruikt, maar hadden tot nu toe nog geen toepassing op het gebied van onderzoek naar leverfibrose gevonden. Deze embryo's zijn goedkoop en de lichamelijke (ontwikkelings-)processen vertonen grote gelijkenissen met de mens. In het onderzoek van **hoofdstuk 4** werd een zebravis embryomodel voor leverfibrose ontwikkeld door gedurende 6 dagen TAA aan het aquarium water toe te voegen. TAA is een toxisch stofje dat schade aan de lever toebrengt. Deze schade leidt tot celdood en vervolgens activatie van de lever fibrogenese. De genexpressie- en eiwit-profielen van dit model lieten zien dat het ziektemechanisme achter deze leverfibrose nagenoeg hetzelfde is als bij de muis en de mens. Om de toepasbaarheid van dit model aan te tonen werden op de vierde dag van TAA behandeling MSCs ter plaatse van de lever ingespoten in de embryo's. Twee dagen na de MSC toediening werd de ernst van de leverfibrose bestudeerd en werden overeenkomstige bevindingen als beschreven in de **hoofdstukken 2 en 3** waargenomen. De MSC behandeling zorgde ook in dit model namelijk voor minder myofibroblasten en minder littekenweefsel.

Alhoewel de pathofysiologie (het onderliggende ziekteproces) van leverfibrose in grote lijnen bekend is, worden er steeds nieuwe ontdekkingen gedaan die in de toekomst mogelijk tot nieuwe behandelmethoden kunnen leiden. Zo werd recent aangetoond dat patiënten met een levercirrose als gevolg van een virusinfectie verhoogde spiegels van het eiwit "Cripto" in hun bloed hadden. Cripto is een eiwit waarvan gedacht werd dat het alleen tijdens de embryogenese (ontwikkeling van baby's) en oncogenese (ontstaan en progressie van

tumoren) een rol speelde. De verhoogde levels van Cripto in het bloed van cirrose patiënten waren dus zeer onverwacht. Het is bekend dat Cripto cellen kan beschermen tegen celdood maar ook de cellen kan aanzetten tot delen en differentiëren. De deling en overleving van levercellen zijn ook belangrijk bij leverfibrose. Daarom hebben we daar onderzoek naar gedaan, beschreven in **hoofdstuk 5**, waaruit bleek dat de levers van mensen met cirrose en levers van zebravis embryo- en muismodellen voor leverfibrose meer Cripto tot expressie brengen dan in de gezonde situatie. De hoogte van deze expressie bleek in de mens ook te correleren met de ernst van de ziekte. Daarnaast vonden we verhoogde Cripto spiegels in het bloed van patiënten met levercirrose en bleek bij de mens dat deze spiegels ook weer normaliseerden als de aangedane lever middels een transplantatie werd vervangen door een gezonde donorlever. Samenvattend geeft dit onderzoek aanwijzingen voor de betrokkenheid van Cripto bij leverfibrose in zowel mens, muis als zebravis. Ook geeft het voldoende aanleiding tot verder onderzoek naar de ware rol van Cripto in leverfibrose. In de toekomst zou dit tot nieuwe inzichten en eventuele alternatieve behandelmethodes kunnen leiden. Zo kunnen we ook speculeren over de mogelijke rol van deze Cripto expressie in de MSC behandelingen van de studies uit **hoofdstukken 2, 3 en 4**. Zo heeft ander onderzoek aangetoond dat MSCs meer HGF gaan produceren als deze met Cripto in aanraking komen. Zoals eerder beschreven wordt er gedacht dat HGF een grote rol speelt bij de effectiviteit van MSC-therapieën in leverfibrose. Volgens deze theorieën zou HGF namelijk direct aangrijpen op de cellen die het littekenweefsel produceren en hiermee de fibrogenese remmen/stilleggen. Daarnaast speelt HGF ook een rol bij de regeneratie (vormen van nieuw weefsel). Samenvattend en heel speculatief zou deze directe relatie tussen de mate van Cripto expressie van de aangedane lever met de mate van HGF expressie van de MSCs het werkingsmechanisme en de dosis response van de MSC-therapieën uit de diverse hoofdstukken kunnen verklaren. Verder onderzoek is echter nodig om deze hypothese te toetsen.

Daarnaast is er ook de bekende betrokkenheid van Cripto bij het ontstaan, de progressie en metastasering (uitzaaiing) van verschillende maligniteiten. Een mogelijke rol van Cripto in de ontwikkeling van het hepatocellulaire carcinomen (HCC ofwel levertumoren) was tot voor kort nog onbekend. In de studie van **hoofdstuk 6** werd de mogelijke expressie en functie van Cripto in het ontstaan en de progressie van HCCs onderzocht. Onze bevindingen laten zien dat er een subpopulatie van HCCs bestaat die Cripto tot expressie brengt en dat juist deze tumoren minder gevoelig voor de bestaande medicamenteuze behandeling (tyrosinekinaseremmers) lijken te zijn. Kortom, patiënten met dit subtype HCC zouden dus mogelijk niet gebaat zijn bij deze zware behandeling. Klinisch relevant is dat we in een experimentele setting hebben aangetoond dat we dit type tumoren weer gevoelig voor de bestaande behandeling kunnen maken door deze medicatie gelijktijdig met een Cripto-remmend eiwit toe te dienen. Er zal echter nog veel onderzoek nodig zijn om de effectiviteit en veiligheid van deze remmers aan te tonen.

Concluderend hebben we met de diverse onderzoeken uit dit proefschrift aangetoond dat een partiële leverresectie tezamen met lokale toediening van MSCs leidt tot een betere aangroei van gezonder leverweefsel dan met een resectie of MSCs alleen. Daarnaast hebben we aanwijzingen gevonden die er op duiden dat er verschillende subpopulaties van MSCs zijn en dat juist de VCAM-positieve subpopulaties de beste anti-fibrotische werking hebben. Ook hebben we laten zien dat zebravis embryo's leverfibrose kunnen ontwikkelen en dat dit ziektemechanisme vergelijkbaar is met dat bij mens en muis. In het tweede deel van het proefschrift staat beschreven dat levercellen, tijdens leverfibrose, Cripto tot expressie brengen en dat de mate van expressie met de ernst van de ziekte correleert. In het laatste hoofdstuk staan de waarnemingen beschreven dat er een kwaadaardige subpopulatie van levertumoren bestaat die Cripto tot expressie brengt en om die reden resistent voor behandeling met een tyrosinekinaseremmer is, welke gevoeligheid terugkomt als een Cripto-remmer toegevoegd wordt.

Kortom, dit proefschrift laat zien dat mesenchymale (stromale) stamcellen een toepassing in de behandeling van leverfibrose zouden kunnen hebben en dat Cripto een nieuwe speler in de fibrose-cirrose-HCC ziektecascade is.

Curriculum vitae

Danny van der Helm werd geboren op 15 januari 1987 te Rotterdam. Na het succesvol afronden van zijn HAVO en VWO, startte hij in 2006 met de studie Bio-farmaceutische wetenschappen aan de Universiteit Leiden. Tijdens zijn studie deed hij 2 wetenschappelijke stages, de eerste onder begeleiding van Prof. Erik Danen op de afdeling Toxicologie aan de Universiteit Leiden, de tweede bij het Albert Einstein College of Medicine te New York in de Verenigde Staten, onder begeleiding van Prof. J. Condeelis. De focus van beide onderzoeken lag op het ontrafelen van de rol van Integrines in de metastasering van borsttumoren. In 2011 keerde hij terug naar Nederland en rondde hij zijn masteropleiding met “zeer veel genoegen” af. Begin 2012 startte hij, onder begeleiding van zijn (co)-promotoren Prof. dr. ir. H.W. Verspaget, Prof. dr. B. van Hoek en dr. M.J. Coenraad, zijn promotie-onderzoek op de afdeling Maag-, Darm- en Leverziekten van het Leids Universitair Medisch Centrum. Gedurende zijn promotie richtte hij zich op het samenspel tussen het natuurlijk regenererend vermogen van de lever en toediening van mesenchymale (stromale) stamcellen als mogelijke behandeling voor levercirrose. Ook ontwikkelde hij een nieuw proefdiermodel voor leverfibrose in zebrafish embryo's. Gedurende het onderzoek raakte hij verder geïnteresseerd in het Cripto-eiwit en haar mogelijke betrokkenheid bij de pathogenese van leverziekten. Met de resultaten van dit onderzoek won hij de “Young investigator bursary” van de “European Association for the Study of the Liver” (EASL). Gedurende zijn studie en beginjaren van zijn promotie-onderzoek was Danny actief roeier en lid bij de K.S.R.V. Njord. Daarnaast zette hij zich als bestuurslid van de service organisatie LEO Clubs Nederland in voor tal van maatschappelijke acties. In 2018 zette hij onder begeleiding van Prof. dr. B van Hoek zijn eerste stappen binnen het data-onderzoek, waarbij hij de levertransplantatie-database uitbreidde, moderniseerde, toegankelijk maakte en gebruikte voor onderzoek. Op 1 mei 2019 maakte hij de overstap naar zijn huidige functie als data-manager/-onderzoeker binnen het transplantatiecentrum van het LUMC. In deze functie richt hij zich voornamelijk op het herstructureren en borgen van data-invoer aan de bron, ontwikkelen van real-time (management-)dashboards, big-data-analyses, onderzoek, waardegedreven zorg, en zal hij de komende jaren de eerste stappen naar artificial intelligence (AI) hiervoor begeleiden.

A

Publications

- Vulnerabilities in kidney transplant recipients with COVID-19: a single center experience
Meziyerh S, van der Helm D, de Vries APJ. Transpl Int. 2020 Aug 7;10.1111/tri.13714. doi: 10.1111/tri.13714 (Letter)
- Donor diabetes mellitus is a risk factor for diminished outcome after liver transplantation: a nationwide retrospective cohort study.
Brüggenwirth IMA, van Reeve M, Vasiliauskaitė I, van der Helm D, van Hoek B, Schaapherder AF, Alwayn IPJ, van den Berg AP, de Meijer VE, Darwish Murad S, Polak WG, Porte RJ. Transpl Int. 2020 Oct 17. doi: 10.1111/tri.13770. Online ahead of print. PMID: 33067844
- Donor hepatectomy time influences ischemia-reperfusion injury of the biliary tree in donation after circulatory death liver transplantation
van Leeuwen OB, van Reeve M, van der Helm D, IJzermans JNM, de Meijer VE, van den Berg AP, Darwish Murad S, van Hoek B, Alwayn IPJ, Porte RJ, Polak WG. Surgery 2020, doi.org/10.1016/j.surg.2020.02.005
- Selected liver grafts from donation after circulatory death can be safely used for retransplantation—a multicenter retrospective study.
van Reeve M, van Leeuwen OB, van der Helm D, Darwish Murad S, van den Berg AP, van Hoek B, Alwayn IPJ, Polak WG, Porte RJ. Transpl Int. 2020 Feb 17, doi: 10.1111/tri.13596
- Local but not systemic administration of mesenchymal stromal cells ameliorates fibrogenesis in regenerating livers
van der Helm D, Barnhoorn MC, de Jonge-Muller ESM, Molendijk I, Hawinkels LJAC, Coenraad MJ, van Hoek B, Verspaget HW. J Cell Mol Med. 2019;00:1–13, DOI: 10.1111/jcmm.14508
- Mesenchymal stromal cells prevent progression of liver fibrosis in a novel zebrafish embryo model
van der Helm D, Groenewoud A, de Jonge-Muller ESM, Barnhoorn MC, Schoonderwoerd JA, Coenraad MJ, Hawinkels LJAC, Snaar-Jagalska BE, van Hoek B, Verspaget HW. Scientific Reports 2018; 8:16005, DOI:10.1038/s41598-018-34351-5

- CRIPTO promotes an aggressive tumour phenotype and resistance to treatment in hepatocellular carcinoma.
van der Helm D, Karkampouna S, Gray PC, Chen L, Klima I, Grosjean J, Burgmans MC, Farina-Sarasqueta A, Snaar-Jagalska EB, Stroka DM, Terracciano L, van Hoek B, Schaapherder AF, Osanto S, Thalmann GN, Verspaget HW, Coenraad MJ, Kruithof-de Julio. M, *J Pathol.* 2018 Jul;245(3):297-310. doi: 10.1002/path.5083
- Endoscopic Administration of Mesenchymal Stromal Cells Reduces Inflammation in Experimental Colitis.
Barnhoorn M, de Jonge-Muller E, Molendijk I, van Gulijk M, Lebbink O, Janson S, Schoonderwoerd M, **van der Helm D**, van der Meulen-de Jong A, Hawinkels L, Verspaget HW. *Inflamm Bowel Dis.* 2018 Jul 12;24(8):1755-1767. doi: 10.1093/ibd/izy130.
- Intraluminal Injection of Mesenchymal Stromal Cells in Spheroids Attenuates Experimental Colitis.
Barnhoorn MC, de Jonge-Muller ES, Mieremet-Ooms MA, van der Reijden JJ, **van der Helm D**, Hommes DW, van der Meulen-de Jong AE, Verspaget HW. *J Crohns Colitis*, 2016 Aug;10(8):953-64. doi: 10.1093/ecco-jcc/jjw047.

Acknowledgements

- Allogeneic bone marrow-derived mesenchymal stromal cells promote healing of refractory perianal fistulas in patients with Chron's disease.
Molendijk I, Bonsing BA, Roelofs H, Peeters KCMJ, Wasser MNJM, Dijkstra G, van der Woude CJ, Veenendaal RA, Zwaginga JJ, Verspaget HW, Fibbe WE, van der Meulen-de Jong AE, Hommes DW. *Gastroenterology*, 2015;149:918-927. doi: 10.1053/j.gastro.2015.06.014.
- β 1 integrin regulates Arg to promote invadopodial maturation and matrix degradation
Beatty BT, Sharma VP, Bravo-Cordero JJ, Simpson MA, Eddy RJ, Koleske AJ, Condeelis J. *Mol Biol Cell.* 2013 Jun 1; 24(11): 1661–1675. doi: 10.1091/mbc.E12-12-0908

Manuscripts in preparation/submitted manuscripts

- VCAM-positive mesenchymal stromal cells are most instrumental in ameliorating experimental liver fibrogenesis.
van der Helm D, Habibe J, Barnhoorn MC, de Jonge-Muller ESM, Hawinkels LJAC, Coenraad MJ, van Hoek B, Verspaget HW.

- Time of administration and disease severity are key factors in achieving efficacy of human bone marrow-derived mesenchymal stromal cells in an experimental model of colitis.
*Molendijk I, van Zuylen V, Swets S, Hennink S, **van der Helm D**, Voorneveld P, van der Meulen-de Jong AE, Fibbe WE, Hommes DW, Roelofs H, Verspaget HW.*
- VCAM-dependent migration of IFN γ and TNF α -stimulated mesenchymal stromal cells ameliorates TNBS-induced colitis.
*Molendijk I, Perez-Galarza J, de Jonge-Muller ESM, **van der Helm D**, van der Reijden JJ, Hoeben RC, Hommes DW, Fibbe WE, Verspaget HW, van Pel M.*
- Local and systemic elevated Cripto levels during liver fibrogenesis.
***van der Helm D**, Karkampouna S, Groenewoud A, Snaar-Jagalska BE, van Hoek B, Verspaget HW, Kruithof-de Julio M, Coenraad MJ.*

Dankwoord

In de eerste plaats wil ik mijn familie bedanken die er met hun onvoorwaardelijke steun, vertrouwen, goede zorgen en gezelligheid voor heeft gezorgd dat ik dit proefschrift tot een mooi einde heb kunnen brengen. In het bijzonder een extra woord van dank voor mijn ouders, Nicole, Dennis en natuurlijk Yara en Nova voor het hechte gezin dat we zijn en de stabiliteit, vaste basis en betrokkenheid die ik hierin heb ervaren. In het bijzonder ben ik mijn grootouders erkentelijk voor de trots die ze over me uitspreken/spraken, wat mij altijd sterkt(e). Deze trots is een grote motivatie om het uiterste uit mezelf te halen en om op het maximale van mijn kunnen te presteren.

Mijn vrienden van het dispuut L.H.D. Vanir en de LEO's wil ik bedanken voor de gezellige en ontspannende momenten die ik ter afwisseling op mijn promotieonderzoek met hen heb meegemaakt. Jullie zijn echte vrienden waar ik altijd op kan bouwen. Het gelach, memorabele "FOMO" feestjes en andere evenementen met jullie zorgde voor een welkome afwisseling op mijn onderzoek. De reizen die we maakten zorgden ervoor dat ik helemaal ontspande. Jullie inspirerende 'young professional spirit', gezelligheid, verbondenheid en dierbare vriendschappen zijn onmisbaar geweest.

Hein, Bart en Minneke, de fijne samenwerking en inzet van de afgelopen jaren hebben bijgedragen tot dit mooie eindresultaat. Het was een hele leerzame periode, waarin ik van jullie zowel wetenschappelijk als daarbuiten veel geleerd heb. In deze periode gaven jullie mij de vrijheid om mij als zelfstandig onderzoeker te ontwikkelen en nieuwe projecten te starten. Hein, tijdens onze sparsessies was je er altijd met je kritische blik, precisie en relativiseringsvermogen. Dit zijn belangrijke eigenschappen waarvan ik dankbaar geleerd heb en welke ik in het vervolg van mijn carrière met mij meeneem. Naast de wetenschappelijke begeleiding ben ik je ook zeer erkentelijk voor het luisterend oor en de mate waarin jij voor je onderzoekers opkomt. We hebben een gezamenlijke interesse voor de golfsport, dus wellicht kom ik je in de toekomst nog eens op de golfbaan tegen. Bart, al vrij snel kwamen we achter onze gemeenschappelijke passie voor het roeien. Dit was dan ook vaak het onderwerp van gesprek. Volgend jaar ga ik het roeien weer oppakken en zal ik jou en je vrouw vast weer vaker bij wedstrijden tegenkomen. Jouw steun en vertrouwen gedurende het promotietraject zijn heel belangrijk voor mij geweest. Voor het sparren over het onderzoek en de mogelijke implicaties voor de kliniek, de samenwerking met andere centra en de bemiddeling naar mijn nieuwe aanstelling ben ik je erkentelijk. Minneke, jouw enthousiasme voor het onderzoek werkt aanstekelijk en liet mij altijd een extra stapje bijzetten. Jouw collegiale en persoonlijke betrokkenheid siert je en maakt het fijn om met je samen te werken.

Daarnaast wil ik natuurlijk ook al mijn collega-onderzoekers bedanken. Ilse en Claire, met jullie begon ik de wetenschappelijke reis van het promoveren. Wat hebben wij daarnaast leuke tijden op het lab en bij de NVGE/NVH beleefd. Toen kwamen Sanne en Annarein op mijn pad. Op het gebied van gezelligheid waren wij enorm aan elkaar gewaagd. We lachten wat af, wat soms tot opmerkelijke blikken van onze promotoren leidde. Hierna kwamen Luuk, Mark, Marieke, Jelte, Maaïke, Gabriëlla, Tom, Sara O. en Sara H. ons onderzoeksteam versterken. Deze verschuiving deed mij landen en zorgde voor een serieuze laatste eindsprint waar jullie mij allemaal mee geholpen hebben. Mede door jullie steun heb ik de laatste periode tot een mooi einde gebracht. Als vaste rotsen in de branding waren daar ook de analisten: Eveline, Johan, Wim, Marij, Stef, Leonie en Annie die mij altijd zeer behulpzaam zijn geweest. Eveline, gedurende het onderzoek was je onmisbaar voor mij. Onze fijne samenwerking, je luisterend oor en het vele werk dat je hebt verricht waren heel belangrijk, zowel voor de uitvoering van de diverse studies als voor mijzelf. Alle andere collega's, dat zijn er te veel om op te noemen, wil ik bedanken voor hun voortdurende support. Ook wil ik de Maag-, Lever- en Darmstichting en de afdeling Maag-, Darm- en Leverziekten bedanken voor het financieel mogelijk maken van mijn promotieonderzoek.

Natuurlijk ook veel dank aan mijn partner, Raymon, voor zijn steun, relativeringsvermogen, luisterend oor en zijn geduld. Raymon, kort samengevat ben je gewoon een topper!

